UNIVERSITY OF HAWAII
LIBRARY
JUL 27 '59

Geochimica et Cosmochimica Acta

JOURNAL OF THE GEOCHEMICAL SOCIETY

xecutive
Editors

itors

C. W. CORRENS, *Göttingen.* E. INGERSON, *Austin, Texas.* L. R. WAGER, *Oxford.*

L. H. AHRENS, *Capetown.* S. R. NOCKOLDS, *Cambridge.* H. C. UREY, *La Jolla, Calif.*
JOHN VERHOOGEN, *Berkeley, Calif.* A. P. VINOGRADOV, *Moscow.*
W. A. WAHL, *Helsingfors.*

CONTENTS VOLUME 16, NOS. 1/3 MAY 1959

K. J. MURATA, C. V. DUTRA, M. TEIXEIRA DA COSTA and J. J. R. BRANCO: Composition of monazites from pegmatites in Eastern Minas Gerais, Brazil . . . 1
W. S. BROECKER and A. WALTON: Geochemistry of C^{14} in the freshwater systems . . 15
D. GREENHALGH and P. M. JEFFERY: A contribution to the pre-Cambrian chronology of Australia . . . 39
N. SEN, S. R. NOCKOLDS and R. ALLEN: Trace elements in minerals from rocks of the S. Californian Batholith . . . 58
J. V. JIZBA: Frequency distribution of elements in rocks . . . 79
D. CARROLL and H. C. STARKEY: Leaching of clay minerals in a limestone environment . 83
G. L. BATE, J. R. HUIZENGA and H. A. POTRATZ: Thorium in stone meteorites by neutron activation analysis . . . 88
H. H. LE RICHE: The distribution of certain trace elements in the lower lias of southern England . . . 101
J. F. G. WILKINSON: The geochemistry of a differentiated teschenite sill near Gunnedale, New South Wales . . . 123
J. D. BURTON, F. CULKIN and J. P. RILEY: The abundances of gallium and germanium in terrestrial materials . . . 151
R. E. BELIN: Radon in the N. Zealand geothermal regions . . . 181
Geochemical Note:
A. E. RINGWOOD: Constitution of the mantle—a revision . . . 192
Letters to the Editors:
H. C. UREY: A typical parent meteorite body—a reply to Dr. J. F. Lovering . . 194
J. F. LOVERING: A typical parent meteorite body—reply to Professor Urey . . 195
R. O. SCOTT and D. J. SWAINE: Further comments on the vanadium–calcium line coincidence at 3185 Å . . . 195
Obituary: F. A. PANETH, 1887–1958. By K. C. DUNHAM . . . 196
Book Review:
"Fundamentals of the Energetic Analysis of Geochemical Processes" by V. I. LEBEDEV (Reviewed by D. J. MILTON) . . . 197
Meeting Announcements . . . 198
Errata . . . 199

QE 351
G 42G

PERGAMON PRESS LONDON • NEW YORK • PARIS • LOS ANGELES

GEOCHIMICA ET COSMOCHIMICA ACTA

EXECUTIVE EDITORS

PROF. C. W. CORRENS (1959) *Sedimentpetrographisches Institut der Universität, Lotzestr.* 13, *Göttingen, Germany*
PROF. E. INGERSON (1959–1960) *Department of Geology, University of Texas, Austin* 12, *Texas, U.S.A.*
PROF. L. R. WAGER, F.R.S. (1959–1961) *Department of Geology and Mineralogy, The University Museum, Oxford, England*

EDITORS

PROF. L. H. AHRENS (1959–1960) *Department of Chemistry, University of Capetown, Rondebosch, Cape Province, South Africa*
DR. S. R. NOCKOLDS (1959) *Department of Mineralogy and Petrology, The University, Cambridge, England*
PROF. H. C. UREY, For. Mem. R. S. (1959) *University of California, La Jolla, California, U.S.A.*
DR. JOHN VERHOOGEN (1959–1961) *Department of Geology, University of California, Berkeley, California, U.S.A.*
PROF. A. P. VINOGRADOV (1959–1961) *Vernadsky Institute, Moscow, U.S.S.R.*
PROF. W. A. WAHL (1959–1961) *Observatoriegaten* 8, *Helsingfors, Finland*

EDITORIAL ADVISORY BOARD

EUROPE

T. F. W. BARTH, *Oslo*
L. CAPDECOMME, *Toulouse*
E. J. CONWAY, *Dublin*
P. ESKOLA, *Helsinki*
P. GALLITELLI, *Modena*
A. HADDING, *Lund*
O. HAHN, *Göttingen*
H. W. HARVEY, *Plymouth*
F. HEIDE, *Jena*
A. HOLMES, *Edinburgh*
W. Q. KENNEDY, *Leeds*
PH. H. KUENEN, *Gröningen*
S. LANDERGREN, *Stockholm*
F. MACHATSCHKI, *Vienna*
A. MUIR, *Harpenden*
J. ORCEL, *Paris*
E. RAGUIN, *Paris*
E. REINHARD, *Basle*
TH. G. SAHAMA, *Helsinki*
C. E. TILLEY, *Cambridge*
T. VOGT, *Trondheim*

AMERICAN CONTINENT

A. F. BUDDINGTON, *Princeton*
D. GUIMARAES, *Belo Horizonte*
G. E. HUTCHINSON, *New Haven*
B. H. MASON, *New York*
F. WHIPPLE, *Cambridge*
R. WILDT, *New Haven*
H. S. YODER, *Washington*

FAR EAST

T. WATANABE, *Tokyo*

Publishing Office: Pergamon Press Ltd., 4 & 5 Fitzroy Square, London W.1 (EUSton 4455)
Four issues per volume, three volumes per year

Subscription *per annum* (including postage) (A) £18. (U.S.A. $51.00); (B) For individual subscribers who write directly to the publisher certifying that the Journal is for their private use, £7.7s (U.S.A. $21.50). Members of the Geochemical Society, or non-members who occasionally publish papers in the Journal, £3. 11s. 6d. (U.S.A. $10.00) *per annum.*

Back numbers, £10 (U.S.A. $28.00) per volume

Single issues, £2. 10s. (U.S.A. $7.00) each

Copyright © 1959 Pergamon Press Ltd.

PERGAMON PRESS LTD.

4 & 5 FITZROY SQUARE, LONDON W.1 122 EAST 55TH STREET, NEW YORK 22, N.Y.

PRINTED IN NORTHERN IRELAND AT THE UNIVERSITIES PRESS, BELFAST.

BOOKS ON PHYSICS AND CHEMISTRY OF THE EARTH AND FUNDAMENTAL PHYSICS

PHYSICS AND CHEMISTRY OF THE EARTH Vol. 3

A Progress Series edited by **L. H. AHRENS** (*Cape Town*), **KALERVO RANKAMA** (*Helsinki*), **FRANK PRESS** (*Pasadena*) *and* **S. K. RUNCORN** (*Newcastle-upon-Tyne*)

CONTENTS

Paleoclimates by **J. W. Durham**; Geophysical Investigations in the Eastern Caribbean by **C. B. Officer, J. I. Ewing, J. F. Hennion, D. G. Harkrider** and **D. E. Miller**; Continental Margins and Geosynclines by **C. L. Drake, M. Ewing** and **G. H. Sutton**; The Origin of the Elements by **A. G. W. Cameron**; Silicate Melt Systems by **E. Roedder**; The Geochemistry of Thorium and Uranium by **J. S. Adams, J. K. Osmond** and **J. J. W. Rogers**; Geochemistry in the USSR by **S. I. Tomkeieff**; The Electrical Properties of the Earth's Interior by **D. C. Tozer**.

£5 net ($15)

CLAYS AND CLAY MINERALS

Proceedings of the Sixth National Conference, Berkeley, edited by **ADA SWINEFORD** (*Kansas*)

An essential reference book for courses in clay mineralogy, ceramics, agronomy and petroleum engineering, these proceedings stress crystal structure of clay minerals, alteration of feldspars, clay mineralogy of soils, morphology of clay particles, water vapour sorption, and diageneses.

60s. net ($8.50)

ATLAS OF CLOUD CHAMBER PHOTOGRAPHS OF THE COSMIC RADIATION

by **G. D. ROCHESTER** *and* **J. G. WILSON**

"The authors of this book are to be congratulated on its production; in bringing together in one volume a very fine collection of photographs, they have paid worthy tribute to the part the cloud chamber has played in revealing the nature and associated properties of the fundamental particles which are found in the cosmic radiation. . . . It cannot be stressed too strongly that all nuclear physicists will benefit from a study of the photographs . . . the outstanding merit of the book is the fact that it describes and discusses, in an interesting manner, real fundamental physics. The quality of the reproduction of the photographs is excellent and is immediately impressive".—*Nature*.

£5 5s. net ($15.50)

CONTRIBUTIONS IN GEOPHYSICS

in honour of Beno Gutenberg

Edited by **H. BENIOFF** (*Pasadena*), **M. EWING** (*Columbia*), **B. F. HOWELL, Jr.** (*Pennsylvania*), **F. PRESS** (*Pasadena*)
These contributions from the world's leading geophysicists picture the status of geophysical research today, and publication of this volume was planned to approximate to the time of Dr. Gutenberg's retirement, because of age, from the Directorship of the Seismological Laboratory of the California Institute of Technology. The diverse nature of the topics chosen by the contributors—a few representatives of his many friends, colleagues, fellow scientists and former students—is a measure of the breadth of Dr. Gutenberg's interests, and the wide geographic distribution of the contributors' homes indicates the range of his influence.

60s. net ($9)

THE STUDY OF ELEMENTARY PARTICLES BY THE PHOTOGRAPHIC METHOD

by **C. F. POWELL, F.R.S.**, *assisted by* **D. H. PERKINS** *and* **P. H. FOWLER**, *University of Bristol*

Describes the development of the photographic method of recording the tracks of charged particles, including the technical methods employed in its application to the discovery of mesons, hyperons and anti-nucleons, and the elucidation of their properties. The illustrations are on a lavish scale and never before has the subject been treated so comprehensively.

In Preparation.

ATLAS OF TYPICAL EXPANSION CHAMBER PHOTOGRAPHS

by **W. GENTNER, H. MAIER-LEIBNITZ** *and* **W. BOTHE**

"An impressive selection of photographs . . . the quality of the reproduction of these photographs is excellent. . . . Not only will this volume be invaluable to the student of nuclear physics but it will appeal also to the non-specialist, for the photographs display in a straight-forward and vivid manner the fundamental processes resulting from interactions in the atomic nucleus".—*Philosophical Magazine*

£5 5s. net ($15.50)

PERGAMON PRESS

LONDON · NEW YORK · PARIS · LOS ANGELES

4 & 5 Fitzroy Square, London W.1. 122 East 55th Street, New York 22, N.Y.

24 rue des Ecoles, Paris Ve.

Pergamon Press International Research Journals

The following 51 International Research Journals provide media for the publication of original research papers in various branches of science, technology and medicine. They are of uniformly high standard scientifically. They are edited by specialists, assisted by International Advisory Boards, and in some cases by regional editors, who control the editorial policy.

Abstracts Journal for Metallurgy of the U.S.S.R.
Acta Metallurgica
Annals of The International Geophysical Year
Annals of Occupational Hygiene
Applied Mathematics and Mechanics
Archives of Oral Biology
A.S.L.E. Transactions
Biochemical Pharmacology
Biophysics
Bulletin of Géodésique
Chemical Engineering Science
Comparative Biochemistry and Physiology
Deep-Sea Research
Electric Technology, U.S.S.R. (Elektrichestvo)
Electrochimica Acta
Health Physics
Human Factors
International Abstracts of Biological Sciences
International Journal of Air Pollution
International Journal of Applied Radiation and Isotopes
International Journal of the Physics and Chemistry of Solids
Journal of Atmospheric and Terrestrial Physics
Journal of Inorganic and Nuclear Chemistry
Journal of Insect Physiology
Journal of the Mechanical Sciences
Journal of the Mechanics and Physics of Solids
Journal of Microbiology, Epidemiology and Immunobiology
Journal of Neurochemistry
Journal of Nuclear Energy:
A—Reactor Science
B—Reactor Technology
C—Plasma Physics—Accelerators and Thermonuclear Research
Journal of Psychosomatic Research
Operational Research Quarterly
Pavlov Journal of Higher Nervous Activity
Physics of Metals and Metallography
Planetary and Space Science
Problems of Hematology and Blood Transfusion
Problems of Oncology
Problems of Virology
Radio Engineering (Radiotekhnika)
Radio Engineering and Electronics (Radiotekhnika i Elektronika)
Rheology Abstracts
Sechenov Physiological Journal of the U.S.S.R.
Semiconductor Technology
Spectrochimica Acta
Talanta
Telecommunications (Electrosviaz)
Tetrahedron
Tetrahedron Letters
U.S.S.R. Patents and Inventions
Vacuum

Fully descriptive leaflets and sample copies of Journals are available on request

PERGAMON PRESS

LONDON . NEW YORK . PARIS . LOS ANGELES

4 & 5 Fitzroy Square, London W.1. 122 East 55th Street, New York 22, N.Y.
24 Rue des Ecoles, Paris Ve.

Geochimica et Cosmochimica Acta, 1958, Vol. 16, pp. 1 to 14. Pergamon Press Ltd. Printed in Northern Ireland

Composition of monazites from pegmatites in eastern Minas Gerais, Brazil*

K. J. Murata†, C. V. Dutra‡, M. Teixeira da Costa‡
and J. J. R. Branco §

(*Received* 19 *March* 1958)

Abstract—Two zoned pegmatites in south-eastern Minas Gerais were sampled in detail for their content of monazite and xenotime and the monazite was analysed for certain of the rare-earth elements and thorium.

The ratio of xenotime to monazite increases in both pegmatites from the wall toward the quartz core. The content of the less basic rare-earth elements and of thorium in monazite rises in the same direction. These variation trends suggest that during the crystallization of these pegmatites there was a fractionation of the elements leading to a more or less steady enrichment of the less basic rare-earth elements and of thorium in the residual fluids. One mode of explaining these observed effects postulates that the rare-earth elements and thorium were present in pegmatitic fluids as co-ordination complexes rather than as simple cations.

Introduction

The ranges of variation of the individual rare-earth elements in the more common rare-earth minerals, such as monazite and xenotime, have now been established quantitatively through the use of spectrophotometric (Wylie, 1950), X-ray fluorescence (Goldschmidt and Thomassen, 1924; Sahama and Vähätalo, 1941; Vainshtein *et al*, 1955, 1956 a,b) and emission spectrochemical (Murata *et al*, 1953, 1957) methods of analysis. The rare-earth composition of the rarer minerals, such as yttrotungstite and lyndochite, has also been studied recently by Butler (1957a,b). Several of the investigators have, in addition, been concerned with tracing the changes in the rare-earth composition of monazite and related minerals during the course of certain geochemical processes, such as the crystallization of a granitic magma.

The present study deals with variations in amount and composition of monazite and xenotime collected from different zones of two well-zoned simple pegmatites in Minas Gerais, and attempts to explain the variations in terms of fractional crystallization of a pegmatitic magma in a closed system. The compositions of isolated monazite crystals from a number of other Brazilian pegmatites are also reported.

The average composition of monazite with respect to the major rare-earth elements, as determined recently in two different laboratories, is given in Table 1. The agreement is remarkably good. Furthermore, the ranges of variations of the individual rare-earth elements which have been reported by the two laboratories are essentially the same. Mertie, Jr. (personal communication, 1957) called our attention to the fact that the proportions of Sm, Gd and Y are somewhat higher in these averages than in average commercial monazite derived from beach sands. This difference in composition is probably attributable to the large number of pegmatitic monazites among the samples analysed by the two laboratories.

* Publication authorized by the Director, U.S. Geological Survey.
† U. S. Geological Survey, Hawaii National Park, Hawaii, T.H.
‡ Instituto de Tecnologia Industrial, Belo Horizonte, M.G., Brazil.
§ Instituto de Pesquisas Radioativas, Escola de Engenharia, Belo Horizonte, M.G., Brazil.

The rare-earth composition of cerium-earth minerals may be conveniently indicated by the quantity Σ, which is the sum of the atomic percentages of La, Ce and Pr with respect to the total rare-earth elements. For example, Σ is 72·4 atomic per cent for the average of twenty-four samples reported in Table 1. This quantity is an index of the concentration of the more basic rare-earth elements in cerium-earth minerals and has been found to vary between 58 and 90 atomic per

Table 1. Average rare-earth composition of monazite as determined in two laboratories, expressed in atomic per cent of total rare-earth elements that were determined

	Lab. 1*	Lab. 2†
Total no. of samples	24	56
La	22·7	25·5
Ce	44·7	45·8
Pr	5·0	5·1
Nd	18·7	18·3
Sm	3·7	3·4
Gd	1·7	1·9
Y	3·5	—
Total	100·0	100·0
Σ La + Ce + Pr	72·4	—
Nd/Ce	0·418	0·400
Y/Ce	0·078	—
La/Ce	0·508	0·557

* Murata *et al.* (1953, 1957)
† Vainshtein *et al.* (1955, 1956 a,b).

cent in monazite. Bastnaesites are consistently high in the more basic elements and have more restricted values of Σ, between 80 and 92 atomic per cent. The individual variations of La, Ce, Pr, Nd, Sm, Gd and Y with Σ have been outlined in a previous paper (Murata *et al.*, 1957) in which a rapid spectrochemical method for determining Σ and the weight percentage of thorium in monazite was also described.

A result of much geochemical interest has been obtained by Vainshtein *et al*, (1956a) by comparing the rare-earth composition of monazite from granites and from their derivative pegmatites. In some examples there is no difference in composition and in others the pegmatitic monazite tends to be higher in Sm, Gd, Tb and other less basic rare-earth elements (in our terminology, the Σ values tend to be smaller). This difference in composition suggests that during the crystallization of a granitic magma, the more basic rare-earth elements tend to be precipitated preferentially so that the rest magma becomes relatively richer in the less basic rare-earth elements. One of the purposes of our work has been to test this interesting relationship further in monazites from successively crystallized zones of granitic pegmatites.

The data obtained in our study are interpreted in terms of the magmatic theory of pegmatite genesis. A basic premise in our interpretation is that the pegmatitic fluid crystallized from the wall inward toward the core, depositing successive zones of distinctive mineralogy through fractional crystallization (CAMERON *et al.*, 1949).

PEGMATITES OF MINAS GERAIS

Numerous pegmatites occur in the Pre-Cambrian metamorphic terrain of eastern Minas Gerais (OLIVEIRA and LEONARDOS, 1943) and have been mined extensively for gemstones, kaolin, mica, beryl and other industrial minerals.

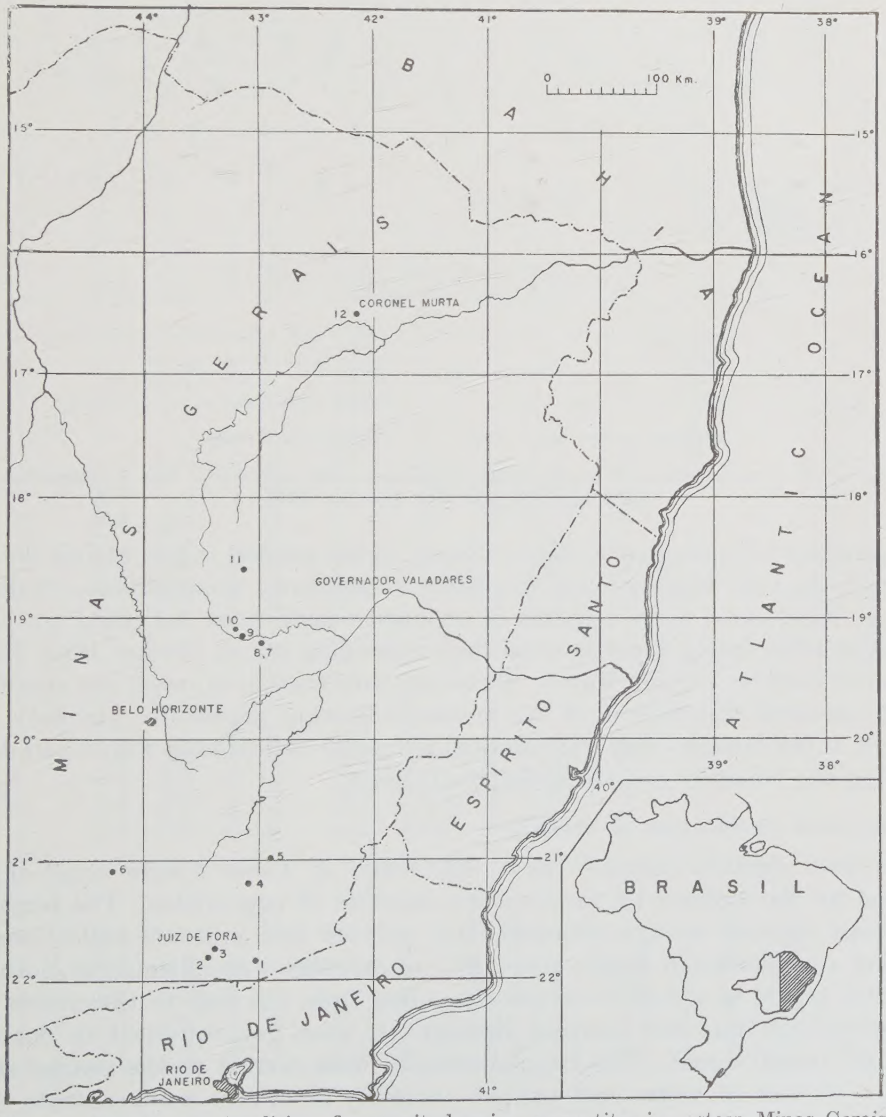

Fig. 1. Map showing localities of monazite-bearing pegmatites in eastern Minas Gerais. The Emprêsa Caolim pegmatite (no. 1) and the Roça Grande pegmatite (no. 2) near Juiz de Fora were studied in detail.

Because most of the pegmatites are deeply weathered they may be sampled for their content of accessory heavy minerals, such as monazite, xenotime and zircon, by panning the saprolite. Not all pegmatites contain monazite and xenotime in concentrations detectable by panning. Thus neither of these minerals could be detected in the mica-producing pegmatites, Pedro Espirito, Cruzeiro no. 1 and Sexta Feira in the Mica Belt north-west of Governador Valadares. The first two of these pegmatites have been described by Pecora *et al.* (1950) and the third is on the same property as the second.

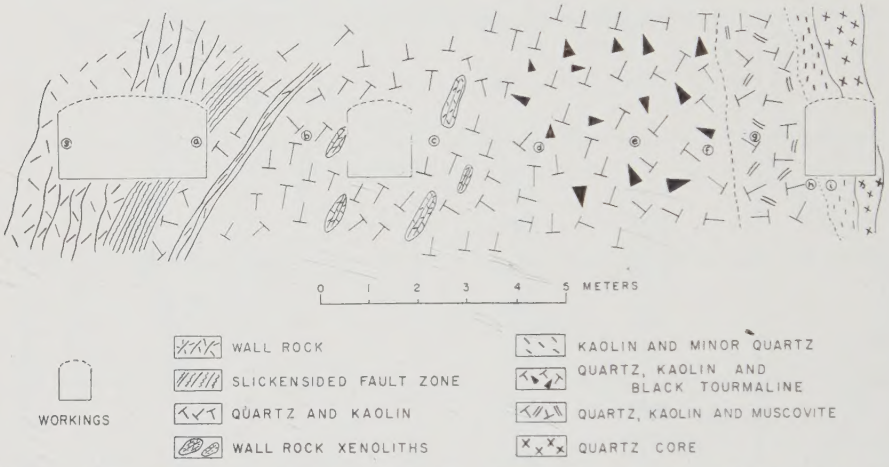

Fig. 2. Transverse section of a part of the Emprêsa Caolim pegmatite, Mar de Espanha, showing the places that were sampled.

Pegmatites of south-eastern Minas Gerais, in the general region of Juiz de Fora, commonly contain monazite and xenotime as accessory minerals recoverable by panning. Occasional large crystals of monazite have been collected by others from pegmatites along a north–south belt extending about 600 km from Juiz de Fora northward to Coronel Murta. However, information is as yet too sketchy to delimit the areal distribution of the monazite-bearing pegmatites precisely. The localities of the samples that were studied by us are indicated in Fig. 1 and details regarding the localities are assembled in Table 2.

Collection and purification of samples

The first eighteen samples (1s to 4A) listed in Table 2 were small crystals collected by the authors by panning the saprolite of pegmatites. The remainder were large crystals mostly obtained from private and museum collections. In sampling a pegmatite in detail, about 15 l. of saprolite was collected in cloth bags at several places in a transverse cut extending from the wall to the quartz core. The quartz core was not sampled because we were not equipped to deal with this hard, massive rock. The bagged samples were carried to the nearest stream or other sources of water and panned carefully to obtain a concentrate of the heavy minerals.

Fig. 2 shows a transverse section of a part of the Emprêsa Caolim pegmatite

Table 2. Localities of monazite samples

No.	Municipality	District	Mine	Source rock	Notes
	State of Minas Gerais				
1s	Mar de Espanha	Estevão Pinto	Emprêsa Caolim	Schist wall rock	Small crystals (<1 mm).
1a–1i	Mar de Espanha	Estevão Pinto	Emprêsa Caolim	Pegmatite	Small crystals. Series of samples across pegmatite.
2s	Juiz de Fora	Ibitiguaia	Roça Grande	Schist wall rock	Small crystals.
2a–2e	Juiz de Fora	Ibitiguaia	Roça Grande	Pegmatite	Small crystals. Series of samples across pegmatite.
3	Juiz de Fora	Juiz de Fora	Linhares	Pegmatite	Small crystals from near contact with wall rock.
4A	Pomba	Tocantins	Fazenda Santa Clara	Pegmatite	Small crystals. Same locality as HESS and HENDERSON (1925) and GUIMARÃES (1926).
4B	Pomba	Tocantins	Fazenda Santa Clara	Pegmatite	Large crystals (>1 cm).
5	Uba	Divino de Uba	—	Pegmatite	Large crystals. Same locality as GUIMARÃES (1925) and FENNER (1928).
6	Nazareno	São João del Rei	—	Pegmatite	Large crystals.
7	Ferros	Ferros	Fazenda Dr. Julio Drummond	Pegmatite	Large crystals.
8	Ferros	Ferros	—	Pegmatite	Large crystals. U.S. Nat. Mus. No. R-8109.
9	Conceicão do Mato Dentro	Brejauba	Fazenda da Posse	Pegmatite	Large crystals.
10	Conceicão do Mato Dentro	Brejauba	Corrego do Tatu	Pegmatite	Large crystals.
11A	Sabinopolis	Brejauba	Gruta da Generosa	Pegmatite	Large crystal. Same locality as LEONARDOS (1936) and PEIXOTO and GUIMÃRAES (1953).
11B	Sabinopolis	Brejauba	Gruta da Generosa	Pegmatite	Another large crystal.
12	Coronel Murta	—	—	Pegmatite	Large crystals.
	Other States				
13	Gramma, São Paulo state	—	—	Pegmatite	Large crystals.
14	São Rafael, Rio Grande do Norte	—	Orquima	Plagioclase pegmatite	Small crystals.
15	ditto	—	10 km SW of locality 14	Granite stock	Small crystals.
16	São Bento Rio Grande do Norte	—	São Bento	Pegmatite	Large crystal.

from the wall to the quartz core going from left to right, and indicates the places where the pegmatite was sampled. This is a typical example of the zoned granitic pegmatites of simple mineralogy which occur in south-eastern Minas Gerais. The presence of a mica-rich zone and a core of massive quartz towards the middle of the pegmatite is characteristic. The portion beyond the quartz core was inaccessible so it is not known whether this pegmatite is zoned symmetrically.

Fig. 3 shows a transverse section across about half of the Roça Grande pegmatite. This pegmatite is about 40 km from the other one and, although much smaller, shows the same type of zonation. The places that were sampled are indicated along the bottom of the section.

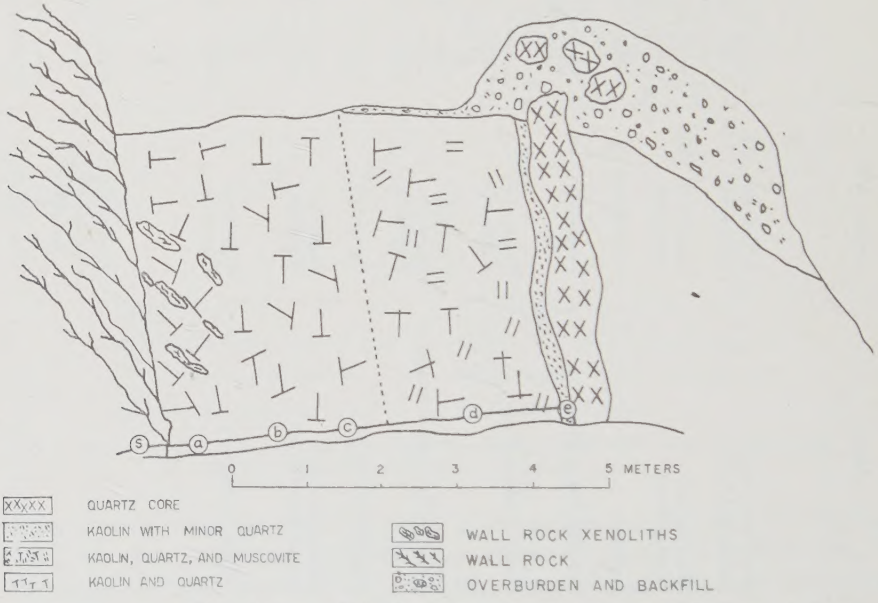

Fig. 3. Transverse section of a part of the Roça Grande pegmatite, Juiz de Fora, showing the places sampled.

How completely monazite and xenotime may be recovered by panning depends on a number of factors, including the density and range of grain size of the two minerals and the amount of preliminary washing required to remove clay from the samples. Theobald (1957) has shown that the recovery of monazite from stream sediments varies between 40 and 80 per cent depending largely on the grain size of the sediment. The percentage recovery of monazite and xenotime in our work is not known, but replicate panning of one test sample showed that we were able to make a consistent recovery. The losses due to our technique are believed to be more or less constant throughout all of the samples. Later in the paper, we will discuss the variation in the ratio of xenotime to monazite within individual pegmatites. We are convinced that these variations in ratio are real and not due to errors in the method used for recovering the two minerals.

In the laboratory, pure monazite and xenotime were separated from the residual sand and other heavy minerals of the panned concentrates by the use of heavy

Table 3. Content of monazite and xenotime in Brazilian pegmatites and composition of the monazite

Sample No.	Monazite (mg per 5 l. of rock)	Xenotime (mg per 5 l. of rock)	Wt. ratio xenotime/monazite	Nd/Ce (Atomic ratio in monazite)	Y/Ce (Atomic ratio in monazite)	La/Ce (Atomic ratio in monazite)	Ce/(Nd + Y) (Atomic ratio in monazite)	Σ* (Atomic ratio in monazite)	ThO_2 in monazite (wt. %)
1s	2	0	0	0·37	0·17	0·59	1·85	70	6·1
1a	46	8	0·18	0·36	0·13	0·52	2·04	73	6·4
1b	484	142	0·29	0·35	0·15	0·51	2·00	73	7·0
1c	375	170	0·45	0·37	0·15	0·51	1·92	71	7·5
1d	119	47	0·39	0·34	0·11	0·48	2·22	75	7·9
1e	165	47	0·28	0·37	0·11	0·63	2·08	73	5·4
1f	246	121	0·49	0·40	0·13	0·53	1·89	71	8·2
1g	182	135	0·74	0·34	0·18	0·43	1·92	71	7·5
1h	390	380	0·97	0·36	0·12	0·46	2·08	73	9·1
1i	19	57	3·0	0·38	0·18	0·47	1·78	69	12·2
Avg. (1a–1i)	225	123	0·55	0·36	0·14	0·50	2·00	72	7·9
Range (1a–1i)	19–484	8–380	0·18–3·0	0·34–0·40	0·11–0·18	0·43–0·63	1·78–2·22	69–75	5·4–12·2
2s	91	0	0	0·37	0·012	0·51	2·63	78	3·3
2a	35	12	0·34	0·45	0·15	0·49	1·67	68	9·7
2b	35	80	2·3	0·46	0·17	0·50	1·59	66	11·7
2c	6·4	29	4·5	0·48	0·20	0·52	1·47	64	15·3
2d	160	670	4·2	0·50	0·18	0·47	1·47	64	10·3
2e	8·7	29	3·3	0·50	0·18	0·47	1·47	64	11·4
Avg. (2a–2e)	49	164	3·3	0·48	0·18	0·49	1·53	65	11·6
Range (2a–2e)	6·4–160	12–670	0·34–4·5	0·45–0·50	0·15–0·20	0·47–0·52	1·47–1·67	64–68	9·7–15·3
3	6·0	1·8	0·30	0·36	0·063	0·59	2·32	76	9·4
4A	—	—	—	0·57	0·16	—	1·38	63	6·6
4B	—	—	—	0·60	0·18	0·39	1·29	61	5·3
5	—	—	—	0·51	0·22	0·40	1·38	63	6·3
6	—	—	—	0·47	0·14	0·34	1·63	67	17·0
7	—	—	—	0·44	0·13	0·48	1·75	69	10·0
8	—	—	—	0·57	0·038	0·34	1·64	66	8·0
9	—	—	—	0·56	0·22	0·35	1·28	61	6·7
10	—	—	—	0·36	0·013	0·44	2·70	79	13·7
11A	—	—	—	0·27	0·008	0·50	3·58	85	9·4
11B	—	—	—	0·29	0·008	0·51	3·39	84	8·7
12	—	—	—	0·28	0·008	0·49	3·41	84	9·1
13	—	—	—	0·59	0·20	0·35	1·26	60	11·4
14	—	—	—	0·30	0·011	0·50	3·21	83	8·4
15	—	—	—	0·42	0·12	0·53	1·83	70	8·1
16	—	—	—	0·48	0·12	0·23	1·68	68	2·6

* Sigma is the sum of the atomic percentages of La, Ce, and Pr with respect to total rare-earth elements in monazite (MURATA *et al.*, 1957).

liquids and the Frantz magnetic separator. The final products were picked free of residual impurities under a binocular microscope illuminated with the unfiltered light of a medium-pressure mercury vapour lamp. Under this light monazite assumes a characteristic green colour (Murata and Bastron, 1956). The purified minerals were weighed and their concentration is given in Table 3 as mg per 5 l. of saprolite. A rough value of the concentration in weight per cent may be obtained by assuming that 5 l. of saprolite weighs 7 kg.

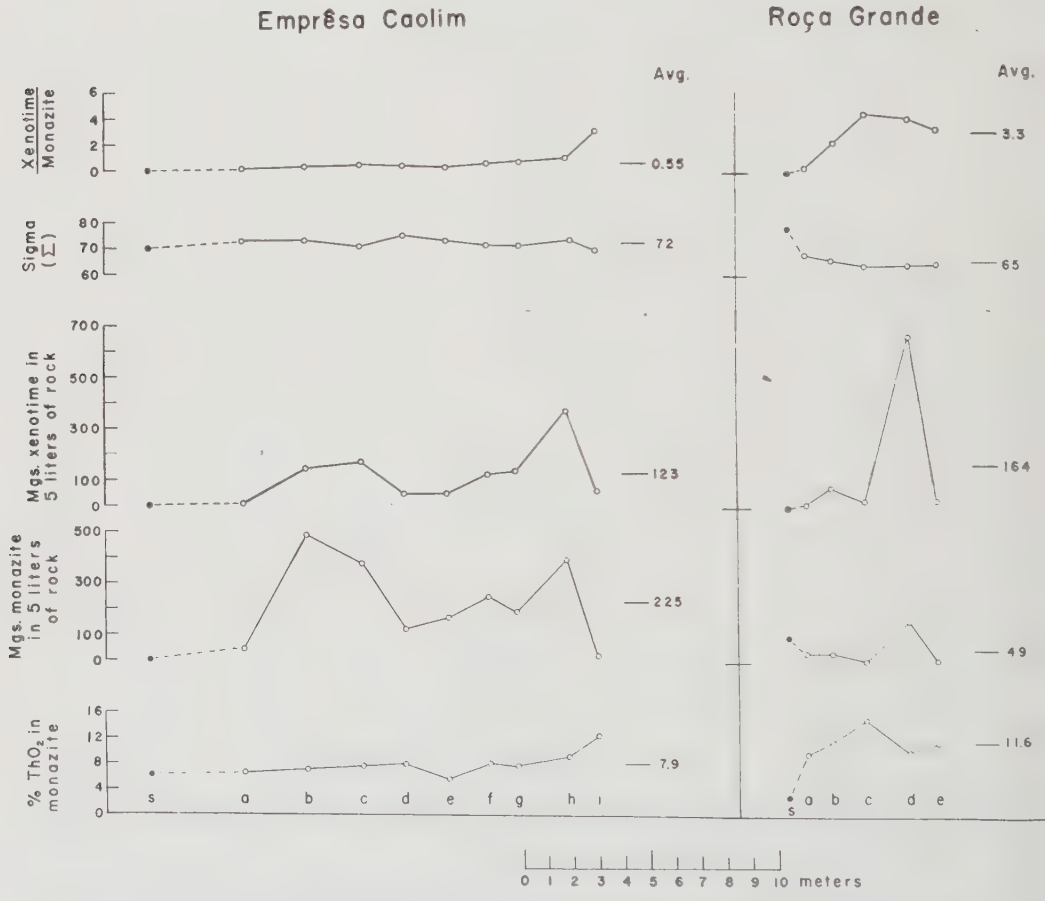

Fig. 4. Content of monazite and xenotime in the Emprêsa Caolim and the Roça Grande pegmatites and the composition of the monazite. Sigma (Σ) is the sum of the atomic percentages of La, Ce and Pr with respect to the total rare-earth elements in monazite.

Methods and Results of Analysis

All the monazite samples and three of the xenotime samples were analysed spectrographically for thorium, following the method of Dutra and Murata (1954). An extension of the method (Murata *et al.*, 1957) also provided data on the atomic ratios of Y, La, Ce and Nd for the monazite samples. The analytical results are presented in Table 3, and those for the sequential samples from the Emprêsa Caolim and Roça Grande pegmatites are also plotted in Fig. 4.

Distribution of monazite and xenotime within the pegmatite

The two zoned pegmatites selected by us for detailed study fortunately have quite different amounts of monazite and xenotime. As shown in Table 3, the Emprêsa Caolim pegmatite averages 225 mg of monazite per 5 l. of rock and monazite is nearly twice as abundant as xenotime. The Roça Grande pegmatite, on the other hand, contains an average of 49 mg of monazite per 5 l. and the concentration of monazite is only a third of that of xenotime.

Figure 4 shows that the concentration of monazite and xenotime varies greatly across both pegmatites and, in general, the two minerals increase or decrease together. From the wall inward there appear to be two zones of enrichment of these minerals, and the inner one is in a mica-rich part near the quartz core. A similar concentration of large crystals of monazite was observed by us in a mica-rich part of the pegmatite at Fazenda Santa Clara (no. 4 of Table 2). In both the Emprêsa Caolim and Roça Grande pegmatites, the kaolin-rich zone in contact with the quartz core, which has been called the "feldspathic sheath of the quartz core" by Pecora *et al.* (1950, p. 256), is low in both monazite and xenotime.

The distribution of the two minerals in these zoned pegmatites of Minas Gerais may be compared with very different distributions found in the unzoned homogeneous pegmatites of Toluca quartz monzonite (Griffitts and Overstreet, 1952) in the region of Shelby, North Carolina. There the monazite is either distributed more or less uniformly across the pegmatite or else is strongly concentrated near the border of the pegmatite, within 30 cm or so of the wall. Xenotime is uncommon in these North Carolina pegmatites.

The ratio of xenotime to monazite in the two Brazilian pegmatites shows an irregular but nonetheless definite tendency to rise going from the wall to the quartz core. In the Emprêsa Caolim pegmatite there is a marked rise in the ratio from 0·5 to 3 among the four innermost samples. In the Roça Grande pegmatite, the ratio increases rapidly among the three outermost samples from 0·3 to a more or less stable value of 4. This increase in the ratio of xenotime to monazite during the crystallization of two pegmatites with very different average contents of the two minerals suggests that there is a general tendency for relatively more of the cerium-group elements to be deposited than the yttrium-group elements throughout the course of fractional crystallization of a pegmatitic fluid and that the residual fluid becomes progressively enriched in yttrium-group elements.

An analysis of the total rare-earths in representative rock samples from different parts of an unweathered zoned pegmatite would definitely prove whether there is such a preferential deposition of the cerium-group elements. Such a study is not possible for our deeply weathered pegmatites. The trend suggested by the xenotime to monazite ratios in the two Brazilian pegmatites, however, is the same as that found by Vainshtein *et al.* (1956a) who demonstrated that monazite of pegmatites tend to be richer in yttrium-group elements than monazite of the parent granites.

Variations in the rare-earth composition of monazite

The rare-earth composition of all the monazites studied by us is denoted by the quantity Σ, which is the sum of the atomic percentages of the three most basic

elements, La, Ce and Pr, with respect to the total rare-earth elements. Sigma has previously been found to vary in monazite between 58 and 90 atomic per cent with an overall average of 72 atomic per cent, and the percentage in all of our Brazilian samples also falls in this range. Monazites with low percentages of Σ are rich in rare-earth elements that are less basic than praseodymium, such as Nd, Sm, Gd and Y.

Monazites of the Emprêsa Caolim pegmatite have an average Σ of 72 atomic per cent and those of the Roça Grande pegmatite an average of 65 atomic per cent. If for the moment only the general averages are considered, the higher content of the less basic rare-earth elements in the monazites of the Roça Grande pegmatite is seen to correlate directly with the greater relative abundance of these elements in this pegmatite as indicated by the xenotime/monazite ratio. It seems reasonable that the average rare-earth composition of monazite should reflect the overall rare-earth composition of the pegmatite in this way.

With regard to the variation of Σ of the monazite within the pegmatite, Fig. 4 shows that in the Emprêsa Caolim pegmatite, Σ fluctuates irregularly about the average of 72 atomic per cent throughout the pegmatite. The minimum percentage of 69 in the innermost monazite (1i) may be significant in relation to the maximum xenotime/monazite ratio found in this part of the pegmatite. In the Roça Grande pegmatite there is a regular decrease in Σ among the three outermost samples—a trend that is in accord with the concurrent increase in the xenotime/monazite ratio. Thus, the variations in Σ of the monazites across the two pegmatites to a certain extent are independent evidence for an enrichment of the less basic rare-earth elements in the residual fluids of a crystallizing pegmatite. The xenotime-monazite ratio, however, seems to be a more sensitive index of this trend.

Variations in the thorium content of monazite

The weight percentage of thoria in all of the monazites listed in Table 3 ranges from 2·6 to 17·0 with an average of 8·9. This result may be compared with a range of from 3·9 to 11·2 with an average of 6·3 found for monazites from 20 pegmatites of North Carolina in an unpublished study by the U.S. Geological Survey. Thoria was also determined in xenotime from three Brazilian samples 1b, 1h and 2d, and found to be 1·0, 1·5 and 2·2 per cent respectively. The thoria content of the monazites from the same samples are from five to seven times higher. Monazites from the Emprêsa Caolim pegmatite average 7·9 per cent ThO_2 and those from the Roça Grande pegmatite 11·6 per cent ThO_2. In these two pegmatites the higher average percentage of thoria, therefore, correlates with a lower average value of Σ in the monazite and a higher average ratio of xenotime to monazite.

In the Emprêsa Caolim pegmatite, the thorium content of monazite, with only an interruption at sample 1c, rises steadily in the direction of the quartz core. A similar rise in the percentage of thoria is found in the three outermost monazites of the Roça Grande pegmatite but there is a sharp drop in the two inner samples. This drop is probably ascribable to the fact that at position 2d a substantial amount of thorium becomes deposited in the abundant xenotime as well as in monazite.

There is an interesting suggestion that the two pegmatites, which are about 40 km apart, may have had a very similar history of crystallization and that the Roça Grande pegmatite merely represents a more advanced stage of differentiation. Some support for this idea is obtained from Fig. 5 in which the percentage of thoria in the monazite of both pegmatites is plotted against the xenotime/monazite ratio. A single line serves roughly to indicate the covariance of these quantities in both pegmatites. Thus the evidence from the two pegmatites, individually and collectively, suggests that during the crystallization of a zoned pegmatite the residual liquid tends to become enriched in the less basic rare-earth elements and in thorium.

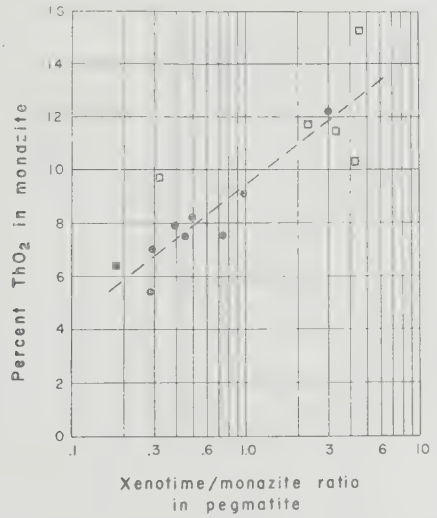

Fig. 5. Relationship between the thoria content of monazite and the xenotime/monazite ratio in two Brazilian pegmatites. Black circles denote samples from the Emprêsa Caolim pegmatite and the open squares, samples from the Roça Grande pegmatite.

Discussion

In order to explain fully the trend of variation of the rare-earth elements and thorium in the two pegmatites, the amount of these elements in all major and minor minerals of the pegmatites must be known. Until such comprehensive information becomes available we can only speculate as to the probable mechanism of fractionation of these elements. The observed variation trends can be explained most simply by assuming that one other mineral like allanite with a ratio of cerium earths to thorium higher than in monazite was deposited throughout the pegmatite along with monazite and xenotime. Silver and Gruenfelder (1957) have emphasized the importance of allanite as carrier of rare-earth elements in certain granites of Georgia but this mineral seems to be absent in the pegmatites of south-eastern Minas Gerais.

Another possible mechanism of fractionating the rare-earth elements and thorium depends upon the relative solubilities of the phosphate minerals, monazite and xenotime themselves, in the pegmatite fluid. Both minerals are deposited

together during the crystallization of a pegmatite but, as seen in the two Brazilian pegmatites, there is an increase in the ratio of xenotime to monazite as the crystallization proceeds from the wall towards the core.

The chemistry of the rare-earth elements in solution can be divided into two general categories depending on whether the elements are present as simple cations or as complex anions. The well-known lanthanide contraction leads to gradations in both the cationic and anionic properties of the rare-earth elements—gradations that would be expected to persist over a wide range of temperature, pressure and composition. Although Ringwood (1955), who recently discussed the role of complex formation in pegmatite genesis, did not consider the rare-earth elements to be among the complex-forming elements, there are many examples of such rare-earth complexes (Keller and Parry, 1956). The sulphato and carbonato complexes are involved in certain classical methods of separating the rare-earth elements into cerium and yttrium groups (Yost, Russell and Garner, 1947).

Existing chemical data indicate that when the rare-earth elements are present in solution as simple cations, the addition of small increments of hydroxides or phosphates results in a preferential precipitation of the less basic yttrium-earth elements by virtue of the greater insolubility of their hydroxides and phosphates compared to those of the cerium-earth elements. Carron *et al.* (1958) have recently synthesized the phosphates of the individual rare-earth elements at 300° C and have shown that their solubility, in general, decreases throughout the lanthanide series in step with the decreasing basicity of the elements. Such a preferential precipitation of the yttrium-earth phosphates leading to an enrichment of the cerium earths in the residual fluid, however, is contrary to the trend observed in the Brazilian pegmatites.

If the rare-earth elements are not present in solution as simple ions but rather as some co-ordination complex, such as the carbonato or sulphato anion, the order of precipitation of the phosphates or hydroxides can become reversed. In general, the less basic the rare-earth element the more stable would be the soluble co-ordination complex it forms and the lower would be the concentration of simple cations in equilibrium with the co-ordination complex. When an increment of phosphate is added to such a system the basic cerium earths which form the least stable co-ordination complexes would, therefore, tend to be preferentially precipitated as observed in the two Brazilian pegmatites.

This dependence of the order of precipitation on the state of the element in solution is also very marked for thorium relative to all of the rare-earth elements. Thorium phosphate is far less soluble than any of the rare-earth phosphates. But thorium also forms soluble co-ordination complexes that are more stable than those of the rare-earth elements. Therefore, like the yttrium earths, thorium would tend to become enriched in residual solutions if it is present in the form of some anionic co-ordination complex.

Acknowledgements—The senior author gratefully acknowledges a grant from the Conselho Nacional de Pesquisas of Brazil which allowed him to participate in this field and laboratory study in Brazil. He expresses his sincere thanks to Dr. D. Guimarães of the Instituto de Tecnologia Industrial of Belo Horizonte for proposing the trip to the Conselho and for providing valuable advice on the pegmatites of Minas Gerais.

Mine owners and employees, particularly those of Emprêsa Caolim Limitada of Rio de Janeiro, extended numerous courtesies that facilitated the work. Drs. J. V. N. Dorr II and M. G. White of joint Brazilian–American geological groups in Brazil kindly made special equipment available. Mr. A. C. Seára, then of the Brazilian Departamento Nacional da Produção Mineral, ably assisted the senior author on a special field trip. We are obliged to the following persons for valuable specimens of monazite: Professor E. Távora of Rio de Janeiro, Professor J. C. Silva of Ouro Preto, Messrs. W. Florencio and F. Peixoto of Belo Horizonte, and Drs. W. D. Johnston, Jr. and G. Switzer of Washington, D.C.

References

Butler J. R. (1957a) Rare earths in yttrotungstite. *Geochim. et Cosmochim. Acta* **12,** 190–194.

Butler J. R. (1957b) Rare earths and thorium in lyndochite. *Amer. Min.* **42,** 671–676.

Cameron E. N., Jahns R. H., McNair A. H. and Page L. R. (1949) The internal structure of granitic pegmatites. *Econ. Geol.* Monograph 2, 115.

Carron M. K., Naeser C. R., Rose H. J., Jr. and Hildebrand F. A. (1958) Fractional precipitation of rare earths with phosphoric acid. *Bull. U.S. Geol. Surv.* 1036–N.

Dutra C. V. and Murata K. J. (1954) Spectrochemical determination of thorium in monazite by the powder-d.c. technique. *Spectrochim. Acta* **6,** 373–382.

Fenner C. N. (1928) Radioactive minerals from Divino de Ubá, Brazil. *Amer. J. Sci.* **16,** 382–391.

Goldschmidt V. M. and Thomassen L. (1924) Geochemische Verteilungsgesetze der Elemente III. Roentgenspektrographische Untersuchungen über die Verteilung der seltenen Erdmetalle in Mineralen. *Skr, Norske Vidensk Akad. Mat.-Naturw. Klasse* No. 5, 1–50.

Griffitts W. R. and Overstreet W. C. (1952) Granitic rocks of the western Carolina Piedmont. *Amer. J. Sci.* **250,** 777–789.

Guimarães D. (1925) Breve Notícia sôbre jazida de samarskita, columbita e monazita. *Serv. Geol. Mineral. Brasil* **13,** 115–118.

Guimarães D. (1926) Nota sôbre o mineral radio-activo da Fazenda Santa Clara, municipio de Pomba. *Inst. Brasileiro Sci. Bol. Anno.* **2,** 114–124.

Hess F. L. and Henderson E. P. (1925) Polycrase from Brazil. *J. Franklin Inst.* **200,** 235–238.

Keller R. N. and Parry R. W. (1956) Modern developments: The electron pair bond and the structure of co-ordination compounds. *Chemistry of Co-ordination Compounds* (Edited by Bailar J. C., Jr.) pp. 157–219. Rheinhold, New York.

Leonardos O. H. (1936) Uma jazida de beryllo, mica, columbita, anneradita, e monazita em Sabinopolis, Minas Gerais. *Minerac. e Metall.* **1,** 15–16.

Murata K. J. and Bastron H. (1956) A convenient method for recognizing non-opaque cerium-earth minerals. *Science* **123,** 888–889.

Murata K. J., Rose H. J., Jr. and Carron M. K. (1953) Systematic variation of rare earths in monazite. *Geochim. et Cosmochim. Acta* **4,** 292–300.

Murata K. J., Rose H. J., Jr., Carron M. K. and Glass J. J. (1957) Systematic variation of rare-earth elements in cerium-earth minerals. *Geochim. et Cosmochim. Acta* **11,** 141–161.

Oliveira A. I. de and Leonardos O. H. (1943) *Geologia do Brasil* (2nd Edn.) pp. 84–87. Ministerio da Agricultura, Rio de Janeiro.

Pecora W. T., Klepper M. R., Larrabee D. M., Barbosa A. L. M. and Frayha R. (1950) Mica deposits in Minas Gerais, Brazil. *Bull. U.S. Geol. Surv.* 964–C, 205–305.

Peixoto F. and Guimarães D. (1953) Problemas de Cronogeologia. *Univ. Minas Gerais, Inst. Pesquisas Radioativas Publ.* **1,** 1–35.

Ringwood A. E. (1955) The principles governing trace-element behaviour during magmatic crystallization.—II. The role of complex formation. *Geochim. et Cosmochim. Acta* **7,** 242–254.

Sahama T. G. and Vähätalo V. (1941) X-ray spectrographic study of the rare earths in some Finnish eruptive rocks and minerals. *Bull. Comm. Géol. Finl.* Nr. 126, 50–83.

Silver L. T. and Grunenfelder M. (1957) Alteration of accessory allanite in granites of the Elberton area, Georgia. *Bull. Geol. Soc. Amer.* **68,** 1796 (abstr.).

Theobald P. K., Jr. (1957) The gold pan as a quantitative geologic tool. *Bull. U.S. Geol. Surv.* 1071–A, 1–54.

Vainshtein E. E., Tugarinov A. I. and Turanskaya N. V. (1955) The distribution of rare earths in monazites. *Dokl. Akad. Nauk. SSSR* **104**, 268–271.

Vainshtein E. E., Tugarinov A. I. and Turanskaya N. V. (1956a) Distribution of rare earths in granitoid monazites. *Dokl. Akad. Nauk. SSSR* **106**, 691–692.

Vainshtein E. E., Tugarinov A. I. and Turanskaya N. V. (1956b) On regularities in the distribution of rare earths in certain minerals. *Geokhimiya* **1**, 36–56.

Wylie A. W. (1950) Composition of some Australian monazites. *Aust. J. Appl. Sci.* **1**, 164–171.

Yost D. M., Russell H., Jr. and Garner C. S. (1947) *Rare-earth elements and their compounds.* Wiley, New York.

Geochimica et Cosmochimica Acta, 1959, Vol. 16, pp. 15 to 38. Pergamon Press Ltd. Printed in Northern Ireland

The geochemistry of C^{14} in fresh-water systems*

W. S. Broecker and A. Walton‡
Lamont Geological Observatory (Columbia University), Palisades, N.Y.

(*Received* 3 *September* 1958)

Abstract—The processes controlling the radiocarbon concentration in the dissolved bicarbonate of fresh-water systems have been investigated in order to allow more precise estimates to be made of the initial C^{14}/C^{12} ratio in materials formed in such systems in the past. Two factors control this ratio: (a) the relative amounts of silicate and carbonate minerals dissolved by the system and (b) the rate of exchange of CO_2 across the water–air interface.

Measurements on samples collected from the Great Basin yield information on both of these factors. As would be expected, the initial C^{14}/C^{12} ratio of the bicarbonate in streams flowing over igneous rocks is close to that in atmospheric CO_2. The CO_2 exchange rates across the surfaces of Mono, Walker, Pyramid and Great Salt Lakes are similar. The results suggest that the exchange rate for lakes is within the range of from 2 to 15 moles/m^2 per year. These values are consistent with published estimates for the average exchange rate for the oceans.

Whereas these data allow the C^{14}/C^{12} ratio in samples formed in ancient Lake Lahonton to be estimated within ± 5 per cent, the error for random fresh-water samples is probably as great as ± 20 per cent.

Thus it appears that whereas considerable uncertainty must be attached to radiocarbon ages on random fresh-water materials, where detailed studies such as the above are made the uncertainty can be reduced to the level of the laboratory error.

Introduction

One of the assumptions of the radiocarbon-age method is that the measurement of a limited number of modern materials allows the initial C^{14} concentration in a sample of unknown age to be precisely estimated. Although this applies to materials formed in the well-mixed atmospheric reservoir, it is not true for those formed in random fresh-water systems. This problem was first recognized by Godwin (1951) and experimentally verified by Deevey *et al.* (1954). Living materials deriving their carbon from the dissolved bicarbonate in alkaline New England ponds were shown to have C^{14}/C^{12} ratios as much as 20 per cent lower than that in contemporary wood. This deficiency was attributed to solution of old carbonate by the waters supplying the ponds.

The current programme was initiated specifically to provide control values for age determination studies on carbonate materials deposited from the waters of the fossil lakes of the Great Basin. A broader aim was to investigate the processes which control the C^{14}/C^{12} ratios in fresh-water systems which in turn would allow radiocarbon dates on fresh-water materials to be evaluated critically.

Theoretical Considerations

Two major factors control the C^{14}/C^{12} ratio of the dissolved bicarbonate in fresh waters: (a) the ratio of the amount of carbonate to the amount of silicate dissolved and (b) the rate of exchange with CO_2 in the atmospheric reservoir.

---

* Lamont Geological Observatory Contribution No. 325.
‡ Present address: National Physical Laboratory, Teddington, England.

The mechanisms which control the ratio of C^{14} to C^{12} in the HCO_3^- added to the system can be demonstrated by the following chemical equations:

(1) $$CaCO_3 + H_2O = Ca^{++} + HCO_3 + OH^-$$
$$OH^- + CO_2 = HCO_3^-$$
$$\therefore \quad CaCO_3 + H_2O + CO_2 = Ca^{++} + 2HCO_3^-$$

(2) $$CaAl_2Si_2O_8 + H_2O = Ca^{++} + 2OH^- + Al_2O_3 + 2SiO_2$$
$$2OH^- + 2CO_2 = 2HCO_3^-$$
$$\therefore \quad CaAl_2Si_2O_8 + H_2O + 2CO_2 = Ca^{++} + 2HCO_3^- + Al_2O_3 + 2SiO$$

The reactions are based on the reasonable assumption that nearly all the dissolved CO_2 in fresh-water bodies is in the bicarbonate ion form. Thus for systems in contact with the atmosphere each equivalent of Ca, Mg, Na and K ions dissolved from silicate minerals is accompanied by the addition of 1 mole of atmospheric CO_2. For carbonates $\frac{1}{2}$ mole of atmospheric CO_2 is added to the system for each equivalent of Ca and Mg ions dissolved. Thus one-half of the total CO_2 is C^{14}-free while the other half has an atmospheric concentration. No C^{14}-free HCO_3^- is added in the case of silicate solution. Once the bicarbonate is formed its C^{14}/C^{12} ratio gradually approaches that in the atmosphere with a rate controlled by the second factor, exchange of CO_2 across the water–air interface.

Estimate of relative contribution of carbonate and silicate

In igneous areas silicate solution will be dominant and the majority of the dissolved bicarbonate will be atmospheric in origin. The C^{14}/C^{12} ratios in such streams should hence be close to the atmospheric value. One process exists, however, which would depress the C^{14}/C^{12} ratio in such systems. Calcium originally leached from silicate minerals may be deposited in soils as $CaCO_3$. This carbonate will eventually be redissolved but in the interim loss of C^{14} through radioactive decay may occur. The magnitude of this effect is difficult to estimate.

Rivers draining sedimentary rock dissolve both silicate and carbonate minerals. An approximate estimate of the relative contribution of the two sources can be made by considering the composition of the cations balancing the bicarbonate. To estimate this composition from chemical analyses of the dissolved salts in the water the contribution of the cations, which entered the system balancing SO_4^{--} and Cl^-, must be eliminated. If the Cl^- results from recycling of oceanic salts or solution of salt deposits an equivalent amount of Na and K must be subtracted from the total Na + K concentration. Although there is some uncertainty as to the origin of freshwater SO_4^{--} (Hutchinson, 1957) the assumption that it is accompanied by Ca^{++} or Mg^{++} is in accordance with most theories. Thus a quantity of Ca^{++} and Mg^{++} equivalent to that of SO_4^{--} must be subtracted from the total $Ca^{++} + Mg^{++}$ concentration. The remaining cations are all derived from the solution of carbonate or silicate rocks. If it is assumed that the cations dissolved from sedimentary silicates are in similar proportions to those derived from igneous rocks, then using the corrected composition of average "igneous" stream water (Conway, 1942) the relative contribution of silicate and carbonate

Table 1. Calculation of the fraction of C^{14}-free bicarbonate in rivers flowing over sedimentary rocks

Ion	Concentration (p.p.m.)	Concentration (equiv./l.)	Concentration corrected for $Cl^- + SO_4^=$ (equiv./l.)	Cation ratios	
Average chemical composition of the dissolved solids in rivers flowing over igneous rocks (Conway, 1942)					
Ca^{++}	6·8	0·340	0·34	2	
Mg^{++}	1·2	0·099			
Na^+	4·9	0·213	0·17	1	
K^+	1·9	0·049			
HCO_3^-	15·5	0·515	0·51		
$SO_4^=$	4·8	0·100	—		
Cl^-	3·2	0·090	—		
Average chemical composition of the dissolved solids in rivers flowing over sedimentary rock (Conway, 1942)					
				Cations from silicates	Cations from carbonates
Ca^{++}	37·5	1·88	1·94	0·46	1·48
Mg^{++}	6·3	0·52			
Na^+	9·6	0·42	0·23	0·23	0·00
K^+	3·5	0·09			
				0·69	1·48
HCO_3^-	126·2	2·07	2·07		
$SO_4^=$	22·0	0·46	—		
Cl^-	10·1	0·28	—		

$$\frac{C^{14}\text{-free } HCO_3^-}{\text{total } HCO_3^-} = \frac{1{\cdot}48/2}{0{\cdot}69 + 1{\cdot}48} = 0{\cdot}34$$

can be estimated. An example of such a calculation is shown in Table 1. The result suggests that the average C^{14}/C^{12} ratio for newly formed HCO_3^- in average "sedimentary" river water is 34 per cent below that in atmospheric CO_2. Because of the large local variations in the composition of silicate rocks, such an approach would not be accurate in specific cases. However, a very high ratio of Ca^{++} to Na^+ would suggest an average C^{14}/C^{12} ratio for newly added bicarbonate of slightly greater than 50 per cent than that in the atmospheric CO_2. On the other hand, a Na : Ca ratio close to that found in "igneous" streams would suggest a ratio only slightly lower than that for atmospheric CO_2.

Estimate of exchange rates

The estimation of exchange rates presents greater difficulties than the initial C^{14}/C^{12} ratio problem. The only reliable estimates of these rates have been obtained from C^{14} data itself. Craig (1957), Arnold and Anderson (1957), Revelle and Suess (1957), Rafter and Fergusson (1957) and Fergusson (1958) give estimates for the average exchange rate across the ocean–atmosphere interface ranging from 7·5 to 90 moles/m^2 per year. Whereas the oceanic estimates supply an order of magnitude for the exchange rate, differences in the degree of surface agitation could cause deviations from this range in specific fresh-water bodies. The oceanic value is sufficiently large that exchange must be an important factor in establishing C^{14}/C^{12} ratios in fresh-water systems.

From the foregoing discussion it is clear that purely theoretical considerations provide only limited information concerning the C^{14}/C^{12} ratios in fresh-water systems. A more precise knowledge of these factors can be obtained only by direct C^{14}/C^{12} measurements on materials from contemporary fresh-water systems.

Analytical Procedures

The procedures used to obtain the C^{14} results have been described by Broecker *et al.* (in press). Errors on these measurements are approximately $\pm 8{\cdot}0$ per mil. For all samples C^{13}/C^{12} ratios were measured with a Consolidated Model 401 mass spectrometer. The techniques used are those described by Ault (1957). The error assigned to these analyses is approximately $\pm 1{\cdot}0$ per mil and arises largely from the uncertainty in the O^{17} correction*. The Cl^-, Mg^{++} and Ca^{++} concentrations in the water samples were determined using standard titration procedures and total CO_2 was determined gravimetrically. The C^{14} results are expressed as the per mil difference from 0·95 the activity of the National Bureau of Standards oxalic acid C^{14} standard where

$$\delta C^{14} = \frac{A_{\text{sample}} - 0{\cdot}95A_{\text{oxalic acid}}}{0{\cdot}95A_{\text{oxalic acid}}} \times 100$$

C^{13}/C^{12} ratios are expressed as the per mil difference from the ratio in the *belemnite* standard (Craig, 1957). To eliminate differences arising from isotopic fractionation the C^{14} results are normalized to the C^{13}/C^{12} ratio of the *belemnite* standard. These final results are expressed as the per mil difference from the normalized δC^{14} value for oak wood grown in Palisades, New York, in 1890 where

$$\Delta C^{14} = \delta C^{14} - 2\delta C^{13}\left(1 + \frac{\delta c^{14}}{1000}\right) - 50{\cdot}0$$

The factor of $-50{\cdot}0$ per mil is added so that 1890 wood becomes zero on the normalized scale (see Table 3).

Choice of Samples

Direct measurement of the dissolved carbonate in fresh-water systems has two major disadvantages: (a) the size of the sample required for an analysis (80–800 l.) makes collection, shipment and laboratory processing difficult and (b) such water samples would not integrate any short-term fluctuations in the C^{14}/C^{12} ratio. It

* See note (1) added in proof, on p. 200.

was thought that both of these problems could be overcome by using materials such as subaqueous plants, shell and animal tissue. To ensure that such materials provide correct estimates of the C^{14}/C^{12} ratio of the dissolved carbonate in the waters in which they grew, several sets of comparison measurements were made on materials formed in the same water body. The results of such comparisons on sets of samples collected from two lakes and two river localities are shown in Table 2. Since fractionation occurs during the formation and possibly during the

Table 2. Comparison measurements on materials from the same freshwater body

Lamont no.	Material†	Collection year	δC^{14}	δC^{13}	ΔC^{14}
		Pyramid Lake (Nevada)			
288–C	Tufa	1954	−11	+6·3	−74
288–I	Algae	1955	−75	−22·7	−83
415–JJ	Plants	1957	−77	−26·3	−78
415–KK	Diss. HCO_3^-	1957	−29	−5·9	−67
447–B	Fish	1957	−60	−22·3	−68
		Walker Lake (Nevada)			
415–ZZ	Plants	1957	−3	−20·6	−12
447–A	Fish	1957	−15	−20·9	−24
		Truckee River (Truckee, Calif.)			
415–NN	Plants	1957	−40	−18·8	−54
415–OO	Shell ($CaCO_3$)	1957	+6	−4·7	−35
415–PP	Shell (organic)	1957	−23	−27·0	−20
		Bear River (Woodruff, Utah)			
415–E	Plants	1957	−138	−22·0	−150
415–F	Shell	1957	−122	−6·7	−160

† See appendix for sample description

chemical processing of these materials only the normalized results should be compared (column 6). The results within both sets of lake samples are in excellent agreement. It should be noted that the Pyramid Lake results include a direct measurement on dissolved bicarbonate. The intercomparisons on river samples show deviations only slightly beyond that expected from measurement errors. From the results it appears therefore that estimates based on the use of subaqueous plants, shell and animal tissue are reliable.

"Bomb" Effect

As a result of the explosion of thermonuclear devices the C^{14} concentration in the atmosphere has increased. Since this increase must be considered when interpreting the results presented in the following sections its magnitude must be established. Rafter and Fergusson (1957) have shown that the increase became measurable in 1955 in the southern hemisphere and had reached 7 per cent by mid-1957. De Vries (1958) has also demonstrated that there has been a

Table 3. Summary of bomb effect data on materials receiving their carbon directly from atmospheric CO_2

Lamont no.	Location	Growth year	Material†	δC^{14}‡	δC^{13}	ΔC^{14}‡
			Great Basin			
353-F	California	1825	Spruce wood	+13	−25·0	+14
353-D	California	1875	Spruce wood	0	−25·0	0
288-M	Lake Winnemucca, Nevada	prior to 1955	Sage brush	+4	−11·2	−23
415-G	Evanston, Wyo.	1957	Tree leaves	+83	−28·2	+94
415-EEE	Salt Lake City, Utah	1957	Tree leaves	+89	−26·0	+96
415-HH	Wadsworth, Nev.	1957	Tree leaves	+85	−27·8	+95
415-QQ	Truckee, Calif.	1957	Tree leaves	+91	−27·2	+100
			East Coast			
314	Palisades, N.Y.	1890	Oak wood	+2	−24·0	0
313	Palisades, N.Y.	1938	Oak wood	−29	−24·1	−32
316-B	Palisades, N.Y.	1954	Tree leaves	−17	−23·2	−21
445	Palisades, N.Y.	1957	Tree leaves	+53	−25·6	+57
			N.B.S. C^{14} *Standard*			
456			Oxalic acid	+53	−16·9	+39

† See appendix for sample description
‡ Corrected for radioactive decay

measurable increase in the northern hemisphere. As shown by our data in Table 3 the increase was negligible in the northern hemisphere until 1954 and reached nearly 120 per mil in the Great Basin by the spring of 1957.

Results

The majority of samples measured as part of this study were collected by the authors during the summer of 1957 from the major lake–river systems of the Great Basin. The locations of the sample stations are given on the maps in Figs. 1 and 2. Where possible, the rivers were sampled at a number of localities to obtain data on the downstream change in C^{14}/C^{12} ratio. A 1 l. sample of water

was collected at each C^{14} station. C^{14}/C^{12}, C^{13}/C^{12}, total CO_2, Cl^-, Ca^{++} and Mg^{++} analyses were made on samples from each station. The results are summarized in Table 4 and complete descriptions of the samples are given in the appendix.

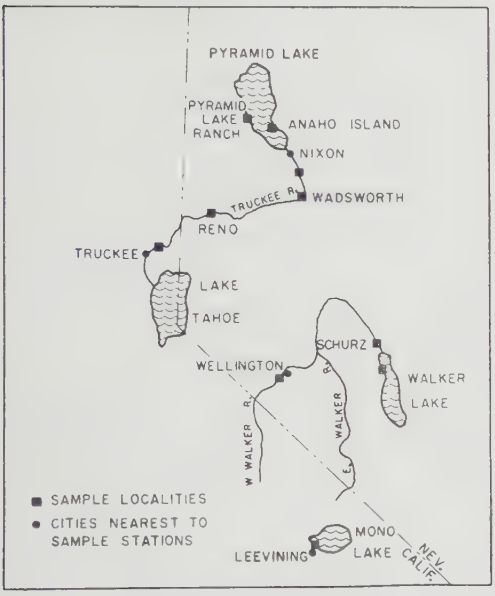

Fig. 1. Map showing Western Great Basin sample localities.

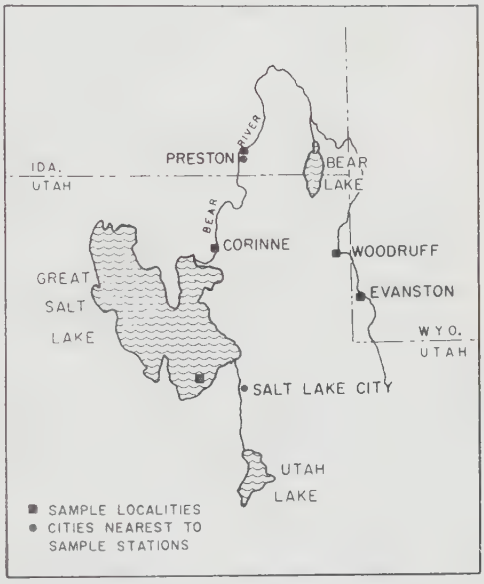

Fig. 2. Map showing Eastern Great Basin sample localities.

Discussion

The data given in Table 4 may be used to obtain estimates of CO_2 exchange rates. Each system will be treated separately.

Pyramid Lake system. Pyramid Lake, which is located in a semi-arid closed basin in north-western Nevada, receives its water supply from the Truckee River system which drains the eastern slopes of the Sierra Nevada mountain range For the purposes of this discussion, the river system may be divided into two parts: the upper Truckee, flowing near the igneous rocks forming the mountains, and the lower Truckee, flowing over the alluvial fans and lacustrine sediments in the basin adjacent to the mountains. Samples were collected from both parts of the river and from Pyramid Lake.

The absence of a measurable change in bicarbonate concentration between the two upper Truckee stations indicates that exchange with the atmosphere is the only process effecting the C^{14}/C^{12} ratio over this stretch of river. Using the relationship developed below, the average rate of exchange can be related to the magnitude of the increase in the C^{14}/C^{12} ratio.

The rate of change of the number of C^{14} atoms, N_R, under a unit of river surface is given by

$$\frac{dN_R}{dt} = RC_A - RC_R \tag{1}$$

Table 4. Summary of measurements

Lamont No.	Location	Cl^- (moles/m³)	CO_2 (moles/m³)	Ca^{++} (moles/m³)	Mg^{++} (moles/m³)	Material‡	δC^{14}	δC^{13}	ΔC^{14}
	Truckee River			Pyramid Lake system					
†	Truckee, Calif.	0·15	1·13	0·17	0·38	†	†	†	
415-LL	Reno, Nev.	0·14	1·04	0·23	0·51	Plants	+6	−18·8	−36
415-GG	Wadsworth, Nev.	0·48	2·27	0·51	0·66	Plants	−33	−27·4	−6
415-II	Nixon, Nev.	1·61	2·53	0·89	1·31	Plants	−112	−34·6	−30
†	Pyramid Lake	55·4	18·8	4·57	0·15	†	†	†	−101
				Walker Lake system					−74
	Walker River								
415-RR	Wellington, Nev.	0·19	—	—	—	Plants	−4	−19·0	−16
415-YY	Schurz, Nev.	0·72	2·36	0·51	1·21	Plants	+5	−24·4	+4
†	Walker Lake	47·5	29·5	4·07	0·21	†	†	†	−18
				Mono Lake system					
415-CCC	Mono Lake	366	240	1·31	0·10	Water	−130	+2·3	−184
				Great Salt Lake system					
	Bear River								
415-C	Evanston, Wyo.	0·22	2·59	0·55	1·02	Plants	−73	−30·1	−67
†	Woodruff, Utah	0·86	6·55	0·87	1·45	†	†	†	−155
415-N	Preston, Idaho	1·63	4·41	2·30	0·64	Plants	−244	−25·9	−255
415-P	Corrine, Utah	10·9	6·22	2·09	1·36	Fish	−152	−21·9	−165
415-FFF	Great Salt Lake	4820	2·85	346	7·81	Brine Shrimp	−111	(−22)	−122

† Based on an average of more than one sample (see Table 2 for summary)
‡ See appendix for sample description

where R is the rate of transfer of CO_2 gas across the interface and C_A and C_R are respectively the concentrations of C^{14} in the CO_2 of the atmosphere and of the dissolved HCO_3^- of the river water. Expressing N_R as the product of C_R, k_R and $\bar{h}$ (where k_R is the concentration of the dissolved HCO_3^- in the river and $\bar{h}$ the mean depth of the river) the equation may be solved for R:

$$R = \frac{k_R \bar{h}}{t} \ln \frac{1 - C_{R_1}/C_A}{1 - C_{R_2}/C_A} \tag{2}$$

C_{R_1} and C_{R_2} represent the C^{14} concentrations at the two stations and t the transit time for the water between the stations.

The values of the parameters used in the calculation of R are given in Table 5. The values of $\bar{h}$ and t were kindly provided by C. H. Carstens of the Carson City Branch of the Water Resources Division of the U.S. Geological Survey. A value for R of 100 moles/m^2 per year is obtained. Because of the range in the C^{14} results from the Truckee station the uncertainty in this estimate is probably ± 50 per cent.

If the other atmospheric gases accompany the CO_2 during the exchange process, the rate computed would correspond to passing 1 l. of air through each 1 l. of river water every 36 min. Since this stream is quite turbulent, having a steep gradient of 37 ft/mile, the calculated exchange rate should be close to a maximum for fresh-water systems.

The two stations below Reno show a progressive decrease in C^{14}/C^{12} ratio accompanied by increases in total CO_2 concentration. No quantitative information concerning the exchange rate can be obtained from these data for two reasons: (a) the C^{14}/C^{12} ratio in the additional CO_2 cannot be estimated and (b) the average transit time of the water is uncertain because of diversion of water for irrigation. The decrease in C^{14}/C^{12} ratio suggests that appreciable carbonate solution occurs in the lower river.

The difference in C^{14}/C^{12} ratio between the last river station and the lake is of particular interest since it is related to the exchange rate across the surface of the lake. Assuming that prior to the bomb era the CO_2 and C^{14} concentrations in the lake had achieved a nearly constant level the following relationships hold:

$$\overset{\text{(input)}}{RA_L + l_E A_L k_R} = \overset{\text{(loss)}}{S + R' A_L} \tag{3}$$

$$C_A R A_L + C_R l_E A_L k_R = (S + R' A_L + V_L k_L \lambda)\, C_L \tag{4}$$

where R and R' are the rates at which CO_2 enters and leaves the lake surface respectively, A_L and V_L, the lake area and volume, and k_R and k_L the concentration of total CO_2 in the water entering the lake and in the lake itself, λ, the decay constant of C^{14}, l_E the linear evaporation rate from the lake surface, and S the rate of loss of CO_2 from the lake through sedimentation of $CaCO_3$. C_A, C_R and C_L are respectively the C^{14} concentrations in the CO_2 of the atmosphere, river and lake.

The following expression is obtained for R:

$$R = l_E k_R \frac{C_L/C_A - C_R/C_A}{1 - C_L/C_A} + \frac{V_L k_L \lambda}{A_L} \frac{C_L/C_A}{1 - C_L/C_A} \tag{5}$$

The first term gives the exchange rate necessary to balance the influx of "old carbon" from the rivers and the second that necessary to balance the loss through radioactive decay in the lake. It should be noted that direct addition of C^{14}-free CO_2 to the lake through sediment solution or hot-spring activity has been considered negligible.

The values selected for the various parameters are summarized in Table 5. The values of C_L/C_A and C_R/C_A must be estimated for the pre-bomb period. The data in Table 2 indicate that the C^{14}/C^{12} ratio in the lake has not changed by a measurable amount over the period of increasing atmospheric C^{14}/C^{12} ratio. This is not unexpected since the amount of bomb C^{14} which could have been added to the lake by river flow or by exchange (assuming the oceanic rate) would be negligible with respect to that already present.

The change in C_R is more difficult to estimate. A minimum estimate of the exchange rate may be obtained if it is assumed that the rivers are as yet unaffected by the bomb C^{14}. Using the result for the Nixon station as the value for C_R, R must be then equal to or greater than 3·7 moles/m^2 per year. In this case the influx of "old carbon" and decay of C^{14} in the lake are equally important in depressing the C^{14}/C^{12} ratio in the lake.

A maximum estimate of the exchange rate may be made if the C^{14}/C^{12} ratio in the river is assumed to show the same percentage increase as that observed for the atmosphere. In this case the C^{14}/C^{12} ratio at the Nixon station would have been 120 per mil lower in 1955 than in 1957. The resulting value of R is 11·5 moles/m^2 per year. Any hot spring activity or carbonate solution in the lake would increase this maximum limit.

An upper limit independent of hot-spring activity can be placed on the exchange rate because of the absence of a measurable increase in the C^{14}/C^{12} ratio for the lake. If R were as large as 100 moles/m^2 per year the C^{14}/C^{12} ratio in the lake should have risen by 15 per mil between 1955 and 1957. The data from Pyramid Lake over this period indicate that the increase was certainly less than this amount (see Table 2). By monitoring the gradual increase in the C^{14}/C^{12} ratio in the lake during the next several years a more precise estimate of the exchange rate can be made.

Walker Lake system. Walker Lake is similar to Pyramid Lake in that it occupies a closed basin and is supplied by run-off from the nearby Sierra Nevada Mountains. Walker River, however, contains no large reservoir analogous to Lake Tahoe in the Truckee River system.

The results on samples from the two river stations yield higher C^{14}/C^{12} ratios than those for corresponding stations in the Truckee River system. This may be partly because of the absence of a large reservoir which holds back some of the bomb C^{14}. Large scale development of irrigation schemes along the lower river prevents the attainment of quantitative information concerning either the source of the bicarbonate or exchange rates for the river.

An estimate of the exchange rate across the lake surface can again be made from the relationship between the C^{14}/C^{12} ratio in the river and that in the lake. For the equilibrium calculation, estimates must be made of the pre-bomb values of C_L and C_R. Since the value of C_L for Pyramid Lake showed little change from

1955 to 1957, it is probable that Walker Lake, which has similar characteristics, would also show little change and hence have a pre-bomb value of C_L within 10 per mil of that in the atmosphere (Table 2).

Since the C^{14}/C^{12} ratio for the Schurz sample exceeds that in the pre-bomb atmosphere by 27 per mil a measurable amount of bomb C^{14} may have entered the river. Depending upon the hold-up time of rainwater in soils the pre-bomb value of C_R could have ranged from equal to, to 90 per mil lower than, the pre-bomb value of C_A.

Because only a minimum estimate of C_A–C_L can be made the range in C_R corresponds to values of R from 5 moles/m^2 per year to at least 39 moles/m^2 per year. Again hot-spring activity or sediment solution would require even higher rates. In the absence of pre-bomb data on the lake no upper limit can be obtained.

Mono Lake system. Mono Lake is situated at the base of the Sierras and receives its water supply from numerous small mountain streams. The lake has an unusually high total CO_2 concentration (240 moles/m^3).

Although no measurements are available for the streams supplying the lake, it is unlikely that their C^{14}/C^{12} ratio would be significantly different from that for the Truckee River at Reno or that for the Walker River at Wellington. Applying the maximum correction for bomb C^{14}, the C^{14}/C^{12} ratio in the streams would be within 100 per mil of the atmospheric value. As can be seen from the data in Table 4 this is at least 70 per mil greater than the C^{14}/C^{12} ratio in Mono Lake. This is possible because the very high CO_2 concentration in the lake leads to a long mean residence time for C^{14} atoms allowing appreciable loss of C^{14} through radioactive decay. For example, replacement of all the CO_2 in the lake by river influx alone would require about one C^{14} half-life. Thus, if exchange with the atmosphere did not occur the lake would have a C^{14}/C^{12} ratio about 50 per cent lower than that in the streams supplying the lake. Using the relationship given above and the data in Table 5, a value of R close to 4 moles/m^2 per year is obtained. Since radioactive decay in the lake dominates in this case, the effect of the uncertainty of the bomb correction on the value of R is negligible.

Appreciable spring activity is known to exist in the Mono Lake basin (Russell, 1886), and thus this value must be considered a minimum. Again future monitoring the growth of the bomb C^{14} concentration in the lake will provide an independent estimate of this rate.

Great Salt Lake system. Great Salt Lake lies on the east side of the Great Basin and receives its water supply from rivers draining the Wasatch Mountains. As in the previous examples, the rivers flow from the mountains across the alluvial and lacustrine sediments of the closed basin.

The results obtained on samples from the Bear River, which supplies about half the influx of water to the lake, are summarized in Table 4. Although the data from the majority of samples show a down-stream decrease in C^{14}/C^{12} ratio, the value at Corinne shows a reverse trend.

The large decrease in C^{14}/C^{12} ratio between Evanston and Woodruff correlates with the transition from a clear mountain stream flowing over a rock-lined channel to a turbid alluvial river flowing over a clay-sand channel. A nearly threefold

Table 5. Parameters used in exchange rate calculations

Rivers	h (m)	k_R† (moles/m³)	t (days)			C_{R^1}/C_A† (1957)	C_{R^2}/C_A† (1957)
Truckee (Truckee to Reno)	0·75	1·0	0·7			0·87	0·90
Lakes	l_E‡ (m/year)	k_R† (moles/m³)	k_L† (moles/m³)	A_L‡ ($m^2 \times 10^{-8}$)	V_L‡ ($m^3 \times 10^{-9}$)	C_R/C_A† (1954)	C_L/C_A† (1954)
Pyramid							
No H-bomb effect on C_R	1·3	2·5	19	5·2	20	0·92	0·95
Best est. of H-bomb effect	1·3	2·5	19	5·2	20	0·84	0·95
Walker							
Min. est. of H-bomb effect	1·5	2·5	29	1·8	4·5	0·98	>0·99
Max. est. of H-bomb effect	1·5	2·5	29	1·8	4·5	0·91	>0·99
Mono							
Max. est. of H-bomb effect	1·2	1·0	240	2·0	5·7	0·91	0·84
Great Salt Lake	1·1	6·2	2·8	42·8	15·3	(see text and Fig. 3)	

† Based on data in Table 4
‡ Based on data summarized by the authors in a separate publication (Broecker and Walton, in press)

increase in bicarbonate concentration occurs along with this transition in channel characteristics. The corresponding decrease in C^{14}/C^{12} ratio is only 88 per mil, indicating that the rise in bicarbonate resulted largely from silicate rather than carbonate solution. Even if only 25 per cent of the additional CO_2 came from dissolved $CaCO_3$ the exchange rate required to yield the C^{14}/C^{12} ratio observed at Woodruff would be higher than that computed for the Truckee River between Truckee and Reno.

The 90 per mil increase in C^{14}/C^{12} ratio between Preston and Corinne is difficult to explain. If the increase is due to exchange with atmospheric CO_2 the rate required would be comparable to that for the much steeper gradient upper Truckee River. An alternative explanation is that the ΔC^{14} result from one of the stations does not provide a reliable index of the average C^{14}/C^{12} ratio for the dissolved bicarbonate at that point in the river. Perhaps the fish collected at Corinne underwent most of their growth further upstream in which case the C^{14}/C^{12} ratio attributed to the river at Corinne would be too high.

The ΔC^{14} value of -122 per mil obtained for the brine shrimp sample collected from Great Salt Lake in June 1958 by R. Cohenour is almost certainly higher than that of the pre-bomb era. The reason for this can be seen from the data in Table 5. From the value of 3·6 m for V_L/A_L and of 1·1 m/year for l_E it can be seen that the water in the lake is replaced every $3\frac{1}{4}$ years. Since the Bear River has a two-fold higher bicarbonate concentration than that in the lake itself the turnover time for carbon must be less than four years. Hence any increase in the C^{14} content of the river would be rapidly recorded in the lake.

An upper limit on the CO_2 exchange rate across the surface of the lake may be obtained by assuming that any change in the lake C^{14}/C^{12} ratio has been due only to exchange with atmospheric CO_2. A lower limit is obtained by assuming the same increase in C^{14}/C^{12} ratio in the river as that observed for the atmosphere. The equations necessary for these calculations are derived below:

(1) No bomb C^{14} added by rivers. The rate of change of the concentration of bomb C^{14} in the dissolved bicarbonate of the lake, b_L, is given by

$$\frac{db_L}{dt} = \frac{R}{k_L\bar{h}}(b_A - b_L) - \frac{k_R l_E}{k_L\bar{h}} b_L \tag{6}$$

where b_A is the concentration of bomb C^{14} in the atmosphere and $\bar{h}$ is the ratio V_L/A_L. The other parameters have the same definitions as those given above. The observed time variation of b_A can be approximated by the relationship $b_A = \varepsilon\{\exp(\gamma t) - 1\}$ where ε and γ are constants. Making this substitution and integrating for the boundary conditions $b_L = 0$ at $t = 0$ (i.e. June 1955) the following relationship is obtained:

$$b_L = R\varepsilon\left[\frac{\exp(\gamma t) - \exp\left\{\frac{-(R + k_R l_E)\,t}{k_L\bar{h}}\right\}}{R + l_E k_R + \gamma k_L\bar{h}} - \frac{1 - \exp\left\{\frac{-(R + k_R l_E)\,t}{k_L\bar{h}}\right\}}{R + l_E k_R}\right] \tag{7}$$

The total C^{14} concentration at any time during the bomb era, $C_L{}^*$, is then given by $C_L + b_L$, where C_L is the equilibrium (pre-bomb) C^{14} concentration.

Table 6. Summary of pre-bomb ΔC^{14} and exchange rate estimates for lakes and rivers*

Location	ΔC^{14} (min. H-bomb effect)	ΔC^{14} (best est.)	ΔC^{14} max. H-bomb effect	R (min. H-bomb effect) (moles/m² per yr.)	R (best est.) (moles/m² per yr.)	R (max. H-bomb effect) (moles/m² per yr.)
Pyramid Lake system						
Truckee River						
Upper River				—	—	—
Truckee, Calif.	-36	−66	-156			
Reno, Nevada	23	−63	−133	—	100	—
				—	—	—
Lower River						
Wadsworth, Nev.	−23	-83	−143			
Nixon, Nev.	−101	181	-221	—	—	—
Pyramid Lake	-	−74	—	4	—	10–100
Walker Lake system						
Walker River						
Upper River						
Wellington, Nev.	23	133	143			
Schurz, Nev.	23	−103	113	—	—	—
Walker Lake		−18		5	- -	-40
Mono Lake system						
Mono Lake		184		3	4	-
Great Salt Lake system						
Bear River						
Upper River						
Evanston, Wyo.	67	-	187	-	-	-
Lower River						
Woodruff, Utah	155	. .	275			
Preston, Idaho	-255		375	—	—	—
Corrine, Utah	-165		-285		—	—
Great Salt Lake	122	162	282	0	2	12

* See note (2) added in proof on p. 200.

Rearrangement of equation (5) yields the following relationship for C_L (since the carbon residence time is small the term involving radioactive decay has been neglected), i.e.

$$C_L = \frac{RC_A + l_E k_R C_R}{R + l_E k_R} \tag{8}$$

Combining equations (7) and (8) and dividing by C_A the ratio of the C^{14} concentration for the lake to that for the pre-bomb atmosphere is related to the exchange rate by the following relationship:

$$\frac{C_L^*}{C_A} = \frac{R\varepsilon}{C_A}\left[\frac{\exp(\gamma t) \quad \exp\left\{\frac{-(R + k_R l_E)t}{k_L \bar{h}}\right\}}{R + l_E k_R + \gamma k_L \bar{h}} - \frac{1 - \exp\left\{\frac{-(R + k_R l_E)t}{k_L \bar{h}}\right\}}{R + l_E k_R}\right] + \left[\frac{R + l_E k_R \, C_R/C_A}{R + l_E k_R}\right] \tag{9}$$

(2) Maximum amount of bomb C^{14} added by rivers. In this case a term expressing the contribution of bomb C^{14} from the rivers must be added to equation (6):

$$\frac{db_L}{dt} = \frac{R}{k_L \bar{h}}(b_A - b_L) + \frac{k_R l_E}{k_L \bar{h}}(b_R - b_L)$$

Since the concentration of bomb C^{14} in the river bicarbonate cannot exceed that in atmospheric CO_2 the maximum contribution from the rivers is obtained when $b_R = b_A$. This equation can now be solved as above and combined with equation (8) yielding:

$$\frac{C_L^*}{C_A} = \frac{\varepsilon}{C_A}\left[\left\{\frac{R + k_R l_E}{R + k_R l_E + \gamma k_L \bar{h}} \exp(\gamma t)\right\} - 1 + \left\{\frac{k_L \bar{h}}{R + k_R l_E + \gamma k_L \bar{h}} \exp\left(\frac{-(R - k_R l_E)\, t}{k_L \bar{h}}\right)\right\}\right] + \left[\frac{R + l_E k_R \, C_R/C_A}{R + l_E k_R}\right] \tag{10}$$

Good agreement with the increase in the C^{14}/C^{12} ratio in the atmosphere is obtained when ε and γ are chosen so that $\varepsilon/C_A = 1$ and $\gamma = 0{\cdot}05$. It has been assumed that there has been a 60 per mil increase in the C^{14}/C^{12} ratio in atmospheric CO_2 between June 1957 and June 1958†. Other data necessary for the calculations are given in Table 5. Because of uncertainties in the choice of the proper value of C_R/C_A, the upper and lower limits of R have been plotted in Fig. 3 as a function of C_R/C_A.

Using the value of C_R/C_A obtained for the fish collected at Corinne a maximum value for R of 1·0 moles/m^2 per year is obtained. As pointed out above, the ratio C_R/C_A at Corinne may be too high. If the Preston result is considered as a more reliable estimate of C_R/C_A then the maximum estimate for R becomes 3·5 moles/m per year. Regardless of which ratio is chosen no lower limit can be placed on R. Since C_R/C_A must be greater than 0·50 the upper limit for R cannot be greater than 12 moles/m^2 per year.

† Recent measurements made at Lamont have confirmed this assumption

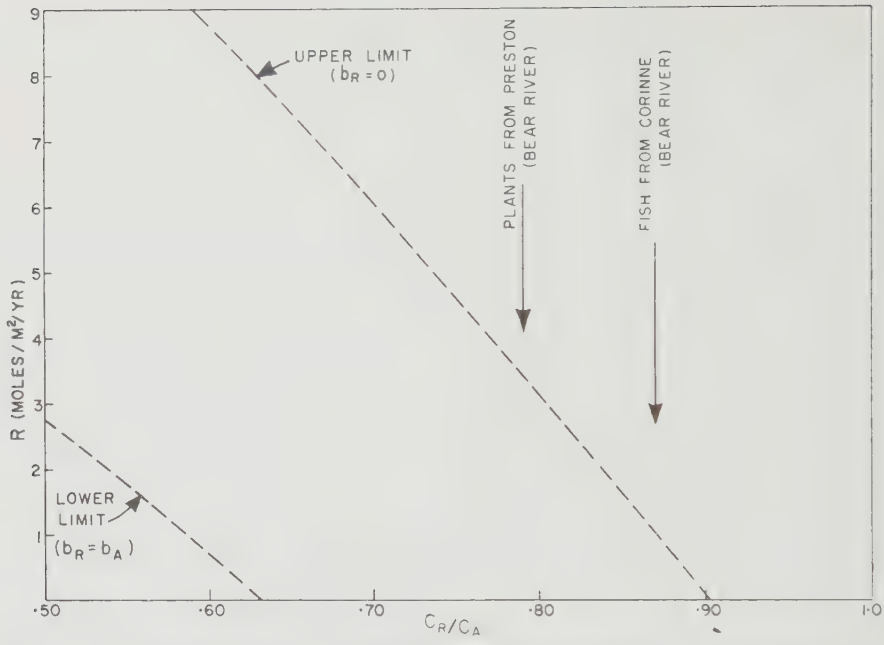

Fig. 3. Relationship between CO_2 exchange rate and the average C^{14} concentration in dissolved bicarbonate of the rivers supplying the lake. The upper curve is drawn assuming that no bomb C^{14} has entered the lake through the rivers and the lower curve assuming that bomb C^{14} concentration in the rivers is equal to that in the atmosphere.

Application to Radiocarbon Dating

C^{14}/C^{12} *ratios in fossil Great Basin Lakes.* The climate changes which caused the large fluctuations in the sizes of the Great Basin lakes also may have influenced their C^{14}/C^{12} ratios. This becomes clear when equation (5) is rewritten as follows:

$$\frac{C_L}{C_A} = \frac{R + l_E k_R \, C_R/C_A}{R + l_E k_R + \dfrac{V_L k_L \lambda}{A_L}}$$

If, for example, R, l_E, k_R, k_L, C_R/C_A or V_L/A_L for the Pyramid Lake system had been different in the past, then the ratio of C_L/C_A would also have differed from its present value (0·950).

Of these parameters only the changes in the ratio of volume to area, V_L/A_L and the linear evaporation rate, l_E, can be quantitatively estimated. Broecker and Walton (in press) have given the following estimates for the magnitudes of these changes for the high water periods of Pyramid Lake:

$$V_L/A_L \quad \text{high-water periods} = 3V_L/A_{L_{\text{present}}}$$

$$l_E \quad \text{high-water periods} = \tfrac{3}{4} l_{E_{\text{present}}}$$

Using these values the ratio of C_L/C_A has been computed for a range of values of the other parameters (see Table 7). Relatively large changes in the parameters produce changes in C_L/C_A of less than 15 per cent if exchange rates close to those

for the contemporary lake apply. (Although there is no reason to believe that R was lower during high-water periods the greater wind-fetch probably resulted in a higher value than at present).

As pointed out by BROECKER and WALTON (in press) the chemical composition of the lower Truckee River has probably been altered considerably by man's activities. Prior to man's presence the lower river may have had a bicarbonate concentration and a C^{14}/C^{12} ratio closer to that measured at Reno. Also during high-water periods the lake covered the lower portion of the river valley. It is possible that volume increases were accompanied by decreases in the bicarbonate concentration. Thus it is probable that the parameters k_R, k_L, C_R/C_A and R changed in directions which would offset the decreases in C_L/C_A introduced by the increase in V_L/A_L.

Table 7. Values of C_L/C_A during high-water periods† of Pyramid Lake for various changes in the present parameters

Change in parameter	C_L/C_A‡	
	R = 3 moles/m² per yr	R = 9 moles/m² per yr
None	0·921	0·939
C_R/C_A = 1·00	0·955	0·973
C_R/C_A = 0·70	0·802	0·911
k_L = 10	0·942	0·948
k_L = 40	0·882	0·907
k_R = 1·0	0·904	0·952
k_R = 5·0	0·925	0·917

† V_L/A_L is assumed to be three times the present value of 40 m and l_E three-quarters the present value of 1·35 m/year for every case.
‡ C_L/C_A at present = 0.950.

It seems justifiable therefore to use the present day value of C_L/C_A for Pyramid Lake as a control value for radiocarbon dates on samples formed in this lake in the past. In view of the above considerations the uncertainty in this estimate is probably no greater than 50 per mil. Since most of the samples of interest exceed 10,000 in age, the error of 400 years introduced by this uncertainty is comparable in magnitude with that resulting from the laboratory error. The choice of C_L/C_A equal to 0·950 for these expanded lakes confirms the preliminary estimate made by BROECKER and ORR (1958) in their age determination work.

Predictions of the C^{14}/C^{12} ratio for Lake Bonneville based on the C^{14} data for contemporary Great Salt Lake system materials are subject to considerable uncertainty. The main reason is the range of possible values for C_R/C_A. Data from the Bear River samples suggest a lower C_R/C_A value than those for the Nevada lakes and since Lake Bonneville had a somewhat greater mean depth it may have had a lower C^{14}/C^{12} ratio than Lake Lahontan. Perhaps the pre-bomb C^{14} concentration in present day Great Salt Lake ($\Delta C^{14} = -120$ per mil) provides the best estimate for the fossil lake. In this case the uncertainty is probably as high as ± 100 per mil. This corresponds to an uncertainty of 800 years in

radiocarbon ages on Lake Bonneville materials. The assumption of Broecker and Orr (1958) that the C^{14}/C^{12} ratio was the same as that in present day Pyramid Lake may therefore be too high. If the −120 per mil value is used all of their ages on materials formed in Lake Bonneville would have to be reduced by 500 years.

Extrapolation to random fresh-water systems. It is important to consider the reliability of radiocarbon ages on fossil materials formed in random fresh-water systems. From the data in Table 4 it is clear that except for special cases such as the Great Basin lakes the uncertainties in the initial C^{14}/C^{12} ratio and hence the sample age will be quite large. Potential samples forming at present in the Great Basin rivers range in C^{14}/C^{12} ratio from 10 per mil to as much as 300 per mil below that in contemporary wood which is normally used as a control for radiocarbon dating. Analyses of a composite of fifteen samples from rivers in Tennessee, Kentucky, Ohio and Pennsylvania yield a result of 328 per mil below the 1890 atmospheric value. Assuming that the influence of exchange is small the latter agrees well with the value of −34 per cent predicted from the chemical data for average sedimentary rivers.

From these data and the theoretical lower limit of 50 per cent of the atmospheric C^{14}/C^{12} ratio, the following averages seem reasonable:

for streams flowing mainly over silicate minerals $C_R/C_A = 0{\cdot}90 \pm 0{\cdot}10$

for streams flowing mainly over limestone terrain $C_R/C_A = 0{\cdot}75 \pm 0{\cdot}15$

and for streams flowing over an unknown sequence $C_R/C_A = 0{\cdot}80 \pm 0{\cdot}20$

Since the corresponding age uncertainties would range from 800 to 1800 years, radiocarbon ages for relatively recent materials (<5000 years in age) would have only limited value. For materials greater than 10,000 years in age, where the laboratory errors would be on the order of 50 per mil, such determinations should prove quite useful.

Of particular interest is the possible application of radiocarbon dating to cave deposits. Since such deposits occur in high carbonate areas and since the underground streams, which carry the carbonate, have only limited direct contact with the atmosphere quite low C^{14}/C^{12} ratios might be expected. Two processes could yield higher ratios for the dissolved bicarbonate than would be predicted from the above reasoning: (a) exchange with atmospheric CO_2 while in a surface system before becoming part of the underground system, and (b) exchange with CO_2 in the air in the cave during transport and deposition. Hence it is possible that sufficient C^{14} is incorporated in cave deposits to allow their ages to be determined.

One stalagmite collected by R. Gurnee in New River Cave in Virginia was measured in connexion with this study. The C^{14}/C^{12} ratio for the outer few millimetres of this formation was 280 per mil below that in the pre-bomb atmosphere. Material from a 2·5 cm core drilled from the centre of the 10 cm diameter stalagmite had only 6 per cent the C^{14} concentration in atmospheric CO_2. Assuming that the difference between the two concentrations is due entirely to radioactive decay about 20,000 years have elapsed since the core of the stalagmite formed.

Although the age uncertainties on this kind of sample will be larger than those on normal samples such as wood and peat, these data suggest that a great deal of information can be obtained from further C^{14} measurements on cave formations. Measurements on a sequence of samples taken from a currently growing deposit will obviously yield more reliable age estimates than those on samples taken at random.

Conclusions

The following conclusions may be drawn from this study:

(1) Materials forming entirely within fresh-water bodies have the same normalized C^{14}/C^{12} ratio as that in the dissolved bicarbonate.

(2) Chemical data on dissolved constituents provide only an approximate estimate of the C^{14}/C^{12} ratio in a given fresh-water body. The C^{14}/C^{12} ratio in water which has dissolved primarily silicate minerals should be close to that in the atmospheric CO_2 while in water which has dissolved primarily carbonate minerals it could be as low as 50 per cent that in the atmospheric CO_2.

(3) Measurements on samples formed in the fresh-water systems of the Great Basin suggest that CO_2 exchange rates for rivers may be as high as 100 moles/m^2 per year while for inland lakes it is closer to 5 moles/m^2 per year.

(4) From the Great Basin data it is concluded that the normalized C^{14}/C^{12} ratio in the dissolved bicarbonate of fossil Lake Lahonton was about 50 per mil lower than that in the pre-bomb atmosphere. The uncertainty in this estimate probably does not exceed 50 per mil allowing radiocarbon ages for materials deposited from this lake to be estimated with ± 400 years.

(5) The data on samples from the river systems of the Great Basin suggest that the C^{14}/C^{12} ratios in random fresh-water systems will show a considerable range. For samples from streams flowing primarily over igneous rocks a C^{14}/C^{12} ratio of 100 ± 100 per mil below the atmospheric value is suggested, while for streams flowing over sedimentary rocks a value of 250 ± 150 per mil should be a good estimate.

(6) Although age uncertainties may be as high as 2000 years considerable information can be obtained from C^{14} measurements on cave formations.

Acknowledgements—The writers are indebted to J. J. Parodiz of the Carnegie Museum, H. van der Schalie of the University of Michigan, T. J. Trelease and Kay Johnson of the Nevada Fish and Game Commission, P. C. Orr of the Western Speleological Institute, R. Gurnee of Closter, N.J., R. Cohenour of Salt Lake City, Utah, L. Jensen of Brigham City, Utah and H. Broecker of Wheaton, Ill., for their help in obtaining and identifying the samples. The assistance of J. Hubbard, E. Olson and M. Zickl in the C^{14} measurement programme is greatly appreciated. G. Erickson and P. Hazlett of the Lamont staff performed the C^{12}/C^{13} analyses. Financial support was provided by the National Science Foundation (Grant NSF G-4191).

References

Arnold J. R. and Anderson E. C. (1957) The distribution of C^{14} in nature. *Tellus* **9**, 28–32.

Ault W. U. (1957) *Isotopic Geochemistry of Sulfur*. Ph.D. Thesis, Columbia University.

Broecker W. S. and Orr P. C. (1958) The radiocarbon chronologies of Lake Lahontan and Lake Bonneville. *Bull. Geol. Soc. Amer.* **69**.

Broecker W. S., Tucek C. S. and Olson E. A. Radiocarbon analyses of oceanic CO_2. To be published.

Broecker W. S. and Walton A. A re-evaluation of the salt chronologies of several Great Basin Lakes. *Bull. Geol. Soc. Amer.* In press.

Conway E. J. (1942) Mean geochemical data in relation to oceanic evolution. *Proc. Roy. Irish Acad.* B **48,** 119–159.

Craig H. (1957a) The natural distribution of radiocarbon and the exchange time of carbon dioxide between atmosphere and sea. *Tellus* **9,** 1–17.

Craig H. (1957b) Isotopic standards for carbon and oxygen and correction factors for mass-spectrometric analyses of carbon dioxide. *Geochim. et Cosmochim. Acta* **12,** 133–149.

Deevey E. S., Gross M. S., Hutchinson G. E. and Kraybill H. L. (1954) The natural C^{14} content of materials from hard-water lakes. *Proc. Nat. Acad. Sci., Wash.* **40,** 285–288.

De Vries. H. (1958) Atomic-bomb effect: variation of radiocarbon in plants, shells and snails in the past 4 years. *Science* **128,** 250–251.

Fergusson G. J. (1958) Reduction of atmospheric radiocarbon concentration by fossil fuel carbon dioxide and the mean life of carbon dioxide in the atmosphere. *Proc. Roy. Soc.* A **243,** 561–574.

Godwin H. (1951) Comments on radiocarbon dating for samples from the British Isles. *Amer. J. Sci.* **249,** 301–307.

Hutchinson G. E. (1957) *A Treatise on Limnology.* Wiley, New York.

Rafter T. A. and Fergusson G. J. (1957) Recent increase in the C^{14} content of the atmosphere, biosphere and surface waters of the oceans. *N.Z. J. Sci. Tech.* B, **38,** 871–883.

Revelle R. and Suess H. E. (1957) Carbon dioxide exchange between atmosphere and ocean and the question of an increase of atmospheric CO_2 during the past decades. *Tellus* **9,** 18–27.

Sample No.	Station location	Hydrologic conditions	Sample description	Collection date	ΔC^{14}
288-C	North-east corner of the Pyramid, Pyramid Lake, Nev.	Water in which material formed is free to mix with rest of lake. Some hot spring activity was noted several hundred feet away	$\frac{1}{4}$ in. thick unlithified fine grained $CaCO_3$ forming on a vertical rock face close to water level	Dec. 1954	−74
288-I	Opposite west side of Anaho Island, Pyramid Lake, Nev.	Open lake	Algae floating on surface of lake. (Presumably rose to surface upon death and were concentrated by wave action)	Sept. 1955	−83
415-JJ	West shore of Pyramid Lake, Nev. near the Pyramid Lake Ranch	Shallow water close to beach	Moss growing on rocks continually washed by waves	Aug. 1957	−78
415-KK	Opposite Pyramid Lake Ranch, Pyramid Lake, Nev.	Open lake. 200 ft from shore (water depth = 5 ft)	Bicarbonate extracted from 50 gal of lake water. (Processed at station by flushing acidified water with CO_2-free air. CO_2 released was absorbed in CO_2-free KOH)	Aug. 1957	67
447-B	Pyramid Lake, Nev.	Open lake	Chubs collected by K. JOHNSON of the Nevada Fish and Game Comm. who states that this type of fish spends its entire life within the lake	Dec. 1957	−68
415-NN	Truckee River at the San Francisco Flycasting Club, Truckee, Calif.	Rapid flowing clear stream (∼100 ft wide and ∼2 ft deep). Bottom lined with boulders and sand	Moss growing on submerged rocks. (Usually within 6 in. of water surface)	Aug. 1957	−54
415-OO	Truckee River at the San Francisco Flycasting Club, Truckee, Calif.	(same as 415-NN)	Shells of *Margaritifera margaritifera falcata* (Gould) living on a sandy shoal	Aug. 1957	−35
415-PP	Truckee River at the San Francisco Flycasting Club, Truckee, Calif.	(same as 415-NN)	Meat from 415-OO shells	Aug. 1957	−20

Appendix—*continued*

Sample No.	Station location	Hydrologic conditions	Sample description	Collection date	ΔC^{14}
415-LL	Truckee River ½ mile west of business district, Reno, Nev.	Clear rapidly flowing water. Silt and cobbled-lined channel ~200 ft wide and from 1 ft to 3 ft deep	Subaqueous plants growing on rocks above rapids	Aug. 1957	−6
415-GG	Truckee River at Route 40 bridge, Wadsworth, Nev.	Slightly turbid water flowing over cobble-silt lined channel	Subaqueous plants growing on cobbles in main channel	Aug. 1957	−30
415-II	Truckee River at Pyramid Lake Indian Reservation. Five miles south of Nixon, Nev.	Clear water flowing over rapids in channel ~50 ft wide and from 1 ft to 3 ft deep	Moss growing on submerged rocks in rapids	Aug. 1957	−101
415-RR	West Walker River at Nevada Route 3 near Wellington, Nev.	Slightly turbid water flowing over rock and silt-lined channel about 100 ft wide and 2 ft deep	Subaqueous plants growing on submerged rocks	Aug. 1957	−16
415-YY	Walker River at Route 93 bridge near Schurz, Nev.	Slightly turbid water flowing over sand- and silt-lined channel	Subaqueous plants attached to small pebbles and debris in main channel	Aug. 1957	+4
415-ZZ	North-west corner of Walker Lake, Nev.	Shallow water (1–2 ft) close to beach	Subaqueous plants attached to rocks and pebbles	Aug. 1957	−12
447-A	Walker Lake, Nev.	Open lake	Chubs collected by T. J. Trelease of the Nevada Fish and Game Comm. who states that this type of fish is confined to the lake	Oct. 1957	−24
415-CCC	West side of Mono Lake 2 miles north of Leevining, Calif.	Shallow water over mud bottom 100 ft from shore	Bicarbonate extracted from 20 gal of water (processed as 415-KK)	Aug. 1957	−184
415-C	Bear River at Route 30 bridge at Evanston, Wyoming	Clear stream flowing rapidly over a cobble-lined channel	Moss forming on submerged rocks within inches of water surface	Aug. 1957	−67

APPENDIX—*continued*

Sample No.	Station location	Hydrologic conditions	Sample description	Collection date	ΔC^{14}
415-E	Bear River 2 miles east of intersection of Utah Routes 39 and 3 at Woodruff, Utah	Slightly turbid water flowing over a silt-lined channel about 100 ft wide and from 2 to 4 ft deep	Subaqueous plants rooted in silt tween scattered pebbles	Aug. 1957	−150
415-F	Bear River (same as 415-E)	(same as 415-E)	Disarticulated shells found on river bottom and shore	Aug. 1957	−160
415-N	Bear River about 8 miles north-east of Preston, Idaho on road to Mink Creek	Rapid flowing water over cobble-lined channel 100 ft wide and 3 ft deep	Moss growing on submerged rocks	Aug. 1957	−255
415-P	Bear River near Corrine, Utah. (Route 30S bridge)	Turbid water flowing in mud-lined channel	Carp collected by L. JENSEN of Brigham City. These fish inhabit the lower Bear River	Sept. 1957	−165
415-FFF	Great Salt Lake	Open water	Brine shrimp collected by R. COHENOUR of Salt Lake City	June, 1958	−122
443-A	New River Cave, Virginia	——	Outer few millimetres of $CaCO_3$ scraped from the surface of 10 cm diameter stalagmite collected by R. GURNEE, Closter, N.J.	1956	−280
443-B	New River Cave, Virginia (same as 443-A)	——	2·5 cm core bored from centre of same stalagmite	1956	−940

Appendix—*continued*

Sample no.	Station location	Sample description	Collection date	ΔC^{14}
448†	Tuscarawas River, Ohio	*Lampsilis ovata* (Say), collected by V. Sterki.	1885	−328
	Ohio River, Beaver Co., Pa.	*Ligumia recta* Raf. Industry, collected by Ortmann.	1908	
	Ohio River	*Plagiola lineolata* Raf. Industry, collected by Ortmann.	1908	
	Schykill River, Monayunk, Pa.	*Ambloxis decisa* (Say), collected by H. J. Gird	1906	
	Mahoning River, Lawrence Co., Pa.	*Ambloxis decisa* (Say), collected by Ortmann.	1907	
	Sandy Creek, Mercer Co., Pa.	*Ambloxis decisa* (Say), collected by S. T. Brooks	1931	
	Aspinwall, Allegheny River, Pa.	*Ambloxis decisa* (Say), collected by Atkinson.	1900	
	Holston River, Tenn.	*Ceriphasia canaliculata undulata* (Say), collected by Goodrich	1924	
	Beaver Creek, Barren Co., Ky.	*Pleurocera obovata* (Say), collected by Goodrich.	1927	
	Tinkers Creek, Ohio	*Helisoma anceps* (Menke), collected by V. Sterki.	1912	
	Tinkers Creek, Ohio	*Gyraulus parvus* (Say), collected by V. Sterki.	1911	
	McKees Rock, Ohio River, Pa.	*Physa heterostrophoa* (Say), collected by Atkinson.	1900	
	Aspinwall, Allegheny River, Pa.	*Physa heterostrophoa* collected by Stupakof.		
	Tinkers Creek, Summit Co., Ohio	*Euamnicola* (*Marstonia*) *lustrica* (Pilsbry), collected by V. Sterki.	1912	
	Tuscarawas River, Ohio	*Euamnicola* (*Cincinnatia*) *cincinnatensis* (Anthony), collected by V. Sterki.	1894	

† Composite of equal weights of samples listed. These samples were supplied by Dr. J. J. Parodiz of the Carnegie Museum, Pittsburgh, Pa.

Geochimica et Cosmochimica Acta, 1959, Vol. 16, pp. 39 to 57. Pergamon Press Ltd. Printed in Northern Ireland

A contribution to the pre-Cambrian chronology of Australia

D. Greenhalgh and P. M. Jeffery
Department of Physics, University of Western Australia, Nedlands,
W. Australia

(*Received* 16 *July* 1958)

Abstract—The results of quantitative chemistry combined with isotope analyses by mass spectrometry have been used to compute a number of mineral ages by the U–Pb method.

The ages of uranium minerals from various parts of Australia have in most cases been in agreement with the previously accepted geologic interpretations. Two periods of uranium mineralization have been confirmed in the Northern Territory uranium mining fields (Late Archaean and Upper Proterozoic), and at Crocker's Well in South Australia (Archaean and Upper Proterozoic). Two periods of mineralization have been postulated for the uranium mineralization at Radium Hill (Archaean and Proterozoic) and for the lead mineralization at Broken Hill (Archaean and Cambrian). The uranium mineralization at Myponga, South Australia, and Hart's Range, Central Australia, has been dated as Upper Proterozoic, and at Woodstock, Western Australia, as Archaean. Where suitable samples were available potassium–argon ages have been used to provide additional evidence as to the correctness or otherwise of the U–Pb determinations. A "concordia" diagram did not satisfactorily resolve discordant ages, and it is concluded that radon losses may generally be expected to vitiate this method.

A set of four figure tables is presented for conversion of isotopic ratios to geological ages.

I. Introduction

The measurements reported here were made during the initial stages of a comprehensive geologic age determination programme which is being developed to outline the geochronology of the Australian continent.

As a first step in this programme the U–Pb, Rb–Sr and K–A age methods are being applied to mineral suites from specific localities so that general age trends may be broadly delineated.

The work described is concerned primarily with uranium minerals whose ages have been determined by mass-spectrometric measurements combined with the results of quantitative chemical analysis.

Areal choice of samples at this stage has been directed rather by availability than by systematic selection, but the geologic significance of the results obtained is of such interest as to warrant an interim report.

II. Experimental

(1) *Instrumentation*

Isotopic analyses were made on a conventional 60° sector-field mass spectrometer (Nier, 1947) using ion source and detector slit-widths of 0·008 and 0·012 in. respectively. These widths were found to give adequate resolution in the lead mass region.

The samples in the form of lead tetramethyl were stored at low pressure over mercury and admitted to the spectrometer through a viscous-flow type of leak. The only departure from standard practice was the use of electron trap control of the ionizing electron beam intensity rather than the normal method of total emission control (Greenhalgh and Jeffery, 1955).

(2) *Sample preparation*

Each mineral specimen was first analysed chemically to determine its uranium, thorium and lead content.

The lead was then extracted from the specimens in the form of lead iodide and converted to lead tetramethyl by the action of methyl magnesium iodide at room temperature, after the manner of Ducheylard *et al.* (1953), although in place of their system of magnetic hammers the lead iodide and Grignard reagent were mixed by rotating a Y-tube, containing one reactant in each arm, about a greased B-10 cone which fitted into the rest of the apparatus, the tube having been previously exhausted by pumping while the arm containing the Grignard reagent was cooled in liquid air.

Ducheylard *et al.* have pointed out the advantages associated with the use of lead iodide rather than lead chloride, namely the speed of the reaction, the lesser complexity of the experimental technique involved and the completeness of the yield without the necessity for excess reagent. The iodide, being less soluble in water than the chloride, is also a more satisfactory end-point for the quantitative extraction of the lead from the minerals.

(3) *Mass-spectral analysis*

The mass spectrum of lead tetramethyl contains ion peaks in the Pb, $PbCH_3$, $Pb(CH_3)_2$, $Pb(CH_3)_3$ and $Pb(CH_3)_4$ regions, each region containing several peaks due to the various isotopes of lead present and also to the loss or gain of extra hydrogen atoms. All analyses in this work were made from the Pb part of the spectrum, where the only complication is due to the fact that each isotope of lead (Pb^{204}, Pb^{206}, Pb^{207}, Pb^{208}) gives rise not only to a peak at its particular mass number, but also to a peak one mass number higher due to the formation of lead hydride ions, PbH. Mercury ions (from the diffusion pump) were also present in the background at mass numbers 198 to 202 and 204, the last adding to the Pb^{204} peak. Mass spectra were consequently drawn, for each specimen, over the mass range 202 to 209, and the peak heights solved mathematically to obtain the lead isotopic abundances using a modification of the method of Dibeler and Mohler (1951).

The results for each specimen were calculated from the mean values obtained from ten spectra, with probable errors in the relative abundances of about $\pm 0{\cdot}5$ per cent. However, when two separate preparations of tetramethyl from the one specimen were analysed some days apart a 3 per cent discrepancy in the relative abundances was obtained. There is some evidence to support the view that this was due to adsorption of previous samples to the walls of the glass sample reservoir, or absorption by the tap grease, the subsequent release contaminating later samples. Systematic outgassing followed by air purging was employed to reduce this effect. Standard samples were used to check on mass discrimination and memory effects. (In particular, a radiogenic lead from Wilberforce, Ontario, Canada, University of Toronto Geophysics Dept., number 432, was found convenient owing to its low common lead content.)

(4) *Calculation of ages*

From the chemical analysis of a mineral specimen and the isotopic analysis of its lead, the isotopic ratios Pb^{206}/U^{238}, Pb^{207}/U^{235}, Pb^{207}/Pb^{206} and Pb^{208}/Th^{232} were calculated, assuming a present day isotopic composition for uranium of $U^{238}/U^{235} = 137{\cdot}7 \pm 0{\cdot}5$ atoms/atom (Giletti and Kulp, 1954).

Before calculating these ratios the non-radiogenic components of the lead isotope abundances were subtracted from them. These were calculated from the observed Pb^{204} abundance, or from the Pb^{208} abundance for minerals containing little thorium.

The first, second and fourth isotopic ratios could then be used to calculate the age t by use of the relation

$$t = \frac{1}{\lambda} \ln (R + 1)$$

where R is the ratio and λ the appropriate decay constant. The Pb^{207}/Pb^{206} ratio gives an age t such that

$$R\,(207/206) = \frac{U^{235}\{\exp(\lambda_{235}\, t) - 1\}}{U^{238}\{\exp(\lambda_{238}\, t) - 1\}}$$

Since this equation is not expressible explicitly in t, it is customarily solved by reference to graphs or nomographs, cf. Kulp *et al.* (1954). However, for this work a table (Table 3) giving the age to the nearest million years for all Pb^{207}/Pb^{206} ratios to four decimal places up to 0·3000 (corresponding to an age of 3526×10^6 years) was drawn up, and subsequently similar tables (Tables 1, 2 and 4), giving the ages corresponding to the other three isotopic ratios, were also contsructed. Analytical data used to calculate these ages, and the constants used in all calculations, are collected in Table 5.

(5) *Probable error of ages*

The ages calculated can be in error for various reasons, which can be summarized as: (a) mass spectrometric error; (b) error in chemical analysis; (c) error in the value of the decay constants used; (d) error in the isotopic composition assumed for the uranium; (e) error in the assumed isotopic composition of common lead used for correction; (f) a departure of the geophysical history of the specimen from the ideal (e.g. leaching, radon loss).

It is difficult to make an accurate estimate of all of these. The first two should be small compared with the others (although as noted previously an error of a few per cent, in this particular case, might have resulted from memory effects due to adsorption in the sample reservoir).

The two chief decay constants used, λ_{238} and λ_{235}, have probable errors (Table 5) of less than 0·2 per cent, and 2·2 per cent, respectively, and will produce similar probable errors in the Pb^{206}/U^{238} and Pb^{207}/U^{235} ages.

A probable error of 0·4 per cent in the U^{238}/U^{235} ratio for present day uranium will be manifested mainly as a similar error in the amount of U^{235} calculated from the chemical analysis for total uranium, and this in turn will cause an additional error in the Pb^{207}/U^{235} age of the same order of magnitude.

Table 1. Table of ages (millions of years) with atom ratio Pb^{206}/U^{238} as argument ($\lambda_{238} = 1{\cdot}541 \times 10^{-10}$/year)

	0	1	2	3	4	5	6	7	8	9	1 2 3	4 5 6	7 8 9
0·0	0	65	128	192	255	317	378	439	499	559	6 13 19 6 12 18	25 32 38 24 30 36	44 50 57 42 48 54
0·1	619	677	735	793	850	907	963	1019	1074	1129	6 12 17 6 11 17	23 29 35 22 28 33	40 46 52 39 44 50
0·2	1183	1237	1290	1343	1396	1448	1500	1551	1602	1652	5 11 16 5 10 15	21 27 32 20 26 31	37 42 48 36 41 46
0·3	1703	1752	1802	1851	1899	1947	1995	2043	2090	2137	5 10 15 5 9 14	20 24 29 19 23 28	34 39 44 33 38 42
0·4	2183	2230	2276	2321	2366	2411	2456	2500	2544	2588	5 9 14 4 9 13	18 23 28 18 22 26	32 37 41 31 35 40
0·5	2631	2674	2717	2760	2802	2844	2886	2927	2968	3009	4 8 13	17 21 25	29 34 38
0·6	3050	3090	3131	3171	3210	3250	3289	3328	3367	3405	4 8 12	16 20 23	27 31 35
0·7	3443	3481	3519								4 8 11	15 19 23	27 30 34

The Pb^{207}/Pb^{206} age is rather more sensitive to errors in decay constants and uranium isotopic composition, and Kulp *et al.* (1954) have calculated that for a mineral with a measured 206/207 age of 1000 million years the probable error is 10 per cent.

The fifth error, the possible error in the assumed isotopic composition of the common lead contamination, results from the observed variations in the composition of common (non-radiogenic) lead, which as listed by Collins *et al.* (1953) are:

$$Pb^{206}/Pb^{204} = 14\text{–}19$$

$$Pb^{207}/Pb^{204} = 14{\cdot}9\text{–}15{\cdot}9$$

$$Pb^{208}/Pb^{204} = 34{\cdot}5\text{–}40$$

An uncertainty therefore exists in the values of the non-radiogenic Pb^{206} and Pb^{207} components calculated from the observed Pb^{204} or Pb^{208} occurrence, with a consequent uncertainty in the calculation of the radiogenic remainders. This can be quite large when a considerable amount of common lead is present.

It is not possible to estimate quantitatively errors of the sixth type, although a qualitative idea may be obtained from the nature of the mineral deposit. The two principal effects are believed to be leaching of uranium, Phair and Levine (1952), and radon loss, Gletti and Kulp (1954). Uranium leaching will increase the apparent 206/238 age, increase the 207/235 age somewhat less, and only very slightly increase the 207/206 age, giving the age pattern (206/238) > (207/235) > (207/206), the last being the most reliable. Radon loss will decrease the 206/238 age, leave the 207/235 age unchanged, and greatly increase the 207/206 age, giving the age pattern (207/206) > (207/235) > (206/238), the 207/235 age being the most reliable. Gletti and Kulp have shown that the error due to radon loss can be less than 0·1 per cent for samarskites, between 0·1 per cent and 10 per cent

for uraninites and pitchblendes, and 20 per cent or more for carnotites and similar secondary minerals.

Errors of the fifth and sixth type are probably the most important.

In the following results the errors are calculated that would result from a maximum possible error in the assumed composition of the common lead. No other errors are estimated, and indeed the discrepancies between the three ages are themselves the best measure of the other effects.

Table 2. Table of ages (millions of years) with atom ratio Pb^{207}/U^{235} as argument ($\lambda_{235} = 9{\cdot}722 \times 10^{-10}$/year)

	0	1	2	3	4	5	6	7	8	9	1 2 3	4 5 6	7 8 9
0·0	0	10	20	30	40	50	60	70	79	89	1 2 3	4 5 6	7 8 9
0·1	98	107	117	126	135	144	153	161	170	179	1 2 3	4 4 5	6 7 8
0·2	187	196	205	213	221	230	238	246	254	262	1 2 2	3 4 5	6 7 7
0·3	270	278	286	293	301	309	316	324	331	339	1 2 2	3 4 5	5 6 7
0·4	346	353	361	368	375	382	389	396	403	410	1 1 2	3 4 4	5 6 6
0·5	417	424	431	437	444	451	457	464	471	477	1 1 2	3 3 4	5 5 6
0·6	483	490	496	503	509	515	521	527	534	540	1 1 2	2 3 4	4 5 6
0·7	546	552	558	564	570	576	581	587	593	599	1 1 2	2 3 4	4 5 5
0·8	605	610	616	622	627	633	638	644	649	655	1 1 2	2 3 3	4 4 5
0·9	660	666	671	676	682	687	692	697	703	708	1 1 2	2 3 3	4 4 5
1·0	713	718	723	728	733	738	743	748	753	758	1 1 2	2 3 3	4 4 5
1·1	763	768	773	778	783	787	792	797	802	806	0 1 1	2 2 3	3 4 4
1·2	811	816	820	825	830	834	839	843	848	852	0 1 1	2 2 3	3 4 4
1·3	857	861	866	870	874	879	883	888	892	896	0 1 1	2 2 3	3 4 4
1·4	901	905	909	913	918	922	926	930	934	938	0 1 1	2 2 3	3 3 4
1·5	942	947	951	955	959	963	967	971	975	979	0 1 1	2 2 2	3 3 4
1·6	983	987	991	994	998	1002	1006	1010	1014	1018	0 1 1	2 2 2	3 3 4
1·7	1022	1025	1029	1033	1037	1040	1044	1048	1052	1055	0 1 1	1 2 2	3 3 3
1·8	1059	1063	1066	1070	1073	1077	1081	1084	1088	1091	0 1 1	1 2 2	3 3 3
1·9	1095	1099	1102	1106	1109	1113	1116	1120	1123	1127	0 1 1	1 2 2	2 2 3
2	1130	1164	1196	1228	1259	1289	1318	1346	1373	1400	3 7 10 3 6 9 3 5 8	13 17 20 12 15 18 11 14 16	23 26 30 21 24 27 19 22 24
3	1426	1451	1476	1500	1524	1547	1570	1592	1613	1635	2 5 7 2 4 6	10 12 14 8 10 13	17 19 22 15 17 19
4	1655	1676	1696	1715	1735	1754	1772	1790	1808	1826	2 4 6	8 10 11	13 15 17
5	1843	1860	1877	1893	1909	1925	1941	1957	1972	1987	1 3 5	6 8 10	11 13 14
6	2002	2016	2031	2045	2059	2073	2086	2100	2113	2126	1 3 4	6 7 8	10 11 13
7	2139	2152	2164	2177	2189	2201	2213	2225	2237	2249	1 2 4	5 6 7	8 10 11
8	2260	2271	2283	2294	2305	2316	2326	2337	2348	2358	1 2 3	4 5 6	8 9 10
9	2368	2379	2389	2399	2409	2419	2428	2438	2448	2457	1 2 3	4 5 6	7 8 9
10 × 1	2466	2556	2638	2715	2785	2852	2914	2973	3029	3081	9 18 27 8 16 24 7 14 21 6 12 18 5 11 16	36 45 54 32 40 48 27 34 41 24 30 36 21 26 32	63 72 81 56 64 72 48 55 62 42 48 54 37 42 48
10 × 2	3132	3179	3225	3269	3311	3351	3390	3427	3464	3498	4 9 13 4 8 11 3 7 10	18 22 27 15 19 23 14 17 20	31 36 40 27 30 34 24 27 31

Table 3. Table of ages (in millions of years) with atom ratio Pb^{207}/Pb^{206} as argument ($\lambda_{238} = 1{\cdot}541 \times 10^{-10}$/year; $\lambda_{235} = 9{\cdot}722 \times 10^{-10}$/year; $U^{238}/U^{235} = 137{\cdot}7$ atoms/atom)

	0	1	2	3	4	5	6	7	8	9	1 2 3	4 5 6	7 8 9
0·04							10	62			5 10 15	21 26 31	36 41 46
									113	162	5 10 14	19 24 29	34 38 43
	209	256	301	345							4 9 13	18 22 27	31 36 40
0·05					388	429	470				4 8 12	16 20 24	28 32 36
								510	548	586	4 8 11	15 19 23	27 30 34
	623	659									4 7 11	14 18 21	25 28 32
0·06			694	729	763	796					3 7 10	13 17 20	23 27 30
							828	860	891	922	3 6 9	12 15 19	22 25 28
0·07	952	981	1010	1038							3 6 9	11 14 17	20 23 26
					1066	1094	1121	1147	1173	1199	3 5 8	11 13 16	18 21 24
0·08	1224	1249	1273	1297	1320	1344	1366	1389	1411	1433	2 5 7	9 12 14	16 18 21
0·09	1455	1477	1498	1518	1539	1559	1579	1599	1618	1637	2 4 6	8 10 12	14 16 18
0·10	1656	1675	1693	1712	1730	1748	1765	1783	1800	1817	2 4 5	7 9 11	13 14 16
0·11	1834	1850	1867	1883	1899	1915	1931	1947	1962	1977	2 3 5	6 8 10	11 13 14
0·12	1993	2008	2022	2037	2052	2066	2080	2095	2109	2122	1 3 4	6 7 9	10 12 13
0·13	2136	2150	2163	2177	2190	2203	2216	2229	2242	2254	1 3 4	5 6 8	9 10 12
0·14	2267	2279	2292	2304	2316	2328	2340	2352	2364	2376	1 2 4	5 6 7	8 10 11
0·15	2387	2399	2410	2421	2433	2444	2455	2466	2477	2487	1 2 3	4 6 7	8 9 10
0·16	2498	2509	2520	2530	2540	2551	2561	2571	2581	2592	1 2 3	4 5 6	7 8 9
0·17	2602	2612	2621	2631	2641	2651	2660	2670	2679	2689	1 2 3	4 5 6	7 8 9
0·18	2698	2707	2717	2726	2735	2744	2753	2762	2771	2780	1 2 3	4 5 5	6 7 8
0·19	2789	2797	2806	2815	2823	2832	2840	2849	2857	2865	1 2 3	3 4 5	6 7 8
0·20	2874	2882	2890	2898	2906	2914	2922	2930	2938	2946	1 2 2	3 4 5	6 6 7
0·21	2954	2962	2970	2977	2985	2993	3000	3008	3015	3023	1 2 2	3 4 5	5 6 7
0·22	3030	3038	3045	3052	3060	3067	3074	3081	3088	3095	1 1 2	3 4 4	5 6 7
0·23	3102	3109	3116	3123	3130	3137	3144	3151	3158	3164	1 1 2	3 3 4	5 5 6
0·24	3171	3178	3185	3191	3198	3205	3211	3218	3224	3230	1 1 2	3 3 4	5 5 6
0·25	3237	3243	3250	3256	3262	3269	3275	3281	3287	3293	1 1 2	3 3 4	4 5 6
0·26	3300	3306	3312	3318	3324	3330	3336	3342	3348	3354	1 1 2	2 3 4	4 5 5
0·27	3360	3366	3371	3377	3383	3389	3395	3400	3406	3412	1 1 2	2 3 3	4 5 5
0·28	3417	3423	3429	3434	3440	3445	3451	3456	3462	3467	1 1 2	2 3 3	4 4 5
0·29	3473	3478	3484	3489	3494	3500	3505	3510	3516	3521	1 1 2	2 3 3	4 4 5
0·30	3526												

Table 4. Table of ages (millions of years) with atom ratio Pb^{208}/Th^{232} as argument ($\lambda_{232} = 4{\cdot}987 \times 10^{-11}$/year)

	0	1	2	3	4	5	6	7	8	9	1 2 3	4 5 6	7 8 9
0·0	0	200	397								20 40 59	79 99 119	139 158 178
				593	786	978	1168				19 38 57	76 96 115	134 153 172
								1357	1543	1728	18 37 55	74 92 111	129 148 166
	1911	2093	2273								18 36 54	72 90 108	126 144 162
0·1				2451	2628	2803					17 35 52	70 87 105	122 140 157
							2976	3148	3319	3488	17 34 51	68 85 102	119 136 153
0·2	3656												

Table 5. Values of decay constants and abundances employed in all calculations

U^{238}	$t_{1/2} = 4{\cdot}498 \times 10^9$ years (Clark *et al.*, 1944; Keinberger, 1949)
	$\lambda = 1{\cdot}541 \times 10^{-10}$/year
U^{235}	$t_{1/2} = 7{\cdot}13 \pm 0{\cdot}16 \times 10^8$ years (Fleming *et al.*, 1952)
	$\lambda = 9{\cdot}722 \times 10^{-10}$/year
Th^{232}	$t_{1/2} = 1{\cdot}39 \pm 0{\cdot}02 \times 10^{10}$ years (Kovarik *et al.*, 1938)
	$\lambda = 4{\cdot}987 \times 10^{-11}$/year
U^{238}/U^{235}	Abundance = $137{\cdot}7 \pm 0{\cdot}5$ atoms/atom (cited by Kulp *et al.*, 1954, p. 349)
	$= 139{\cdot}46 \pm 0{\cdot}5$ g/g
	Percentage composition of uranium by weight is
	$U^{235} = 0{\cdot}7119$ g %
	$U^{238} = 99{\cdot}29$ g %
K^{40}	$t_{1/2} = 1{\cdot}31 \times 10^9$ years
	$\lambda_e = 0{\cdot}583 \times 10^{-10}$/year ; $\lambda_\beta = 4{\cdot}72 \times 10^{-10}$/year
Rb^{87}	$t_{1/2} = 50 \times 10^9$ years
	$\lambda_\beta = 1{\cdot}39 \times 10^{-11}$/year

III. Results and Discussion

The ages computed from the mass spectra and quantitative chemical analyses are collected in Table 7.

(1) *The South Australian specimens*

The two main uranium deposits in South Australia occur at Radium Hill and Crocker's Well (Fig. 1). Radium Hill lies at the western edge of the Archaean Willyama Complex, which extends east into New South Wales and includes the rich ore deposits at Broken Hill. Crocker's Well, 50 miles to the north west of Radium Hill, lies within the general region of the later Proterozoic Adelaide system, but is part of an extensive area of Archaean porphyritic granitic rocks which outcrop as prominent hills, overlain unconformably by the Adelaide system, and separated by broad areas of alluvial flats.

The uranium mineralization at Crocker's Well is mainly thorian brannerite ("absite"), which occurs as fracture filling and replacement in a brecciated shear zone in an adamellite, believed to be a late stage local intrusive into the Archaean sequence. In addition, davidite has been found in pegmatites and primary quartz veins in the main granitic rocks.

The ages for the absite and davidite specimens are in complete agreement with this geological picture, dating the absite mineralization as Upper Proterozoic and the pegmatite as Archaean. Kulp, of the University of Columbia, has also dated a specimen of Crocker's Well absite on behalf of the S.A. Department of Mines (1954) and obtained the four lead ages of 520, 600, 915 and 585 million years respectively, which are in reasonable concord with our absite ages.

One might expect some radon loss in a mineral such as this absite which has been situated in a porous shear zone since its formation in Upper Proterozoic times. The high 207/206 ages obtained in both measurements on the mineral indicate that this is the case. The generally greater ages reported here could be due to some leaching of uranium, which tends to increase the apparent ages. The

Table 6. Analytical data

Mineral and location*	Chemical composition (%)			Isotopic composition							Common lead (%)
	U	Th	Pb	U^{235}	U^{238}	Th^{232}	Pb^{204}	Pb^{206}	Pb^{207}	Pb^{208}	
Uraninite. Brocks Creek, N.T.	2·76	0·729	0·482	6·15	846	230·9	1·23	100	24·26	45·92	51
Uraninite. Adelaide River, N.T.	4·20	0·0172	1·630	2·464	339·4	1·436	0·87	100	19·0	33·0	41
Tanteuxenite. Woodstock, W.A.	3·41	2·59	1·61	2·083	286·9	225·0	0·15	100	20·85	36·11	6·3
Samarskite. Hart's Range, C.A.	1·05	1·49	0·28	4·685	645·5	945·8	1·65	100	30·15	67·59	59
Davidite. Radium Hill, S.A.	2·300	0·1098	0·3761	5·126	706·2	34·83	0·40	100	13·52	20·15	26·5
Uraninite. Sleisbeck, N.T.	40·13	0·001	2·327	13·97	1923	0·04	0·407	100	12·78	16·37	24
Uraninite. Myponga, S.A.	50·8	0·97	3·81	8·99	1238	24·4	0·03	100	6·35	1·63	1·8
Thorian Brannerite. Crocker's Well, S.A.	21·33	8·196	2·228	7·321	1009	400·4	0·036	100	7·33	15·04	2·1
Davidite. Crocker's Well, S.A.	1·942	0·660	0·6811	2·409	331·7	116·5	0·350	100	15·04	19·67	17
Uraninite 1. El Sharana, N.T.	52·67	0·3005	5·001	7·342	1011	5·957	0·056	100	8·85	2·70	4·3
Uraninite 2. El Sharana, N.T.	67·92	0·1116	3·923	11·71	1613	2·74	0·028	100	6·92	1·38	2·6
Uraninite 1. Palette Lode, N.T.	64·6	0·336	6·60	6·533	899·6	4·833	0·017	100	6·41	0·46	0·48
Uraninite 2. Palette Lode, N.T.	74·7	0·50	7·12	7·30	1005	6·97	0·076	100	7·68	3·68	5·9
Uraninite 3. Palette Lode, N.T.	75·9	0·48	5·69	9·00	1239	8·10	0·034	100	6·33	1·67	2·6
Uraninite 4. Palette Lode, N.T.	73·6	0·12	5·63	8·83	1216	2·05	0·037	100	6·35	1·824	3·1
Uraninite 5. Palette Lode, N.T.	74·7	0·10	5·37	9·47	1304	1·80	0·036	100	7·26	1·73	2·9
Galena.† Baker's Prospect, N.S.W.	—	—	—	—	—	—	1·000	18·04 (x)	15·93	38·32 (z)	—

* C.A.: Central Australia.
N.S.W.: New South Wales.
N.T.: Northern Territory.
S.A.: South Australia.
W.A.: Western Australia.

† Galena ages were calculated from the relations:

$$t_{206} = 6{\cdot}51 \times 10^9 \ln (1 + (18{\cdot}80 - x)/11{\cdot}02) \text{ years}$$
$$t_{208} = 20{\cdot}04 \times 10^9 \ln (1 + (39{\cdot}10 - z)/40{\cdot}8) \text{ years}$$

(Wilson, 1955).

better internal consistency of these figures compared with KULP's may be due to a combination of uranium loss and radon loss.

Since radon loss leaves the 207/206 age unchanged, and leaching of uranium increases it, KULP's estimate of 580 ± 30 million years as a "best age" for the absite deposit is probably reasonable. A specimen of biotite hand picked from the thorian brannerite was found to have an age, determined by potassium–argon measurements, of 520 million years which is further evidence in favour of KULP's estimate.

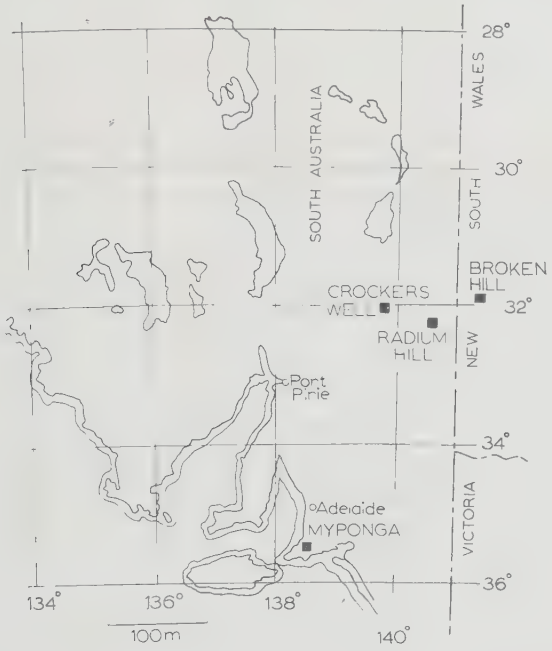

Fig. 1. Location of South Australian specimens.

As far as is known no previous age determinations have been made on the Crocker's Well country rock, the Archaean granitoid in which the davidite occurs, but the value obtained here for our specimen is reasonably close to that determined by COLLINS *et al.* (1953), (207/206 age only, 1510 million years) for davidite from Radium Hill, confirming that the Archaean rocks of Crocker's Well are part of the Willyama Complex to which Radium Hill and Broken Hill belong. Other age determinations on the Willyama Complex include figures of 1730 million years for the 207/206 age of the Radium Hill uranium mineralization, and 1680 million years for the common lead galena mineralization at Broken Hill (WILSON, 1951).

The ages calculated for the Radium Hill davidite, and the Broken Hill galena (included in this section because of the close relationship between the New South Wales Broken Hill deposits and the South Australian deposits) do not fit in so easily with accepted geological interpretations, and other measurements. The fact that the 207/206 age of the Radium Hill davidite is lower than the other two ages suggests uranium leaching, with little or no radon or lead losses, in which case this age should be the most reliable of the three, and if in error should be too high. This suggests that the age is not greater than 690 million years. This is surprisingly

low compared with the two determinations of 1510 and 1730 million years respectively for Radium Hill by Collins and Wilson, quoted above.

There are reputed to have been several periods of mineralization at Radium Hill (Sprigg, 1951, p.7) with uranium introduction, as shear replacements and in-fillings along faults in the granitized metasediments, being the last. This result, if it can be confirmed by further work on Radium Hill minerals, would indicate at least two periods of uranium mineralization, Archaean and Proterozoic.

The specimen of galena from Baker's Prospect in the Thackaringa area of the Broken Hill district, New South Wales, is a common lead ore. Its age is calculated by use of the formulae given by Russell *et al.* (1954), as revised by Wilson (1955), and the probable error implicit in these formulae is large. Even so, the values seem to be significantly lower than the figures quoted above obtained by Wilson on Broken Hill ores.

Recently Wilson (1955) has reported common lead ages made on galenas from Broken Hill (his specimen numbers 721, 725 and 723) with the values 490 ± 250, 240 ± 275 and 210 ± 280 million years respectively. He does not state whether these ores were of the Thackaringa type or the Broken Hill type, but the results suggest that they were of the same type as our specimen from Baker's Prospect. It would seem that the existence of two widely separated periods of lead mineralization at Broken Hill has been established, the first (the Broken Hill ore type) about 1500 million years ago, and the second (probably the Thackaringa ore type) considerably younger. Russell *et al.* (1957) have concluded that the Thackaringa ore is anomalous owing to intermixing of radiogenic and ordinary leads and set a maximum age for this ore type of 1020 ± 150 million years.

The Myponga uraninite specimen is from the lode outcrop which occurs in Archaean gneisses at Myponga 30 miles south of Adelaide. The mineral is reported to be found in brown, richly biotitic rocks as lumps of up to 5 cm in size, singly, or in clusters surrounded by smaller fragments dispersed through its alteration products, gummite and meta-autunite. The softness and ease of etching suggest that this is an ancient deposit.

The sample received from the South Australian Department of Mines was a heavy mineral concentrate from which as much gummite, etc., as possible had been removed.

The ages obtained have the characteristic radon-loss pattern making the 207/235 age of 520 million years the most reliable. This would make the lode Upper Proterozoic or Cambrian, much younger than expected. Further evidence in the form of potassium argon ages on two biotite samples from this region suggest a slightly greater age than that given by the 207/235 data. One sample in close association with the uraninite was dated at 650 million years while biotite from a pegmatite dyke adjacent to the lode appeared to be some 390 million years old. Both ages were computed by assuming complete argon retention. Further investigations on samples from this area appear to be necessary.

(2) *The Northern Territory specimens* (*Katherine–Darwin Region*)

Uranium mineralization has been discovered in the Northern Territory at Rum Jungle, Adelaide River, Brock's Creek (the Fleur de Lys mine), Sleisbeck,

El Sharana and the Palette Lode (Fig. 2). The samples dated include uraninite specimens from each of these fields except the first.

The geological history of the Katherine–Darwin region in which all of these deposits lie, according to NOAKES (1949), opened with the deposition, in Lower Proterozoic time, of the marine sediments which were later folded and metamorphosed by granitic intrusions to form the Brock's Creek Group. These slates,

Table 7. Australian U–Pb ages (millions of years)

Specimen	206/238	207/235	207/206	208/232
South Australia				
Davidite (Radium Hill)	787 ± 10	764 ± 35	691 ± 200	—
Thorian Brannerite (Crocker's Well)	610 ± 1	674 ± 3	895 ± 15	675 ± 5
Davidite (Crocker's Well)	1628 ± 10	1660 ± 25	1702 ± 60	1252 ± 150
Uraninite (Myponga)	502 ± 1	521 ± 2	609 ± 10	—
Galena (Baker's Prospect)	$t_{206} = 430 \pm 400$			
	$t_{208} = 308 \pm 680$			
Northern Territory				
Brock's Creek	576 ± 17	627 ± 80	816 ± 400	
Adelaide River	1450 ± 30	1110 ± 75	470 ± 250	
Sleisbeck	305 ± 3	370 ± 25	816 ± 150	
El Sharana 1	605 ± 1	743 ± 5	1196 ± 18	
El Sharana 2	388 ± 1	447 ± 2	766 ± 12	
Palette Lode 1	683	695	729 ± 2	
Palette Lode 2	612 ± 2	635 ± 7	719 ± 30	
Palette Lode 3	500 ± 1	507 ± 3	533 ± 20	
Palette Lode 4	509 ± 1	506 ± 3	494 ± 18	
Palette Lode 5	476 ± 1	542 ± 4	830 ± 20	
Central Australia				
Samarskite (Hart's Range)	683 ± 30	692 ± 120	729 ± 600	139 ± 100
Western Australia				
Tanteuxenite (Woodstock)	1900 ± 5	2360 ± 10	2790 ± 25	2590 ± 25

sandstones, conglomerates, quartzites, phyllites and schists constitute the basement rock of this region, which outcrops extensively. Later, the considerably eroded formation was submerged again and the Upper Proterozoic sediments of the Buldiva Quartzites were laid down. This was followed by isolated outbursts of vulcanism in early Cambrian times, and finally by the deposit of Lower Cambrian limestones and sandstones, since when there has been little change.

FISHER (personal communication) Chief Geologist of the Bureau of Mineral Resources, Canberra, has also stated that some of his geologists have long maintained that there are two periods of mineralization in the Northern Territory, the first thought to be directly associated with granitic intrusions of presumed Lower Proterozoic age and the second with a post-granite movement of Upper Proterozoic

age. The Adelaide River occurrence was considered to be associated with the granite, the Brock's Creek deposit was doubtful and the occurrences in the South Alligator region were supposed to be associated with the post-granite movement.

The age determinations on the Adelaide River uraninite places the mineralization in the Upper Archaean, although the discordance of the three ages makes further determinations desirable.

The results for the Brock's Creek uraninite are characteristic of radon loss, with the second age therefore the most reliable and possibly high. This would place the mineralization at the Fleur de Lys mine as Upper Proterozoic.

The South Alligator River region, as indicated by Fisher, is to be associated with the Upper Proterozoic post-granite movement and includes the Palette Lode and El Sharana deposit, which are within a few miles of one another. Newton (1955) who has extensively investigated the uranium occurrence at Sleisbeck, approximately 25 miles to the south-east, states that this is probably of similar origin to the South Alligator leases.

Fisher states that the host rock at the Palette Prospect is a sandstone considered to be of Upper Proterozoic age, noncomformably underlain by a Lower Proterozoic siltstone, both rocks being intersected by a fault. The exposure at this lode showed secondary mineralization in the siltstone, and uraninite and secondary minerals in the sandstone, adjacent to and spreading out from the fault. Other uranium orebodies in the South Alligator area were localized in favourable structures, faults and shears in the vicinity of the nonconformity; where the faults and shears transgressed the unconformity the mineralization commonly extended into the Upper Proterozoic. It seems that the uraniferous orebodies in this area were virtually confined to locations not far away from outcrops of Upper Proterozoic volcanic rock. Fisher has postulated that the lodes could be due either to crystallization from the instrusive magmatic phases themselves, or to mobilization of uranium, copper, etc., from the carbonaceous sediments by heat and vadose solutions derived from the intrusive phases, followed by subsequent precipitation in shears and faults.

The five Palette Lode specimens (Table 7) give results which indicate an age of close to 500 million years. Specimens 3 and 4 were collected from a small uraninite-rich face exposed at the side of an adit driven about 20 ft below the surface outcrop. They should therefore yield reliable ages and the results may be accepted as reasonably close to the true age. Specimen 2 was taken from the surface and had undergone a good deal of alteration, being completely surrounded by secondary minerals. It had probably undergone considerable leaching (of uranium) resulting in generally high ages, while radon loss had also occurred, judging from the characteristic order of the three ages.

Specimen 5, as supplied by the Bureau of Mineral Resources, Canberra, was prepared by separating small (up to 1 in.) masses of uraninite which were interspersed in a specimen of sandstone closer to the surface than 3 and 4. Such an occurrence would favour radon loss, and the order of the ages bears out this premise. Any uranium leaching has probably been smaller than for the surface specimen, with the result that the 206/238 age is still low.

Specimen 1 was submitted by Shepherd (Chief Geologist of United Uranium,

N.L.) who reported that it had been taken from a surface occurrence and was surrounded by haloes of weathered products. He believed it had suffered extensive leaching and weathering. This would explain the high ages, due to uranium leaching, and radon loss is again manifested in the age pattern.

The Palette mineralization should probably be dated as about 500 million years, in the Upper Proterozoic.

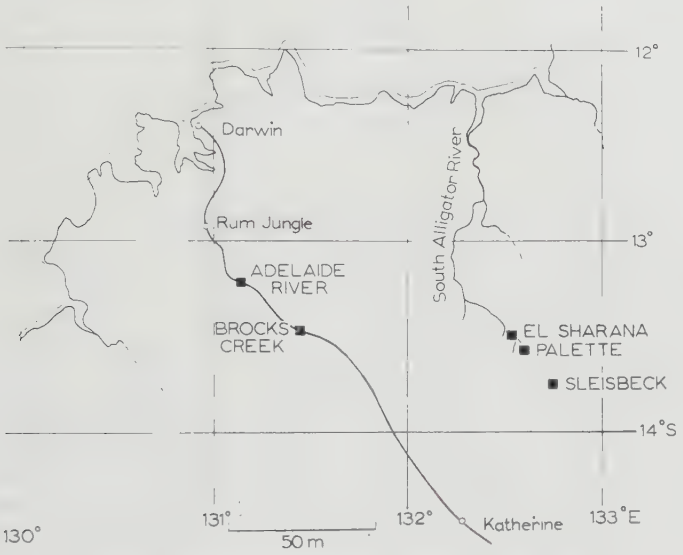

Fig. 2. Location of Northern Territory specimens.

The two El Sharana specimens are more difficult to interpret. The level at which sample 1 was taken was not known, although it has obviously undergone losses. Sample 2 is part of a drill core taken from the 55 ft level, and should be more reliable. Until specimens giving more internally consistent ages can be obtained, no definite age assessment of this area can be made, although it would seem likely that if it is not of the same age as the Palette lode, then it must be younger.

The single Sleisbeck specimen also needs augmenting, although here it seems even more likely that the age is less than that of the Palette Lode. The original assumption that the Sleisbeck and Palette lodes are of the same origin may be in error.

Newton (1955) reports that the Sleisbeck deposits occur as uranium micas and pitchblende, associated with carbonaceous schists, and occurring against the quartzite hills which outcrop the surrounding strongly eroded chloritic schists. The quartzite and schists form the Basement Rocks, and have been unconformably overlain by cover rocks of rudaceous, arenaceous and volcanic beds, of which only a few remnants which have escaped erosion remain at protected places on the prospect hills. Newton interprets this field evidence as showing that the mineralization is pre-cover rocks (pre-vulcanism?) in age, which certainly does not explain the possibly lower age obtained for this specimen.

(3) *Other specimens*

Hart's Range (Fig. 3) in Central Australia, the southern portion of the Northern Territory, lies at the north-eastern edge of the Arunta Block, in which the metamorphism and folding of the gneisses and schists is to an extent which suggests they are the oldest rocks in the Northern Territory, and of Archaeozoic age

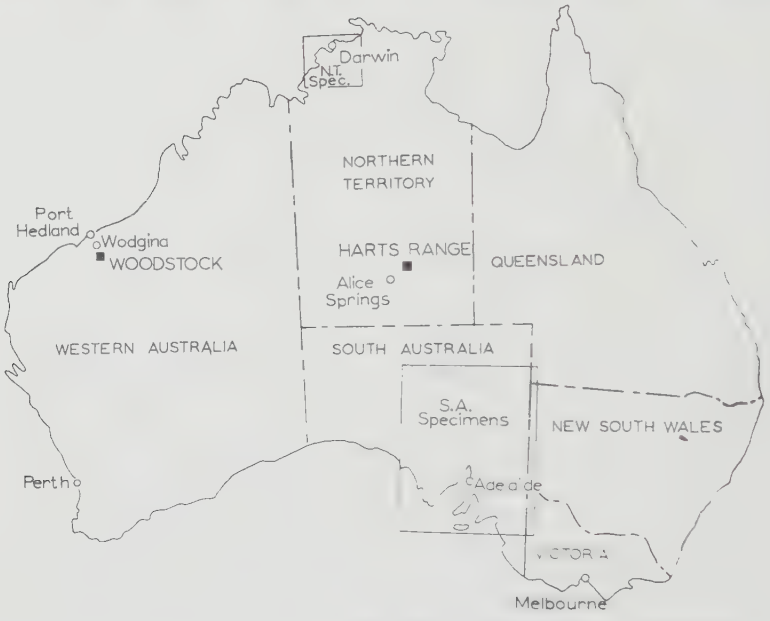

Fig. 3. Other specimens, and locality map for N.T. and S.A. specimens.

(Noakes, 1953). In the Range, muscovite and some radioactive minerals are found in pegmatites intruding the gneisses and crystalline schists. Most of the commercial mica has been won from pegmatites which intrude the two formations, the most productive dykes being those that transgress the foliation of the host rock. Noakes regards this mineralization also as probably Archaeozoic. Potassium–argon dates on muscovite and microcline minerals from these pegmatites have all yielded ages less than 600 million years so that even assuming extensive argon losses the mineralization is almost certainly Proterozoic.

Joklik (1953) describes a complex dome structure 20 miles in diameter at the eastern portion of the mica field, erosion of which has exposed a granite core regarded as the parent of the quartz–felspar–mica pegmatites.

The ages calculated for the Hart's Range samarskite, taken from one of these pegmatites, are Middle or Upper Proterozoic, which is not in agreement with Noakes' interpretation. The extremely low 208/232 age is apparently characteristic of thorium minerals, which tend to lose Pb^{208} preferentially, according to the work of Gledtisch and Qviller (1932) and of Tilton (1956). The "best" age, allowing for some apparent radon loss, is probably a little less than 700 million years.

The tanteuxenite, from Woodstock, W.A., is the oldest specimen measured. Woodstock, in the Pilbara mining province, lies 90 miles to the south of Port

Hedland. The specimen was taken from a pegmatite intruding the rocks of the Warrawoona System, generally accepted to be of early Archaeozoic age. The calculated ages agree with this interpretation.

Once again the radon-loss age-pattern is evident, but the value of the 208/232 age, the "thorium age," gives an overall pattern difficult to interpret, although Nier (Nier, 1939b; Nier *et al.*, 1941) has measured two samples with similar patterns (uraninite from Besner, Ont., and samarskite from Glastonbury, Conn.). The 207/235 age is independent of radon loss, and is increased by leaching (assuming that this affects uranium more than lead, as Phair and Levine (1952) have shown), and, if in error, will be too great. The thorium age under the same conditions would be too low, according to common observation. Yet in this case the thorium age is higher than the 207/235 age.

It is possible that for a thorium mineral such as samarskite the results of Phair and Levine are not valid, and predominant lead loss has occurred, thus lowering the 207/235 age. It has also been noted by Kulp *et al.* (1954) that where the uranium and thorium contents of a mineral are both high (as in this case), the tendency for a low thorium age seems to disappear, and this age takes its place with the others as a credible measure of the true age. The age of the tanteuxenite specimen, therefore, unless some further insight into the processes to which the mineral has been subjected can be obtained, must be stated as somewhere in the vicinity of 2400 to 2600 million years.

Muscovite and microcline from a pegmatite at Wodgina, about 35 miles north-west of Woodstock and geologically similar, have been dated by one of us (Jeffery, 1956) using rubidium–strontium and potassium–argon techniques. The ages, which have been recalculated using the most recent decay constants and branching ratio, are, for the two techniques, respectively 2930 and 2300 million years for the muscovite, and 2840 and 2100 for the microcline. Argon loss (with a resultant low potassium–argon age) has probably seriously affected the potassium–argon ages in these samples. There appears every likelihood that further studies in this area will indicate that its age lies between 2600 and 2800 million years as this period appears to have been one of intense igneous activity through the western half of Australia, judging from other measurements which have been made in this laboratory.

(4) *"Concordia" plot of Northern Territory specimens*

Recently Wetherill (1956) devised a new method for dealing with discordant uranium–lead ages, using a "D/P" diagram, in which the abscissa represents the Pb^{207}/U^{235} ratio of a specimen, and the ordinate represents the Pb^{206}/U^{238} ratio. Every point on the surface of the diagram is therefore associated with a particular 207/235 age, and a particular 206/238 age, and the points for which these two ages are equal lie along a curve referred to as "concordia". The two Pb/U ratios for any uranium mineral specimen can be plotted as a single point which will lie on concordia only if the mineral has suffered neither losses nor gains of any sort.

Wetherill has shown that if various minerals of the same age τ_0 have undergone varying amounts of uranium or lead leaching at some time τ_1, then the points corresponding to the present-day ratios of the various minerals will all lie

on the straight line joining the two points on "concordia" corresponding to the ages τ_0 and τ_1. The point plotted for each mineral will divide this line $\tau_1\tau_0$ in the ratio R = (Pb/U after leaching)/(Pb/U before leaching) so that for uranium loss, when R must be greater than unity, the point will divide $\tau_1\tau_0$ externally and lie on $\tau_1\tau_0$ produced.

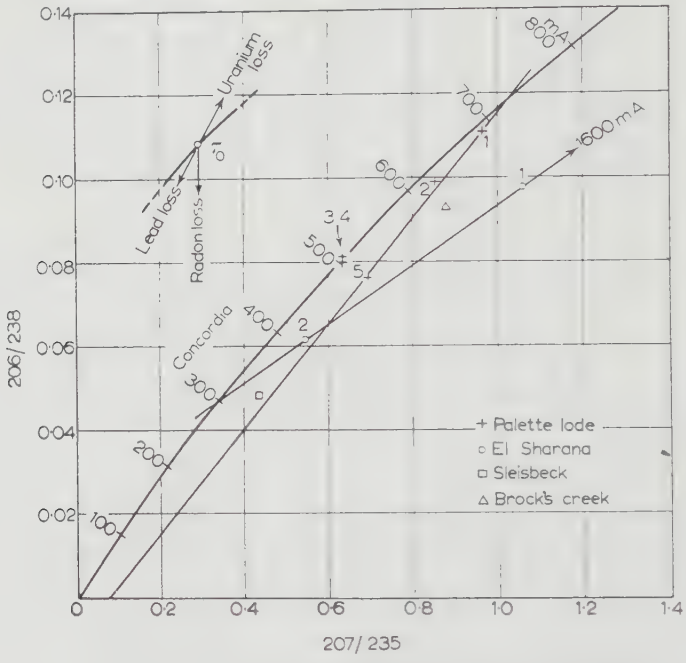

Fig. 4. Concordia plot of Northern Territory specimens.

Wetherill devised this method originally as a method of predicting the effect of a given geological history on the present day ratios of a mineral specimen, but the value of the method for working backwards from the measured ratios of a suite of uranium minerals, which might reasonably be supposed to be of the same age and to have undergone leaching at the same time, although to varying degrees, was immediately obvious. The ratios of such a suite, whose measured ages would be discordant as a result of this leaching, should, when plotted on the diagram, give a series of points lying in a straight line which cuts the curve concordia at two points corresponding respectively to the true age and the time at which the leaching occurred.

It should not be forgotten, however, that minerals that have undergone leaching are also likely to be in a physical form that would permit radon loss, and this, since it reduces the measured 206/238 ratio while not affecting the 207/235 ratio, will cause the points plotted on the diagram to move vertically downwards (Fig. 4). If all the specimens of a suite of minerals whose ratios are plotted have undergone the same radon loss, the points will still lie in a straight line, although this, having moved downwards, will now cut concordia at points which represent times greater than the true age and less than the age at which original leaching occurred.

If on the other hand they have undergone radon loss in amounts proportional to the individual degrees of leaching (either of uranium or of lead, but not both), points on the straight line will drop distances proportional to their distance from the point τ_0, the true age, at which the line intersects concordia. The line will therefore rotate about τ_0, and still indicate the age correctly, although the other point of intersection (supposedly indicating the time of leaching) will no longer be significant. The second possibility, that radon loss proportional to the extent of leaching has occurred, is by no means unlikely, since this also depends on the degree of porosity of a mineral.

The Northern Territory uraninites, that is, the Palette lode, El Sharana and Sleisbeck specimens, constitute a group of minerals which from field evidence appear likely to be of the same age. Consequently these were plotted on a concordia diagram, Fig. 4.

Of the five Palette specimens, three yield approximately collinear points, the line cutting concordia at a point corresponding to an age of about 730 million years. The indicated time of leaching is negative (though small) and could be regarded as an indication of recent leaching. However the other two Palette specimens 3 and 4 give points close to each other and on concordia (since the two ages of each are very nearly equal to one another), at the 500 million year mark. This is well removed from the line of the other three.

If the age of 730 million years is to be believed, it follows that all specimens have undergone lead leaching, but that specimen 1 has undergone the least. However this is refuted by field evidence as specimen 1 was surrounded by haloes of weathered products. Uraninite 2 also appeared to have been leached.

Specimens 3 and 4 showed no evidence of leaching, and since they were collected from an adit driven about 20 ft below the outcrop, they have probably suffered only small losses of metals or radon. The consistent ages they give, of about 500 million years, are therefore the most likely to be correct. The other three specimens, then, may be supposed to have undergone varying degrees of uranium leaching (which would shift them up and to the right of the 500 million years mark), plus radon loss to an almost equal extent for each, thus shifting them vertically downwards but leaving them still approximately in a straight line. The point of intersection of this line with concordia (730 million years) however, would have no significance.

The Sleisbeck specimen gives a point which also lies near the straight line of the three Palette specimens. Of the two El Sharana specimens, one lies near this line and the other is well below it. The line joining these two points gives an age of 1600 million years, with leaching occurring about 300 million years ago. However, it is not felt that any significance can be placed in these results owing to the likelihood once again of radon loss.

IV. Conclusion

Some of the age determinations that have been made have confirmed previous geological knowledge; others have been at variance.

Thirteen of the sixteen radioactive specimens dated have given age patterns

(207/206) > (207/235) > (206/238), which are characteristic either of radon loss or of lead loss, with radon loss the more probable.

Two periods of mineralization, Archaean and Upper Proterozoic have been confirmed at Crocker's Well, South Australia, in agreement with the geological interpretation of field evidence.

An unexpectedly young specimen, apparently Proterozoic, has been dated from Radium Hill, South Australia, where the mineralization has all been reported to be Archaean. Further determinations here will be necessary before this problem can be resolved.

The common lead age of a galena from the Thackaringa Area of Broken Hill has yielded an age (Cambrian or later) at variance with present geological opinion and some other worker's results (Archaean). However, recent results by Wilson in Toronto seem to support the Cambrian age and suggest two periods of lead mineralization at Broken Hill.

A young age (Upper Proterozoic) has also been obtained for a specimen from Myponga, South Australia. Potassium–argon ages from this area also agree with this result.

The suspected existence of two periods of mineralization in the Northern Territory has been confirmed, the first Late Archaean (Adelaide River), the second Upper Proterozoic (Brock's Creek, El Sharana, Palette Lode, Sleisbeck).

The mineralization at Hart's Range has been dated as Middle or Upper Proterozoic, although it is generally accepted that this also is Archaean. Potassium–argon determinations support the younger age.

Mineralization at Woodstock, in the Pilbara region, has been dated as early Archaean, as expected.

It appears that radon loss (which has affected most minerals that have undergone leaching) renders the "concordia" method of resolving discordant ages unsatisfactory.

Acknowledgements—For providing the mineral specimens on which these age determinations were made, the authors would like to thank the Director of the South Australian Department of Mines, the Director of the Bureau of Mineral Resources, Melbourne, the Acting Senior Geologist of the Geological Survey, New South Wales, the Chief Geologist of United Uranium N.L., Darwin, the Senior Geologist of the North Australian Uranium Corporation N.L., Darwin, the Mine Manager, Uranium Development and Prospecting Mine, Adelaide River, the Director of the Government Chemical Laboratories, Perth and Mr. D. E. Gardner, of the Bureau of Mineral Resources, Canberra. The authors are grateful to Dr. N. H. Fisher the Chief Geologist of the Bureau of Mineral Resources, Canberra, for providing the extracted lead and chemical analyses of some of the Northern Territory specimens.

They also acknowledge their indebtedness to Professor C. J. B. Clews for his direction and encouragement, to Mr. K. Malinowski for carrying out the chemical analyses and extractions of lead from mineral specimens, to Dr. W. Compston for his assistance generally and guidance in geological matters, and to Mr. D. D. B. McNaughton for help with the construction of some of the electronic equipment. Thanks are also due to Mr. D. W. Everson and the staff of the Physics Department Workshop for the engineering work necessary in assembling the mass spectrometer.

The research was made possible by a generous gift from the Carnegie Institution of Washington and has been supported by the Research Grants Committee of the University of Western Australia.

References

Clark F. L., Spencer Palmer H. J. and Woodward R. N. (1944) *British Atomic Energy Projects Reports* BR-521, 522.

Collins C. B., Russell R. D. and Farquhar R. M. (1953) *Canad. J. Phys.* **31,** 402.

Dibeler V. H. and Mohler F. L. (1951) *J. Res. Nat. Bur. Stand.* **47,** 337.

Ducheylard G., Lazard B. and Roth E. (1953) *J. Chim. Phys.* **50,** 497.

Fleming E. H., Jr., Ghiorso A. and Cunningham B. B. (1952) *Phys. Rev.* **88,** 642.

Giletti B. J. and Kulp J. L. (1954) *Amer. Min.* Cited by Kulp *et al.* (1954).

Gleditsch E. and Qviller B. (1932) *Phil. Mag.* **14,** 233.

Greenhalgh D. and Jeffery P. M. (1955) *J. Sci. Instrum.* **32,** 36.

Jeffery P. M. (1956) *Geochim. et Cosmochim. Acta* **10,** 191.

Joklik G. F. (1953) *The Geology of Australian Ore Deposits* p. 336. Australasian Institute of Mining and Metallurgy, Melbourne.

Keinberger C. A. (1949) *Phys. Rev.* **76,** 1561.

Kovarik A. F. and Adams N. E., Jr., (1938) *Phys. Rev.* **54,** 413.

Kulp J. L., Bate G. L. and Broecker W. S. (1954) *Amer. J. Sci.* **252,** 345.

Newton H. J. (1955) *The Occurrence of Uranium Ore at Sleisbeck, N.T.* Proc. 176, Australasian Institute of Mining and Metallurgy, Melbourne.

Nier A. O. (1939) *Phys. Rev.* **55,** 153.

Nier A. O., Thompson R. W. and Murphy B. F. (1941) *Phys. Rev.* **60,** 112.

Nier A. O. (1947) *Rev. Sci. Instrum.* **18,** 398.

Noakes L. C. (1949) *A Geological Reconnaissance of the Katherine Darwin Region. Bull. Bur. Min. Resour. Aust.* No. 16.

Noakes L. C. (1953) *The Geology of Australian Ore Deposits* p. 284. Australasian Institute of Mining and Metallurgy, Melbourne.

Phair G. and Levine H. (1952) *U.S. Geol. Surv., Prelim. Rep.* Cited by Kulp *et al.* (1954).

Russell R. D., Farquhar R. M., Cumming G. L. and Wilson J. T. (1954) *Trans. Amer. Geophys. Un.* **35,** 301.

Russell R. D., Farquhar R. M. and Hawley J. E. (1957) *Trans. Amer. Geophys. Un.* **38,** 557.

Sprigg R. C. (1951) Uranium Deposits in South Australia. *Bull. Geol. Surv. S. Aust.* No. 30.

Tilton G. R. (1956) *Trans. Amer. Geophys. Un.* **37,** 224.

Wetherill G. W. (1956) *Trans. Amer. Geophys. Un.* **37,** 320.

Wilson J. T. (1951) Uranium Deposits in South Australia. *Bull. Geol. Surv. S. Aust.* No. 30, 12.

Wilson J. T. (1955) *Common Lead Isotope Abundances* Pamphlet, University of Toronto.

Geochimica et Cosmochimica Acta, 1959, Vol. 16, pp. 58 to 78. Pergamon Press Ltd. Printed in Northern Ireland

Trace elements in minerals from rocks of the S. Californian batholith

N. Sen,* S. R. Nockolds and R. Allen
Dept. of Mineralogy and Petrology, The University of Cambridge, England

(*Received* 31 *July* 1958)

The rocks of the S. Californian batholith have been described in detail by Larsen (1948), and trace element determinations made on some of them by Nockolds and Allen (1953). A number of minerals from these rocks have been examined and chemically analysed for the major elements by Larsen and Draisin (1950).

Professor Larsen kindly provided us with a set of analysed rocks from the batholith and it is from these that the minerals used in the present study were separated. It must be noted, therefore, that we did not have available the actual sample of any mineral analysed by Larsen and Draisin, but our material has been separated in each case from the same rock. The rock-names and specimen numbers used throughout are those used by Larsen. In addition we give first the number of the specimen in the rock collection of the Department of Mineralogy and Petrology, Cambridge.

I. The Plagioclase Felspars

Trace element determinations on a number of plagioclase felspars will be found in Table 1, together with their anorthite contents, as given by Larsen, and the major element composition determined by chemical analysis for nos. 1, 5 and 13. The major element compositions of the remainder have been obtained by calculation from the known anorthite content and are given in brackets. The position of the rock from which the plagioclase felspar has been separated is also given in terms of the modified Larsen function (Nockolds and Allen, 1953).

Most of the common trace elements are below their limits of sensitivity and the only ones found in detectable amounts are Ga, Sr, Ba, V†, Li and Cr (in one instance). The values of these for nos. 6–14 are given in brackets because these determinations were made on mixtures of plagioclase and quartz and the values adjusted to allow for the quartz content. This obviously introduces some possibility of error but the values are believed to be of the right order. Nos. 1–5 come from accumulative rocks, nos. 6–14 from rocks whose elements fall on more or less smooth curves believed to represent the liquid line of descent.

The early accumulative felspars are richer in anorthite and are correspondingly richer in Sr and poorer in Ba, than the later plagioclase felspars. Ga tends to be a little higher here than in the later felspars, and they are the only ones to show appreciable, though small, amounts of V. In the plagioclase felspars from rocks on the supposed liquid line of descent, Sr decreases steadily as the anorthite content decreases, while Ga and Ba do not show much change.

* Present address: Chemistry Division, I.A.R.I., New Delhi 12, India

† The V content may be fictitious (see D. M. Shaw, *Geochim. et Cosmochim. Acta* **15,** 159)

Table 1. Plagioclase felspars*

	1	2	3	4	5	6	7	8	9	10	11	12	13	14
Si	205.10^3	(238.10^3)	(219.10^3)	(251.10^3)	247.10^3	(262.10^3)	(265.10^3)	(276.10^3)	267.10^3	(285.10^3)	(282.10^3)	(283.10^3)	296.10^3	(296.10^3)
Al	192.10^3	(167.10^3)	(181.10^3)	(157.10^3)	156.10^3	(148.10^3)	146.10^3	(138.10^3)	142.10^3	(130.10^3)	(133.10^3)	(132.10^3)	117.10^3	(122.10^3)
Fe^{3+}	tr.	—	—	—	6.10^3	—	—	—	4.10^3	—	—	—	7.10^3	—
Mg	tr.	—	—	—	—	—	—	—	—	—	—	—	—	—
Na	5.10^3	(26.10^3)	(12.10^3)	(36.10^3)	30.10^3	(44.10^3)	(47.10^3)	(55.10^3)	47.10^3	(62.10^3)	(59.10^3)	(60.10^3)	68.10^3	(70.10^3)
Ca	134.10^3	(100.10^3)	(123.10^3)	(84.10^3)	90.10^3	(72.10^3)	(67.10^3)	(54.10^3)	61.10^3	(43.10^3)	(47.10^3)	(46.10^3)	26.10^3	(30.10^3)
K	8.10^2	—	—	—	25.10^2	—	—	—	40.10^2	—	—	—	40.10^2	—
Ga	35	32	30	28	35	(25)	(25)	(22)	(21)	(20)	(25)	(26)	(30)	(28)
Cr	*	8	*	*	*	*	*	*	*	*	*	*	*	*
†V	10	20	20	10	10	*	(5)	*	*	*	*	*	*	*
Li	*	*	3	2	2	(4)	*	*	*	*	*	(5)	*	(28)
Sr	1000	1300	1100	1250	900	(895)	(990)	(600)	(785)	(250)	(410)	(430)	(140)	(140)
Ba	10	85	80	45	50	(130)	(80)	(225)	(255)	(165)	(150)	(170)	(120)	(235)
Rock position	−8·2	−6·5	−5·3	−3·0	−2·9	+1·3	+1·9	+5·6	+5·6	+9·4	+10·9	+11·3	+13·3	+13·9
Ga × 1000/Al	0·18	0·19	0·17	0·18	0·22	0·17	0·17	0·16	0·15	0·15	0·19	0·20	0·26	0·23
Na × 10/Ca	0·4	2·6	1·0	4·3	3·3	6·1	7·0	10·2	7·7	14·4	12·6	13·0	26·2	23·3
Sr × 1000/Ca	7·5	13·0	9·0	14·9	10·0	12·4	14·8	11·1	12·9	5·8	8·7	9·3	5·4	4·7
Ba × 1000/Ca	0·1	0·9	0·6	0·5	0·7	1·8	1·2	4·2	4·2	3·8	3·2	3·7	4·6	7·8
Composition	An_{93}	An_{70}	An_{86}	An_{59}	An_{64}	An_{50}	An_{47}	An_{38}	An_{42}	An_{30}	An_{33}	An_{32}	An_{22}	An_{21}

(Ni, Co, Mo, Sc, Zr, Y, La, Rb below limits of sensitivity in all).

1. From 58245, olivine norite (also described as "olivine-hornblende troctolite" and as "calcic gabbro"), SLR, M 354 (Larsen and Draisin, 1950, Table 4, no. 1).
2. From 58212, noritic hornblende gabbro, SLR, M 299.
3. From 58240, calcic hornblende gabbro (rich in iron-ore), El 303.
4. From 58243, norite (rich in iron-ore), SLR 218.
5. From 58241, typical norite, SLR, M 334 (Larsen and Draisin, 1950 Table 4, no. 2).
6. From 58255, coarse quartz-biotite norite, El 230.
7. From 58271, Bonsall tonalite, SLR 1016.
8. From 58256, Green Valley tonalite, SLR 138.
9. From 58259, Bonsall tonalite, SLR, El 38–28 (Larsen and Draisin, 1950, Table 4, no 3).
10. From 58251, Green Valley tonalite, SLR 685.
11. From 58237, granodiorite, W of Lakeview, El 38–126.
12. From 58219, Bonsall tonalite (granodiorite), SLR 2242.
13. From 58220, Woodson Mountain granodiorite, SLR 596 (Larsen and Draisin, 1950, Table 4, no. 4).
14. From 58227, coarse granite of Rubideaux Mountain, El 38-167.

* All values in this and following tables are in p.p.m. An asterisk indicates that the element is below its limit of sensitivity (Nockolds and Allen, 1953, Table 1).

† These values may be fictitious (See D. M. Shaw, *Geochim. et Cosmochim. Acta* **15,** 159).

The ratio Ga/Al does not vary much throughout the whole series and shows no definite trend, but with increase in the ratio Na/Ca there is a rise in the ratio Ba/Ca, as would be expected. The ratio Sr/Ca also rises in the same direction in the earlier plagioclase felspars but falls in the later numbers of the series. This is probably due to the fact that the latter are accompanied by appreciable amounts of potash felspar which is capturing some Sr.

It should be noted that while in general the anorthite content of the plagioclase decreases steadily for rocks on the supposed liquid line of descent as the modified Larsen function increases in value, nos. 8 (from Green Valley tonalite, 58256) and 10 (from Green Valley tonalite, 58251) are exceptions to this.

Table 2. Potash felspars

	1	2	3	4	5
Si	$305 . 10^3$	$299 . 10^3$	$301 . 10^3$	$297 . 10^3$	—
Al	$97 . 10^3$	$101 . 10^3$	$102 . 10^3$	$103 . 10^3$	
Fe^{3+}	$4 . 10^3$	$2 . 10^3$	$3 . 10^3$	$2 . 10^3$	—
Na	$21 . 10^3$	$13 . 10^3$	$15 . 10^3$	$11 . 10^3$	$26 . 10^3$
Ca	$4 . 10^3$	$2 . 10^3$	$2 . 10^3$	$2 . 10^3$	—
K	$103 . 10^3$	$102 . 10^3$	$111 . 10^3$	$120 . 10^3$	$88 . 10^3$
Ga	10	10	10	10	10
Li	*	3	3	4	10
Sr	200	200	200	110	130
Ba	2000	3000	2500	2500	2500
Rb	450	400	600	600	600
Rock position	+9·4	+10·9	+11·3	+13·3	+13·9
Ga × 1000/Al	0·10	0·10	0·10	0·10	—
Na × 10/K	2·0	1·3	1·4	0·9	3·0
Sr × 1000/K	1·9	2·0	1·8	0·9	1·5
Ba × 1000/K	19·4	29·4	22·5	20·8	28·4
Rb × 1000/K	4·4	3·9	5·4	5·0	6·8

(Cr, V, Ni, Co, Mo, Sc, Zr, Y, La, below limits of sensitivity in all.)

1. From 58251, Green Valley tonalite, SLR 685 (Larsen and Draisin, 1950, Table 5, no. 1).
2. From 58237, granodiorite, W. of Lakeview, El 38-126 (Larsen and Draisin, 1950, Table 5, no. 2).
3. From 58219, Bonsall tonalite (granodiorite), SLR 2242 (Larsen and Draisin, 1950, Table 5, no. 3).
4. From 58220, Woodson Mountain granodiorite, SLR 596 (Larsen and Draisin, 1950, Table 5, no. 4).
5. From 58227, coarse granite of Rubideaux Mt., El 38–167 (Larsen and Draisin 1950, Table 5, no. 5).

II. The Potash Felspars

Potash felspar is not an important constituent in the earlier rocks of the batholith and is lacking entirely in some, while we have not had the opportunity

of separating potash felspar from the latest rocks of the batholith. Consequently our samples come from rocks with a rather restricted range of composition, their modified Larsen function ranging from +9·4 to +13·9 (Table 2).

Of the common trace elements only Ga, Li, Sr, Ba and Rb rise above their limits of sensitivity. Ga is low in all five samples, Ba is relatively high and shows little change within the range covered. Sr, on the other hand, does decrease in the later potash felspar while Rb increases in the same direction. The small amounts of Li present in four out of the five samples are perhaps to be attributed to incipient sericitization.

Comparison between plagioclase and associated potash felspar is possible in five cases (58220, 58251, 58237, 58219 and 58237). In all the plagioclase shows higher Ga and Sr (though this may be only a little higher) and lower Ba and Rb than the potash felspar. The same relations are to be found in associated plagioclase and potash felspars from the Scottish Caledonian igneous rocks (Nockolds and Mitchell, 1948, Tables XX and XXI).

III. Olivine, Hypersthene and Augite

A single olivine has been separated, namely that occurring in the olivine norite (Table 3, no. 1). This has a composition about $Fo_{72}Fa_{28}$. Like most olivines elsewhere the only common trace elements present in important amounts are Ni and Co. But unlike most magnesian olivines analysed so far, the Co is in excess of Ni. This is a feature characteristic of the ferromagnesian constituents from the rocks of this batholith and, indeed, of many of the rocks themselves (Nockolds and Allen, 1953, Table 1).

Hypersthenes separated from various rocks are shown in Table 3 (nos. 2–7). The first four come from accumulative rocks, the next one from a rock at the beginning of the supposed liquid line of descent and the final example from a granite relatively late in the liquid line of descent. In general, the early hypersthenes tend to be richer in Cr, V, Mo, Ni and Co than the late hypersthene. Ga is present in small, but appreciable, amounts in all, while a little Sc is present in all but one. Lk is interesting in that it is present in small amounts in the two hypersthenes from rocks on the supposed liquid line of descent, but is below the limit of sensitivity (1 p.p.m.) in hypersthenes from the accumulative rocks.

All the hypersthenes have Co > Ni and this is particularly marked in the hypersthene from calcic hornblende gabbro (no. 3) and in that from norite (no. 4). These two are also low in Cr. This marked excess of Co over Ni and low content of Cr is a feature of these two rocks, both of which are rich in iron-ore (Nockolds and Allen, 1953, Table 1, nos. 3 and 4). It is further reflected in the augite from the norite (Table 3, no. 8).

A comparison of olivine and hypersthene from the same rock (Table 3, nos. 1 and 2) shows the latter to be richer in Ga, Cr, V and Mo but poorer in Ni and Co. This is in harmony with the behaviour of co-existing olivines and hypersthenes elsewhere.

Augite is an important constituent only in some of the earlier rocks of the batholith. Of the two separated, one (Table 3, no. 8) comes from an accumulative rock, the other (Table 3, no. 9) from a rock at the beginning of the supposed

Table 3. Olivine, hypersthenes, augites

	1	2	3	4	5	6	7	8	9
Si					$243 . 10^3$		$208 . 10^3$		
Al					$11 . 10^3$		$26 . 10^3$		
Ti					$20 . 10^2$		$84 . 10^2$		
Fe^{3+}					$14 . 10^3$		$9 . 10^3$		
Mg					$125 . 10^3$		$40 . 10^3$		
Fe^{2+}					$154 . 10^3$		$301 . 10^3$		
Na					tr.		$3 . 10^3$		
Ca					$20 . 10^3$		$10 . 10^3$		
K					—		$1 . 10^3$		
Ga	*	10	2	4	8	8	5	5	4
Cr	20	100	8	5	45	140	4	15	500
V	*	40	200	60	110	170	*	200	480
Mo	*	2	2	*	2	3	*	*	*
Li	*	*	*	*	*	10	7	1	20
Ni	150	22	*	5	60	40	10	*	55
Co	250	60	55	70	85	65	12	40	60
Sc	*	*	30	60	60	60	30	250	120
Y	*	*	*	*	*	25	*	30	70
Sr	*	*	*	*	*	*	*	10	*
Ba	*	*	*	*	*	*	*	*	*
Zr	*	*	*	45	*	*	*	35	65
Rock position	−8·2	−8·2	−5·3	−3·0	−2·9	+1·3	+13·9	−3·0	+1·3

(La, Rb, below limits of sensitivity in all).

1. Olivine from 58245, olivine norite, SLR, M 354.
2. Hypersthene from 58245, olivine norite, SLR, M 354.
3. Hypersthene from 58240, calcic hornblende gabbro (rich in iron-ore), El 303.
4. Hypersthene from 58243, norite (rich in iron-ore), SLR 218.
5. Hypersthene from 58241, typical norite, SLR, M 334 (Larsen and Draisin, 1950, Table 1, no. 1).
6. Hypersthene from 58255, coarse quartz-biotite norite, El 230.
7. Hypersthene from 58227, coarse granite of Rubideaux Mt., El 38–167 (Larsen and Draisin, 1950, Table 1, no. 2).
8. Augite from 58243, norite (rich in iron-ore), SLR 218.
9. Augite from 58255, coarse quartz-biotite norite, El 230.

liquid line of descent. The latter shows quite typical features; relatively high Cr and V; appreciable Li, Ni, Co, Sc and Y; and small amounts of Ga. The former has very low Li, low Y and high Sc in harmony with its earlier formation, but is unduly low in Cr, Ni and Co. As mentioned previously, however, this comes from an unusual rock, rich in iron-ore.

If co-existing augites and hypersthenes are compared (Table 3, nos. 9 and 6; nos. 8 and 4), the former have higher Cr, V, Li, Sc and Y. Co and Ni are about evenly distributed in the first pair, but in the second pair (of earlier formation) the hypersthene has rather more Co and Ni than the augite. Very similar features

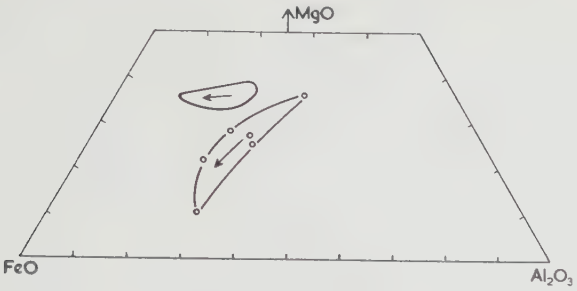

Fig. 1. Hornblendes.

Table 4. Hornblendes

	1	2	3	4	5	6	7	8	9	10	11	12
Si	$209 . 10^3$					$205 . 10^3$	$217 . 10^3$				$211 . 10^3$	$185 . 10^3$
Al	$89 . 10^3$					$61 . 10^3$	$45 . 10^3$				$51 . 10^3$	$65 . 10^3$
Ti	$36 . 10^2$					$90 . 10^2$	$80 . 10^2$				$102 . 10^2$	$87 . 10^2$
Fe^{3+}	$5 . 10^3$					$32 . 10^3$	$28 . 10^3$				$24 . 10^3$	$29 . 10^3$
Mg	$92 . 10^3$					$65 . 10^3$	$66 . 10^3$				$63 . 10^3$	$26 . 10^3$
Fe^{2+}	$64 . 10^3$					$104 . 10^3$	$105 . 10^3$				$113 . 10^3$	$180 . 10^3$
Na	$13 . 10^3$					$9 . 10^3$	$9 . 10^3$				$11 . 10^3$	$13 . 10^3$
Ca	$74 . 10^3$					$77 . 10^3$	$83 . 10^3$				$82 . 10^3$	$71 . 10^3$
K	$8 . 10^2$					$50 . 10^2$	$6 . 10^3$				$7 . 10^3$	$12 . 10^3$
Ga	2	5	8	12	10	15	15	15	15	20	15	20
Cr	100	250	20	2	370	100	125	85	90	15	35	30
V	90	270	1000	220	240	200	235	265	240	125	190	175
Li	*	*	1	1	1	5	5	5	15	20	5	15
Ni	20	30	80	*	15	30	40	20	55	5	15	5
Co	20	35	35	40	28	45	30	30	35	12	30	10
Sc	*	80	95	90	80	125	100	100	100	150	150	200
Y	*	20	25	15	15	65	200	95	250	130	300	2000
La	*	*	*	*	*	*	*	*	200	*	90	300
Sr	15	25	10	50	20	10	3	5	15	5	*	10
Ba	15	25	45	20	30	80	45	50	15	50	10	60
Rb	*	*	*	*	*	*	*	*	*	10	?5	10
Zr	15	50	70	40	30	180	50	50	110	170	100	250
Rock position	−8·2	−6·5	−5·3	−3·0	−2·9	+1·9	+5·6	+5·6	+9·4	+10·9	+11·3	+13·9

(Mo below limits of sensitivity in all).

1. From 58245, olivine norite, SLR, M 354 (reactional) (Larsen and Draisin, 1950, Table 3, no. 1).
2. From 58212, noritic hornblende gabbro, SLR, M 299.
3. From 58240, calcic hornblende gabbro (rich in iron-ore), El 303.
4. From 58243, norite (rich in iron-ore), SLR 218.
5. From 58241, typical norite, SLR, M 334.
6. From 58271, Bonsall tonalite, SLR 1016 (Larsen and Draisin, 1950, Table 3, no. 6).
7. From 58256, Green Valley tonalite, SLR 138 (Larsen and Draisin, 1950, Table 3, no. 7).
8. From 58259, Bonsall tonalite, SLR El 38–28.
9. From 58251, Green Valley tonalite, SLR 685.
10. From 58237, granodiorite, W of Lakeview, El 38–126.
11. From 58219, Bonsall tonalite (granodiorite), SLR 2242 (Larsen and Draisin, 1950, Table 3, no. 9).
12. From 58227, coarse granite of Rubideaux Mt., El 38–167 (Larsen and Draisin, 1950, Table 3, no. 11).

are shown by co-existing augites and hypersthenes from the rocks of the Madras charnockite series (Howie, 1955, Tables IX and X); by the augite and hypersthene from the pyroxene-mica diorite at Garabal Hill (Nockolds and Mitchell, 1948, p. 555); by the augites and rhombic pyroxenes from the olivine-rich inclusions in basaltic rocks (Ross *et al.*, 1954); and by the augites and rhombic pyroxenes from certain pyroxenites (DeVore 1955, Table 13). Where Ga has been determined, this element is behaving as in the pyroxenes from the rocks described here. It is about the same in both pyroxenes or slightly greater in amount in the rhombic pyroxene.

IV. The Hornblendes

A number of hornblendes have been analysed by Larsen and Draisin (1950) for their major elements and we have made trace-element determinations on some of these and on others which have not been analysed (Table 4).

Larsen and Draisin recognize three types of hornblende—hydrothermal, reactional, and normal hornblendes occurring as individual grains and prisms. Fig. 1 gives a plot of the analysed normal hornblendes on the basis MgO + total Fe as FeO + Al_2O_3 = 100. The general trend shown by the arrow is towards enrichment in FeO, and contrasts with the trend of normal hornblendes from Scottish Caledonian igneous rocks where relatively little enrichment in iron took place.

The first hornblende, from an accumulative rock (Table 4, no. 1), is said to be reactional and is characterized by its high Al and low V, Sc, Ga and Y. The next four hornblendes also come from accumulative rocks (Table 4, nos. 2 to 5). All have very low Li, moderate Sc, and low Y and Ga. Two (nos. 2 and 5) show the relatively high Cr that one might expect in early amphibole, but two (nos. 3 and 4) are abnormal in this respect and have low Cr. Once again, these minerals come from the calcic hornblende gabbro (rich in iron-ore) and the norite (rich in iron-ore), respectively. Each is abnormal in other ways as well. The hornblende from the calcic hornblende gabbro has high V and Ni > Co, while in that from the norite Ni has fallen below the limit of sensitivity.

Turning now to hornblendes from rocks on the supposed liquid line of descent (Table 4, nos. 6 to 12), certain general tendencies can be distinguished. In passing from hornblende in basic tonalite (no. 6) to hornblende in granite (no. 12), Cr, V, Ni and Co tend to decrease, while Li, Sc, Y, La (and Rb) tend to increase in amount. Ga remains more or less constant, Ba is low but rather variable as is also the low Sr content (which, however, is usually somewhat higher in the early hornblendes from the accumulative rocks).

On closer scrutiny it will be observed that anomalies in these tendencies are provided largely by the hornblendes from the Green Valley tonalite (nos. 7 and 9). In both these Cr is somewhat high for the position their rocks occupy while both have Ni > Co, the reverse of what is usual for ferromagnesian minerals from the rocks of this batholith. Both are relatively high in Y and, in one case, La.

With these two exceptions, contents of Ni and Co are much the same in the hornblendes from the earlier rocks on the liquid line of descent, but Co is definitely in excess of Ni in the later hornblendes.

In the few cases where we can compare ratios of associated trace elements to major elements for the normal hornblendes (Table 6, nos. 6, 7, 11, 12), the ratio Ga/Al shows little change. The ratios Ni/Mg, Co/Mg, Ni/Fe^{2+}, Co/Fe^{2+} and Cr/Fe^{3+} all decrease on passing from early to late hornblende, as we should expect. The ratios Sc/Fe^{2+} and V/Fe^{3+} remain fairly constant, while the ratio Li/Mg is higher in late hornblende.

V. The Biotites

Chemical analyses of a number of biotites have been made by Larsen and Draisin (1950) and from these the data on major elements given in Table 5 have been produced. When plotted on the basis MgO + total Fe as FeO + Al_2O_3 = 100 (Fig. 2), the trend of these biotites is very different from that shown by the biotites of the Scottish Caledonian calc-alkali rocks and, moreover, the early biotites are considerably richer in iron than the early biotites of the Scottish Caledonian rocks. This is in harmony with the more iron-rich nature of the supposed parental magma of the rocks of the S. Californian batholith (Nockolds and Allen, 1953, Table 8).

All the biotites shown in Table 5 come from rocks lying on the supposed liquid line of descent and on passing from early to late biotites there is a general tendency for Mg and Al to decrease in amount while the content of *total* Fe increases in the same direction. Cr V, Ni and Co tend to decrease on passing from early to late biotite while Li and Rb increase in amount. Ga increases a little in later biotites; Sc and Ba do not show any detectable trend.

It should be noted that three of the biotites are behaving exceptionally. The first two (Table 5, nos. 4 and 6) come from samples of the Green Valley tonalite and are richer in Cr, V, Ni and Co than they should be from their position in the sequence. Both are also relatively poor in Ba. We have already found other minerals from the Green Valley tonalites behaving in an exceptional manner. The third example (Table 5, no. 8) comes from the Bonsall tonalite (granodiorite). This is richer in Cr, V, Ni and Co, and poorer in Li, than it should be. These discrepant biotites can be readily accounted for if the rocks from which they come have been contaminated to some extent with earlier basic material. This, too, would account for the aberrant behaviour of the other minerals in the Green Valley tonalite where we may suppose the degree of contamination to have been greater than in the case of the Bonsall granodiorite.

Considering now the ratios between the trace elements and associated major elements (Table 6), and remembering that nos. 4 and 8 are aberrant, the following ratios increase on passing from early to late biotite: Ga/Al, Li/Mg, Fe^{2+}/Mg, Rb/K, while the following decrease in the same direction: Ni/Mg, Co/Mg, Ni/Fe^{2+}, Co/Fe^{2+}, Cr/Fe^{3+}, V/Fe^{3+}. These changes in ratios are all of the kind we should expect and similar changes occur among the biotites of the Scottish Caledonian igneous rocks (Nockolds and Mitchell, 1948). The only difference lies in the ratio Ba/K, which decreases on passing from early to late biotites in the Caledonian rocks, as we might expect it to, but here does not show much change.

We can compare the trace-element contents of seven associated hornblendes and biotites (58271, 58256, 58259, 58251, 58237, 68219 and 58227). In every case

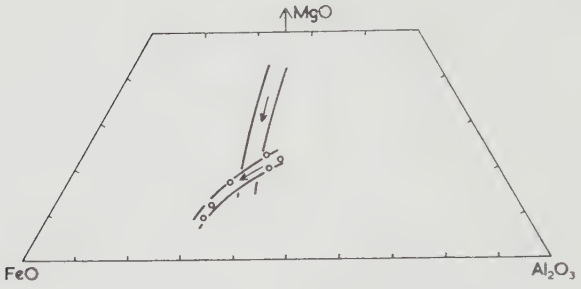

Fig. 2. Biotites.

Table 5. Biotites

	1	2	3	4	5	6	7	8	9	10
Si	$175 . 10^3$	$177 . 10^3$	$171 . 10^3$	$174 . 10^3$				$178 . 10^3$		$168 . 10^3$
Al	$84 . 10^3$	$96 . 10^3$	$91 . 10^3$	$87 . 10^3$				$63 . 10^3$		$76 . 10^3$
Ti	$318 . 10^2$	$183 . 10^2$	$204 . 10^2$	$180 . 10^2$				$210 . 10^2$		$318 . 10^2$
Fe^{3+}	$31 . 10^3$	$25 . 10^3$	$32 . 10^3$	$24 . 10^3$				$54 . 10^3$		$10 . 10^3$
Mg	$62 . 10^3$	$63 . 10^3$	$55 . 10^3$	$66 . 10^3$				$58 . 10^3$		$34 . 10^3$
Fe^{2+}	$120 . 10^3$	$120 . 10^3$	$128 . 10^3$	$131 . 10^3$				$139 . 10^3$		$204 . 10^3$
Na	$4 . 10^3$	$5 . 10^3$	$2 . 10^3$	$3 . 10^3$				$4 . 10^3$		$4 . 10^3$
Ca	$9 . 10^3$	$11 . 10^3$	$3 . 10^3$	$19 . 10^3$				$3 . 10^3$		$4 . 10^3$
K	$68 . 10^3$	$61 . 10^3$	$76 . 10^3$	$60 . 10^3$				$69 . 10^3$		$70 . 10^3$
Ga	15	15	17	20	20	25	25	25	30	25
Cr	110	80	30	125	50	65	10	80	15	5
V	400	350	270	340	200	285	150	295	120	55
Li	80	110	125	100	125	150	175	175	250	260
Ni	70	30	15	90	15	55	5	20	15	<5
Co	50	50	45	50	35	70	25	35	20	15
Sc	15	5	8	5	—	10	25	7	35	15
Sr	*	*	*	*	*	*	*	*	*	*
Ba	1600	1825	2500	1200	2100	500	2500	2500	1500	2000
Rb	1100	1000	1000	1000	1100	1250	1000	1100	1500	1750
Zr	35	45	30	45	30	30	50	40	50	45
Rock position	+1·3	+1·9	+4·0	+5·6	+5·6	+9·4	+10·9	+11·3	+13·3	+13·9

(Mo, Y, La below limits of sensitivity in all)

1. From 58255, coarse quartz-biotite norite, El 230 (Larsen and Draisin, 1950, Table 2, no. 1).
2. From 58271, Bonsall tonalite, SLR 1016 (Larsen and Draisin, 1950, Table 2, no. 4).
3. From 58250, Lakeview tonalite, El 38–134 (Larsen and Draisin, 1950, Table 2, no. 3).
4. From 58256, Green Valley tonalite, SLR 138 (Larsen and Draisin, 1950, Table 2, no. 2).
5. From 58259, Bonsall tonalite, SLR, El 38–28.
6. From 58251, Green Valley tonalite, SLR 685.
7. From 58237, granodiorite, W of Lakeview, El 38–126.
8. From 58219, Bonsall tonalite (granodiorite), SLR 2242 (Larsen and Draisin, 1950, Table 2, no. 5).
9. From 58220, Woodson Mt. granodiorite, SLR 596.
10. From 58227, coarse granite of Rubideaux Mt., El 38–167 (Larsen and Draisin, 1950, Table 2, no. 7).

Table 6. Trace/major-element ratios for hornblendes and biotites

	Hornblendes					Biotites					
	1	6	7	11	12	1	2	3	4	8	10
Ga × 1000/Al	0·02	0·25	0·33	0·29	0·31	0·18	0·16	0·19	0·23	0·40	0·33
Li × 1000/Mg	<0·01	0·08	0·08	0·08	0·58	1·3	1·7	2·3	1·5	3·0	7·6
Ni × 1000/Mg	0·2	0·5	0·6	0·24	0·19	1·1	0·5	0·3	1·4	0·4	<0·15
Co × 1000/Mg	0·2	0·7	0·5	0·5	0·4	0·8	0·8	0·8	0·8	0·6	0·4
Fe^{2+}/Mg	0·7	1·6	1·6	1·8	6·9	1·9	1·9	2·3	2·0	2·4	6·0
Ni × 1000/Fe^{2+}	0·3	0·3	0·4	0·13	0·03	0·6	0·25	0·12	0·7	0·16	<0·02
Co × 1000/Fe^{2+}	0·3	0·4	0·3	0·3	0·06	0·4	0·4	0·35	0·4	0·25	0·07
Sc × 1000/Fe^{2+}	<0·2	1·2	1·0	1·3	1·1	0·12	0·04	0·06	0·04	0·05	0·07
Fe^{3+}/Fe^{2+}	0·08	0·3	0·27	0·2	0·16	0·26	0·2	0·25	0·18	0·39	0·05
Cr × 1000/Fe^{3+}	20	3·1	4·5	1·5	1·0	3·5	3·2	1·0	5·2	1·5	0·5
V × 1000/Fe^{3+}	18	6	8	8	6	13	14	8	14	6	5·5
Sr × 1000/Ca	0·2	0·1	0·04	*	0·1	*	*	*	*	*	*
Sr × 1000/Ca + K	0·2	0·1	0·03	*	0·1	*	*	*	*	*	*
Ba × 1000/K	19	16	7·5	1·4	5	24	30	33	20	36	29
Ba × 1000/Ca + K	0·2	1·0	0·5	0·1	0·7	21	25	32	15	35	27
Rb × 1000/K	*	*	*	*	0·8	16	16	13	17	16	25

the hornblende has higher Sc, Y (also La when present) and Sr, and lower Li, Ba and Rb than its associated biotite.

V, Co and Ga are normally somewhat lower in the hornblende (though this is reversed for V in the granite 58227), while Cr is usually a little higher (except in the Bonsall granodiorite 58219). Ni is about equally distributed between a hornblende and its associated biotite, the only exception to this being the Green Valley tonalite (58256) where Ni in biotite is definitely in excess.

We can also compare the ratios of certain trace elements and associated major elements for co-existing hornblende and biotite in four cases (Table 7). In each case the ratios Li/Mg, Ba/K or Ba/Ca + K, and Rb/K are higher in the biotite than its associated hornblende and the ratios Sc/Fe^{2+} and Fe^{3+}/Fe^{2+} (with one exception) are lower. The ratio Fe^{+2}/Mg is a little higher in the biotite, except in the latest one where it is lower. but the ratios Co/Mg, Co/Fe^{2+}, Ni/Mg and Ni/Fe^{2+} tend to be the same in both the biotite and its associated hornblende (except in the case of the Green Valley tonalite, 58256). The ratio V/Fe^{3+} is higher in early biotites but becomes essentially the same as that of associated hornblende in later biotites. The ratio Cr/Fe^{3+} is much the same in both minerals, except in the case of the latest biotite from the granite 58227, where it is definitely lower than that of the associated hornblende. The ratio Ga/Al is higher in hornblende in the earlier rocks but tends to become higher in biotite in later rocks.

The distribution of trace elements between biotite and associated hornblende here is very similar to that found in these minerals in the Caledonian plutonic rocks of Scotland (Nockolds and Mitchell, 1948, p. 551 and Table XII). On the other hand, the biotite and hornblende from an intermediate member of the charnockite series (Howie, 1955, Table VII, no. 2270) and three examples from

hornblende schists (DeVore, 1955, Table 13) behave like the biotite and hornblende from the Green Valley tonalite, 58256, in that the ratios Ni/Mg and Ni/Fe^{2+} are definitely greater in the biotite than in the associated hornblende. This is perhaps to be connected with the simultaneous crystallization of the two minerals in these examples.

Table 7

	58271		58256		58219		58227		
	Horn.	Biot.	Horn.	Biot.	Horn.	Biot.	Horn.	Biot.	Hyp.
Ga × 1000/Al	0·25	0·16	0·33	0·23	0·29	0·40	0·31	0·33	0·19
Ni × 1000/Mg	0·5	0·5	0·6	1·4	0·24	0·4	0·19	<0·15	0·25
Li × 1000/Mg	0·08	1·7	0·08	1·5	0·08	3·0	0·58	7·6	0·2
Co × 1000/Mg	0·7	0·8	0·5	0·8	0·5	0·6	0·4	0·4	0·3
Fe^{2+}/Mg	1·6	1·9	1·6	2·0	1·8	2·4	6·9	6·0	7·5
Ni × 1000/Fe^{2+}	0·3	0·25	0·4	0·7	0·13	0·16	0·03	<0·02	0·03
Co × 1000/Fe^{2+}	0·4	0·4	0·3	0·4	0·3	0·25	0·06	0·07	0·04
Sc × 1000/Fe^{2+}	1·2	0·04	1·0	0·04	1·3	0·05	1·1	0·07	0·1
Fe^{3+}/Fe^{2+}	0·3	0·2	0·27	0·18	0·2	0·39	0·16	0·05	0·03
Cr × 1000/Fe^{3+}	3·1	3·2	4·5	5·2	1·5	1·5	1·0	0·5	0·4
V × 1000/Fe^{3+}	6	14	8	14	8	6	6	5·5	*
Sr × 1000/Ca	0·1	*	0·04	*	*	*	0·1	*	*
Sr × 1000/Ca + K	0·1	*	0·03	*	*	*	0·1	*	*
Ba × 1000/K	16	30	7·5	20	1·4	36	5	29	*
Ba × 1000/Ca + K	1·0	25	0·5	15	0·1	35	0·7	27	*
Rb × 1000/K	*	16	*	17	*	16	0·8	15	*

58271 = Bonsall tonalite, SLR 1016.
58256 = Green Valley tonalite, SLR 138.
58219 = Bonsall tonalite (granodiorite), SLR 2242.
58227 = coarse granite of Rubideaux Mountain, El 38–167.

Table 8

	58219		58227	
	Biot.	K-Fels.	Biot.	K-Fels.
Ga × 1000/Al	0·40	0·10	0·30	—
Sr × 1000/K	<0·03	1·8	<0·03	1·5
Ba × 1000/K	36	22·5	21	28·4
Rb × 1000/K	18	5·4	19	6·8

58219 = Bonsall tonalite (granodiorite), SLR 2242.
58227 = coarse granite of Rubideaux Mountain, El 38–167.

We may further consider biotite and associated potash felspar with respect to their contents of Sr, Ba, Rb and Ga in five examples (58220, 58251, 58237, 58219, 58227). In all the biotite has higher Ga and Rb, lower Ba (except 58219 where the Ba content is the same in both) and much lower Sr than the accompanying potash felspar. In two cases (58219, 58227) we can compare ratios of trace elements and associated major elements (Table 8). The ratios Ga/Al and Rb/K are considerably higher in the biotite while the ratio Sr/K is much lower. The ratio Ba/K is greater in biotite than in potash felspar for the rock 58219, but is slightly less in the biotite for the later rock 58227.

These results agree with those found for co-existing biotite and potash felspar from Scottish Caledonian igneous rocks (Nockolds and Mitchell, 1948, p. 554, Table XIII, p. 555).

VI. Spinel and Magnetite

Spinel occurs in an accumulative norite and may be compared with magnetite from the same rock (Table 9, nos. 1 and 2). The spinel is richer in Ga and Co, has about the same amount of Ni and is poorer in Cr and much poorer in V, than the associated magnetite.

The magnetites represented by nos. 2 to 6 in Table 9 all come from early accumulative rocks. In general, they all show appreciable amounts of Ga, high Cr and V (all three presumably replacing Fe^{3+}), moderate amounts of Ni and Co (replacing Fe^{2+}) and small amounts of Mo. Ni and Co tend to occur in about equal amounts but there are two exceptions to this (nos. 4 and 5). These two magnetites are exceptional in other ways. Both have low Cr and Co much in excess of Ni, features which, as already mentioned, are reflected in the trace-element contents of the rocks from which they come. No. 4 also shows very low V, although the

Table 9. Spinel and magnetites

	1	2	3	4	5	6	7	8	9	10	11	12	13
Ga	200	65	55	50	120	70	95	120	70	70	120	120	100
Cr	5000	12000	3500	55	100	1200	3000	1800	2500	1500	200	1250	250
V	400	6000	4500	50	5000	5000	6000	3500	2200	3500	1750	2500	1100
Mo	*	20	20	20	20	20	30	25	25	40	20	25	100
Ni	200	225	215	320	20	350	200	30	125	70	10	25	20
Co	500	210	200	1000	150	210	70	60	50	30	40	40	40
Rock position	−8·2	−8·2	−6·5	−5·3	−3·0	−2·9	+1·3	+1·9	+5·6	+9·4	+10·9	+11·3	+13·9

(Zr, Y, La below limits of sensitivity in all.)

1. Spinel from 58245, olivine norite, SLR, M 354.
2. Magnetite from 58245, olivine norite, SLR, M 354.
3. Magnetite from 58212, noritic hornblende gabbro, SLR, M 299.
4. Magnetite from 58240, calcic hornblende gabbro (rich in iron-ore), El 303.
5. Magnetite from 58243, norite (rich in iron-ore), SLR 218.
6. Magnetite from 58241, typical norite, SLR, M 334.
7. Magnetite from 58255, coarse quartz–biotite norite, El 230.
8. Magnetite from 58271, Bonsall tonalite, SLR 1016.
9. Magnetite from 58256, Green Valley tonalite, SLR 138.
10. Magnetite from 58251, Green Valley tonalite, SLR 685.
11. Magnetite from 58237, granodiorite, W. of Lakeview, El 38–126.
12. Magnetite from 58219, Bonsall tonalite (granodiorite), SLR 2242.
13. Magnetite from 58227, coarse granite of Rubideaux Mt., El 38–167.

rock from which it comes is not poor in this element. This is perhaps accounted for by the fact that the hornblende occurring with the magnetite is exceptionally rich in vanadium (Table 4, no. 3).

The magnetites represented by columns 7 to 13 in Table 9 are from rocks on the supposed liquid line of descent. The early magnetite here is relatively rich in Cr and V with a moderate amount of Ni and with Ni > Co. In the later magnetites Cr and V gradually decrease in amount, Ni decreases rapidly and Co less rapidly, so that Co soon becomes greater in amount than Ni. Ga and Mo both tend to be present in somewhat greater amounts than in the magnetites from the accumulative rocks, but Ga shows little change on passing from early to late magnetite in rocks on the liquid line of descent. Mo, however, does show a definite increase in amount in the latest magnetite. It will be seen that, just as in the case of the biotites, the magnetites from the Green Valley tonalites (Table 9, nos. 9 and 10) and that from the Bonsall tonalite (granodiorite) (Table 9, no. 12), occupy anomalous positions in the series. They are richer in Cr, V and Ni than they should be for the positions occupied on the liquid line of descent by the rocks from which they come. Once again, this can be accounted for if it is assumed that these rocks have suffered appreciable contamination from earlier basic material.

Early and late magnetites from the Skaergaard intrusion (Wager and Mitchell, 1951, p. 153 and Table B) show much the same features as the early and late magnetites here, but owing to high fractionation, Cr, V and Ni all fall below their limits of sensitivity. Early and late magnetites from the rocks of the Madras charnockite series (Howie, 1955, Table XIV) are also very similar in their behaviour but V is more variable and Ni is usually greater than Co in amount.

Eleven examples of the association hornblende–magnetite and seven examples of the association biotite–magnetite are available for comparison. In almost every case the magnetite has higher Ga, Cr, V, Mo, Ni and Co, and lower Sc than its associated hornblende or biotite. The only marked exception to this comes from an accumulative rock already mentioned, namely the calcic hornblende gabbro where the magnetite has much lower vanadium than the associated hornblende.

VII. Distribution of Trace Elements Among the Minerals of the Same Rock

It is possible to show the distribution of trace elements among the various minerals of a given rock in a number of cases, and this has been done in Tables 10 to 16. The modes used in these tables are those given by Larsen (1948), while the trace element contents of the rocks are taken from Nockolds and Allen (1953, Table 1). There is good agreement, on the whole, between the determinations made on the rock and the calculated trace element composition in terms of the mode. The worst discrepancies occur with Li, Sr, Ba and Rb, all determined on long-range plates which are apt to be difficult to read satisfactorily. The amounts of Zr and Y are always greater in the rock than in the mineral summation but this is to be expected, owing to the presence of accessory zircon, apatite, sphene and allanite which are not included in the mineral summation.

Table 10. 58245. Olivine norite, SLR, M 354 (LARSEN, 1948, Table 5, no. 1)

	Plagio-clase	Olivine	Hypers-thene	Horn-blende	Spinel	Mag-netite	Plagio-clase 67%	Olivine 18%	Horn-blende 10%	Hypers-thene 2%	Spinel 1·5%	Mag-netite 1%	Σ Mins	Rock
Ga	35	*	10	2	200	65	23·4	*	0·2	0·2	3·0	0·7	28	45
Cr	*	20	100	100	5000	12000	*	3·6	10·0	2·0	75·0	120·0	211	200
V	10	*	40	90	400	6000	6·7	*	9·0	0·8	6·0	60·0	83	80
Mo	*	*	2	*	*	20	*	*	*	0·04	*	0·2	0·2	*
Li	*	*	*	*	—	—	*	*	*	*	—	—	*	<2†
Ni	*	150	22	20	200	225	*	27·0	2·0	0·4	3·0	2·2	35	30
Co	*	250	60	20	500	210	*	45·0	2·0	1·2	7·5	2·1	58	55
Sc	*	*	*	*	*	*	*	*	*	*	*	*	*	*
Zr	*	*	*	15	*	*	*	*	1·5	*	*	*	2	10
Y	*	*	*	*	*	*	*	*	*	*	*	*	*	*
La	*	*	*	*	*	*	*	*	*	*	*	*	*	*
Sr	1000	*	*	15	—	—	670	*	1·5	*	—	—	672	500
Ba	10	*	*	15	—	—	6·7	*	1·5	*	—	—	8	5
Rb	*	*	*	*	—	—	*	*	*	*	—	—	*	*

† Revised determination.

Table 11. 58255. Coarse quartz–biotite norite, El 230 (Larsen, 1948, Table 5, no. 9)

	Plagioclase and quartz	Hypersthene	Augite	Biotite	Magnetite	Ilmenite	Plagioclase and quartz 62%	Biotite 16%	Hypersthene 9%	Augite 8%	Hornblende 3%	Ilmenite 1½%	Mt. ½%	Σ Mins	Rock
Ga	20	8	4	15	95	40	12·4	2·4	0·7	0·3	(1·2)	0·6	0·5	18	30
Cr	*	140	500	110	3000	250	*	17·6	12·6	40·0	(11·1)	3·7	15·0	100	75
V	*	170	480	400	6000	900	*	64·0	15·3	38·4	(7·2)	13·5	30·0	168	150
Mo	*	3	*	*	30	*	*	*	*	*	(*)	*	0·2	0·2	*
Li	3	10	20	80	—	—	1·9	12·8	0·9	1·6	(tr.)	—	—	17	20†
Ni	*	40	55	70	200	20	*	11·2	3·6	4·4	(0·5)	0·3	1·0	21	30
Co	*	65	60	50	70	*	*	8·0	5·8	4·8	(0·8)	*	0·4	20	20
Sc	*	60	120	15	*	*	*	2·4	5·4	9·6	(2·4)	*	*	20	25
Zr	50	*	65	35	*	*	31·0	5·6	*	5·2	(0·9)	*	*	43	75
Y	*	25	70	*	*	*	*	*	2·3	5·6	(0·5)	*	*	8	20
La	*	*	*	*	*	*	*	*	*	*	*	*	*	*	*
Sr	750	*	*	*	—	—	465·0	*	*	*	(0·6)	—	—	466	275
Ba	110	*	*	1600	—	—	68·2	256·0	*	*	(1·2)	—	—	325	300
Rb	*	*	*	1100	—	—	*	176·0	*	*	*	—	—	176	100

† Revised determination.

Table 12. 58271. Bonsall tonalite, SLR 1016 (Larsen, 1948, Table 8, no. 2)

	Plagioclase and quartz	Hornblende	Biotite	Magnetite	Plagioclase and quartz 65%	Hornblende 18%	Biotite 14%	Magnetite 2%	Σ Mins	Rock
Ga	20	15	15	120	13·0	2·7	2·1	2·4	20	25
Cr	*	100	80	1800	*	18·0	11·2	36·0	65	45
V	5	200	350	3500	3·2	36·0	49·0	70·0	158	150
Mo	*	*	*	25	*	*	*	0·5	0·5	*
Li	*	5	110	—	*	0·9	15·4	—	16	25
Ni	*	30	30	30	*	5·4	4·2	0·6	10	10
Co	*	45	50	60	*	8·1	7·0	1·2	16	20
Sc	*	125	5	*	*	22·5	0·7	*	23	30
Zr	*	180	45	*	*	32·4	6·3	*	39	75
Y	*	65	*	*	*	11·7	*	*	12	20
La	*	*	*	*	*	*	*	*	*	*
Sr	800	10	*	—	520·0	1·8	*	—	522	250
Ba	65	80	1825	—	42·2	14·4	255·5	—	312	250
Rb	*	*	1000	—	*	*	140·0	—	140	100

Table 13. 58251. Green Valley tonalite (granodiorite), SLR 685 (Larsen, 1948, Table 7, no. 1)

	Plagio-clase and quartz	Potash felspar	Hornblende	Biotite	Magnetite	Plagioclase and quartz 76%	Potash felspar 10%	Biotite 8%	Hornblende 4%	Magnetite 2%	Σ Mins	Rock
Ga	15	10	15	25	70	11·4	1·0	2·0	0·6	1·4	16	20
Cr	*	*	90	65	1500	*	*	5·2	3·6	30·0	39	30
V	*	*	240	285	3500	*	*	22·8	9·6	70·0	102	100
Mo	*	*	*	*	40	*	*	*	*	0·8	0·8	*
Li	5	*	15	150	—	3·8	*	12·0	0·6	—	16	25
Ni	*	*	55	55	70	*	*	4·4	2·2	1·4	8	15
Co	*	*	35	70	30	*	*	5·6	1·4	0·6	8	15
Sc	*	*	100	10	*	*	*	0·8	4·0	*	5	15
Zr	*	*	110	30	*	*	*	2·4	4·4	*	7	300
Y	*	*	250	*	*	*	*	*	10·0	*	10	40
La	*	*	200	*	*	*	*	*	8·0	*	8	*
Sr	200	200	15	*	—	152·0	20·0	*	0·6	—	173	250
Ba	100	2000	15	500	—	76·0	200·0	40·0	0·6	—	317	400†
Rb	*	450	10	1250	—	*	45·0	100·0	0·4	—	145	100

† Revised determination.

Table 14. 58237. Granodiorite, W of Lakeview, El 38–126 (LARSEN, 1948, Table 8, no. 1)

	Plagio-clase and quartz	Potash felspar	Hornblende	Biotite	Magnetite	Plagioclase and quartz 77%	Potash felspar 14%	Biotite 5%	Hornblende 3%	Magnetite 1%	Σ Mins	Rock
Ga	15	10	20	25	120	12·0	1·4	1·3	0·6	1·2	17	20
Cr	*	*	15	10	200	*	*	0·5	0·5	2·0	3	3
V	*	*	125	150	1750	*	*	7·5	3·8	17·5	29	40
Mo	*	*	*	*	20	*	*	*	*	0·2	0·2	*
Li	*	3	20	175	—	*	0·4	8·8	0·6	—	10	20†
Ni	*	*	5	5	10	*	*	0·3	0·1	0·1	0·5	*
Co	*	*	12	25	40	*	*	1·3	0·4	0·4	2	3
Sc	*	*	150	25	*	*	*	1·3	4·5	*	6	<10
Zr	*	*	170	50	*	*	*	2·5	5·1	*	8	125
Y	*	*	130	*	*	*	*	*	3·9	*	4	15
La	*	*	*	*	*	*	*	*	*	*	*	*
Sr	250	200	5	*	—	192·5	28·0	*	0·2	—	221	250†
Ba	90	3000	50	2500	—	69·3	420·0	125·0	1·5	—	616	1000†
Rb	*	400	10	1000	—	*	56·0	50·0	0·3		106	200

† Revised determination.

Table 15. 58219. Bonsall tonalite (granodiorite), SLR 2242 (Larsen, 1948, Table 8, no. 5)

	Plagio-clase and quartz	Potash felspar	Hornblende	Biotite	Magnetite	Plagioclase and quartz 76%	Potash felspar 14%	Biotite 7%	Hornblende 2%	Magnetite 1%	Σ Mins	Rock
Ga	15	10	15	25	120	12·0	1·4	1·8	0·3	1·2	17	20
Cr	*	*	35	80	1250	*	*	5·6	0·7	12·5	19	15
V	tr.	*	190	295	2500	*	*	20·7	3·8	25·0	50	75
Mo	*	*	*	*	25	*	*	*	*	0·2	0·2	*
Li	3	2	5	175	—	2·3	0·3	12·3	0·1	—	15	15
Ni	*	*	15	22	25	*	*	1·5	0·3	0·3	2	5
Co	*	*	30	35	40	*	*	2·5	0·6	0·4	4	10
Sc	*	*	150	7	*	*	*	0·5	3·0	*	4	<10
Zr	20	*	100	40	*	15·2	*	2·8	2·0	*	20	150
Y	*	*	300	*	*	*	*	*	6·0	*	6	30
La	*	*	90	*	*	*	*	*	1·8	*	2	*
Sr	250	200	*	*	—	190·0	28·0	*	*	—	218	250
Ba	100	2500	10	2500	—	76·0	350·0	175·0	0·2	—	601	700
Rb	*	600	?5	1100	—	*	84·0	77·0	*	—	161	250

Table 16. 58227. Coarse-grained granite, Rubideaux Mt., El 38–167 (LARSEN, 1948, Table 18, no. 1)

	Plagioclase and quartz	Potash-felspar	Hypersthene	Hornblende	Biotite	Magnetite	Plagioclase and quartz 64%	Potash-felspar 32%	Biotite 2%	Hornblende 1%	Hypersthene ½%	Magnetite ½%	Σ Mins	Rock
Ga	15	10	5	20	25	100	9·6	3·2	0·5	0·2	tr.	0·5	14	15
Cr	*	*	4	30	5	250	*	*	0·1	0·3	tr.	1·3	2	*
V	*	*	*	175	55	1100	*	*	1·1	1·8	*	5·5	8	15
Mo	*	*	*	3	*	100	*	*	*	tr.	*	0·5	0·5	*
Li	15	10	7	15	260	—	9·6	3·2	5·2	0·2	tr.		18	50
Ni	*	*	10	5	<5	20	*	*	0·1	0·1	0·1	0·1	0·4	*
Co	*	*	12	10	15	40	*	*	0·3	0·1	0·1	0·2	0·7	*
Sc	*	*	30	200	15	*	*	*	0·3	2·0	0·2	*	3	*
Zr	*	*	*	250	45	*	*	*	0·9	2·5	*	*	3	100
Y	*	*	*	2000	*	*	*	*	*	20·0	*	*	20	30
La	*	*	*	300	*	*	*	*	*	3·0	*	*	3	50
Sr	75	130	*	10	*	—	48·0	41·6	*	0·1	*		90	125
Ba	125	2500	*	60	2000	—	80·0	800·0	40·0	0·6	*		921	1000†
Rb	*	600	*	10	1750	—	*	192·0	35·0	0·1	*		227	250

† Revised determination.

VIII. Summary and Conclusions

In general, each mineral series studied is behaving as one might expect on the assumption that the rocks whose elements fall on smooth curves in the variation diagrams (Nockolds and Allen, 1953, Figs. 1, 9a, 10a, 13a) belong to a liquid line of descent controlled largely by processes of crystallization–differentiation but modified to some extent, as in the case of the Green Valley tonalite, by assimilation of earlier gabbroic material. The early gabbroic rocks of the batholith mostly lie off the supposed liquid line of descent and are believed to represent accumulative types. The composition of the members of the various mineral series from such rocks supports this view.

Such assumptions would be in harmony with the views expressed by Larsen (1948): "It is therefore concluded that the differentiation was due to crystal settling modified by assimilation". More recently, Chayes (1956) has expressed the view that the intermediate types in the batholith are all hybrids between a quartz-free gabbro and a granodiorite devoid of hornblende, pyroxene and ores. This could well be the case for intermediate rocks such as the Green Valley tonalite, but seems less likely to be the whole story for those like the Bonsall tonalite.

References

Chayes F. (1956) Modal composition of the major members of the Southern California batholith. *Ann. Rpt. Director of the Geophysical Laboratory*, 1955–56, pp. 214–216.

De Vore G. W. (1955) Crystal growth and the distribution of elements. *J. Geol.* **63,** 471–494.

Howie R. A. (1955) The geochemistry of the charnockite series of Madras, India. *Trans. Roy. Soc. Edinb.* **62,** 725–768.

Larsen E. S., Jr. (1948) Batholith and associated rocks of the Corona, Elsinore and San Luis Rey quadrangles, southern California. *Mem. Geol. Soc. Amer.* **29.**

Larsen E. S. Jr. and Draisin W. M. (1950) Composition of the minerals in the rocks of the southern California batholith. *Rept. 18th Internat. Geol. Congress*, 1948. Part II, Proc. Sect. A, pp. 66–79.

Nockolds S. R. and Mitchell R. L. (1948) The geochemistry of some Caledonian plutonic rocks. *Trans. Roy. Soc. Edinb.* **61,** 533–575.

Nockolds S. R. and Allen R. (1953) The geochemistry of some igneous rock series. *Geochim. et Cosmochim. Acta* **4,** 105–142.

Ross C. S., Foster M. D. and Myers A. T. (1954) Origin of dunites and of olivine-rich inclusions in basaltic rocks. *Amer. Min.* **39,** 693–737.

Wager L. R. and Mitchell R. L. (1951) The distribution of trace elements during strong fractionation of basic magma. *Geochim. et Cosmochim. Acta* **1,** 129–208.

Geochimica et Cosmochimica Acta, 1959, Vol. 16, pp. 79 to 82. Pergamon Press Ltd. Printed in Northern Ireland

Frequency distribution of elements in rocks

Z. V. Jizba
California Research Corporation, La Habra, California.

(*Received* 20 *August* 1958)

Abstract—Two models are suggested as possible mechanisms to generate frequency distribution of elements in nature. One model leads to a three-parameter β-distribution. The second model leads to a distribution which approaches lognormality for trace elements.

In recent years there has been considerable controversy on the subject whether elements and minerals follow the lognormal distribution or not: Ahrens (1954 a, b; 1957), Miller (1955), Aubrey (1954), Chayes (1954). Ahrens, a strong proponent of the theory of lognormal distribution in nature, bases his arguments primarily on empirically observed data and none of his papers justify this distribution theoretically. The critics of the theory of lognormal distribution in nature have two types of arguments. First, they point to illustrations of distributions which obviously can not be lognormal (Aubrey, 1954, p. 142). Second, they plead for a more realistic evaluation of the processes that generate specific frequency distributions. Unfortunately no step has been taken beyond this second argument except to state the plea.

One way to settle the question of frequency distribution of rocks, minerals and elements in nature is to set up, or attempt to set up, realistic models of processes occurring in nature and to derive the frequency distributions theoretically. The mathematical machinery for this has been with us for many years, but it has not been put to use in geochemistry.

This note describes two models of geological (or astronomical) processes and the corresponding frequency distributions.

Two approaches to the theory of frequency distribution have been highly successful in the past. One approach, that of Pearson (1894 and later), is based on a differential equation derived from the binomial distribution. The second approach, that of Kapteyn (1903), considers the effect of a large number of random impulses in time (or space).

Pearson's approach stems from a generalized treatment of the urn problem. Let us assume that the universe is made of an infinite number of different types of spheres (atoms) and that each sphere can be identified according to some characteristic (atomic weight, charge in nucleus). In the entire universe the relative abundance of the elements is fixed, so we have a distinct probability of picking any particular sphere or combination of spheres. In fact, if the individual spheres did not interact and if the universe were thoroughly mixed we could easily compute the probability of selecting a sample of, say, ten elements of a specified composition. Pearson considers the case of spheres being drawn from an urn and computes the rate of change in the probability that the number of spheres of a particular kind will be increased by 1. This type of treatment gave Pearson a differential equation

from which he derived a number of frequency distributions known as the Pearson's curves. This differential equation may be written as

$$\frac{d(\log f)}{dx} = \frac{x - a}{B_0 + B_1(x - a) + B_2(x - a)^2} \qquad \text{(see Kendall, 1948, p. 138) (1)}$$

where a is the mode of the distribution, B_0, B_1 and B_2 are arbitary constants and f is the frequency distribution.

When we deal with compositions, x is a percentage. Therefore the value of x cannot go beyond the limits 0 and 1. In fact in rocks which are saturated with oxygen the maximum content of an element cannot exceed the percentage of that element in its oxide. The maximum element content permissible in the structure of a particular mineral limits the element content of some rocks; the maximum solubility of certain ions in water limits their maximum occurrence in sea water. With these considerations, equation (1) becomes

$$\frac{d(\log f)}{dx} = \frac{1}{C} \cdot \frac{x - mk}{x(x - k)} \qquad (2)$$

Here mk is the mode when x is in per cent, k is the maximum theoretical content of an element and C is an arbitrary constant. The x in the denominator means that the lower limit of x is 0. Integration gives

$$f(x) = A\{x^m (k - x)^{1-m}\}^{1/C} \qquad (3)$$

which is a Pearson type I distribution with three constants.

In this equation C can be thought of as a constant which depends on the degree of mixing of the elements. It might be linked to the entropy of the element in the rock-forming process.

The second model of processes in nature is that of Kapteyn (1903) and is associated with a derivation of the central limit theorem. Assume that a large number of random increments E act in time on an original value x_0. In the central limit theorem, the increments are assumed to be not only random, but also independent of each other. Kapteyn extended this criterion by making each additional increment a function of the last value of the variable x. Thus where the normal criterion can be expressed by equation (4):

$$x_n = x_0 + E_0 + E_1 + \ldots + E_{n-1} \qquad (4)$$

the extended Kapteyn criterion can be written by

$$x_n = x_{n-1} + E_{n-1}G(x_{n-1}) \qquad (5)$$

where $G(x_{n-1})$ is any function of x. In some problems each additional increment is not a random variable but is proportional to x. This is a special case of Kapteyn's criterion, which leads to the lognormal distribution. Because this distribution has been postulated in geochemistry, let us see how this criterion satisfies the underlying processes leading towards the distribution of elements. Almost immediately we see that it violates the geometry of the problem. If the random increment in x is proportional to x itself, then x must have no upper bound. This cannot be reconciled with the fact that we deal with percentages, and x cannot exceed 1

(100 per cent). Because the lognormal distribution is fundamentally incorrect, let us see if some other criterion better satisfies the geochemical processes.

Suppose we have a closed system, for example an intrusive body. This body has a fixed composition and may or may not be thought of as perfectly homogeneous. If we split the body into two equal volumes by an imaginary plane we can think of the plane as an imaginary membrane which allows elements to pass back and forth from one half to the other. Suppose that element A has a relative abundance of the order of magnitude 10^{-6}. Then if we move half of the available amount from one side of the plane to the other, then the change in composition cannot exceed the order of magnitude 10^{-6}. Suppose now that the body is composed of one element C^{D} which makes up 99·9999 per cent of the body. Then the maximum change in composition that one might expect is of the order of magnitude of 10^{-4}. For if we move 50 per cent of element C_{D} from one side of the membrane to the other, then about 50 per cent of the same element must also come back. The above argument means that the random changes in composition depend not only on the previous value of the composition, but also depend on the complement, i.e. what the rock is likely to get back when it trades some of its contents. Mathematically this argument applied to the Kapteyn criterion can be expressed as

$$x_n = x_{n-1} + E_{n-1}x_{n-1}(1 - x_{n-1}) \tag{6}$$

This criterion does not lead to a lognormal distribution, but to a type which has been studied by Johnson (1949) and designated by the symbol S_B. This distribution is given by equation (7):

$$p(x) = \frac{\delta e^{-\frac{1}{2}\gamma^2}}{\sqrt{(2\pi)}} x^{-\frac{1}{2}\delta^2 \log x - (\gamma\delta+1)} (1 - x)^{-\frac{1}{2}\delta^2 \log(1-x) + \gamma\delta - 1} e^{\delta^2 \log x \log(1-x)} \tag{7}$$

A better way to study this equation is to take the logarithm of the function

$$\log p(x) = k - \log x - \log(1 - x) - \tfrac{1}{2}\{\gamma + \delta \log x - \delta \log(1 - x)\}^2 \tag{8}$$

where $k = \log\left(\frac{\delta}{\sqrt{(2\pi)}}\right)$

Note that for trace elements, $\log(1 - x) \simeq 0$ and expression (8) becomes

$$\log p(x) = -\tfrac{1}{2}\delta^2(\log x)^2 - (\gamma\delta + 1)(\log x) - (\gamma^2/2 - k) \tag{9}$$

which is essentially the equation corresponding to a lognormal distribution. Thus the Kapteyn criterion applied to a feasible process in nature leads to a distribution function which tends to become lognormal for trace elements but not for major elements.

Acknowledgement—I am indebted to A. E. Stoddard for many hours of critical discussion of this problem.

References

Ahrens L. H. (1954a) The lognormal distribution of the elements -I. *Geochim. et Cosmochim. Acta* **5**, 49–73.

Ahrens L. H. (1954b) The lognormal distribution of the elements—II. *Geochim. et Cosmochim. Acta* **6**, 121–131.

Ahrens L. H. (1957) Lognormal-type distributions—III. *Geochim. et Cosmochim. Acta* **11,** 205–212.

Aubrey K. V. (1954) Frequency distribution of the concentrations of elements in rocks. *Nature, Lond.* **174,** 141–142.

Aubrey K. V. (1956) Frequency distributions of elements in igneous rocks. *Geochim. et Cosmochim. Acta* **9,** 83–89.

Chayes F. (1954) The lognormal distribution of the elements: a discussion. *Geochim. et Cosmochim. Acta* **6,** 119–120.

Johnson N. L. (1949) Systems of frequency curves generated by methods of translation. *Biometrika* **36,** 149–176.

Kapteyn J. C. (1903) *Skew Frequency Curves in Biology and Statistics,* Noordhoff, Groningen.

Kendall M. C. (1948) *The Advanced Theory of Statistics,* Vol. II. London.

Miller R. L. and Goldberg E. D. (1955) The normal distribution in geochemistry. *Geochim. et Cosmochim. Acta* **8,** 53–62.

Pearson K. (1894) Contributions to the mathematical theory of evolution. *Phil. Trans.* **185,** 71; (1895) *Ibid.* **186,** 343; (1901) *Ibid.* **197,** 443; (1916) *Ibid.* **216,** 429.

Geochimica et Cosmochimica Acta, 1959, Vol. 16, pp. 83 to 87. Pergamon Press Ltd. Printed in Northern Ireland

Leaching of clay minerals in a limestone environment*

Dorothy Carroll and H. C. Starkey
U.S. Geological Survey, Washington 25, D.C.

(*Received* 20 *June* 1958)

Abstract—Water saturated with CO_2 at about 25°C was percolated through mixed beds of limestone or marble fragments and montmorillonite, "illite" and kaolinite in polyethylene tubes for six and forty-five complete runs. The leachates were analysed for SiO_2, Al_2O_3 and Fe_2O_3, but only SiO_2 was found. The minerals lost SiO_2 in this order: montmorillonite > kaolinite > "illite". The differential removal of SiO_2 during the short period of these experiments suggests a mechanism for the accumulation of bauxite deposits associated with limestones.

Introduction

It has been observed in many parts of the world that limestones give rise to reddish brown soils known as *terra rossa*, and that gibbsite or other hydrated aluminium oxides are also often associated with the weathering products of limestone. The presence of impurities in the limestones causes the formation of both brown soils and bauxite deposits, but the mechanism of their formation has not been studied in detail. The limestone soils of Guam, western Pacific Ocean, owe their character in part to the presence of detrital clay minerals originally deposited in the accumulating carbonate muds that later consolidated as limestones (Hathaway and Carroll, personal communication). Study of the mineralogy of these limestones suggested that an investigation of the effect of percolating water containing CO_2 on the solubility of clay minerals in a limestone environment would be interesting.

Limestones may contain clay minerals as individual flakes distributed throughout the rock as clumps of aggregated flakes or as thin beds and lenses. Small flakes of clay have a large surface area that can be attacked by solutions. If the clay occurs in beds the individual flakes are closely packed together and are therefore protected from percolating waters. Limestones that contain small quantities of insoluble residue, including clay minerals, generally form thin soils with little profile development, but limestones with lenses or beds of clay develop thicker soils with profiles characteristic of the climate in which they occur.

The solubility of clay minerals in a limestone environment was examined by setting up an experiment to simulate the percolation of carbonated water through limestone containing only a small quantity of clay mineral. The minerals used for this experiment were montmorillonite (Osage, Wyo., API standard no. 25b), "illite" (Fithian, Ill., API standard no. 35) and kaolinite (Bath, S. C., API standard no. 5).

The experiment was based on the production of $CaHCO_3$ and H_2CO_3 from limestone by leaching with carbonated water. Miller (1952, p. 162) gives the

* Publication authorized by the Director, U.S. Geological Survey, Washington 25, D.C.

following equilibrium equations for the reaction:

$$H_2O + CO_2 \rightleftharpoons H_2CO_3 \rightleftharpoons H^+ + (HCO_3)^-$$

$$CaCO_3 + H^+ + (HCO_3)^- \rightleftharpoons Ca^{2+} + 2(HCO_3)^-$$
(in solution)

The amount of CO_2 soluble in water under one atmosphere pressure of CO_2 at 25°C is 1·45 g/l. This produces a weak acid solution, 0·0329 M that reacts with the calcium carbonate and any other minerals, such as clay minerals, that may be present. Under 1 atm P_{CO_2} the solubility of calcium carbonate is 0·044 g/l.; in equilibrium with P_{CO_2} of the atmosphere the solubility is 0·86 g/l. (Miller, 1952). Garrels and Dreyer (1952) have shown that the amount of $CaCO_3$ soluble in water varies with the amount of CO_2 in solution, temperature, pressure, added salts and pH.

Experimental Procedure

The experiment consisted of two parts. The first part was a trial run to test the equipment and procedure. A layer of limestone (2–4 mm grain diameter) about 20 mm deep was placed in one end of a polyethylene drying tube* (15 × 150 mm) and held in position with filter paper so that it would not move downwards when the tube was placed vertically. Alternate thin layers of montmorillonite and limestone were added until 0·5 g of montmorillonite had been used. Tubes containing kaolinite and illite were prepared in the same way, and a blank was made with limestone alone. Each of the four tubes was connected to an aspirator bottle (1 l.). A volume of 1 l. distilled water for each of the aspirator bottles was saturated with 1 atm CO_2 by bubbling CO_2 into it until the pH was lowered to 5. The aspirator bottles were each filled with the carbonated water and attached by tubing to the drying tubes so that the water would drip vertically through the mixtures of clay minerals and limestone. The aspirator bottles were partly stoppered to prevent free access of air which would have raised the pH of the water by removal of CO_2. The tubing that connected the aspirator bottles to the drying tubes was constricted with pinchcocks to regulate the flow of the percolating water so that 1 l. of water took approximately a day to flow through the limestone clay bed. At the end of each run the pH of each water was measured. Carbon dioxide was bubbled through each solution to lower the pH to 5; the solutions were returned to the aspirator bottles and the cycle was repeated six times in all.

The clays were washed off the limestone, combined with any clay that had passed the filter paper and was present in the leaching water, and allowed to dry at room temperature. X-ray diffraction patterns were made of oriented aggregates and unoriented powders of the clays. These patterns were compared with patterns of the untreated clays.

With some modifications the second part of the experiment was run in a similar way to the first. Marble chips (4–8 mm grain diameter) were used instead of the limestone because they had less tendency to break up into clay-size particles which were difficult to separate from the clay minerals. Because the filter

* Polyethylene was used for all equipment because glass could introduce silica.

Table 1. pH readings of water before and after percolating through limestone–clay beds.

Run	Date	Blank		Montmorillonite		Kaolinite		"Illite"	
		finish	start	finish	start	finish	start	finish	start
1	4 Sept.	7·0	5·0	7·0	5·0	6·8	5·0	7·0	5·0
2	5 Sept.	6·1	5·0	6·0	5·0	6·5	5·0	6·5	5·0
3	6 Sept.	6·1	5·0	5·7	5·0	5·9	5·0	5·9	5·0
4	7 Sept.	5·8	5·0	5·6	5·0	6·0	5·0	6·2	5·0
5	8 Sept.	5·9	5·0	5·5	5·0	5·6	5·0	5·9	5·0
6	9 Sept.	5·8	5·0	5·5	5·0	6·1	5·0	5·8	5·0
7	10 Sept.	6·0	5·3	5·7	5·1	6·0	5·2	6·4	5·3
8	11 Sept.	6·0	5·4	5·6	5·1	5·9	5·3	6·3	5·4
9	12 Sept.	5·8	5·4	5·8	5·2	5·7	5·3	5·8	5·4
10	13 Sept.	6·1	5·3	5·8	5·4	6·0	5·4	6·4	5·4
11	14 Sept.	6·1	5·4	5·9	5·3	6·1	5·3	6·4	5·4
12	15 Sept.	6·0	5·4	5·8	5·4	6·1	5·3	6·4	5·4
13	16 Sept.	6·1	5·4	6·0	5·3	6·0	5·4	6·3	5·4
14	17 Sept.	6·1	5·3	5·9	5·4	6·1	5·4	6·3	5·4
15	18 Sept.	6·2	5·4	5·9	5·4	6·4	5·4	6·4	5·4
16	19 Sept.	6·0	5·4	5·9	5·4	6·1	5·4	6·5	5·4
17	20 Sept.	6·0	5·6	5·9	5·5	6·1	5·5	6·2	5·5
18	23 Sept.	6·5	5·5	6·2	5·5	6·1	5·5	6·2	5·5
19	24 Sept.	6·1	5·5	5·9	5·4	6·3	5·4	6·2	5·5
20	25 Sept.	6·2	5·4	5·9	5·4	6·2	5·4	6·5	5·5
21	26 Sept.	6·0	5·4	5·9	5·4	6·2	5·4	6·4	5·5
22	27 Sept.	6·3	5·5	6·1	5·5	6·3	5·5	6·6	6·5
23	28 Sept.	6·2	5·5	6·0	5·4	6·3	5·5	6·6	5·5
24	29 Sept.	6·1	5·5	6·0	5·4	6·2	5·5	6·4	5·5
25	30 Sept.	6·0	5·5	5·9	5·5	6·1	5·5	6·7	5·5
26	1 Oct.	6·0	5·5	6·0	5·5	6·0	5·5	6·4	5·5
27	2 Oct.	6·1	5·5	6·1	5·5	6·1	5·5	6·4	5·6
28	3 Oct.	6·0	5·5	6·1	5·5	6·2	5·5	6·4	5·6
29	4 Oct.	6·1	5·5	6·1	5·5	6·2	5·5	6·6	5·5
30	5 Oct.	6·1	5·5	5·9	5·5	6·2	5·5	6·7	5·5
31	6 Oct.	6·0	5·5	5·9	5·5	6·2	5·5	6·5	5·6
32	7 Oct.	5·9	5·4	5·9	5·5	6·1	5·5	6·5	5·6
33	8 Oct.	5·9	5·4	6·0	5·5	6·1	5·4	6·6	5·5
34	9 Oct.	6·0	5·5	6·1	5·5	6·2	5·5	6·6	5·5
35	10 Oct.	6·2	5·5	6·1	5·5	6·2	5·5	6·7	5·5
36	11 Oct.	6·0	5·5	6·1	5·5	6·0	5·5	6·7	5·5
37	12 Oct.	6·1	5·5	6·1	5·4	6·1	5·5	6·8	5·5
38	13 Oct.	6·0	5·5	—	—	6·1	5·5	6·6	5·5
39	14 Oct.	6·0	5·5	6·0	5·5	6·0	5·5	6·6	5·5
40	15 Oct.	6·1	5·5	6·1	5·5	6·1	5·5	6·4	5·5
41	16 Oct.	6·1	5·5	6·0	5·5	6·3	5·6	6·6	5·6
42	17 Oct.	6·3	5·6	6·0	5·5	6·2	5·5	6·6	5·5
43	18 Oct.	6·5	5·5	6·1	5·5	6·2	5·6	6·8	5·6
44	19 Oct.	6·6	5·5	6·1	5·5	6·1	5·6	6·5	5·6
45	20 Oct.	6·2		5·9		6·0		6·3	

Table 2. Silica removed from 0·5 g samples of montmorillonite, "illite" and kaolinite by leaching with carbonated water in a limestone enviroment

	Montmorillonite* (mg)	"Illite" (mg)	Kaolinite (mg)	Blank† (mg)
six runs	1·9	1·1	0·9	0·4
forty-five runs	3·7	1·1	1·7	0·1

* This montmorillonite contained feldspar and quartz (about 1 per cent) as impurities, but no cristobalite was detectable by X-ray diffraction.

† The blank for six runs contained 0·05 mg Al_2O_3 and 0·05 mg Fe_2O_3; the blank for forty-five runs contained 0·1 mg Al_2O_3 and 0·05 mg Fe_2O_3.

The figures for Al_2O_3 and Fe_2O_3 were identical with the figures for the blanks, and were therefore omitted from Table 2.

paper became clogged with clay, spiral paper cores of (smoking) pipe filters were placed in the lower ends of the drying tubes to prevent the clay from being washed out of the tubes. This was not entirely successful, but the amount of clay removed was less than in the first procedure. Forty-five runs were made in the second part of the experiment. Bubbling CO_2 through the solutions failed to lower the pH to 5 after the sixth run. The CO_2 was passed through the solutions until equilibrium was reached, i.e. the pH remained constant after continued additions of CO_2. The pH readings obtained during the 45 runs are given in Table 1.

After the solutions had been filtered they were made up to volume and an aliquot was analysed for SiO_2, Al_2O_3 and Fe_2O_3 by Shapiro, U.S. Geological Survey. The results are given in Table 2.

Results

The analyses of the percolating water (Table 2) showed that only silica was removed from these minerals. The greatest quantity of SiO_2 was removed from montmorillonite and the least from "illite". There was as much SiO_2 removed from montmorillonite by six runs as from kaolinite by forty five runs. The pH of the leaching water ranged from 5·0 to 6·2 for montmorillonite, from 5·0 to 6·2 for kaolinite, and from 5·0 to 6·8 for "illite". Silica is soluble within this range (Krauskopf, 1956), but Al_2O_3 (Correns, 1941) and Fe_2O_3 (Cooper, 1937) are not. Table 2 shows that time of leaching increases the amount of SiO_2 removed, so that a continuation of this process under natural conditions could cause a considerable quantity of the SiO_2 originally present in a clay mineral to be removed leaving Al_2O_3 to accumulate as gibbsite. In this experiment the attack on the tetrahedral layer of the minerals was insufficient to cause any change in their X-ray diffraction patterns.

It was found that the rate of solution of calcium carbonate decreased as described by Garrels and Dreyer (1952, p. 343) because the water becomes saturated with calcium and the pH increases. The addition of CO_2 to the water each day reduced the pH and allowed more calcium carbonate to be dissolved, thus maintaining the original leaching conditions. No Al_2O_3 went into solution because at the pH range of the solutions it is insoluble.

Conclusions

This experiment shows that carbonated water percolating through limestone containing clay minerals will remove silica from these minerals. A continuation of this process could remove most of the SiO_2 leaving Al_2O_3 and Fe_2O_3 neither of which are soluble at the pH of the leaching water. The experiment probably gives the minimum effects as ground waters passing through soils into limestone may contain very high amounts of CO_2 derived in part from organic matter, and have a pH low enough to dissolve alumina (Foster, 1950, p. 35). Circulation of water is necessary because the effect of the solution of $CaCO_3$ is to raise the pH which would maintain the exchangeable cations in the clay minerals and therefore stabilize them. However, continuation of high pH conditions would cause the aluminium octahedral layer to be attacked. The limestone environment gives rather uniform pH conditions, and it is to be expected that alumina and ferric oxide will be concentrated from the clay minerals by the continuous passage of surface waters through porous limestones containing them, and that in less porous limestones the clay minerals will either remain unattacked or silica and ferric oxide will accumulate and the alumina be removed. Both can be explained by the pH relationships.

References

Cooper L. H. N. (1937) Some conditions governing the solubility of iron. *Proc. Roy. Soc.* **124,** 299–307.

Correns C. W. (1941) Über die Löslichkeit von Kieselsäure in schwach sauren und alkalischen Lösungen. *Chem. d. Erde* **13,** 92–96.

Foster M. D. (1950) The origin of high sodium bicarbonate waters in the Atlantic and Gulf Coastal Plains. *Geochim. et Cosmochim. Acta* **1,** 33–48.

Garrels R. M. and Dreyer R. M. (1952) Mechanism of limestone replacement at low temperatures and pressures. *Bull. Geol. Soc. Amer.* **63,** 325–380.

Krauskopf K. B. (1956) Dissolution and precipitation of silica at low temperatures. *Geochim. et Cosmochim. Acta* **10,** 1–26.

Miller J. P. (1952) A portion of the system calcium carbonate-carbon dioxide–water, with geological implications. *Amer. J. Sci.* **250,** 161–203.

Geochimica et Cosmochimica Acta, 1959, Vol. 16, pp. 88 to 100. Pergamon Press Ltd. Printed in Northern Ireland

Thorium in stone meteorites by neutron activation analysis*

G. L. Bate†, J. R. Huizenga and H. A. Potratz‡
Argonne National Laboratory, Lemont, Illinois

(*Received* 22 *August* 1958)

Abstract—Radiochemical procedures for assay of Pa^{233} following neutron activation of Th^{232} in stone meteorites are described in detail. Eight analyses of five chondrites yielded an average concentration of $(3{\cdot}96 \pm 0{\cdot}20) \times 10^{-8}$ g Th/g which, with proper assumptions, leads to a cosmic atomic abundance of 0·026 for thorium (per 10^6 Si atoms). The thorium concentrations in two achondrites were found to differ by nearly two orders of magnitude. On comparison with uranium concentrations in stones determined by neutron activation analysis, the Th/U ratio in chondrites and achondrites agrees to nearly 5 per cent, yielding an average weight ratio of about 3·6.

Introduction

The abundance and distribution of thorium in those terrestrial rocks and meteorites in which the thorium concentration is less than 1 p.p.m. have defied accurate assay until very recent times, owing to the inadequate sensitivity of conventional techniques, compounded with the problem of reagent contamination in chemical processing of the sample. With the advent of high neutron flux densities in modern reactors, the application of neutron activation analysis to thorium has provided an appropriate method for assay of low-level thorium concentrations in meteorites and terrestrial rocks.

Jenkins (1955) has summarized the analytical difficulties encountered in low-level thorium analysis with conventional techniques. By radiochemical assay for thorium-233 following slow neutron irradiation, he has demonstrated the two major advantages of the method of neutron activation—namely, high sensitivity and freedom from effects of reagent contamination during chemical processing after irradiation. Further work on analysis for thorium by neutron activation via radiochemical assay for protoactinium-233 has been reported by Leddicotte and Mahlman (1956). Following an initial investigation of thorium in stone meteorites (Bate, Huizenga and Potratz, 1957) as determined by neutron activation analysis, a continuing study of this problem has been carried on at Argonne. Additional analyses completed together with the various procedures and refinements effected to date are reported in this paper, and comparison with other results and the general significance of data are further discussed.

Sample Preparation and Activation

The samples received from our immediate sources, which had previously been ground and powered (Modoc, Richardton, Holbrook and Nuevo Laredo), were placed directly in quartz vials for activation in about 0·2–0·4 g portions. Interior

* Based on work performed under the auspices of the United States Atomic Energy Commission.
† Permanent address: Department of Physics, Wheaton College, Wheaton, Ill.
‡ Permanent address: Department of Chemistry, Washington University, St. Louis 5, Missouri.

portions were taken from meteorites otherwise available in solid form (Forest City, Beardsley and Johnstown), ground and powdered in diammonite mortars, and similarly deposited in quartz vials for activation. Appropriate precautions were observed at all times to prevent possible contamination of the samples before activation.

Slow neutron activation of the samples was carried out in the "Thimble" of the Argonne CP-5 heavy water reactor, where the neutron flux density was of the order of 3×10^{13} n-cm^{-2} sec^{-1} and the Cd ratio for In activation was about 10 to 1. Thorium-232 by slow neutron absorption produces Th^{233} which decays with a 23 min half-life to protoactinium-233. In this work, radiochemical assay of the samples was based on Pa^{233}, rather than Th^{233}, both because the longer half-life of Pa^{233} provides greater convenience in working time, and because Pa^{233} has intense γ-radiation of 310 keV energy which permits convenient detection by scintillation counting. Although Pa^{233} is also β-active its 310 keV γ-activity was the preferred radioactive index because of greater ease (by use of a multiple-channel analyser) of discrimination against extraneous activity.

The course of Pa^{233} generation during activation may be described by the differential equation

$$\frac{dN_3}{dt} = \lambda_2 N_2 - \lambda_3 N_3 - F\sigma_3 N_3 \tag{1}$$

where (also for equations to follow) N_1, N_2 and N_3 are the numbers of atoms of Th^{232}, Th^{233} and Pa^{233} respectively present in the sample at time t, and λ_1, λ_2 and λ_3 are the corresponding decay constants; F represents the neutron flux density (neutrons cm^{-2} sec^{-1}) and σ_1, σ_2 and σ_3 are the respective slow neutron capture cross-sections of Th^{232}, Th^{233} and Pa^{233}. The last term in equation (1) accounts for secondary activation of Pa^{233}.

N_2 appearing in equation (1) is also a time-dependent function obeying a similar differential equation, the integration of which equation yields

$$N_2 = \frac{F\sigma_1 N_1}{\lambda_2 + F\sigma_2}\,[1 - \exp\{-(\lambda_2 + F\sigma_2)t\}]. \tag{2}$$

Substitution of equation (2) into equation (1) then permits direct integration with respect to time which, by means of a Laplace transformation and subsequent inverse transformation, gives

$$N_3 = \frac{\lambda_2 F\sigma_1 N_1}{(\lambda_2 + F\sigma_2)(\lambda_3 + F\sigma_3)}\,[1 - \exp\{-(\lambda_3 + F\sigma_3)t\}] + \frac{\lambda_2 F\sigma_1 N_1}{(\lambda_2 + F\sigma_2)(\lambda_3 + F\sigma_3 - \lambda_2 - F\sigma_2)}\,[\exp\{-(\lambda_3 + F\sigma_3)t\} - \exp\{-(\lambda_2 + F\sigma_2)t\}] \tag{3}$$

Equation (3) involves $N_2 = N_3 = 0$ at $t = 0$ as boundary conditions and moreover assumes that N_1, the number of Th^{232} atoms, is essentially constant throughout the time of activation. For the flux level used, $F\sigma_2 \ll \lambda_2$ and $F\sigma_3 \ll \lambda_3$ ($\sigma_2 = 1400$

barns and $\sigma_3 = 66$ barns) for Th^{233} and Pa^{233} respectively, so that secondary activation effects may be neglected in both cases. Noting further that $\lambda_3 \ll \lambda_2$, the Pa^{233} activity A_3 at a time τ following the end of an irradiation of duration t may be obtained from equation (3) to a good degree of approximation as

$$A_3 = F\sigma_1 N_1 \exp(-\lambda_3\tau)\left[\{1 - \exp(-\lambda_3 t)\} - \frac{\lambda_3}{\lambda_2}\{\exp(-\lambda_3 t) - \exp(-\lambda_2 t\right] \quad (4)$$

Inspection of equation (4) shows that since the half-life of Pa^{233} is 27·4 days, its activity increases at an approximately linear rate for the first several days of activation (the contribution of the last exponential from the 23 min Th^{233} becomes negligible within a few hours). Moreover, the irradiation time required to produce saturation activity is about $5\frac{1}{2}$ months. With the slow neutron flux available in the Argonne CP-5 reactor, it was found that an irradiation of 1 week produced initially, in a sample containing $\sim 10^{-9}$ g Th^{232}, several hundred counts/min of the 310 keV Pa^{233} γ-activity, well above counter background. For most samples it was therefore found unnecessary to even approach the irradiation time required for saturation activity.

By measuring the Pa^{233} activity A_3, at a time τ, the amount of Th^{232} initially present, N_1, can in principle be calculated from equation (4). Since this calculation involves the absolute determination of flux density and neutron capture cross-section, absolute counter calibration, etc., it is found in practice much easier and more accurate to compare the activity of the sample with that of a known amount of thorium irradiated under the same conditions (hereafter referred to as the flux monitor) and to calculate the amount of Th^{232} present in the sample from its proportionate activity. By counting the flux monitor under the same geometry that the sample is counted, the counter efficiency need not be determined. Other variables, not amenable to accurate experimental evaluation, are also conveniently eliminated by use of the flux monitor.

Thorium flux monitors used in this work were prepared in two ways: (a) by introducing a known amount of thorium into a meteorite matrix and (b) by mounting a known amount of thorium directly on aluminium foil. Following activation, the type (a) flux monitor is processed chemically in the same way the samples are, and for this reason will be referred to as a chemical flux monitor. The type (b) flux monitor is counted after activation without any chemical processing and hence for convenience will be designated as a physical flux monitor.

A standard thorium solution was made up with a concentration of approximately 1 μg per 25 λ (1 λ = 10^{-3} ml). A 25 λ micropipette was used for volumetric transfer of the standard solution, the 25 λ volume being considered minimal for accurate (within 1–2 per cent) transfer. Although pipetting errors would be smaller for larger volumes, the concentration of the thorium would have to be reduced proportionately in order to maintain 1 μg delivery, and it was desired to avoid weaker concentrations in order to minimize the contribution of thorium unavoidably present in the distilled water used for the standard solution. After delivery from the pipette, the pipette was washed twice with distilled water of about $\frac{1}{3}$ vol, adding the washing to the aliquot initially transferred.

Chemical flux monitors were prepared by micropipetting the 25 λ aliquot of

standard thorium solution onto a narrow strip of filter paper together with the pipette washings. The filter paper was dried under a heat lamp and then "buried" in a matrix of 0·2 g powdered chondrite contained in the same kind of quartz vial as used for the samples. The thorium present in the meteorite matrix was known to be not more than 1 per cent of the standard and hence could be corrected for with a second order correction at most. The chemical flux monitor was centrally positioned among a number of samples being activated simultaneously. Following activation the entire chemical flux monitor including meteorite powder and filter paper, was chemically treated in the same manner as the samples.

For the preparation of physical flux monitors, the standard thorium aliquot, with pipette washings, was transferred onto a $\frac{3}{4}$ in. diameter aluminium foil 0·00075 in. thick. After evaporation under a heat lamp, an identical foil was then placed on top as a cover and the edges of the pair of foils were crimped slightly to hold the cover firmly in place. The cover was retained in place during subsequent counting after activation; in fact it was never removed for any purpose.

Since the aluminium after irradiation was found to contain impurities contributing to the 310 keV γ-line (most likely chromium-51 from original Cr^{50}) two more pairs of foil were used as monitor blanks, one pair being placed on each side of the monitor and its cover. The 310 keV γ-activities of the two blank pairs of foil were subsequently measured, averaged together, and subtracted from the total 310 keV γ-activity of the flux monitor with its cover, to give the corrected activity due to the standard thorium alone.

Each sample (including the chemical monitors) was monitored by two physical flux monitors, wrapped around the quartz vials from opposite sides. A monitor "sandwich" of the $\frac{3}{4}$ in. diameter foils consisting of a blank pair of foils beneath the flux monitor proper and its cover, with another blank pair above the monitor, was found to be quite flexible, and could be conveniently wrapped around the quartz vial. The two monitor "sandwiches" were in turn held in place around the vial by a firm wrapping of ordinary commercial aluminium foil.

The variations in γ-activity (integrated counts/min at 310 keV under about 37 per cent geometry) of flux monitors of adjacent samples are displayed in Fig. 1. The twenty-six flux monitors are from a single irradiation in which the samples were arranged in two groups about 3 in. apart in an aluminium irradiation can. Each group contained six or seven vials of samples (one of which was a chemical flux monitor), all of which lay approximately in a plane within a circle of 1 in. radius. Even-numbered samples were placed in one group and odd-numbered samples were arranged in the other. This division is reflected in the figure, since the average activity differed by about 12 per cent between the two groups of samples.

The activities of the two physical flux monitors for each sample are both plotted at the same abscissa in Fig. 1 and separated by a vertical line, the length of which directly reflects their difference. It is seen that the activities of a given pair of monitors differed by no more than 5 per cent at most, and for about 75 per cent of the samples the agreement was closer to 2 per cent. For a given sample, the average of the activities of the two monitors was used to calculate the proportionate amount of thorium present in the sample.

It should be observed that, in addition to actual variations of flux density in pile space, the differences in activities of the physical flux monitors reflect the effects of other variables as well, e.g. variations in volumetric delivery of the standard thorium solution from the micropipettes, inhomogeneity of impurity content (giving rise to extraneous 310 keV γ-activity) of the aluminium foil (i.e. from piece to piece), etc. With reference to the last-named factor, the variation in

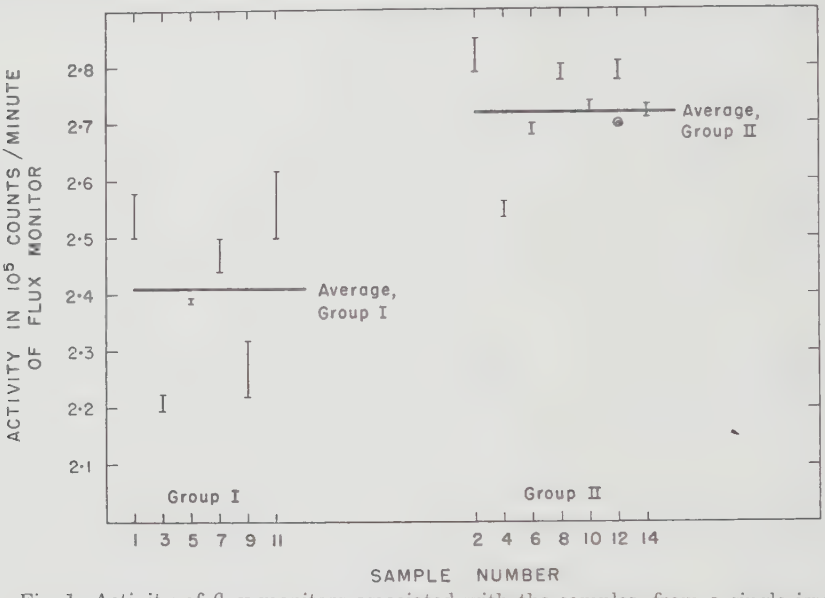

Fig. 1. Activity of flux monitors associated with the samples, from a single irradiation. The samples were divided into two groups as indicated, separated by a distance of about 3 in. along the axis of the irradiation can of 1 in. diameter. The horizontal marks at each sample number abscissa show the activities of the two physical flux monitors for that sample, and the vertical line segment between each pair of marks reflects their difference. The encircled point at abscissa 12 represents the chemical flux monitor for the Group II samples.

total 310 keV γ-activity between the two blank monitor pairs for each monitor usually amounted to about 2 per cent of their average, in rare cases to as much as 20 per cent (most of this activity was general "background" activity —not more than 5 per cent was specifically 310 keV energy).

Since the counting of the monitors shown in Fig. 1 was not all done at the same time under conditions of identical geometry, corrections were made for geometry and decay of activity with time. For the latter, half-life uncertainty would introduce a systematic rather than a statistical-type error, but may account in part for the observed spread in activities of flux monitors. Sample 12 of Group II was the chemical monitor for that group and the encircled point plotted in Fig. 1 on the abscissa for sample 12 shows the comparable activity of the chemical flux monitor for Group II samples. This value agrees to about 3 per cent with the average of the two physical flux monitors affixed to the tube of the chemical flux monitor and to within 1 per cent of the average of the physical flux monitors of Group II. This agreement is also regarded as evidence for the general reliability of the chemical procedure used, in particular of complete isotopic equilibration of

Pa^{233} with the Pa^{231} tracer used, as discussed below. A chemical flux monitor for Group I was also analysed, but the results were invalidated because of an indicated loss of a portion of the monitor activity in initial chemical processing.

The agreement of activity of the chemical flux monitor with the activities of the physical flux monitors is further regarded as evidence for the absence of self-shadowing effects in the samples. If the meteorite material possessed a large average capture cross-section, it would be expected that the charge of standard thorium in the chemical flux monitor, located as it was on a strip of filter paper centrally buried in the meteorite matrix, would exhibit a reduced activity relative to that of the physical flux monitors. Since such an effect was not observed and since the known general composition of chondrites does not admit appreciable amounts of nuclides of very large capture cross-section, it is concluded that for the sample geometry utilized (essentially cylindrical in shape, ca. 10 mm height by 3 mm diameter), self-shadowing effects are negligible.

Although several experimental variables thus far enumerated could account for the scatter of activities within a given group in Fig. 1, it is believed the spread is largely real, i.e. due to actual spatial variation in neutron flux in the pile. Since the two groups of samples were separated by a distance of 3 in. along the axis of the irradiation can, it is evident from Fig. 1 that an axial flux gradient of nearly 4 per cent per in. is indicated. This may be an indication of the magnitude of the transverse flux gradient, but the situation appears to be further compounded by local effects, since the mean deviation of the activities in Group I is substantially larger than that of Group II. Moreover, the relatively small number of data involved does not warrant a rigid interpretation because of possible statistical effects. The principal reason for regarding the variation in activity as a reflection of actual flux variation is based on an inference from the final analyses of the chondrites: namely, the thorium contents of the chondrites are more divergent (even for portions of the same meteorite) when calculated with the average activity of the group of samples than with the specific activity of the two physical monitors affixed to each given sample. This effect would not be obtained if a highly uniform flux distribution prevailed over the entire region of sample irradiation. Since the argument hinges upon an assumed uniformity of thorium distribution in the chondrites analysed, for which there is no *a priori* justification (intuitively reasonable though it may be), the conclusion stated cannot be rigorously defended.

In any event, unless special precautions are taken to ensure a demonstrably uniform neutron flux distribution for sample irradiation, it appears that the close control of flux density afforded by profuse use of flux monitors is to be highly recommended, especially if an experimental accuracy within 5 per cent is a *desideratum*.

Radiochemical Procedures

The problem of isolation and purification of Pa^{233} after irradiation was simplified by permitting samples to "cool off" for at least a week thereby eliminating the activity of many short-lived nuclides. The typical radiation level after such time was about 100 mr/hr at 2 in., with the β- and γ-activity from iron predominating.

Although the chemistry of protoactinium is not extensively defined, it is sufficiently well known to permit the isolation of trace amounts of adequate purity and good yield (Golden and Maddock, 1956) even in the presence of nearly the entire periodic table of elements, as in the

case of stone meteorites. The processing of protoactinium is complicated by its tendency toward adsorption on glass, especially in solutions of low acidity. As general precautions to minimize irreproducible behaviour and to secure maximum yield therefore, platinum and polyethylene containers were used exclusively in this work and where possible the Pa was carried in strong acid (preferably HCl) solutions at least 6 N in concentration. The separation procedures developed utilized primarily the following properties of protoactinium: co-deposition with certain precipitates (especially manganese dioxide and barium fluo-zirconate), extraction into appropriate organic solvents (di*iso*propyl ketone and di*iso*propyl carbinol) and pronounced complexing tendency with HF (forming a highly stable and tractable anion, presumably PaF_7^{2-}).

Two essentially different radiochemical procedures for Pa isolation have been developed to date, and both are given here for comparison and contrast. Comparable results with identical samples are obtained by both methods. They differ in the methods of initial opening up of the samples, as well as in subsequent cycles of purification.

Radiochemical procedure A. After weighing the activated sample in a 25 ml platinum crucible, 2 ml 6 N HCl containing ~130 α-counts/min of Pa^{231} was added. Free metallic iron in the sample was dissolved by the strong acid in a short time when the crucible was placed under the heat lamp. If hydrogen evolution persisted as the solution neared dryness, another 2 ml portion of 6 N HCl was added and the mixture taken to dryness under the heat lamp. (The initial dissolution of free iron in strong acid was effected to prevent a possible rendering of the iron into an inert form in the subsequent treatment with concentrated acids). To the dried mixture were added 3 ml concentrated HNO_3, 1 ml concentrated $HClO_4$ and 1 ml concentrated HF, and the solution was taken to moist fuming of $HClO_4$ under the heat lamp. This process was repeated two or three times, omitting HNO_3, until a clear solution was obtained, which was then taken through strong $HClO_4$ fuming to near-dryness. The overall sample digestion generally required about 2 hr time. Possible loss of Pa by volatilization during heating is regarded as negligible on the basis of the work of Golden and Maddock (1956).

The sample digestion by concentrated acid attack, especially HF, served two purposes: (a) elimination of silica via formation of volatile SiF_4; and (b) isotopic equilibration of tracer Pa^{231} with Pa^{233}. The initial removal of silica is essential since it interferes in reactions with Pa. The high HF concentration at moderate temperatures for a sustained period of time is considered ideal for true solution and equilibration of the Pa isotopes.

The residue remaining after concentrated acid digestion was taken up in a 10 ml 6 N HNO_3 solution 1 N in $Al(NO_3)_3$, Al^{3+} serving to complex any remaining F^- which might otherwise interfere with subsequent Pa separation. It was found that a trace of fine black residue remained after the nitric acid solution was transferred (by careful pipetting to permit settling of the residue) from the crucible into a 40 ml polyethylene tube. $KHSO_4$ (1 g) was added to the crucible containing the acid-insoluble residue and the mixture fused for 2–3 min. The fused mass was then dissolved in another 10 ml portion of HNO_3–$Al(NO_3)_3$ solution (with no evidence of insoluble matter), which was added, together with a small rinse, to the preceding nitrate solution. Subsequent separate analysis of the acid insoluble residue showed no evidence of Pa and the $KHSO_4$ fusion step was generally omitted.

To the combined nitrate solutions were added ½ ml $Mn(NO_3)_2$ solution (containing ~70 mg Mn per ml) and 1 ml saturated $KMnO_4$ solution. The MnO_2 precipitate was digested on the steam bath for 15–20 min. After centrifuging and washing with 5 ml 1 N HNO_3 solution, the MnO_2 precipitate was taken up in 2 ml 7 N HCl and sufficient $NH_2OH.HCl$ was added to reduce Mn^{4+} to soluble Mn^{2+}. The solution was transferred to a 15 ml polyethylene tube and contacted with an equal volume of di*iso*propyl ketone for 3–5 min. Vigorous stirring was achieved by rapid rotation of a specially designed glass stirring rod attached to the shaft of a variable speed electric motor. The ketone was removed and the aqueous solution again contacted with an equal volume of fresh ketone after adding several drops of strong HCl to the aqueous phase to raise the acidity. Each portion of ketone was washed with an equal volume of 8 N HCl and then was reduced by air-jet evaporation to a 1 ml volume. The two ketone portions were then combined and washed with 2 ml 8 N HCl.

The protoactinium in the organic phase was next back-extracted into 2 ml 6 N HCl containing 0·1 ml concentrated HF (see Moore, 1955). The aqueous phase was washed four times with 2 ml

portions of ketone which had previously been contacted with 6 N HCl. Following the washing, 0·2 g of anhydrous $AlCl_3$ was added, after which the Pa was extracted from the aqueous phase by contacting twice with 2 ml portions of ketone. Several drops of concentrated HCl were added to the aqueous phase before extracting the second time. The ketone extracts were combined, reduced by air-jet evaporation to 2 ml, and then washed with 2 ml 8 N HCl.

It was found that the aluminium carried in the organic solvent at this stage interfered with subsequent extractions and the following cycle of basic precipitation was therefore introduced to remove the aluminium. The Pa was back-extracted into 2 ml 0·1 N HCl and the process repeated. The aqueous solutions were combined and $\frac{3}{4}$ ml $La(NO_3)_3$ solution (containing 3 mg La^{3+}) was added. On the addition of ~2 ml 20% NaOH solution, $La(OH)_3$ was precipitated, carrying down Pa. After centrifuging and withdrawal of the supernate, the precipitate was washed with a 5% NaOH solution. The precipitate was then dissolved in 2–3 ml 6 N HNO_3, to which were added 0·1 ml $Mn(NO_3)_2$ solution and 1 mg each Hg^{2+} and Cr^{3+} in nitrate solution. The latter solution served as hold-back carrier for 280 keV, 48 day Hg^{203} γ-activity and 320 keV, 27 day Cr^{51} γ-activity. Lanthanum already present in solution also serves as hold-back carrier for the rare earths. The addition of $\frac{1}{4}$ ml of saturated $KMnO_4$ solution caused precipitation of MnO_2 which was treated and washed as before. The MnO_2 precipitate was dissolved in 2 ml 6 N HCl with $NH_2OH.HCl$ as previously described and the acid phase was contacted with 2 ml di*iso*propyl ketone. Following two washings with 2 ml portions of 8 N HCl and evaporation of the ketone to 1 ml volume, the Pa was back-extracted from the ketone by two successive contacts with 1 ml portions of 0·1 N HCl. The aqueous phases were combined and an equal volume of concentrated HCl added to bring normality of the solution to about 6.

A final extraction of the Pa was made into an equal volume of benzene solution $\frac{1}{4}$ M in TTA (thenoyltrifluoroacetone). After washing with 8 N HCl the TTA solution was evaporated on a platinum disk by induction heating. The final chemical yield was ascertained by α-counting the Pt disk for Pa^{231} activity. Pulse analysis verified the expected absence of extraneous α-activity. Yields averaged around 25 per cent, varying from a low of about 10 per cent to a high of over 40 per cent. It was found convenient to process two samples simultaneously, the total working time for radiochemical processing amounting to about 14 hr, equivalent to 7 hr per sample.

Radiochemical procedure B. After weighing the activated sample in a 25 ml zirconium (metal) crucible, 1 g Na_2O_2 was added and mixed with the sample. Pa^{231} tracer (~130 α-counts/min) was evaporated on a small strip of filter paper and placed in the crucible on top of the sample-peroxide mass. (Simultaneous analyses were also made for chromium, scandium and europium and appropriate carriers were added at this point. These analyses are still in progress and since they do not materially affect the Pa separation procedure, they are omitted from this report). The tracer and sample were completely covered with another 1 g portion of Na_2O_2 and the mixture was fused in the open crucible. The melt was brought to and maintained at a cherry-red heat with constant swirling for about 5 min.

The filter paper carrying the tracer underwent vigorous and rapid oxidation, which was regarded as a possible means of losing the tracer by volatilization. This difficulty was circumvented in about half of the analyses by using a strip of fibre glass cloth instead of filter paper. Although there was no observable difference in the final results by both methods of tracer introduction (loss of tracer would be reflected by unduly high apparent thorium content), the use of fibre glass cloth is the preferred technique.

After cooling, the crucible was placed in a 250 ml glass beaker, to which was added 100 ml distilled H_2O. After the fused mass had dissolved, the crucible was rinsed with 1 ml concentrated HCl followed by a small amount of H_2O, accompanied by gentle heating of the crucible in each case. At this point the solution was a muddy brown colour, of rather homogeneous appearance, dominated by $Fe(OH)_3$; no evidence of residue undissolved by fusion was detected. The mixture was allowed to sit for 10 min after dissolving 10 g NH_4Cl. The increased NH_4^+ concentration was designed to lower the pH of the solution, thereby enhancing precipitation of silicic acid. This in turn, was intended to promote quantitative scavenging of any Pa remaining in solution.

Isolation of insoluble precipitates was effected by centrifuging the solution in 35 ml portions

and decanting the supernate. Experiments with Pa tracer showed that essentially 100 per cent of the Pa introduced before fusion was carried through on the precipitate up to this point in the procedure. This evidence confirmed (a) negligible loss of Pa by volatilization during fusion and (b) quantitative carrying of Pa out of basic solution by combined $Fe(OH)_3$ and $SiO_2.H_2O$ precipitations. The precipitate was washed with 35 ml 0·1 N NH_4Cl solution. After adding 1 ml concentrated HNO_3, 1 ml concentrated $HClO_4$ and 1 ml concentrated HF, the mixture was transferred to a 100 ml platinum evaporating dish and evaporated under a heat lamp. Alternate portions of concentrated HF and concentrated $HClO_4$ were added and evaporated until a clear solution was obtained with complete elimination of SiO_2. The solution was then taken down to a very small volume with strong $HClO_4$ fuming, which was subsequently taken up in about 15 ml of 2 N HCl. At this point isotopic equilibration of the Pa isotopes was considered complete. Presumably, good isotopic mixing would be obtained in the initial fusion, with the melt at a sustained elevated temperature. This assumption need not necessarily be realized however, since both isotopes are quantitatively carried through to the treatment with concentrated HF, which as noted previously, is believed to promote ideal conditions for equilibration of the Pa isotopes.

To the 2 N HCl solution of the sample were added several ml strong NH_4OH to precipitate the hydroxides, with 1 ml in excess. After centrifuging and decanting the supernate, the precipitate was washed in 20 ml 0·1 N NH_4Cl solution and subsequently dissolved in sufficient concentrated HCl to give a 6 N acid solution. Next, 6 N HCl was added as required to bring the total volume to 10 ml in a 40 ml polyethylene centrifuge tube. After adding 0·1 ml concentrated HF, this solution was contacted with 10 ml di*iso*propyl ketone which had previously been washed with 6 N HCl. By this treatment Fe^{3+} was extracted into the organic phase while the Pa remained complexed with F^- in the aqueous phase. Next were added 1 ml saturated H_3BO_3 solution, 1 ml concentrated HCl and 0·3 g H_3BO_3 crystals. On stirring vigorously for 2 min, most of the H_3BO_3 crystals were dissolved.

On contacting the boric acid solutions with 10 ml di*iso*propyl ketone, the Pa was extracted out of the aqueous phase, leaving carrier scandium and europium in the aqueous phase. The ketone solution was washed with an equal volume of 8 N HCl and the Pa then back-extracted into an aqueous solution consisting of 2·5 ml H_2O, 0·5 ml 2 N HCl and 1 ml concentrated HF, followed by transfer to a 15 ml polyethylene centrifuge tube. To this aqueous solution (the next steps through the back-extraction from di*iso*propyl carbinol follow Potratz and Bonner, 1954) were added $\frac{3}{4}$ ml concentrated HNO_3, $\frac{1}{2}$ ml zirconyl nitrate solution (10 mg Zr per ml in 1 N HNO_3), and $\frac{1}{2}$ ml concentrated HF, and Pa was co-precipitated with barium fluo-zirconate on the addition of $\frac{3}{4}$ ml $BaCl_2$ solution (30 mg Ba per ml). The precipitate was allowed to sit for 15 min and was then washed in 2 ml H_2O. After dissolving the precipitate by heating in $\frac{3}{4}$ ml saturated H_3BO_3 solution and $\frac{1}{4}$ ml concentrated HNO_3 together with a small amount of H_2O subsequently added, the Pa was brought down with an iodate precipitate on the addition of 4 ml 1 N HIO_3 solution. The precipitate was allowed to sit for 10–15 min, washed in 2 ml H_2O, and then dissolved in 1·25 ml concentrated HCl on heating, with the subsequent addition of $\frac{1}{2}$ ml H_2O. The solution was brought to a 10 ml volume 6 N in HCl and contacted with di*iso*propyl carbinol (redistilled) in a 40 ml polyethylene centrifuge tube for 3–5 min.

After washing the carbinol twice with an equal volume of 6 N HNO_3, the Pa was then back-extracted from the organic phase into an aqueous solution consisting of 2·5 ml H_2O, 0·5 ml 1 N HNO_3 and $\frac{1}{4}$ ml concentrated HF. A basic precipitation was effected to eliminate F^- ion, by adding 0·1 ml $Mn(NO_3)_2$ solution and 2 ml concentrated NH_4OH. The $Mn(OH)_2$ precipitate was washed in a weak NH_4OH solution and dissolved in 2 ml 6 N HNO_3. A nitrate solution containing 1 mg each Hg^{2+} and Cr^{3+} was added as hold-back carrier, together with 1 ml concentrated HNO_3 and 1 ml saturated $Al(NO_3)_3$ solution to tie up any residual F^- ion. The addition of $\frac{1}{2}$ ml saturated $KMnO_4$ solution precipitated MnO_2, which was digested and washed as in procedure *A*. The precipitate was dissolved in 2 ml 6 N HCl with a trace of $NH_2OH.HCl$ and the Pa was extracted by contacting with 2 ml di*iso*propyl ketone. Following two washes with 2 ml portions of 8 N HCl, the ketone was evaporated by induction heating on a Pt disk for counting. The overall chemical yield as determined by α-counting the Pa^{231} tracer, averaged about 25 per cent. The α purity of the final yield was again verified by pulse analysis. As in

procedure *A*, it was found convenient to process two samples simultaneously, which involved a total time of about 12 hr.

The Pa^{233} γ-spectra from samples processed by both radiochemical procedures were identical to that of our standard Pa^{233} source, and no (less than 1 per cent) extraneous γ-activity was found in any of the purified sample spectra. Measurements of the half-lives of final sample activity agreed with the reported 27·4 day value for Pa^{233}, so that the identification of the final sample activity as that of Pa^{233} is quite conclusive. Possible production of γ-activity at 310 keV by fast neutron fission of Th^{232} during activation was ruled out both because the ratio of fast to slow neutrons at the immediate site of sample irradiation was known to be small, and because of the absence of fission-product γ-activity in the physical flux monitors.

α-Counting was effected with an internal 2π, continuous flow gas counter and the γ-activity was detected by means of a 3 in. $\times$ 3 in. NaI crystal (37 per cent maximum geometry) and photomultiplier tube, the output of which was fed into a 256 channel pulse height analyser. A minimum of 10^4 counts was obtained for all α- and γ-activity measurements so that statistical errors due to counting are of the order of 1 per cent in the data reported.

Results and Discussion

As a typical illustration of the experimental data obtained, sample 6–8, Forest City, weighed 0·4459 g and when analysed 81 days after activation gave a Pa^{233} 310 keV γ-activity of 293·1 counts/min (integrated over a peak width of 54 channels), which when corrected for a background of 57·9 counts/min gives a sample activity of 235·2 counts/min. In order to minimize the correction for dead-time of the analyser, the physical flux monitors, because of their much larger activity, were counted at smaller geometry. The first monitor attached to this sample gave on the same date a corresponding activity of 27,740 counts/min (corrected from 24,440 counts/min for analyser live time factor of 0·881) which when reduced by the average blank activity of 817 counts/min, gives a monitor activity of 26,920 counts/min. Corresponding numbers for the second monitor were gross activity, 27,350 counts/min; average blank activity, 722 counts/min; which gives a monitor activity of 26,630 counts/min. The average of the monitor activities becomes therefore, 26,780 counts/min which when adjusted by the geometry factor of 3·682, yields 98,600 counts/min for the monitor activity at sample geometry. From an initial tracer 127·8 α-counts/min, a final 19·25 α-counts/min were recovered in the purified sample. Since the monitor activity corresponds to 1·093 μg Th^{232}, the thorium concentration in the meteorite is calculated by direct proportion as $3{\cdot}87 \times 10^{-8}$ g Th/g Forest City.

The Argonne thorium analyses previously published (Bate *et al.*, 1957) were based on procedure *A*. Subsequent analyses effected by procedure *B* are given in Table 1. In comparing the two sets of data, the previous Holbrook datum should be ignored since subsequent analyses for other elements have also yielded spurious results and it is concluded that our original material was contaminated. The Holbrook analyses appearing in Table 1 are for a sample from a different source, as indicated in the table. The Beardsley and Forest City analyses here reported are for the identical specimen used for the analyses previously given (analyses labelled (b) in our 1957 publication). The Beardsley data nearly agree within experimental error (present reproducibility is considered close to 5 per cent) while the Forest City analyses differ by a much wider margin. The agreement on the achondrite Johnstown is poor, and our present analysis of Nuevo Laredo differs

considerably from the Los Alamos result (54×10^{-8} g Th/g) in our earlier report. In general the analyses herein reported are regarded as more accurate due to closer control of the flux monitors than realized in previous work.

Table 1 shows that with the exception of Beardsley, the thorium concentration in chondrites is quite uniform, the average deviation amounting to less than 3 per cent about a mean of $3{\cdot}84 \times 10^{-8}$ g Th/g chondrite. Since this scatter is within experimental error, the actual distribution of thorium in chondrites generally may be highly uniform.

Table 1. Thorium content of stone meteorites

Meteorite	Sample No.	10^{-8} g Th/g meteorite	Average 10^{-8} g Th/g meteorite
Chondrites			
Modoc*	3	3·90	
	4	3·94	3·92
Richardton†	5	3·96	
	6	3·64	3·80
Forest City‡	8	3·87	3·87
Holbrook†	9	3·81	
	10	3·79	3·80
Beardsley‡	14	4·77	4·77
		Average: $3{\cdot}96 \pm 0{\cdot}20$	
Achondrites			
Nuevo Laredo†	1	45·6	
	2	49·6	47·6
Johnstown, Colorado §	7	0·587	0·587

* The authors are indebted to Urey of the University of Chicago for the supply of this sample.

† These samples were supplied through the courtesy of Reed of Argonne National Laboratory, sources as follows: Richardton from Marshall of the University of Chicago, Holbrook from Urey of the University of Chicago and Nuevo Laredo from Patterson of California Institute of Technology.

‡ Samples procured from Nininger, American Meteorite Museum, Sedona, Arizona.

§ Sample procured through the good offices of Mason, American Museum of Natural History, New York, N.Y.

The high thorium concentration for Beardsley is not easily accounted for. Although the possibility of experimental error may not be ruled out, there are no reasons to ascribe this result to experimental error. A spurious result occasioned by tracer introduction on filter paper as previously discussed, is not admissible since in this analysis fibre glass material was used for tracer introduction. Contamination before activation remains a real possibility, although natural contamination by terrestrial weathering is not easily admitted since Beardsley is a dated fall, as are all the chondrites listed in the table. An alternate accounting may be afforded by statistical effects from the size of the sample: metallic iron with presumably a very low thorium content (Bate, Potratz and Huizenga, 1958) is randomly scattered throughout chondrites, and in a 0·2 g size sample, it is statistically possible for a given portion to be depleted in the iron with the result that the thorium content will appear higher than otherwise warranted.

The average of all chondrites in Table 1 is $(3{\cdot}96 \pm 0{\cdot}20) \times 10^{-8}$ g Th/g (using the first column of data instead of the averages in the second column, to avoid undue weighting of the single Beardsley result which may not be a true value) which may also be taken as the cosmic abundance of Th if chondrites constitute a valid average composition of the non-volatile part of solar matter (Urey, 1952). In terms of atomic abundance (per 10^6 atoms Si) the cosmic abundance of thorium is computed (by the same assumption) to be 0·026 using an average Si content of 0·185 by weight in primitive solar non-volatile material (Suess and Urey, 1956). This value of 0·026 for thorium may be contrasted with Goldschmidt's value of 0·59 (atomic abundance) and a more recent value of 0·136 (using their Si weight ratio of 0·178 with their reported 2×10^{-5} per cent Th) given in a review by Soviet investigators (Levin *et al.*, 1957). It appears that differences in original chemical analyses rather then diversity of weighting factors, largely account for the considerable discordance among these thorium abundance values.

Accepting the cosmic abundance of uranium, $1{\cdot}14 \times 10^{-8}$ g U/g, reported by Hamaguchi, Reed and Turkevich (1957) from analyses of chondrites, a weight ratio of cosmic thorium to uranium of 3·47 is obtained. For the achondrite Nuevo Laredo also analysed ($12{\cdot}6 \times 10^{-8}$ g U/g) by Hamaguchi *et al.* (1957) a Th/U weight ratio of 3·78 is similarly determined. The essential agreement of these two Th/U ratios is indeed noteworthy, in view of the widely different chemical compositions (and hence of chemical history) of the two types of meteorites. These values may in turn be compared with the Th/U weight ratio for terrestrial sandstones, $3{\cdot}8 \pm 0{\cdot}8$, published by Murray and Adams (1958), which may well represent an independent determination of the overall crustal Th/U ratio. These results taken together are broadly consistent with a uniform Th/U ratio in the sources of both meteoritic and terrestrial material and with the similar geochemical properties of thorium and uranium (whereby a constant Th/U ratio is generally maintained during different cycles of geochemical differentiation).

The validity of the method of neutron activation analysis applied to thorium has been discussed in our previous reports (Bate *et al.*, 1957 and 1958) and while it cannot yet be regarded as conclusively proven, there are still no known reasons to discount the method. The general internal consistency of the data herein reported, and compatibility with uranium abundances determined by neutron activation analysis might be viewed as further evidence in favour of the thorium neutron activation method, but cannot rigorously be regarded as more than a plausibility demonstration. Pending the availability of an absolute thorium standard permitting calibration with quantities of the order of 10^{-9} g Th, no conclusive statements as to absolute accuracy of the data may be made. An experimental reproducibility of 5 per cent is the best indication of relative accuracy that may be made at this time.

Areas for improvement in further research needed to broaden the base of thorium abundance data are, as indicated by this work: (a) preparation of an absolute thorium standard of low concentration and (b) removal of metallic phase (by simple magnetic extraction) prior to analysis of silicate phase, in order to minimize the role of statistical fluctuation of metallic content in small samples. The latter step is considered essential for optimum experimental reproducibility;

by weighing the metallic portion so removed, correction to gross thorium concentration may be easily made.

Acknowledgement—The authors are indebted to D. W. Engelkemeir for the use of his 256 channel scintillation spectrometer.

References

Bate G. L., Huizenga J. R. and Potratz H. A. (1957) *Science* **126**, 612.
Bate G. L., Potratz H. A. and Huizenga J. R. *Geochim. et Cosmochim. Acta* **14**, 118.
Golden J. and Maddock A. G. (1956) *J. Inorg. Nucl. Chem.* **2**, 46.
Hamaguchi H., Reed G. W. and Turkevich A. (1957) *Geochim. et Cosmochim. Acta* **12**, 337.
Jenkins E. N. (1955) *Analyst* **80**, 301.
Leddicotte G. W. and Mahlman H. A. (1956) *Proceedings of the International Conference on the Peaceful Uses of Atomic Energy* Vol. VIII, Paper P117. p. 250. United Nations, New York.
Levin B. Y., Kozlovskaia S. V. and Starkova A. G. (1957) *Geochim. et Cosmochim. Acta* **13**, 76.
Moore F. L. (1955) *Analyt. Chem.* **27**, 70.
Murray E. G. and Adams J. A. S. (1958) *Geochim. et Cosmochim. Acta* **13**, 260.
Potratz H. A. and Bonner N. A. (1954) *Los Alamos Scientific Laboratory Report* LA-1721, p. 230.
Suess H. E. and Urey H. C. (1956) *Rev. Mod. Phys.* **28**, 53.
Urey H. C. (1952) *Phys. Rev.* **88**, 248.

Geochimica et Cosmochimica Acta, 1959, Vol. 16, pp. 101 to 122. Pergamon Press Ltd. Printed in Northern Ireland

The distribution of certain trace elements in the Lower Lias of southern England

H. H. Le Riche
Soil Survey of England and Wales, Rothamsted Experimental Station, Harpenden, England

(*Received* 8 *October* 1958)

Abstract—The apparent rarity of the conditions which give rise to the teart disease of cattle in central Somerset has led to a study of the distribution of molybdenum in the Lower Lias shales from which the teart soils are derived.

Analyses of numerous specimens of shale from two boreholes and from outcrops on the coasts of Dorset and Glamorgan have shown considerable variation to occur over the formation but correlations have been found between the concentrations of molybdenum, vanadium, copper and nickel. The amounts of these elements in the shales are related to the organic carbon content and these together are related to the percentage of calcium carbonate, reaching a maximum with 20–50% $CaCO_3$.

Detailed study of one shale specimen has shown that despite the correlation of these elements with organic carbon, they are not all associated with it. Some of the molybdenum is associated with the silicates and pyrite, while nearly all the vanadium resides in the silicates. Copper and nickel appear to be mainly organically bound, although some of the latter is in exchangeable form.

Introduction

It has been known for over 100 years that in certain areas of Somerset cattle suffer from a scouring disease locally known as teart. Evidence that it was due to a condition of the pasture and not to a bacterial infection was provided by the fact that when animals were removed to other areas they rapidly recovered. Clarke (1855) and Gimingham (1914) showed that teart only occurred in areas where the soil was directly derived from the Lower Lias and the latter reported instances of it in Warwickshire and Lincolnshire. Gimingham (1914) and Muir (1936) reported a suspected association between the incidence of teart and poor soil drainage, but Ferguson *et al.* (1943) found no such association and showed that the trouble was caused by an excessive quantity of molybdenum in the soil and in the parent shale below. A solution to this apparently conflicting evidence is probably provided by Mitchell (1955) who has shown that in poorly drained soils, a number of trace elements including molybdenum are more readily available to plants than in nearby well-drained ones.

Ferguson *et al.* also found that the symptoms of teart could be suppressed by the administration of copper to the animals.

A point of interest in this matter is the apparent rarity of teart, which would seem to suggest either that such toxic concentrations of molybdenum are very unusual or that a number of predisposing factors are involved, of which high molybdenum is only one. Trouble with grazing animals due to excess molybdenum has been reported from other parts of the world but in no case do conditions appear to have been quite similar. Cunningham (1949) found that lambs grazing on reclaimed peat lands in New Zealand suffered from a copper deficiency, which in some cases was aggravated by an excess of molybdenum. Barshad (1951)

reported teart symptoms due to excess molybdenum in California, but conditions here were different since he showed that the molybdenum in the soil was largely water-soluble, decreased with depth and was derived from drainage of the surrounding high ground. In the Lias soils it is only slightly water-soluble and Lewis (1943) showed that it increases with depth to the parent material. Walsh *et al.* (1953) reported high molybdenum in pastures growing on strongly acid soils in Eire. Here again conditions appear to be quite different since in the teart soils of Somerset molybdenum is only appreciably taken up by the pasture on neutral or alkaline soils.

It might be expected that formations similar to the Lower Lias in other parts of the world would give rise to teart conditions, but little seems to have been reported. According to Goldschmidt (1954, p. 560) the Permian copper shales in Germany contain 100–200 p.p.m. Mo over wide areas; but soils derived from materials such as these would be expected to produce pasture abnormally high in copper which would suppress the ill effects of molybdenum.

It would therefore seem that the incidence of teart conditions resulting from a high level of molybdenum in the soil parent material probably requires several favourable factors:

(1) The absence of abnormally high available copper, which would act as an antidote;

(2) The presence of calcium carbonate to provide neutral or alkaline soils;

(3) Imperfect drainage conditions.

Spectrochemical analysis of a large number of Lower Lias shales has shown that big variations occur in their molybdenum contents and that these are in general accompanied by variations in the amounts of copper, nickel and vanadium and the distribution of this whole group of elements has been investigated.

Existing evidence as to the sources of molybdenum in the Lower Lias formation

Kuroda and Sandell (1954) have pointed out that molybdenum tends to become concentrated in carbonaceous shales and Goldschmidt (1954, p. 496) has shown that molybdenum, vanadium, copper and nickel, together with several other elements, tend to become concentrated in bituminous materials. It has been suggested by Bromehead (1943), quoting Dunham and Oakley, that the excessive molybdenum responsible for the teart disease probably originated in ore bodies in the Mendip Hills, which formed an island at the time of deposition in the Liassic sea. During the preceding Triassic period, molybdenum present in the galena deposits would have been oxidized to lead molybdate (wulfenite) and this would have been readily weathered during the wetter Liassic times, passing into the sea as molybdate.

Krauskopf (1956) has shown that the concentrations of Zn, Cu, Pb, Bi, Cd, Ni, Co, Hg, Ag, Cr, Mo, W and V in sea water are thousands of times less than the calculated amounts of these elements supplied to the sea during geological time and are far below the saturation levels with respect to the anions commonly present, except that in the case of Cu, Zn, Hg, Ag, Cd, Bi and Pb, precipitation as sulphide may occur under reducing conditions. A mechanism must therefore be postulated to account for their removal. He concludes that with the exception of

this latter group the removal of these elements from sea water must be brought about by adsorption, coprecipitation or organic reactions. Experiments in which he precipitated ferrous sulphide from sea water in the presence of Ni, Co, Mo, W and V showed that of these only V suffered any appreciable reduction in concentration and this reduction was to nothing like as low a concentration as occurs in sea water.

While this evidence may be relevant, it has to be borne in mind that conditions were almost certainly very different in the Liassic sea from those prevailing at present. From the worldwide distribution of black shales, it would appear that anaerobic conditions have been much more common in past geological ages than at present.

Methods of Investigation

For this investigation some 190 specimens of Lower Lias shale were analysed from two boreholes, one at Northleach, Gloucestershire and the other in central Somerset, and also from the outcrops on the coasts of Dorset and Glamorgan. In addition to the comparative study of these, one particular specimen from the *angulatum* zone at Lyme Regis, Dorset, was studied in detail to ascertain with which of the components of the shale the trace elements were associated.

All trace element determinations were made spectrochemically with a Hilger Large Quartz spectrograph, E 492, using the d.c. carbon arc cathode layer method. Determinations of Fe, K, Mg and Mn were made by the Lundegårdh flame method. Both techniques were used as described by Mitchell (1948) with a modification of the former method. The iron-variable internal standard was replaced by palladium, all standards and unknowns being mixed with an equal weight of carbon containing 0·1% Pd. The reference lines used were Pd 3242·70 Å and Pd 3460·77 Å.

The analysis lines used were those quoted by Mitchell, except in the case of vanadium. In these calcareous materials V 3185·40 was found to be interfered with by a calcium line which is not listed in the *M.I.T. Wavelength Tables* (Harrison, 1939). V 3183·41 is unaffected and proved satisfactory.

Rapid determinations of oxidizable material were made by the wet oxidation method of Tinsley (1950). Where a more accurate assessment of the organic carbon (independent of pyrite) was required, a more elaborate method was used, based on those of Clark and Ogg (1952) and Shaw (1958). One sample of the finely powdered material was heated in the reaction vessel of a gas analysis train with dilute hydrochloric acid containing ferrous chloride, the liberated CO_2 being collected and weighed in U-tubes. A second sample was subsequently heated in the same apparatus with powdered dichromate and a 60 : 40 mixture of sulphuric and phosphoric acids. The difference in weight of CO_2 obtained by the two treatments was taken to represent organic carbon.

I. Trace Element Survey of the Lower Lias

The Stowell Park borehole, Northleach

The most comprehensive set of specimens was obtained from this borehole, extending over a depth range from 760 ft below the surface (*margaritatus* zone, Middle Lias) through the entire range of the Lower Lias to 2080 ft (Rhaetic). Samples were obtained at about 20 ft intervals with their zonal identifications. All samples were ground to 100 mesh and examined spectrographically, qualitatively at first in order to ascertain which contained sufficiently high concentrations

of trace elements to warrant further investigation. Determination of percentage $CaCO_3$ and percentage oxidizable material were carried out on all the samples. The latter were done in order to obtain a quick, though fairly rough indication of organic matter content, an error being introduced by the presence of pyrite. Iron, potassium, magnesium, manganese and sulphur were also determined on most of the samples.

Analytical data for typical specimens from different zones are set out in Table 1. In view of the very variable amount of calcium carbonate, all the data (except $\%$ $CaCO_3$) are expressed on the non-calcareous basis in order to avoid spurious correlations due to the dilution effect of the carbonate.

One point which becomes apparent when the data are expressed in this manner is the remarkably constant amounts of potassium and cobalt. In some seventy-five specimens, from which those in Table 1 are selected, the former quantity nearly always lay between 2 and 3 per cent, the great majority lying between 2·4 and 2·8 per cent. The cobalt content nearly always lay between 20 and 30 p.p.m. This constancy suggests that the depositing clay was of a very uniform composition throughout the period of deposition in spite of the extremely variable amounts of calcium carbonate with which it is associated.

The *margaritatus* (Middle Lias), *davoei* and *ibex* (Lower Lias) zones were found to contain barely detectable amounts of molybdenum, although measurable amounts of all the other elements sought were found. These zones also contained quite small quantities of calcium carbonate, generally below 10 per cent. From the *jamesoni* zone downwards, the majority of shales contained from 20 to 50 per cent $CaCO_3$ and relatively large quantities of molybdenum occurring quite irregularly.

In Fig. 1, the amounts of molybdenum, vanadium, nickel, copper and oxidizable material are plotted logarithmically against depth. It is seen that, in general, the fluctuations in molybdenum content are reflected in those of the other elements, but that molybdenum varies to a much greater extent, up to a hundredfold, whereas none of the others varies more than tenfold. The molybdenum content of shales down to 1250 ft was below the limit of detection and a straight line is drawn indicating the order of concentration normally occurring in soils and clays.

The Dorset coast (*Lyme Regis*)

The detailed description by Woodward and Ussher (1911) of this classical Lias exposure greatly facilitated the sampling of particular zones. In the lower zones up to the *angulatum* the deposits consist of a succession of alternating bands of shale and limestone, the latter being usually up to about 1 ft thick, while the former are of more variable thickness. In the higher zones comprising the Black Ven Marls (*bucklandi* and *raricostatum*) and the Belemnite Marls (*jamesoni* and *ibex*) the limestone bands are fewer. All the specimens were analysed for the same elements as were those from Stowell Park: in addition, direct determinations of organic carbon were made. The analytical data are set out in Table 2.

The simultaneous variation in the contents of Mo, V, Cu, Ni and organic C is illustrated in Fig. 2, which also shows that the concentrations of Fe and S are less markedly related to the others.

Table 1. Analytical data for Stowell Park specimens
(all figures except % $CaCO_3$ expressed on non-calcareous basis)

Zone	Depth (ft)	$CaCO_3$ (%)	Fe_2O_3 (%)	K (%)	Mg (%)	Mn (%)	S (%)	Oxidizable material (as C) (%)	Mo (p.p.m.)	V (p.p.m.)	Cu (p.p.m.)	Ni (p.p.m.)	Co (p.p.m.)
Davoei	880	<1·0	3·89	1·87	0·64	<0·02	0·95	1·02	<3	77	7	45	15
	960	1·7	7·10	2·30	0·07	0·13	2·79	1·83	<3	180	20	100	26
Ibex	1059	3·9	6·88	2·14	1·02	0·05	1·86	1·34	<3	240	14	35	
	1100	53·7	11·4	2·27	1·66	0·20	3·33	2·01	<3	220	15	75	17
Jamesoni	1240	57·1	9·07	2·86	5·00	<0·04	2·49	2·26	<3	280	27	91	22
	1261	32·2	7·05	2·39	1·48	0·05	5·12	5·69	28	380	55	160	15
Raricostatum	1360	48·0	9·69	2·77	4·17	0·16		2·25	15	230	25	87	29
	1399	12·0	6·50	2·58	1·25	0·04		1·51	5	180	43	110	32
Oxynotum	1440	25·9	6·70	2·56	1·59	0·06	3·02	3·29	22	190	45	110	23
	1450	35·2	6·91	2·72	2·13	0·07		4·95	23	280	45	110	14
Obtusum	1481	15·9	6·77	2·13	0·15		5·72	3·70	89	160	32	110	21
	1540	9·7	8·86	2·06	0·11	0·06	7·90	4·59	35	190	37	140	23
Turneri	1582	6·3	7·05	2·49	1·20	0·05		2·55	7	120	26	82	26
	1596	16·8	6·52	2·44	0·79	0·02	4·74	5·75	85	320	38	150	22
Semicostatum	1659	20·3	6·67	2·64	1·97	0·06		2·32	10	160	30	97	24
	1720	24·2	7·72	2·32	1·73	0·07		6·30	150	340	61	210	33
Bucklandi	1780	14·4	9·05	2·14	1·09	0·06	8·94	5·78	120	160	40	94	19
	1822	31·5	7·69	2·28	2·45	0·09		9·59	320	270	77	220	31
Angulatum	1883	29·8	6·50	2·95	2·88	0·09		2·48	14	170	83	100	23
	1960	21·5	8·56	3·14	2·31	0·12	6·20	3·14	11	150	47	98	24
Planorbis	1982	12·2	7·37	2·77	1·63	0·13		1·93	6	170	19	93	25
	2020	16·9	7·95	2·70	1·76	0·11		2·79	19	120	44	180	34

The Somerset borehole

A further large number of specimens was examined from a borehole in central Somerset. Analytical data were obtained for the same suite of trace elements as

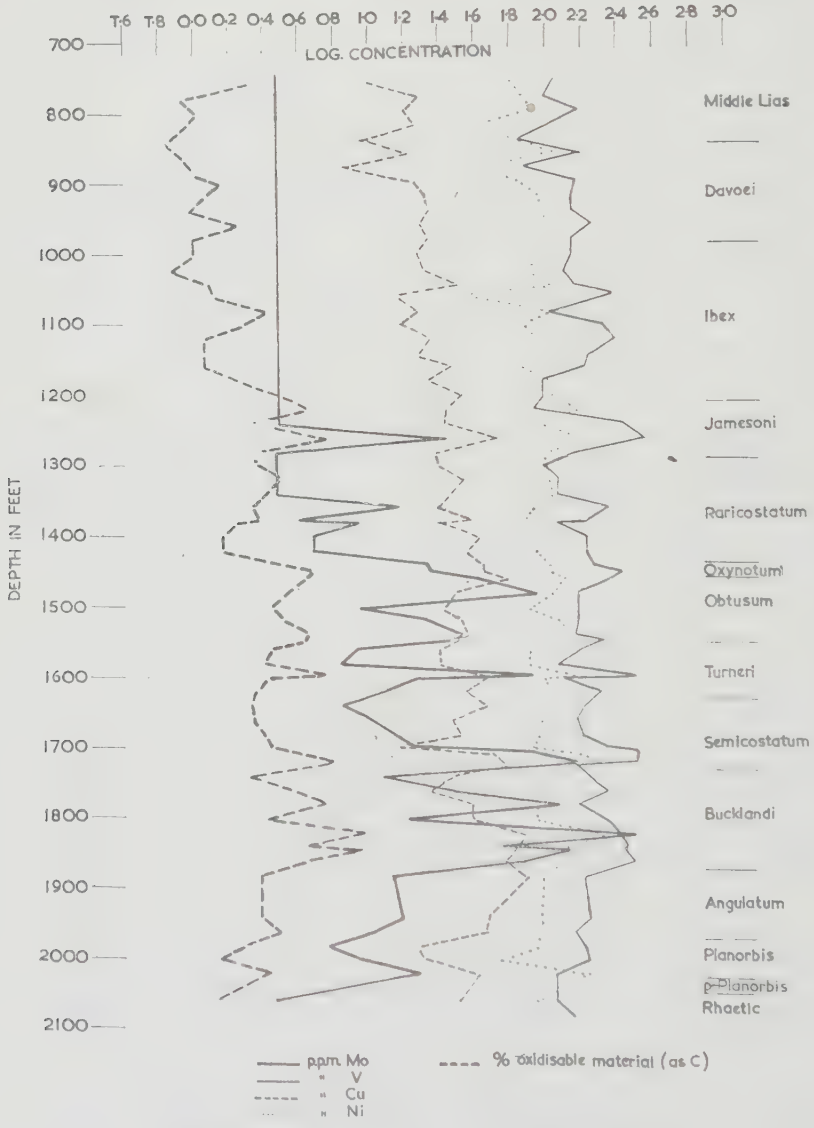

Fig. 1. Trace elements in the Lower Lias of the Stowell Park borehole.

at the two previous sites and the relationships illustrated in Figs. 1 and 2 were again found to occur. These data, being very similar to those in Tables 1 and 2 are not given here but they have been used in Figs. 3–8.

Table 2. Analytical data for Lyme Regis specimens
(all figures except % $CaCO_3$ quoted on non-calcareous basis)

Stratigraphical divisions	Zones	$CaCO_3$ (%)	Fe_2O_3 (%)	K (%)	Mg (%)	Mn (%)	S (%)	Organic carbon (%)	Mo (p.p.m.)	V (p.p.m.)	Cu (p.p.m.)	Ni (p.p.m.)	Co (p.p.m.)
Belemnite Marls	jamesoni	42·1	5·85	3·37	2·09	0·11	1·38	5·58	5	220	49	150	16
Belemnite Marls	jamesoni	17·6	7·91	2·44	1·41	0·06	3·25	1·47	<3	220	28	110	27
Black Ven Marls	oxynotum	37·9	10·4	2·70	5·35	0·18	3·28	3·32	65	290	40	130	25
Black Ven Marls	obtusum	71·6	21·4	4·90	6·03	0·17	2·57	5·95	22	220	44	78	12
Black Ven Marls	obtusum	21·7	7·19	0·95	7·87	0·19	3·08	5·69	210	340	63	130	28
Black Ven Marls	obtusum	11·0	6·70	1·85	1·26	0·06	2·19	2·99	<3	230	54	120	24
Black Ven Marls	obtusum	25·4	8·24	3·27	1·61	0·06	3·31	0·87	<3	220	32	110	40
Black Ven Marls	obtusum	14·4	7·79	2·58	1·49	0·04	3·21	5·66	50	400	69	200	29
Black Ven Marls	obtusum	14·9	7·80	2·20	1·32	0·04	3·07	2·46	13	280	47	130	24
Black Ven Marls	obtusum	40·0	7·24	2·28	4·10	0·11	1·93	2·97	6	160	40	95	19
Blue Lias	bucklandi	31·0	7·44	3·43	2·90	0·08	2·75		26	330	50	130	41
Blue Lias	angulatum	27·5	6·83	2·89	2·28	0·06	2·90	5·70	190	420	74	180	23
Blue Lias	angulatum	25·5	13·2	2·53	1·41	0·05	7·60	8·35	260	460	84	250	30
Blue Lias	angulatum	23·2	8·30	2·87	1·97	0·06	4·04	7·94	240	450	95	260	41
Blue Lias	angulatum	17·2	7·34	3·21	1·82	<0·04	3·20	6·28	85	360	78	190	39
Blue Lias	planorbis	35·4	4·95	2·84	2·06	<0·05	2·48	10·3	24	210	72	100	16
Pre-planorbis beds	pre-planorbis	55·9	6·70	2·44	1·69	0·07	2·92	10·2	7	200	53	100	31

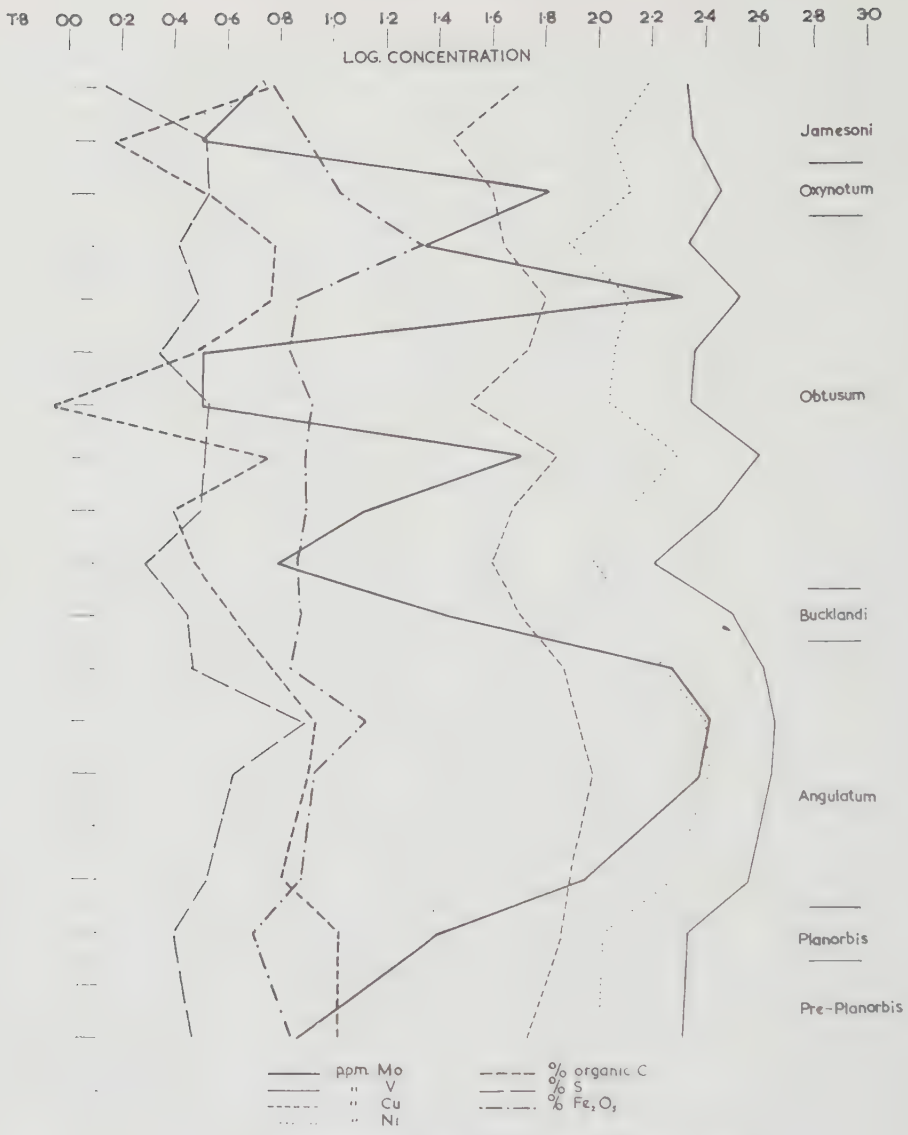

Fig. 2. Trace elements in the Lower Lias at Lyme Regis.

The relationship between trace elements and organic carbon in shales from Lyme Regis and Somerset

From the foregoing evidence it is clear that no direct proportionality exists between the amounts of these trace elements and of organic carbon in the shales, but a relationship emerges more clearly when Mo (p.p.m.) is plotted against organic carbon (%) as in Fig. 3.

The high concentrations of molybdenum always occur in shales containing organic carbon in excess of 2 per cent. The line AB can be drawn such that no points lie to the left of it, i.e. high molybdenum is always associated with high

organic carbon, whereas high organic carbon is not necessarily accompanied by high molybdenum. This would seem to suggest the presence of two distinct forms of organic matter, one of which is present in all these shales usually to the extent of at least 2 per cent, while the other is more variable in amount and is associated with molybdenum. When the content of vanadium is similarly plotted (Fig. 4) it is again found that abnormally high concentrations are associated with organic carbon in excess of 2 per cent, but that all shales contain a minimum basic level of about 150 p.p.m. V. It is therefore reasonable to postulate that the original inorganic constituents of the sediment as deposited contained this basic quantity of 150 p.p.m. and that the excess has been accumulated by the agency of the same constituent of the organic matter which accumulated the molybdenum.

Fig. 3. Somerset and Lyme Regis shales: Mo (p.p.m.) (non-calcareous basis) organic C (%).

In Figs 5 and 6 copper and nickel contents are similarly plotted and here again there appears to be a minimum basic level which with both these elements is about 60 p.p.m. By contrast, Fig. 7 shows a corresponding plot of cobalt for which there appears to be no obvious relationship, the level remaining between about 10 and 30 p.p.m. independently of organic carbon.

In the light of these observations an explanation is provided for the fact that the variations in molybdenum content as seen in Figs. 1 and 2 are so much greater than those of the other elements. In the case of vanadium, for instance, these fluctuations are superimposed on a basic content of about 150 p.p.m. which is independent of organic carbon. This figure roughly corresponds to the average amount found in clays and soils. On the other hand, the average amount of molybdenum to be expected in such materials is of the order of 2 p.p.m. only. Consequently the extra molybdenum above the basic amount is proportionately much greater than is the case with vanadium.

The relationship between trace element and calcium carbonate content in shales from Stowell Park, Lyme Regis and Somerset

In the analytical data for shales from these three sites a relationship appears between the amounts of molybdenum, vanadium, copper and nickel (non-calcareous basis) on the one hand and of calcium carbonate on the other. An inspection of the figures showed that high values for these elements occur most frequently when the

Fig. 4. Somerset and Lyme Regis shales: V (p.p.m.) (non-calcareous basis) organic C%.

calcium carbonate content lies between 20 and 50 per cent. This is illustrated in Fig. 8, in which mean values are shown for trace elements (in log. p.p.m.) in shales containing 0–10, 10–20, etc., per cent $CaCO_3$. This is only taken as far as 60 per cent $CaCO_3$ since the number of specimens with higher contents was too small to give reliable mean values. As in Figs. 1 and 2 the effect is most marked in the case of molybdenum, but the trend is similar with vanadium, copper and nickel.

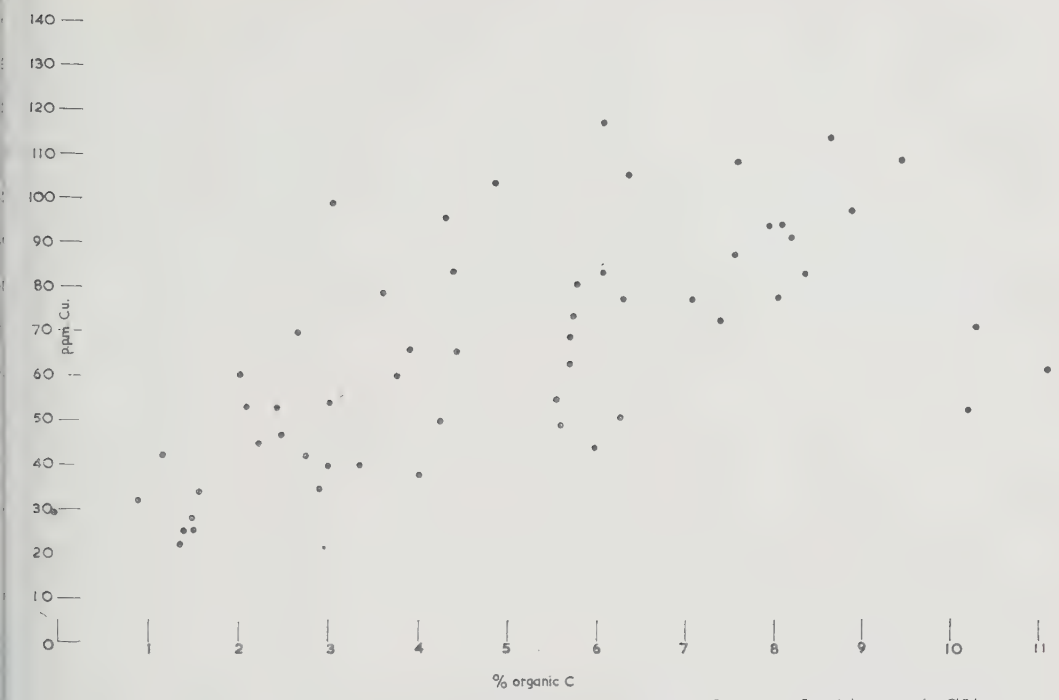

Fig. 5. Somerset and Lyme Regis shales: Cu (p.p.m.) (non-calcareous basis) organic C%.

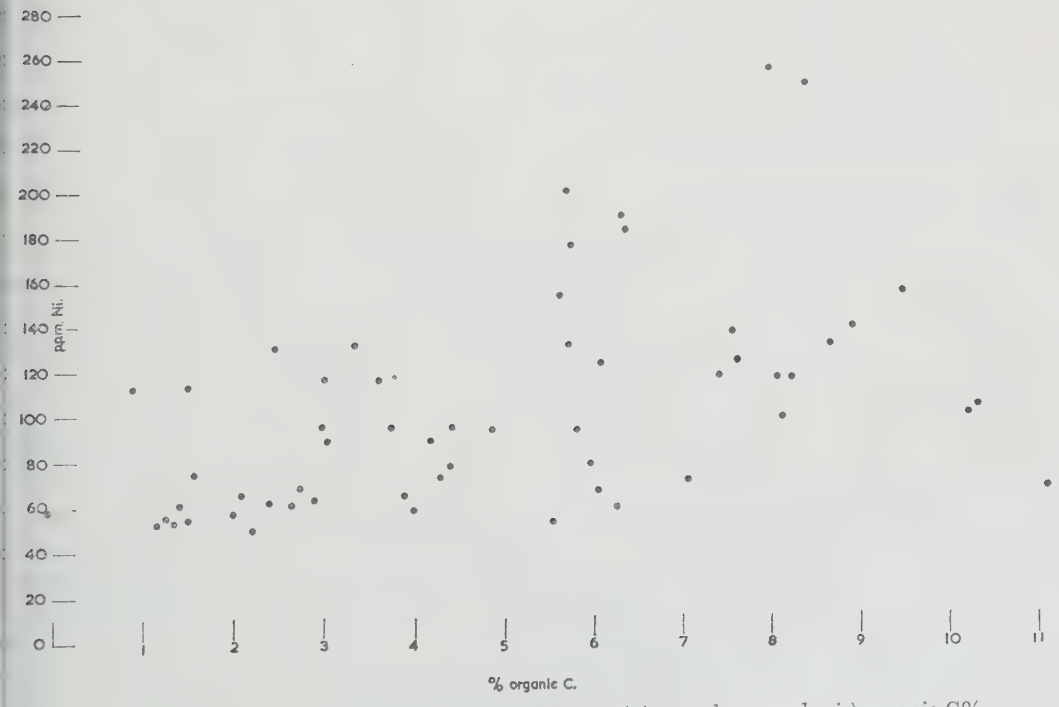

Fig. 6. Somerset and Lyme Regis shales: Ni (p.p.m.) (non-calcareous basis) organic C%.

Cobalt shows no appreciable effect. In view of the relationship shown above between these elements and organic carbon, one might likewise be expected between calcium carbonate and organic carbon and in Fig. 8 this is shown to occur. These relationships between the trace elements and calcium carbonate are therefore probably not direct, but are a result of one between the carbonate and the organic matter with which the trace elements are associated. Twenhofel (1926, p. 240) described a mechanism which could account for this relationship. He suggested that under anaerobic conditions, decaying organic matter will liberate ammonia, which forms ammonium carbonate with dissolved CO_2, so precipitating calcium salts from solution as carbonate.

Fig. 7. Somerset and Lyme Regis shales: Co (p.p.m.) (non-calcareous basis) organic C%.

Shales from the Glamorgan coast

According to Trueman (1922) the Lower Lias zones from *planorbis* to *bucklandi* are represented in the section extending around the coast of Glamorgan from Southerndown to Barry and in the outlier at Lavernock. Specimens were collected from this area for comparison with those from the same zones on the Dorset coast. In appearance the two exposures are very similar, consisting of many interstratified shale and limestone bands. At its western end, however, the Glamorgan exposure develops a littoral character and rests on Carboniferous limestone. While these zones were found to contain high levels of trace elements and organic carbon at the other three sites, analysis showed that this was not the case in Glamorgan; no high values were found comparable with those in the same zones in Dorset. It would seem likely that this is attributable to the proximity of the shore being unfavourable to the deposition of the type of organic matter with which the trace elements are associated.

The significance of this in relation to the absence of any reported cases of teart in Glamorgan is discussed elsewhere (Le Riche, 1959).

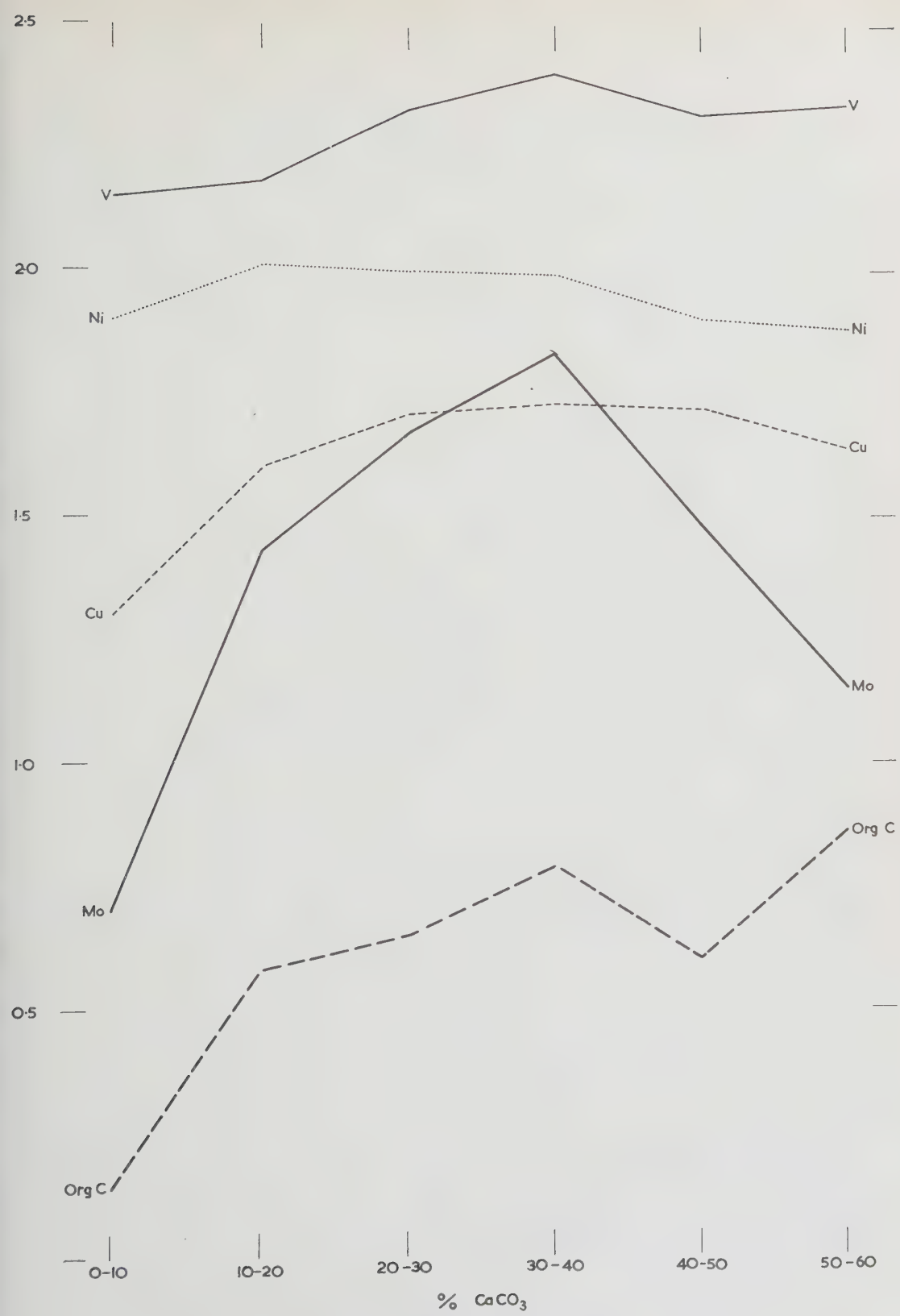

Fig. 8. Relationship between the trace element and organic carbon contents of shales (non-calcareous basis) and percentage $CaCO_3$.

II. Detailed Study of One Shale Specimen

In order to find out more about the association of molybdenum, vanadium, copper, nickel and cobalt in these shales, a detailed study was made of one specimen from the *angulatum* zone at Lyme Regis, which had been found to be particularly rich in these elements. Some 500 g of this shale were ground to 100 mesh and all experimental work performed with this fine material. Three investigations were made. In the first, after treatment with various extractants, it was separated into sand, silt and clay-sized fractions and the distribution of the elements was studied in these fractions and in the liquids used. In the second and third the shale was subjected to more drastic extraction methods and the residues again examined.

Extraction and mechanical fractionation

Samples (5 g) of shale were shaken successively with water, ammonium acetate (at pH 7 and 9), alcohol and chloroform, the residues decalcified with hydrochloric acid and separated as far as possible into sand, silt and clay sized fractions by sedimentation. The sand was further separated into heavy and light fractions with bromoform. All the liquids involved were concentrated by the method of Mitchell (1948) and were examined spectrochemically together with the solid fractions. In Table 3 analytical data are given for the untreated shale and for the separated fractions, while Table 4 shows the amount of trace elements removed by the extractants and by the water used in mechanical fractionation.

Table 3. Analytical data for original shale and mechanical fractions

Material	Oxidizable material (as C) (%)	Fe (%)	S (%)	Mo (p.p.m.)	V (p.p.m.)	Cu (p.p.m.)	Ni (p.p.m.)	Co (p.p.m.)	Amount of fraction in shale (%)
Original shale	8·16	6·89	5·66	190	315	80	110	22	—
Heavy sand (pyrite)	50·4	45·4	48·4	390	<20	100	55	<20	4·90
Light sand	14·3	6·74	6·00	180	200	115	240	36	13·2
Silt	10·9	6·70	5·06	180	190	105	140	26	22·9
Clay	2·8	4·74	0·28	30	400	60	120	28	28·7

Table 4. Amounts of trace elements extracted from shale (on original weight basis)

Method of extraction	Mo (p.p.m.)	V (p.p.m.)	Cu (p.p.m.)	Ni (p.p.m.)	Co (p.p.m.)
Water extraction	14	0·06	—	0·40	0·04
Ammonium acetate (pH 7)	5·8	0·17	—	10	0·88
Ammonium acetate (pH 9)	7·0	0·36	—	7·8	0·09
Alcohol	0·10	0·28	—	0·34	—
Chloroform	0·06	0·10	—	0·32	—
HCl	5·2	5·6	0·50	3·0	0·50
Water used in fractionation	25	1·6	6·2	6·2	1·2

From Table 4 it is seen that all the solvents except alcohol and chloroform removed appreciable quantities of molybdenum. The fact that the final water treatment removed the largest quantity can be ascribed to the larger volume of liquid used here. The behaviour of nickel and cobalt is noteworthy in that ammonium acetate removed more than did the first water extraction, suggesting that this fraction is in exchangeable form. Vanadium and copper dissolved only slightly.

Determination of oxidizable material before and after extraction and on the fractions showed little loss. Compared with the original 8·16 per cent the extraction residue contained 8·02 per cent and the fractions added together contained 7·66 per cent, indicating that the organic matter and pyrite had been virtually unaffected.

The mechanical separation did not succeed in completely dispersing the shale and the coarser fractions, apart from the pyrite, consisted of unbroken shale fragments. Therefore, while the pyrite and clay fractions can be regarded as homogeneous, the light sand and silt fractions were mixtures of varying proportions of clay, organic matter and fine pyrite.

Examination of the data in Table 3 for the separated fractions indicates that appreciable amounts of molybdenum, copper and nickel occur in the pyrite but that it contains no detectable vanadium or cobalt, while the clay fraction contains the bulk of the vanadium but is lowest in molybdenum, copper, nickel and oxidizable material. This is in marked contrast to the relationship shown to exist between these constituents in different specimens of shale, where the concentrations of molybdenum, vanadium, copper, nickel and oxidizable material showed a common general trend. Whereas the relationship between the amounts present suggests that their accumulation is due to a single cause, they are not all bound in the same manner.

Trace elements in the pyrite

If it is assumed that the sulphur in the various fractions is present entirely as pyrite and that its trace element content is independent of particle size, maximum figures are obtained for the amount of pyrite and of the elements associated with it in each fraction. Thus from the figures for the different elements in Table 3 it is possible to assess the maximum proportion in each fraction which is attributable to the pyrite (Table 5).

Table 5. (A) maximum amounts of trace elements in fractions attributable to their pyrite content (p.p.m.); (B) minimum amounts not attributable to pyrite (p.p.m.)

Material	Mo		V		Cu		Ni		Co	
	A	B	A	B	A	B	A	B	A	B
Light sand	44	136	<2·3	>198	11	104	6	234	<2·3	>34
Silt	37	143	<1·9	>188	9·5	95	5·2	130	<1·9	>24
Clay	2·0	28	<0·11	>400	0·53	60	0·29	115	<0·11	>28

These figures clearly show that the bulk of these elements does not reside in the pyrite and while much of the vanadium is apparently in the clay, this is not true of molybdenum, copper and nickel.

Loss of trace elements by solution

An important factor in regard to the contents of trace elements in the different fractions is the fact that more is likely to be dissolved from the finer fractions in the process of separation. The significance of this factor is illustrated in Tables 3 and 4 from which it can be seen that appreciable proportions of molybdenum, nickel and, to a lesser extent, cobalt were dissolved. It is therefore not justifiable to assume that the amounts of these found in the fractions are a true indication of their distribution between pyrite, organic matter and clay, although little will have been dissolved from the pyrite. The figures for vanadium and copper can be regarded as reliable since much smaller amounts of these dissolved.

Prolonged water extraction

In a second experiment the solubility of these elements was further investigated. It is to be expected that any elements which are not incorporated in large insoluble crystals (e.g. pyrite) or very strongly adsorbed, would be ultimately removable by prolonged extraction with water in a Soxhlet apparatus. Those which are present in the organic matter, pyrite or as free sulphides should be rendered relatively soluble by ignition, since elements forming anions on oxidation would be expected to form calcium salts, while the others would be converted to sulphates or oxides. Such sparingly soluble substances as calcium molybdate might be expected to dissolve in view of the small amount involved and the fact that they are continually subjected to the action of pure solvent.

Two samples, one of which had previously been ignited to 500° C, were treated with redistilled hydrochloric acid to dissolve the carbonate and the residues washed free of soluble salts, the acid and washings being retained for analysis. Both samples were then subjected to two successive extractions with water in a Soxhlet apparatus, each lasting 2 days. Some pyrite was separated from the unignited extraction residue and the remaining "light" fraction treated with dilute HF HCl mixture to remove the silicates. The extracts and aliquots from the various residues were analysed, the results being given in Table 6.

Molybdenum. From the unignited material, the acid removed 13 μg and the two water treatments 62 μg and 3·4 μg respectively. This suggests the presence of about 75 to 80 μg of molybdenum in a relatively soluble form most of which had been removed before the second water extraction. A further 39 μg were removed with the silicates. In the ignited material the rate of solution of molybdenum was reduced but it was still being extracted at the same rate in the second 2 days as in the first two, from which it would appear that although less soluble, more could have been removed by prolonged extraction.

Some evidence as to the distribution of molybdenum between the various constituents of the shale is obtained by consideration of that present in the pyrite, the specimen separated being found to contain 320 p.p.m. The total content of pyrite in the shale is not ascertainable by direct means, as it was not possible to

remove it from the finer material. However, in an earlier experiment some 6 per cent was separated, and if it is assumed that all the sulphur present (5·65 per cent) is in this form a maximum figure of 10·6 per cent pyrite is obtained. It therefore follows that the total amount of molybdenum associated with it must be between 19 and 34 μg/g of shale. Thus since the unignited residue 6 contains 76 μg Mo/g of shale it contains between 42 and 57 μg which are not associated with pyrite.

Table 6. Amounts of trace elements extracted from unignited (A) and ignited (B) shale (expressed as μg/g of original shale)

	Mo		V		Cu		Ni		Co	
	A	B	A	B	A	B	A	B	A	B
(1) Untreated shale	190		315		80		110		22	
(2) HCl extract	13	3·4	2·2	1·9	—	1·2	61	4·6	6·8	1·4
(3) HCl residue	140	150	270	300	77	83	52	94	12	18
(4) First water extract	62	22	4·2	11	0·82	4·4	0·30	0·96	<0·12	0·16
(5) Second water extract	3·4	20	2·4	15	0·24	—	0·28	0·14	<0·12	<0·12
(6) Water residue	76	110	240	220	78	79	49	87	12	15
(7) pyrite from (6)	14		—		4·0		2·2		2·3	
(8) "Light" fraction from (6)	63		230		87		45		12	
(9) Residue from HF–HCl treatment of (8)	25		8·6		43		18		5·4	

In view of the very big difference between the amounts of molybdenum removed from the unignited shale in the first and second water extractions, it may be inferred that the acid and the first water extraction removed nearly all that was relatively soluble. It would therefore appear that that present in the original shale can be divided into three distinct categories:

(1) About 80 μg relatively soluble;

(2) Between 19 and 34 μg insoluble and directly associated with pyrite;

(3) Between 42 and 57 μg insoluble but not associated with pyrite, of which 38 μg were removed by HF.

According to Barshad (1951) the solubility of molybdenite in water is 50 μg/l.; consequently any molybdenum present in this form would be expected to be in the relatively soluble fraction (1). On ignition, that associated with organic matter or sulphides would be expected to be converted to molybdate, which is probably the material which slowly dissolves out from the ignited shale.

Vanadium. Very little vanadium was removed from either sample by HCl or water, but it was almost entirely removed by HF.

Copper. Little was removed from the unignited sample, but more was extracted from the ignited sample, which is to be expected as a result of the oxidation of sulphides. An appreciable amount was removed by HF.

Nickel and cobalt. The acid treatment removed much more of both these elements from the unignited than from the ignited material, but no appreciable amount of either was removed by subsequent treatments. From this it appears that about one-half of the nickel and one-third of the cobalt are in a relatively soluble form which becomes insoluble on ignition.

Direct treatment of shale with HF–HCl *mixture*

A further investigation of this shale consisted in treating the decalcified material with successive quantities of a mixture of dilute HF and HCl, the residues at each stage being analysed for Mo, V, Cu, Ni, Co, S and ignition loss at 500° C (Table 7).

Table 7. The removal of trace elements from shale by 5% HF–HCl mixture (all figures except ignition loss expressed on original weight basis)

Material	Mo (p.p.m.)	V (p.p.m.)	Cu (p.p.m.)	Ni (p.p.m.)	Co (p.p.m.)	S (p.p.m.)	Ign. loss (%)
Original shale	190	315	80	110	22	5·7	
Decalcified residue	150	315	72	46	12	4·8	18·6
First HF residue	140	170	54	28	8·0	5·0	18·6
Second HF residue	84	36	62	26	6·0	5·0	24·6
Third HF residue	54	20	56	22	6·0	5·0	29·0
Fourth HF residue	20	6	54	24	6·0	4·8	56·4

Throughout this treatment the sulphur content has remained constant except for a small loss during decalcification, probably due to the presence of soluble sulphates. The FeS_2 is thus virtually unaffected.

Molybdenum and vanadium. Despite the very much smaller volume of solvents used here as compared with the Soxhlet extraction, about 90 per cent of the molybdenum has been removed. It is probable that the 20 p.p.m. remaining is in the pyrite.

A comparison of the behaviour of molybdenum and vanadium in the Soxhlet extraction and in this treatment shows that in the former, where vanadium was practically unaffected by leaching with water, some 50 per cent of the molybdenum was removed. In this HF–HCl extraction all the molybdenum has been removed except for a small amount attributable to the pyrite together with some 98 per cent of the vanadium. The following conclusions therefore seem probable:

(1) The vanadium is almost entirely combined with the silicates although previous examination of the different shales indicated an original association with organic matter;

(2) The bulk of the molybdenum is in a relatively soluble form loosely adsorbed on the organic matter or the clay minerals. Of the remainder, a part resides in the pyrite and a part in the silicates similarly to vanadium.

Copper, nickel and cobalt. The copper content was only slightly reduced by HF treatment as well as by water extraction, indicating that it is very firmly bound to some non-siliceous material. As with molybdenum, an appreciable proportion of the nickel and cobalt was removable by HCl. A further amount was removed by HF–HCl, but removal stopped abruptly after the second HF treatment, leaving about a quarter of the original amounts of both unattacked and apparently in a different state of combination.

Pyrite was separated from the HF–HCl residue and these three elements

together with iron were determined on the "heavy" and "light" fractions so obtained. The ratios of these elements to iron were found to be much greater in the "light" fraction, indicating that they could not be ascribed to pyrite remaining in it (see Table 8). They must therefore reside either in the organic matter or in some other non-siliceous residue.

Table 8. Ratios of copper, nickel and cobalt to iron in "heavy" and "light" fractions of HF–HCl residue

Fraction of HF–HCl residue	Cu (p.p.m.) / Fe (%)	Ni (p.p.m.) / Fe (%)	Co (p.p.m.) / Fe (%)
"Heavies"	5·1	0·7	0·7
"Lights"	28	12	3·6

Discussion

The accumulation of trace elements in reduced sediments

Except in the case of elements incorporated as intrinsic constituents of depositing minerals, the accumulation of particular elements in reduced sediments must be ultimately related to their abundance in the waters in which the sediments were laid down, whether or not any contemporary organism acted as an accumulator. Certain present-day marine animals are known to require unusual elements for their metabolic processes. Copper occurs in the respiratory pigment haemocyanin in crustaceans and molluscs, and vanadium in the blood of ascidians and holothurians. It is quite probable that such phenomena occurred in Mesozoic times; indeed, it has been suggested by Pirie (1957) that a number of the rarer elements were used in biological processes in former geological eras and that the present use of vanadium is a relic of a much wider use in the past.

Vanadium is known to be frequently present in relatively high concentrations in bituminous sediments and the mechanism of its accumulation is of considerable interest. Rankama and Sahama (1949, p. 600) suggest the possibility of its transportation as vanadate in weathering solutions and deposition as sulphide under anaerobic conditions. Goldschmidt (1954 p. 492) has stated that in the presence of reducing agents it can be precipitated as the vanadium mica, roscoelite. Jost (1932) found the vanadium content of bituminous sediments to increase with bitumen content, but Assarsson (1941) found no such relationship for vanadium or molybdenum and suggested that they were combined with sulphur. Bøgvad and Nielsen (1945) also found no relationship between vanadium and organic matter content in Swedish alum shales; they also found no vanadium whatever in the sulphides.

Bird and Calcott (1914) in a series of experiments to investigate the mutual interactions of vanadate solutions, petroleum and sulphur compounds, found that the mixture of a vanadate solution and petroleum produced a fine precipitate of sulphide in the presence of sulphide ions. This precipitate remained in suspension, but could be made to settle by the introduction of carbon dioxide. Furthermore,

exposure of such a suspension to air or oxygen over a long period produced an asphalt-like mass. They concluded that vanadate solutions could thus be transported by petroleum and deposited either as a sulphide ore or in a bituminous mass on coming into contact with carbon dioxide or air respectively.

The present work has shown that in a Lias shale, no vanadium was found in the pyrite and that nearly all of it resided in the silicate minerals. At the same time it has been shown that over a large number of shales the amount of vanadium in excess of about 150 p.p.m. is related to that of organic carbon. From this it would appear that organic matter has been directly or indirectly responsible for its accumulation and that the vanadium has subsequently migrated into a silicate crystal lattice. In these shales the organic matter has remained *in situ*, hence the rough correlation between the two. But it is possible that in certain circumstances the organic matter could lose some or all of its vanadium to the silicates and subsequently migrate elsewhere, in which case no such correlation would be found. Such an explanation could account for the apparently conflicting findings of Jost, Assarsson, and Bøgvad and Nielsen.

It seems likely that when molybdenum, copper and nickel are available in the water, they are similarly adsorbed by organic matter. Relatively large quantities of copper are not uncommon in reduced sediments. An exceptionally high concentration (up to 3 per cent) occurs in the Permian copper shales of central Europe and in the Ordovician shales of Scandinavia. By comparison with these the amount in the Lias shales is very small, being nearly always below 100 p.p.m.

It has been shown that in these Lias shales, while the nickel content is related to that of organic carbon, that of cobalt apparently is not. This may not be due to any inherent difference of properties between the two elements, but to there having been little cobalt available in the water. The fairly constant amount found in all the shales suggests that it was almost entirely deposited as a constituent of the clay, but it is possible that the small amount remaining after removal of the silicates is organically bound.

The present work indicates that when they are available, molybdenum, vanadium, copper, nickel and possibly cobalt are all apparently accumulated by organic matter. If a biological mechanism is postulated for this it requires either the existence at the time of deposition of an organism capable of accumulating all of these elements or the simultaneous presence of several different species which together could accumulate them, either of which might appear rather improbable. On the other hand, if adsorption on decomposed material is postulated it might be expected that the adsorptive capacity of such material would be greatly in excess of the amount of trace elements available for adsorption. This would produce a correlation with the amount in the water and not the relatively constant concentration in the organic matter necessary to produce the correlation which is found. Thus the evidence cannot be said to be conclusively in favour of either mechanism.

The relationship illustrated in Fig. 8 between the amounts of organic carbon and calcium carbonate implies that little change can have occurred in the relative proportions of the two since the deposits were laid down. This would appear to be at variance with the views of Richardson (1923) and Kent (1936) who have

produced strong evidence suggesting that the limestone bands occurring in the Lower Lias have been produced by post-depositional segregation. It may not necessarily be so, however, since with the majority of the shales on which Fig. 8 is based, their disposition in relation to limestone bands is unknown. It is possible that a more detailed study of those closely interstratified with limestone would not produce such a relationship.

Conclusions

The association of a proportion of the molybdenum, vanadium, copper and nickel in Lower Lias shales with organic matter seems clearly to indicate that these fractions must have been adsorbed in some way from solution. It follows from this that the water itself must at the time have contained an abnormally high concentration of molybdenum. It has been shown that the high concentrations in the shale are not confined to central Somerset and the suggestion of Bromehead (1943) that the molybdenum originated in the weathering of ore bodies in the Mendip Hills, although possibly true, would not appear to be an adequate explanation; a much larger land mass than they then comprised must be considered to have been its source.

The apparent rarity of the particular conditions which give rise to molybdenum toxicity in this case is largely due to what is evidently the unusual combination of an abnormally large amount of molybdenum and a relatively small amount of copper being brought into the sea at the time of deposition. The effect is accentuated by what little copper there is being organically bound in a form very unavailable to plants. This, added to the calcareous nature of the shales and the rather poor drainage conditions in the resulting soil all combine to produce the toxic effect.

Acknowledgements—The author is indebted to the Director of the Geological Survey of Great Britain for making available numerous specimens of shale used in this investigation, and to Dr. I. Stephen and Mr. D. F. Ball for help in the collection of specimens from the coastal exposures, also to Dr. A. Muir for much helpful discussion. This paper is based on part of a thesis approved by the University of London for the Ph.D. degree.

References

Assarsson G. (1941) See Rankama and Sahama (1949) *Geochemistry* p. 601.

Barshad I. (1951) Factors affecting the molybdenum content of pasture plants. I: Nature of soil molybdenum, growth of plants and soil pH. *Soil Sci.* **71,** 297.

Bøgvad R. and Nielsen A. H. (1945) See Rankama and Sahama (1949) *Geochemistry* p. 602.

Bird R. M. and Calcott W. S. (1914) The association of vanadium with petroleum and asphalt. *Bull. Phil. Soc. Univ. Va.* **1,** 365.

Bromehead C. E. N. (1943) Geology and health. *S. East. Nat.* **48,** 1.

Clark N. A. and Ogg C. L. (1942) A wet combustion method for determining total carbon in soils. *Soil Sci.* **53,** 27.

Clarke J. A. (1855) On the scouring lands of central Somerset. *J. Bath W. S. Co. Ass.* (2nd. Series) **3,** 52.

Cunningham I. J. (1949) Trace mineral and vitamin deficiencies in animals in New Zealand. *Proceedings of Special Conference in Agricucture, Australia* p. 272.

Ferguson W. S., Lewis A. H. and Watson S. J. (1943) The teart pastures of Somerset. I: The causes and cure of teartness. *J. Agric. Sci.* **33,** 44.

Gimingham C. T. (1914) The scouring lands of Somerset and Warwickshire. *J. Agric. Sci.* **6,** 328.
Goldschmidt V. M. (1954) *Geochemistry* (Edited by Muir A.) Clarendon Press, Oxford.
Harrison G. R. (Editor) (1939) *M. I. T. Wavelength Tables.* Wiley, New York.
Jost K. (1932) Über dem Vanadiumgehalt der Sedimentgesteine und sedimentären Lagerstätten. *Chem. d. Erde* **7,** 177.
Kent P. E. (1936) The formation of the hydraulic limestones of the Lower Lias. *Geol. Mag.* **63,** 476.
Krauskopf K. B. (1956) Factors controlling the concentrations of thirteen rare metals in sea water. *Geochim. et Cosmochim. Acta* **9,** 1.
Kuroda P. K. and Sandell E. B. (1954) Geochemistry of molybdenum. *Geochim. et Cosmochim. Acta* **6,** 35.
Le Riche H. H. (1959) Molybdenum in the Lower Lias of England and Wales in relation to the incidence of teart. *J. Soil. Sci.* In press.
Lewis A. H. (1943) The teart pastures of Somerset. II: Relation between soil and teartness. *J. Agric. Sci.* **33,** 52.
Mitchell R. L. (1948) *The Spectrographic Analysis of Soils, Plants and Related Materials.* Commonwealth Bureau of Soil Science. Tech. Comm. No. 44.
Mitchell R. L. (1955) In *Chemistry of the Soil* p. 253. (A.C.S. Monograph 126). Reinhold, New York.
Muir W. R. (1936) The teart pastures of Somerset. *Agric. Prog.* **13,** 53.
Pirie N. W. (1957) The origins of life: Moscow symposium. *Nature, Lond.* **180,** 886.
Rankama K. and Sahama T. G. (1949) *Geochemistry.* University of Chicago Press.
Richardson W. A. (1923) On the petrology of the shales-with-beef. *Quart. J. Geol. Soc. Lond.* **79,** 88.
Shaw K. (1958) Studies in nitrogen and carbon transformations in soil. Unpublished Thesis, University of London.
Tinsley J. (1950) The determination of organic carbon in soils by dichromate mixtures. *Transactions of International Congress on Soil Science, Amsterdam,* **1,** 161.
Trueman A. E. (1922) The Liassic rocks of Glamorgan. *Bull. Geol. Soc. Amer.* **33,** 245.
Twenhofel W. H. (1926) *Treatise on sedimentation.* Baillère, Tindall and Cox, London.
Walsh T., Neenan M. and O'Moore L. B. (1953) High molybdenum in herbage on acid soils. *Nature, Lond.* **171,** 1120.
Woodward H. B. and Ussher W. A. E. (1911) *The Geology of the Country around Sidmouth and Lyme Regis.* Memoirs of the Geological Survey of England and Wales, Explanation of sheets 326 and 340.

Geochimica et Cosmochimica Acta, 1959, Vol. 16, pp. 123 to 150. Pergamon Press Ltd. Printed in Northern Ireland

The geochemistry of a differentiated teschenite sill near Gunnedah, New South Wales

J. F. G. Wilkinson
Department of Geology, University of New England, Armidale, New South Wales

(*Received* 8 *October* 1958)

Abstract—Data for the commoner trace elements in the rock and component mineral series of a differentiated teschenite sill are presented. The most important trace elements in the various mineral series are: olivines, Ni, Co; clinopyroxenes, Cr, Ni, Co, V, Zr, Sc, Sr; titanomagnetites, Ga, Cr, Ni, Co, V; plagioclase feldspars, Ga, Sr, Ba; analcites, Ga, Zr, Ba, Rb. With differentiation Cr, Ni, Co and V reveal the most extreme variation, both in the rock and mineral series; these elements are absent in a vein of microcrystalline mesostasis (approximating in its composition to analcite syenite) from the uppermost levels of the sill. Zr, Ba and Rb are enriched in this liquid. Fractionation crystallization is considered to have been the differentiation mechanism responsible for the variations in the rock and mineral series.

Introduction

Although trace element data on igneous, sedimentary or metamorphic rocks, or minerals from various localities are steadily increasing, only in a few instances has emphasis been placed on trace-element distribution and trends in both the rocks and coexisting component minerals from a single intrusion, a petrographic province, or metamorphic facies. Trace element studies on both rock and component mineral series have been carried out by Nockolds and Mitchell (1948; Scottish Caledonian calc-alkaline plutonic rocks), Wager and Mitchell (1951; strongly fractionated tholeiitic Skaergaard intrusion), Howie (1955; Madras charnockite series), de Vore (1955a; various metamorphic facies) and Cornwall and Rose Jr. (1957; Keeweenawan lavas). The present study deals with major and trace element distributions and trends within the rock and mineral series of the Black Jack teschenite sill, a differentiated intrusion approximately 500 ft thick, situated 3 miles south-west of Gunnedah, New South Wales. The general geology and petrology of this intrusion have already been discussed (Wilkinson, 1958). The locations of the analysed specimens within the intrusion are shown on Fig. 2 of this paper.

The Black Jack sill is a product of alkali olivine–basalt magma (Tilley, 1950). Higazy (1952) has dealt with the distribution of trace elements in the teschenites of the Braefoot Outer Sill, Fife, described by Campbell *et al.* (1933). The behaviour of the commoner trace elements with respect to major constituents in some well-known alkali igneous rock series has been discussed by Nockolds and Allen (1954). To facilitate comparison with the latter studies, the rock analyses from the Black Jack sill have been calculated and plotted on the same basis.

In previous studies of this kind, the distribution and entry of trace elements into crystal lattices have been generally discussed primarily on the basis of the Goldschmidt rules of trace element camouflage, capture and admission. This

procedure is generally followed in the present study, although in those cases where the strict validity of these rules has been questioned (e.g. Shaw, 1953; Ringwood, 1955a), attention has been directed also to possible alternative interpretations. However, in the final assessment of the amounts of trace elements present in a series of coexisting igneous minerals, factors that are essentially petrological (e.g. the position of a particular mineral in the crystallization sequence) may prevail in addition to crystal chemical factors.

The minerals in the present study were separated by the writer, using appropriate combinations of heavy liquid centrifuging and isodynamic magnetic separation. All the spectrographic analyses were carried out by S. R. Nockolds and R. S. Allen in the Department of Mineralogy and Petrology, Cambridge, using techniques they have described elsewhere (Nockolds and Allen, 1953). The values for the various ionic radii are those for standard sixfold co-ordination (Ahrens, 1952).

The Distribution of Trace Elements in the Mineral Series

With the exception of the olivines, apatites and alkali feldspar, members of the other principal mineral series (titaniferous clinopyroxene, titanomagnetite, plagioclase feldspar, analcite) were separated from teschenites representative of the 500 ft thickness of the sill. The teschenites submitted for spectrographic analysis are listed in Table 1, together with their positions in relation to the lower intrusion contacts, and their modal compositions (weight per cent). In all tables the order of specimens (B1 → H8), with the exception of B3 which is slightly abnormal in its composition in relation to its position in the intrusion (Wilkinson, 1958), corresponds to the rock sequence on a variation diagram illustrating degree of differentiation.

Wherever possible, the major element compositions of the various mineral series, derived either from chemical analyses or from optical properties/composition diagrams (in the case of the olivines and plagioclases) are presented along

Table 1. Modal compositions and positions of analysed teschenites

Specimen	Height above lower contacts (ft)	Olivine	Clinopyroxene	Iron ore*	Feldspar†	Mesostasis and zeolite
B1	20	24·8	20·6	15·6	31·8	7·2
B2	20	21·0	22·8	17·6	23·7	14·9
B3	120	8·5	25·9	10·2	42·4	13·0
B4	270	17·2	24·8	12·3	34·5	11·2
B7	420	7·4	24·6	15·7	38·7	13·6
B9	500	2·4	31·7	17·5	27·5	20·9
H1	450–500	2·8	18·5	18·5	19·0	41·2
H8	approx. 500	0·6	24·8	18·6	13·4	42·6

Modal compositions in weight per cent.
* Dominantly titanomagnetite.
† Dominantly plagioclase, with minor anorthoclase mantling plagioclase or occurring as individual crystals.

with the minor elements. It was not considered advisable to correlate individual mineral trace element contributions with the total amount of any trace element present in each rock, owing to petrographic difficulties in determining modal primary analcite, alkaline mesostasis and alkali feldspar. However, reasonable correlation along these lines may be generally obtained in the case of Cr, Ni and Co, trace elements present in the dark minerals.

(1) *The olivines*

The olivines form an unbroken compositional sequence from Fa_{28} to Fa_{68} (weight per cent). Both individual crystals and successive crops of crystals become more fayalitic with progressive differentiation. The amount of modal olivine decreases with increasing height in the intrusion (Table 1). Olivine zoning is widespread, e.g. olivine from teschenites B3 and B7 is zoned from Fa_{37}–Fa_{59} and Fa_{46}–Fa_{57} respectively. In teschenites B1–B7, olivine was the first mineral to crystallize, although subophitic plagioclase indentations on zonal olivine margins indicate a certain amount of overlapping of crystallization of these two minerals in the final stages of consolidation. The olivines were finally separated by centrifuging in heavy liquids with specific gravities appropriate to the olivine core compositions. The present study does little to settle the debatable question of whether chromium definitely enters the olivine structure (Table 2). A small amount of Cr may be camouflaged in the minor amounts of Fe^{3+} usually reported in olivine analyses. Sandell and Goldich (1943) and Lundegårdh (1949) have reported small amounts of Cr in highly forsteritic olivines. The replacement of Cr for either Mg or Fe^{2+} requires the entry of univalent ions with ionic radius similar to Cr and with sixfold co-ordination. Lithium, which partly satisfies these requirements, is present in the Black Jack olivines only in small amounts (1–4 p.p.m.) Goldschmidt (1954) has pointed out the possibility that solid Mg_2SiO_4 at high temperature may dissolve a small amount of chromite. The Black Jack olivines all carry occasional minute dots of an opaque mineral (probably a chrome spinel) which could not be eliminated during separation (cf. Wager and Mitchell, 1951). Allotment of the olivine chromium values as contributions to the Cr content of the rock reveals a decided excess over the measured rock values. Consequently the values for chromium are bracketed and are not regarded as signifying anything other than the high insolubility of chrome spinel at a very early stage in the crystallization sequence.

The small amounts of lithium (1–4 p.p.m.) are admitted by Mg. The Skaergaard olivines contain 2–15 p.p.m. (Wager and Mitchell, 1951).

In the olivines from teschenites B1–B7, nickel remains steady at 1000 p.p.m. and thus tends to reveal enrichment relative to Mg with differentiation. This behaviour is contrary to the findings of Vogt (1923) who demonstrated a decrease in Ni with decreasing Mg. It has been customary to regard the Ni–Mg diadochy as a perfect example of camouflage. Recently Ringwood (1955a, 1956) has questioned this relationship on crystal chemical grounds and advocated that Ni in olivine is camouflaged principally by Fe^{2+} rather than by Mg. The analysed olivines, always richer in $(Mg + Fe^{2+})$ than the associated clinopyroxene or titanomagnetite, have a higher Ni content than these minerals whose Ni contents

Table 2. Major and trace elements in olivines*

Element	r	s	B1	B2	B3	B4	B7	I	II	III
Mg^{2+}	0·66		(249 . 10^3)	(221 . 10^3)	(218 . 10^3)	(207 . 10^3)	(187 . 10^3)	(240 . 10^3)	63 . 10^2	
Fe^{2+}	0·74		(153 . 10^3)	(197 . 10^3)	(202 . 10^3)	(219 . 10^3)	(252 . 10^3)	(165 . 10^3)	504 . 10^3	
Ga^{3+}	0·62	2	*	*	*	*	*	*	5	*
Cr^{3+}	0·63	2	(500)	(400)	(100)	(500)	(50)	20	*	*
Li^{+}	0·68	1	1	4	2	3	2	2	15	—
Ni^{2+}	0·69	2	1000	1000	1000	1000	1000	2000	*	820
Mo^{4+}	0·70	5	5	7	7	5	7	3	30	—
Cu^{2+}	0·72	—	—	—	—	—	—	20	20	35
Co^{2+}	0·72	5	320	320	235	235	225	150	20	230
V^{3+}	0·74	5	20	25	20	25	20	*	*	20
Mn^{2+}	0·80	—	—	—	—	—	—	2000	7800	6300
Sr^{2+}	1·12	5	*	*	*	*	*	10	20	20
Ba^{2+}	1·34	5	*	*	*	*	*	*	10	*
	Ni × 1000/Mg		4·0	4·5	4·6	5·0	5·4	8·3	—	
	Ni × 1000/Fe^{2+}		6·5	5·1	5·0	4·6	4·0	12·1	—	
	Co × 1000/Mg		1·3	1·4	1·1	1·1	1·2	0·6	3·3	
	Co × 1000/Fe^{2+}		2·1	1·6	1·2	1·1	0·9	0·9	0·04	
Compositions (weight %)†			Fa_{28}	Fa_{36}	Fa_{37}	Fa_{40}	Fa_{46}	Fa_{30}	Fa_{97}	

Sc (10), Rb (5) Cs (10) below the limits of sensitivity (in brackets) for the Black Jack olivines.

B1–B7: Olivines from teschenites, Black Jack sill (see Table 1).

I: Olivine from olivine–gabbro (1846), Skaergaard intrusion (WAGER and MITCHELL, 1951, Table B).

II: Olivine from fayalite–ferrogabbro (1881), Skaergaard intrusion (WAGER and MITCHELL, 1951, Table B).

III: Olivine from ophitic basalt (3·89) in plagioclase-rich zone, 774 ft below top of Greenstone Flow, Michigan (CORNWALL and ROSE JR., 1957, Table 2). Also present: Y 60, Sc 10, Ti 1200.

* For this and all succeeding tables, an asterisk indicates that an element is present in amounts less than the sensitivity(s).

† In the case of the Black Jack olivines, these values refer to the average compositions of the cores of the olivines, taken as the mean of compositions derived from both refractive index and Universal stage determinations.

Table 3. Major and trace elements in clinopyroxenes

Element	*r*	*s*	B1	B2	B3	B4	B7	B9	H8	I	II	III	IV	V
Si^{4+}	0·42		$218 . 10^3$						$225 . 10^3$	$235 . 10^3$	$235 . 10^3$	$199 . 10^3$	$239 . 10^3$	
Al^{3+}	0·51		$305 . 10^2$						$189 . 10^2$	$78 . 10^2$	$187 . 10^2$	$277 . 10^2$	$159 . 10^2$	
Fe^{3+}	0·64		$129 . 10^2$						$126 . 10^2$	$72 . 10^2$	$136 . 10^2$	$261 . 10^2$	$172 . 10^2$	
Mg^{2+}	0·66		$735 . 10^2$						$698 . 10^2$	$752 . 10^2$	$954 . 10^2$	$28 . 10^2$	$929 . 10^2$	
Ti^{4+}	0·68		$192 . 10^2$						$145 . 10^2$	$74 . 10^2$	$52 . 10^2$	$101 . 10^2$	$55 . 10^2$	$42 . 10^2$
Fe^{2+}	0·74		$561 . 10^2$						$734 . 10^2$	$913 . 10^2$	$658 . 10^2$	$245 . 10^3$	$414 . 10^2$	
Na^{+}	0·97		$60 . 10^2$						$52 . 10^2$	$36 . 10^2$	$52 . 10^2$	$76 . 10^2$	$25 . 10^2$	
Ca^{2+}	0·99		$159 . 10^3$						$158 . 10^3$	$151 . 10^3$	$132 . 10^3$	$877 . 10^2$	$148 . 10^3$	
K^{+}	1·33		$8 . 10^2$						$10 . 10^2$	tr.	$12 . 10^2$	$19 . 10^2$	—	
Ga^{3+}	0·62	2	15	12	15	15	12	15	15	5	3	10	6	*
Cr^{3+}	0·63	2	1000	1000	200	1000	800	65	*	10	3000	*	2500	270
Li^{+}	0·68	1	10	10	10	10	6	6	6	*	3	50	5	—
Ni^{2+}	0·69	2	175	150	80	125	125	90	20	10	200	*	90	160
Co^{2+}	0·72	5	50	50	60	50	60	60	50	35	60	15	30	75
V^{3+}	0·74	5	900	500	800	750	900	800	400	300	300	*	250	520
Zr^{4+}	0·79	10	225	200	225	225	200	225	200	90	30	*	25	30
Mn^{2+}	0·80	—	(1000)	—	—	—	—	—	(1500)	(1900)	(1500)	(6000)	(1500)	(2900)
Sc^{3+}	0·81	10	100	100	80	100	100	100	60	75	80	80	30	100
Y^{3+}	0·92	15	35	35	40	40	30	40	30	55	*	*	*	100
Sr^{2+}	1·12	5	175	150	125	125	125	125	150	20	10	100	30	60
La^{3+}	1·14	20	*	*	*	*	*	*	*	—	200	300	*	*
Ba^{2+}	1·34	5	?10	?10	?10	5	5	5	?10	—	*	60	*	*
Ga × 1000/Al			0·5						0·8	0·6	0·2	0·4	0·4	
Li × 1000/Mg			0·1						0·1	—	0·03	1·9	0·1	
Ni × 1000/Mg			2·4						0·3	0·1	2·1	—	1·0	
Co × 1000/Mg			0·7						0·7	0·5	0·6	5·4	0·3	
Fe^{2+}/Mg			0·8						1·0	1·2	0·7	88	0·4	
Ni × 1000/Fe^{2+}			3·1						0·3	0·1	3·0	—	2·2	
Co × 1000/Fe^{2+}			0·9						0·7	0·4	0·9	0·1	0·7	
Sc × 1000/Fe^{2+}			1·8						0·8	0·8	1·2	0·3	0·7	
Fe^{3+}/Fe^{2+}			0·2						0·2	0·1	0·2	0·1	0·4	
Cr × 1000/Fe^{3+}			77						—	1·4	220	—	145	
V × 1000/Fe^{3+}			70						32	42	22	—	14	

Table 3 (*contd.*)

Element	B1	B2	B3	B4	B5	B6	B7	H8	I	II	III	IV
Sr × 1000/Ca	1·1							0·9	0·1	0·1	1·1	0·2
Compositions (atom %)	$Ca_{48}Mg_{37}Fe_{15}$							$Ca_{47}Mg_{34}Fe_{19}$	$Ca_{48}Mg_{36·5}Fe_{20·5}$	$Ca_{45}Mg_{37·5}Fe_{17·5}$	$Ca_{30}Mg_{2}Fe_{68}$	$Ca_{43}Mg_{44}Fe_{13}$

For the Black Jack clinopyroxenes, Mo (5), Rb (5) and Cs (10) below the limits of sensitivity (in brackets) in all cases.

B1–H8 Bulk titaniferous clinopyroxenes from teschenites, Black Jack sill (see Table 1).

I: Clinopyroxene from pyroxene-rich laminated layer in crinanite, Eilean Mhuire sill, Shiant Isles (DREVER, 1957).

II: Clinopyroxene from olivine gabbro (4289 and 1846), Skaergaard intrusion (WAGER and MITCHELL, 1951, Table B).

III: Clinopyroxene from fayalite ferrogabbro (1881), Skaergaard intrusion (WAGER and MITCHELL, 1951, Table B). Also present: Cu 100, Rb 50.

IV: Clinopyroxene from peridotite, Garabal Hill–Glen Fyne complex (NOCKOLDS and MITCHELL, 1948, Table XV).

V: Clinopyroxene (augite) from ophitic basalt (3–89) in plagioclase-rich zone, 774 ft below top of Greenstone flow, Michigan. (CORNWALL and ROSE JR., 1957, Table 2) Also present: Cu 51.

reveal a progressive decrease with differentiation. The Ni contents of the clinopyroxene and titanomagnetite from teschenite B7 are approximately two-thirds the values in these minerals from teschenite B1. At any particular differentiation stage, the early separation of olivine no doubt facilitated the entry of Ni into the olivine structure. The relatively high Ni content of the olivine from teschenite B7 may have resulted from its lower content of modal olivine; at a given Ni concentration in the melt but with fewer olivine crystallization centres, greater opportunity for entry of Ni probably existed. Applying Ringwood's (1955b) extensions of the original Goldschmidt rules in terms of relative ionic radii and electronegativities, the distribution of Ni in the olivines is consistent with its camouflage by either Fe^{2+} or Mg, the former relationship probably being the better approximation

Molybdenum (5–7 p.p.m.) is present in all the olivines. Wager and Mitchell (1951) encountered 3–30 p.p.m. Mo in the Skaergaard olivines, suggesting that it was present replacing silicon within the oxygen tetrahedra. However Kuroda and Sandell (1954) found only 0·0–0·5 p.p.m. Mo in two dunites. On a basis of ionic radii alone, these authors do not discount the substitution of Mo for Mg or Fe^{2+}.

Cobalt is moderately concentrated in the olivines and shows a gradual decrease with differentiation. As in the Skaergaard intrusion, it is present in olivine in greater amounts than in the associated clinopyroxene or titanomagnetite. Cobalt in the olivines is camouflaged principally by Fe^{2+}. The early enrichment of Co relative to Fe^{2+} accords well from a consideration of their respective ionic radii.

Vanadium appears in all the olivines (20–25 p.p.m.). In view of the minute opaque inclusions, the presence of vanadium is treated with caution, although part may be camouflaged by the small amounts of Fe^{3+} in olivines. Lundegårdh (1946) has reported 50 p.p.m. of vanadium in an olivine (20 per cent Fe_2SiO_4) from Eastern Uppland, Sweden. De Vore (1955b) reports V and Cr in olivines from the Laramie Range anorthosites; olivines from the Keeweenawan lavas contain 20–40 p.p.m. V (Cornwall and Rose Jr., 1957).

(2) *The clinopyroxenes*

On the basis of the varied major element content of pyroxenes, Wager and Mitchell (1951) anticipated a high degree of minor element substitution in the Skaergaard clinopyroxenes. Of all the mineral series in the Black Jack sill, the clinopyroxenes exhibit the greatest variety of trace elements (Table 3). With differentiation, Cr, Ni and to a lesser extent V, decrease, while Sc and Zr are significant trace elements generally absent in the other mineral series.

In the Black Jack sill, the range in bulk clinopyroxene composition is from $Ca_{48}Mg_{37}Fe_{15}$ to $Ca_{47}Mg_{34}Fe_{19}$ (atom per cent), the clinopyroxenes in teschenites B1 and H8 respectively. Analyses of the Mg rich and Fe rich fractions of the above indicate an overall clinopyroxene composition range of $Ca_{49}Mg_{37}Fe_{14}$ to $Ca_{47}Mg_{33}Fe_{20}$. This range in composition is not comparable to that exhibited by the associated olivine, titanomagnetite or plagioclase feldspar. The most significant clinopyroxene major element variation with differentiation is replacement of Mg by Fe^{2+}. The clinopyroxenes are titaniferous salites, occasionally mantled by

a thin rim of aegirine–augite. Isolated aegirine crystals are present in the alkaline mesostasis in teschenites from the upper levels of the sill. In all four analysed pyroxenes, there is considerable substitution of Al for Si in the *z*-group. In the bulk pyroxene from teschenite H8, Ti replaces Si to a minor extent in the *z*-group.

In assessing the nature and amount of trace element substitution in the clinopyroxenes, the following factors have been considered:

(1) In view of the relatively limited variation exhibited by the major elements, any appreciable variation of a particular trace element, e.g. Cr, reflects in large part its concentration in the magma at the time of pyroxene precipitation;

(2) The substitution of Al for Si in the *z*-group no doubt favoured the entry of trivalent ions (particularly Cr, V and Sc) into the *y*-group;

(3) The position of a particular clinopyroxene in the crystallization sequence, e.g. in relation to the distribution of Cr.

Gallium (12–15 p.p.m.) is present in all the clinopyroxenes and shows little significant change with differentiation.

Of all the trace elements, chromium shows the greatest variation (1300 p.p.m. to less than 2 p.p.m.). Except in teschenite B1, the clinopyroxene is richer in Cr than the associated titanomagnetite (Table 4); the opaque mineral in the later differentiates tends to be later than the pyroxene in the crystallization sequence. The ease of entry of Cr into the *y*-group is shown by the presence of 0·8 per cent Cr in chrome diopsides and chrome augites (Hess, 1949). In the earliest Skaergaard gabbros, Wager and Mitchell (1951) recorded a high distribution factor for Cr in clinopyroxenes.

Lithium (10–6 p.p.m.) tends to decrease slightly in the later pyroxenes, and is admitted by Mg, the Li/Mg ratio remaining approximately constant.

The behaviour of nickel and cobalt is similar to that observed in the titanomagnetites (Table 4). Whereas Ni decreases fairly rapidly with differentiation (175–20 p.p.m.), Co, camouflaged by Fe^{2+}, has a relatively uniform distribution (50–60 p.p.m.). Ni is concentrated relative to Fe^{2+}, in accordance with their respective ionic radii. The associated titanomagnetite is generally richer in Ni than the pyroxene, a relationship present in the Lambertville diabase sill where the Ni content of the pyroxene varies from 240–9 p.p.m. in a thickness of approximately 1570 ft (Storm and Holland, 1957).

Vanadium, camouflaged by Fe^{3+}, undergoes moderate concentration in the pyroxenes. V appears to show an initial decrease, then increases in the middle of the series, finally decreasing to values (400 p.p.m. in H8) approximately half the vanadium content of the early pyroxene from B1. The V/Fe^{3+} ratios accord well with the respective electronegativities (Ringwood, 1955a). It may be noted that pyroxene H8 contains a smaller percentage of Al in the *z*-group, compared with pyroxene B1; in addition the V content of the magma was decreasing at this stage, since the associated titanomagnetite also reveals a sharp decrease in its V content.

The titaniferous salites from the Black Jack sill all reveal enrichment in zirconium (200–225 p.p.m.). Such values are greater than those recorded in the Skaergaard, Scottish Caledonian or Madras clinopyroxenes; Cornwall and Rose Jr. (1957) have recorded 180–2000 p.p.m. in impure Keeweenawan clinopyroxenes.

Washington and Merwin (1927) and Degenhardt (1957) have indicated the concentration of Zr in aegirines (up to 0·5 per cent Zr). The relatively higher zirconium content of the Black Jack clinopyroxenes, compared with other clinopyroxene series from different environments, resulted from their crystallizing in an alkaline environment, leading to the development of the occasional aegirine–augite rims, which are most prevalent where the salites abut against the residual alkaline mesostasis. This mesostasis in teschenite H4 contains 450 p.p.m. Zr. According to Wager and Mitchell (1951) and Ringwood (1955b), Zr replaces Ca in pyroxenes; Degenhardt (1957) suggests that the replacement is Zr^{4+} for $NaFe^{3+}$, the Fe^{3+} being responsible for the capture of the Zr.

Scandium, captured principally by Fe^{2+}, is present in moderate amounts (100 p.p.m.) and tends to show little change with differentiation until in the latest pyroxene H8 (60 p.p.m. Sc). Sc is concentrated in the pyroxene rather than in the associated olivine or titanomagnetite, a relationship found also by Wager and Mitchell (1951), Goldschmidt (1954) and Cornwall and Rose Jr. (1957). The charge balance may be attained by the substitution of Al for Si (cf. Osborn, 1950).

Yttrium, captured by calcium, shows little change with differentiation. Despite the fact that the clinopyroxenes are lime-rich members of the diopside-hedenbergite series, their strontium content is from one-thirtieth to one-fortieth that of the associated plagioclase feldspar. Similar relationships for the two mineral series have been found by Wager and Mitchell (1951) and Howie (1955). The limited Sr substitution is in agreement with the experimental work of Eskola (1922) who was unable to prepare a strontium analogue of diopside, although a strontium anorthite existed.

(3) *The titanomagnetites*

Titanomagnetite, generally homogeneous, is the most important opaque mineral in the teschenites; ilmenite grains are rare. Titanomagnetites B1 and B4 are essentially Fe_3O_4·Fe_2TiO_4·$FeTiO_3$ solid solutions, containing approximately 44 and 27 weight per cent recalculated Fe_2TiO_4 (Wilkinson, 1957). Recalculation of the analysis of titanomagnetite H8 reveals a predominantly Fe_3O_4·$FeTiO_3$ solid solution; Fe_2TiO_4 is absent. Magnetite (2308) from the Skaergaard intrusion (Table 4, analysis I) is similar in its chemistry to titanomagnetite B1, and contains 43 per cent calculated Fe_2TiO_4; in magnetite (2308) ulvöspinel is present as a separate phase.

The trace elements of the titanomagnetites are presented in Table 4. Of the three significant major elements present, namely Fe^{2+}, Fe^{3+} and Ti^{4+}, di- and trivalent iron have the greatest influence on the trace element contents. With progressive differentiation, Fe^{3+} and Ti^{4+} both increase whilst Fe^{2+} decreases.

Gallium is consistently four times as abundant in the titanomagnetites (70–80 p.p.m.) than in the associated plagioclase feldspar, a relationship encountered also by Howie (1955) in certain Madras charnockites. Both Wager and Mitchell (1951; 20–60 p.p.m.), Howie (1955; 10–120 p.p.m.) and Cornwall and Rose Jr. (1957; 10–20 p.p.m.) found Ga to be a significant trace element of magnetite but not ilmenite. Although most of the Ga in the titanomagnetites is replacing Fe^{3+}, a small percentage is camouflaged by Al.

Table 4. Major and trace elements in titanomagnetites

Element	r	s	B1	B2	B3	B4	B7	B9	H8	I	II	III
Si^{4+}	0·42		$15 . 10^2$			$25 . 10^2$			$13 . 10^3$	$11 . 10^2$	$84 . 10^2$	$22 . 10^2$
Al^{3+}	0·51		$122 . 10^2$			$188 . 10^2$			$130 . 10^2$	$41 . 10^2$	$22 . 10^2$	$1 . 10^2$
Fe^{3+}	0·64		$148 . 10^3$			$162 . 10^3$			$211 . 10^3$	$226 . 10^3$	$277 . 10^3$	$443 . 10^3$
Mg^{2+}	0·66		$116 . 10^2$			$141 . 10^2$			$47 . 10^2$	$119 . 10^2$	$4 . 10^2$	$23 . 10^2$
Ti^{4+}	0·68		$160 . 10^3$			$164 . 10^3$			$178 . 10^3$	$115 . 10^3$	$118 . 10^3$	$179 . 10^2$
Fe^{2+}	0·74		$352 . 10^3$			$325 . 10^3$			$228 . 10^3$	$335 . 10^3$	$288 . 10^3$	$251 . 10^3$
Mn^{2+}	0·80		$47 . 10^2$			$53 . 10^2$			$91 . 10^2$	$26 . 10^2$	$50 . 10^2$	—
Ca^{2+}	0·99		$42 . 10^2$			$19 . 10^2$			$188 . 10^2$	$30 . 10^2$	$58 . 10^2$	$16 . 10^2$
Ga^{3+}	0·62	2	80	80	70	80	80	80	70	20	30	15
Cr^{3+}	0·63	2	1300	450	450	350	25	30	*	200	*	5000
Ni^{2+}	0·69	2	250	250	125	320	150	125	15	300	*	150
Mo^{4+}	0·70	2	20	20	20	20	25	20	25	5	3	tr.
Co^{2+}	0·72	5	200	200	225	200	200	200	120	80	3	80
V^{3+}	0·74	5	1250	1000	1000	1500	1500	1500	1000	2000	*	4500
	$Ga \times 1000/Fe^{3+}$		0·5			0·5			0·3	0·1	0·1	0·04
	$Cr \times 1000/Fe^{3+}$		8·8			2·2			—	1·0	—	11·3
	$V \times 1000/Fe^{3+}$		8·5			9·3			4·7	8·8	—	10·2
	$Ni \times 1000/Fe^{2+}$		0·7			1·0			0·1	0·9	—	0·6
	$Co \times 1000/Fe^{2+}$		0·6			0·6			0·5	0·2	0·01	0·3

B1–H8: Titanomagnetites from teschenites, Black Jack sill (see Table 1).
I: Magnetite from hypersthene–olivine–gabbro (2308), Skaergaard intrusion. Also present: Cu 20, Sr 10, Ba 10.
II: Magnetite from fayalite–ferrogabbro (4142), Skaergaard intrusion. Also present: Cu 400, Sr 30, Ba 20. (Major elements for I and II from Vincent and Phillips, 1954, Table 2; trace elements from Wager and Mitchell, 1951, Table B).
III: Magnetite from norite (2941), Nagaramalai, Salem (Howie, 1955, Table XIV). Also present: Sn 50, Zr 30, Pb 45.

Chromium, showing enrichment relative to Fe^{3+}, shows a strong decrease with differentiation (from 1300 p.p.m. to less than 2 p.p.m.). Wager and Mitchell found chromium (200 p.p.m.) only in the magnetite from the Skaergaard hypersthene–olivine–gabbro (2308) and point out that its absence from the later magnetites is due to the chromium in large part entering earlier precipitated pyroxene and chromite. In the teschenites, titanomagnetite B1, an early precipitation mineral, is richer in Cr (1300 p.p.m.) than the associated clinopyroxene (1000 p.p.m.). In succeeding differentiates, the titanomagnetite tends to crystallize after the clinopyroxene which is then always the richer in Cr.

All the titanomagnetites are enriched in vanadium (1000–1500 p.p.m.) camouflaged by Fe^{3+} in the spinel structure. The V content and the V/Fe^{3+} ratio tend to increase in the middle stages of differentiation and then decrease. A similar trend is shown in the parent rocks, and to a lesser extent, in the associated clinopyroxene. Wager and Mitchell, and Howie found that the magnetites studied by them carried two to three times more vanadium than the associated ilmenite; Landergren (1948) states that the greater part of the vanadium enters the magnetite structure in titaniferous iron ores. There is apparently little admission of V by Ti^{4+}, despite the similarity in ionic radii. The facility with which V can enter the magnetite structure is illustrated by the V content (1000 p.p.m.) of the titanomagnetite from teschenite H8, compared with 400 p.p.m. V in the earlier crystallized associated clinopyroxene. Titanomagnetite H8 occurs as skeletal phenocrysts in a microcrystalline alkaline mesostasis which comprises approximately 40 per cent of the rock. At this advanced stage of differentiation, the removal of V from the late stage liquids by the titanomagnetite was so effective that the vanadium content of a vein of similar mesostasis (Fe^{3+} = 2·5 per cent) from teschenite H4 occurring at comparable levels in the sill is less than 5 p.p.m.

Molybdenum (20–25 p.p.m.) is present in all the titanomagnetites. Howie (1955) records up to 150 p.p.m. Mo in magnetites from the Madras charnockite series; the associated ilmenites generally have Mo less than 2 p.p.m. Kuroda and Sandell (1954) have noted the concentration of Mo in magnetite–ilmenite (up to 37 p.p.m.). The Mo probably replaced Fe^{3+} in magnetite.

Nickel and cobalt are both camouflaged by Fe^{2+} in the titanomagnetites. While Co remains steady at 200 p.p.m., dropping to 120 p.p.m. in the ore from the most differentiated teschenite H8, Ni reveals a more extreme variation (320–15 p.p.m.). The Ni/Fe^{2+} and Co/Fe^{2+} ratio trends accord reasonably well from a consideration of the respective ionic radii. The Ni content of magnetite in the tholeiitic Lambertville sill, New Jersey, decreases markedly towards the top of the sill (range 383–96 p.p.m. Ni) (Storm and Holland, 1957). The titaniferous iron ores analysed by Landergren (1948) contain on an average 200 p.p.m. Co. The relatively even distribution of Co and the progressive decrease of Ni (and Cr) in differentiated titanomagnetites has been found by Lundergårdh (1949) and Wager and Mitchell (1951).

(4) *The plagioclase feldspars*

Plagioclase feldspars in the Black Jack sill are generally lime-rich types and range in composition from An_{71} to An_{42} (weight per cent). A large percentage

Table 5. Major and trace elements in plagioclase feldspars

Element	r	s	B1	B2	B3	B4	B7	B9	H8	I	II	III	IV
Al^{3+}	0·51		(165 . 10^3)	(160 . 10^3)	(158 . 10^3)	(158 . 10^3)	(154 . 10^3)	(153 . 10^3)	(147 . 10^3)	(162 . 10^3)	(131 . 10^3)	(157 . 10^3)	
Na^{+}	0·97		(276 . 10^2)	(336 . 10^2)	(349 . 10^2)	(349 . 10^2)	(386 . 10^2)	(396 . 10^2)	(455 . 10^2)	(308 . 10^2)	(616 . 10^2)	(360 . 10^2)	
Ca^{2+}	0·99		(980 . 10^2)	(892 . 10^2)	(864 . 10^2)	(864 . 10^2)	(804 . 10^2)	(792 . 10^2)	(692 . 10^2)	(932 . 10^2)	(432 . 10^2)	(850 . 10^2)	
Ga^{3+}	0·62	2	20	25	20	15	20	20	15	35	200	20	40
Cr^{3+}	0·63	2	3	3	3	*	*	*	*	10	*	10	4
Li^{+}	0·68	1	1	*	*	2	*	1	*	2	*	7	—
Ni^{2+}	0·69	2	3	5	*	*	*	*	(4)	10	*	10	7
Cu^{2+}	0·72	—	—	—	—	—	—	—	—	15	10	30	20
Co^{2+}	0·72	5	*	*	*	*	*	*	*	*	*	30	10
V^{3+}	0·74	5	15	15	20	10	15	15	10	10	*	15	*
Zr^{4+}	0·79	10	10	10	*	10	*	*	*	*	30	(40)	*
Mn^{2+}	0·80	—	—	—	—	—	—	—	—	100	100	200	70
Y^{3+}	0·92	15	*	*	*	*	*	*	15	*	*	*	*
Sr^{2+}	1·12	5	3000	3000	3000	3000	3000	3000	2300	1000	2000	3000	600
La^{3+}	1·14	50	*	*	*	*	*	*	*	*	*	10	*
Pb^{2+}	1·20	10	*	*	30	*	*	*	*	*	*	10	—
Ba^{2+}	1·34	5	350	300	200	550	230	550	350	80	600	1500	300
Rb^{+}	1·47	10	*	*	*	*	*	*	*	*	*	200	—
Compositions (weight %)†			An_{68}	An_{62}	An_{60}	An_{60}	An_{56}	An_{55}	An_{48}	An_{65}	An_{30}	An_{59}	—
Ga × 1000/Al			0·1	0·2	0·1	0·1	0·1	0·1	0·1	0·2	1·5	0·1	—
Sr × 1000/Ca			31	34	35	35	37	38	33	10	46	35	—

Mo (5) and Sc (10) below the limits of sensitivity (in brackets) in all cases.

B1–H8: Plagioclase feldspars from teschenites, Black Jack sill (see Table 1).

I: Plagioclase from olivine–gabbro (1851), Skaergaard intrusion (Wager and Mitchell, 1951, Table B).

II: Plagioclase from fayalite–ferrogabbro (4142), Skaergaard intrusion (Wager and Mitchell, 1951, Table B).

III: Plagioclase from main gabbro, Garabal Hill–Glen Fyne complex (Nockolds and Mitchell, 1948, Table XX).

IV: Plagioclase (labradorite) from ophitic basalt (3–89) in plagioclase-rich zone, 774 ft below top of Greenstone flow, Michigan (Cornwall and Rose Jr., 1957, Table 2). Also present: Ti 400.

† For the Black Jack plagioclases, these values refer to the average compositions of the feldspar cores, taken as the mean value of both refractive index and Universal stage determinations.

shows normal zoning. The plagioclase is invariably analcitized to varying degrees: despite repeated centrifuging it was not possible to eliminate occasional veneers of analcite along cleavage traces.

Gallium, camouflaged by Al, shows little significant variation with differentiation (15–25 p.p.m.) (Table 5).

Chromium (3 p.p.m.) and nickel (3–5 p.p.m.) are both present in the earlier plagioclases, while vanadium (10–20 p.p.m.) is present throughout the whole series. All these elements have been recorded in plagioclases from Skaergaard, Caledonian and Keeweenawan rocks, and in the case of Ni, in plagioclase from the Lambertville diabase (Storm and Holland, 1957). Although a contamination origin for the above elements might be suggested, it is highly likely that they are actually present in the plagioclase structure, camouflaged by the small amounts of Fe^{2+} (in the case of Ni) and Fe^{3+} (Cr and V) usually reported in analyses of plagioclases. Very small amounts of Ni and Cr would be expected in the earlier plagioclases when these two elements were relatively abundant in the magma.

The strontium content of the plagioclases remains steady (3000 p.p.m.) over the major part of the crystallization of the sill, but shows an appreciable decrease in the plagioclase (An_{48}) from teschenite H8. As Ca is decreasing, the Sr/Ca ratio tends to increase, in accordance with the larger radius of Sr; similar Sr/Ca relationships have been found in plagioclase from the Skaergaard and Stillwater intrusions (Turekian and Kulp, 1956). Nockolds and Mitchell (1948) found little variation in the Sr content of the plagioclases from the Caledonian plutonic rocks until a composition of An_{20}, after which Sr decreased appreciably. The decrease in Sr in the plagioclase from teschenite H8 (a relatively late differentiation product), at the comparatively calcic composition of An_{48}, reflects the decreasing Sr

Table 6. Trace elements of analcites

Element	*r*	*s*	B1	B2	B3	B4	B7	B9	H8
Na^+	0·97		$836 . 10^2$			$901 . 10^2$	$927 . 10^2$		$897 . 10^2$
K^+	1·33		$144 . 10^2$			$123 . 10^2$	$88 . 10^2$		$92 . 10^2$
Ga^{3+}	0·62	2	7	10	7	7	7	5	7
Li^+	0·68	1	2	*	*	2	*	3	*
Zr^{4+}	0·79	10	45	30	15	40	15	10	*
Sr^{2+}	1·12	5	(275)	(125)	(100)	(220)	(250)	(300)	(100)
Ba^{2+}	1·34	5	50	20	30	125	40	180	200
Rb^+	1·47	5	25	15	15	25	*	15	*
Cs^+	1·67	10	<10	<10	10	<10	<10	10	*
	Ba × 1000/K		3·5			10·2	4·5		21·7
	Rb × 1000/K		1·7			2·0	—		—

Cr(2), V(5), Mo(5), Ni(2), Co(5), Sc(10), Y(15), La(20) and Pb(10) below the limits of sensitivity (in brackets) in all cases.

B1–H8: Analcites from teschenites, Black Jack sill (see Table 1).

content of the magma at this stage, culminating in a marked impoverishment in Sr in the residual mesostasis H4 (Table 7).

Barium (200–550 p.p.m.) shows little significant trend. Despite its larger radius, it apparently replaces Ca. Rubidium is below the limit of sensitivity (10) in every case.

(5) *The analcites*

A large percentage of the analcite is a product of direct magmatic precipitation, a small amount of analcite having formed by deuteric analcitization of plagioclase. With differentiation, Na increases slightly while K decreases (Table 6). Care is necessary in interpretation of the trace elements of the analcites. The mineral is often laced with fibres of apatite; the values for Sr have accordingly been bracketed. In addition the crystals sometimes reveal a certain amount of turbidity; the chemistry of this change is not known.

Table 7. Trace elements of apatites

Element	*r*	*s*	B9	H8	I	II	III
Ga^{3+}	0·62	2	*	*	3	*	*
Cr^{3+}	0·63	2	*	*	3	*	10
Li^{+}	0·68	1	*	*	*	1	*
Ni^{2+}	0·69	2	*	*	*	*	20
Mo^{4+}	0·70	5	35	35	*	*	—
Cu^{2+}	0·72	—	—	—	*	200	100
V^{3+}	0·74	5	60	60	*	*	90
Zr^{4+}	0·79	10	?10	*	30	(50)	100
Mn^{2+}	0·80	—	—	—	400	500	200
Sc^{3+}	0·81	10	*	*	30	*	9
Y^{3+}	0·92	15	450	450	4000	5000	4000
Sr^{2+}	1·12	5	4000	4000	1000	2000	400
La^{3+}	1·14	20	1300	1350	1200	1000	2000
Pb^{2+}	1·20	10	15	15	10	—	—
Ba^{2+}	1·34	5	30	30	30	5	90

Co(5), Rb(5) and Cr(10) below the limits of sensitivity (in brackets) in all cases.
B9–H8: Apatites from teschenites, Black Jack sill (see Table 1).
I: Apatite from fayalite–ferrogabbro (4142), Skaergaard intrusion (Wager and Mitchell, 1951, Table B).
II: Apatite from main gabbro, Garabal Hill–Glen Fyne complex (Nockolds and Mitchell, 1948, Table XIV).
III: Apatite from ophitic basalt (4–376), 501 feet below top of Greenstone flow, Michigan (Cornwall and Rose Jr., 1957, Table 2). Also present: Ti 500.

The analcite represents a crystallization product of residual liquids representative of different differentiation stages of the 500 ft thickness of the sill. Table 6 illustrates the monotony of the analcite trace element content, in particular Ni, Co, V, Cr, etc., (trace elements in the dark minerals) being below the limits of sensitivity in all cases. Although rejection of the above elements would be anticipated, both from a consideration of the major elements present and the basic Goldschmidt

rules, it was not expected that their rejection would be so complete, since presumably the late liquids, particularly from the early stages of differentiation, contributed to the minor element content of later differentiation products.

The small amounts of gallium (5–10 p.p.m.) are camouflaged by Al. The small amounts of lithium in three analcites may be a result of late hydrothermal alteration. Except in the case of the analcite from teschenite H8, zirconium is always present and tends to decrease with differentiation; this trend for zirconium is the opposite to that shown by the rock series. According to Ringwood (1955b), the magmatic behaviour of the zirconium ion is dominated by its tendency to form a complex of the ZrO_4^{4} type, becoming accumulated in residual magmas relatively to SiO_4^{4-}. The presence of free Zr^{4+} in the magma is indicated by its constant presence in the clinopyroxenes, in every case precipitated earlier than the coexisting analcite. It is possible that with decreasing temperature, concomitant with greater hydrothermal activity the tendency for zirconium to form a complex increased, such a complex not being readily accepted into the analcite structure. Data on the Zr contents of Na–Al silicates has been presented by Degenhardt (1957).

Strontium shows an irregular distribution. It is possible that some of the Sr should be considered as captured by K. If all the Sr is to be referred to contaminating apatite, lanthanum would be expected to be present in amounts considerably above its limit of sensitivity.

The behaviour of barium is difficult to interpret. While the K content of the analcites decreases with differentiation, the values for Ba indicate an increase in this element. It may be noted that although their K contents remain approximately constant (0·38 0·46 per cent K_2O), the plagioclase feldspars from the layered Skaergaard series show a definite increase in their Ba contents (80–600 p.p.m.) with differentiation; however, Wager and Mitchell (1951) emphasize that the distribution factors for barium remain fairly steady whilst this increase in the plagioclase Ba contents takes place. Thus in the case of the analcites, the increased Ba may have resulted from the progressive building-up of this element in the various teschenite residual solutions; consequently the actual K content of the analcite is no criterion of the amount of barium to be expected. In the early stages of differentiation, the Ba in the magma was only partly eliminated by the plagioclases; in the teschenites themselves, the maximum concentration of barium (450 p.p.m.) was reached in H8, from the roof of the sill, a rock containing the lowest modal plagioclase but maximum microcrystalline mesostasis and zeolite. A more advanced differentiation product, namely the mesostasis from H4, shows a definite decrease in its Ba content, despite further enrichment in K.

The amount of rubidium in the analcites is closely related to their K content and the amounts of each element decreases with differentiation.

(6) *The apatites*

Trace element data is available on only two apatites (Table 7), separated from teschenites B9 and H8, which are representative of the later stages of differentiation. The apatites (fluorapatites) are characterized by enrichment in yttrium, lanthanum and strontium. Both yttrium and lanthanum have a pronounced

affinity for fluorine and commonly are concentrated in the apatites of igneous rocks (Sahama and Rankama, 1950), and like strontium, are probably replacing Ca. Barium (30 p.p.m.) is camouflaged by Ca. Both apatites contain 15 p.p.m. lead (cf. Goldschmidt, 1954, p. 399).

(7) *Alkali feldspar (anorthoclase)*

Sufficient anorthoclase (Or_{26}) was separated only from teschenite I2, approximately 500 ft above the lower contacts, for determination of the following elements (p.p.m.).: Li^+ 5; Sr^{2+} 650; Ba^{2+} 1000; Rb^+ 50.

The anorthoclase shows noticeable enrichment in Ba and Rb, compared with the plagioclase feldspars (Table 5).

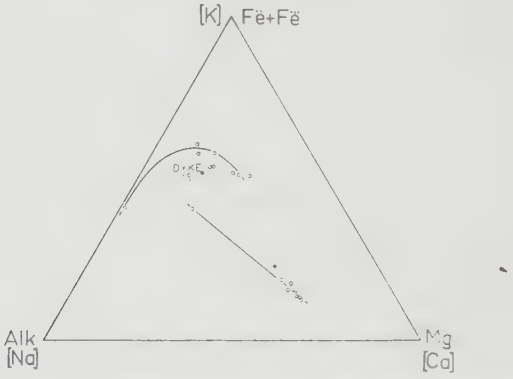

Fig. 1. Course of crystallization of the Black Jack teschenites.

Major and Trace Elements of the Teschenites

For the major elements, chemical data on the teschenites (Wilkinson, 1958, Table 6) were recalculated on a water-free basis (Table 8). The method of plotting the major and minor elements is the same as that used by Nockolds and Allen (1954) where the amount of a given element is plotted against the value $(\frac{1}{3}Si - K) - (Ca + Mg)$ (Figs. 2a, b). In discussing the geochemistry of the teschenites, reference will be made mainly to the alkali igneous rock series investigated by Nockolds and Allen (1954), namely the Scottish Tertiary alkali series, the alkali rocks of the Hawaiian islands and three series of alkali igneous rocks found in the Polynesia Islands. Nockolds and Allen (1954) have also plotted the major and trace elements of the Braefoot Outer Sill (Higazy, 1952; Table 8, analyses I–III).

(1) The variation diagram on a basis of Mg, $(Fe^{2+} + Fe^{3+})$ and $(Na + K)$, and Ca, Na and K, is presented in Fig. 1. The general trend is the same as that obtained using a plot of the respective oxides on a weight per cent basis. The Fe–Mg–alk. curve is strongly concave downwards, while the Ca–Na–K curve is virtually a straight line. In the former case, the initial trend, namely one of enrichment in Fe relative to Mg, resulted primarily from the increasing fayalite content of the olivines and ever diminishing amounts of modal olivine with differentiation. Olivine is virtually absent from teschenite H8 at the maximum of the curve, and thenceforth alkali enrichment predominated over Fe–Mg enrichment. The Scottish Tertiary, Hawaiian and Polynesian alkali-basalt–trachyte series all show a

Table 8. Major and trace elements of teschenites from the Black Jack sill

Element	r	s	B1	B2	B3	B4	B7	B9	H1	H8	H4	I	II	III
Si^{4+}	0·42		$213 . 10^3$	$216 . 10^3$	$217 . 10^3$	$217 . 10^3$	$220 . 10^3$	$213 . 10^3$	$216 . 10^3$	$214 . 10^3$	$255 . 10^3$	$196 . 10^3$	$220 . 10^3$	$287 . 10^3$
Al^{3+}	0·51		$76 . 10^3$	$79 . 10^3$	$94 . 10^3$	$80 . 10^3$	$91 . 10^3$	$77 . 10^3$	$81 . 10^3$	$88 . 10^3$	$95 . 10^3$	$59 . 10^3$	$84 . 10^3$	$73 . 10^3$
Fe^{3+}	0·64		$29 . 10^3$	$21 . 10^3$	$19 . 10^3$	$22 . 10^3$	$20 . 10^3$	$28 . 10^3$	$24 . 10^3$	$30 . 10^3$	$25 . 10^3$	$13 . 10^3$	$11 . 10^3$	$20 . 10^3$
Mg^{2+}	0·66		$59 . 10^3$	$50 . 10^3$	$29 . 10^3$	$46 . 10^3$	$28 . 10^3$	$30 . 10^3$	$22 . 10^3$	$19 . 10^3$	$24 . 10^2$	$90 . 10^3$	$43 . 10^3$	$17 . 10^3$
Ti^{4+}	0·68		$15 . 10^3$	$16 . 10^3$	$17 . 10^3$	$16 . 10^3$	$17 . 10^3$	$25 . 10^3$	$23 . 10^3$	$22 . 10^3$	$36 . 10^2$	$10 . 10^3$	$13 . 10^3$	$52 . 10^2$
Fe^{2+}	0·74		$72 . 10^3$	$76 . 10^3$	$67 . 10^3$	$75 . 10^3$	$64 . 10^3$	$76 . 10^3$	$78 . 10^3$	$78 . 10^3$	$46 . 10^3$	$70 . 10^3$	$56 . 10^3$	$30 . 10^3$
Na^{+}	0·97		$25 . 10^3$	$27 . 10^3$	$30 . 10^3$	$29 . 10^3$	$30 . 10^3$	$30 . 10^3$	$32 . 10^3$	$31 . 10^3$	$51 . 10^3$	$18 . 10^3$	$32 . 10^3$	$34 . 10^3$
Ca^{2+}	0·99		$59 . 10^3$	$61 . 10^3$	$75 . 10^3$	$61 . 10^3$	$74 . 10^3$	$71 . 10^3$	$72 . 10^3$	$61 . 10^3$	$25 . 10^3$	$41 . 10^3$	$48 . 10^3$	$14 . 10^3$
K^{+}	1·33		$15 . 10^3$	$17 . 10^3$	$15 . 10^3$	$16 . 10^3$	$16 . 10^3$	$16 . 10^3$	$22 . 10^3$	$21 . 10^3$	$51 . 10^3$	$58 . 10^2$	$11 . 10^3$	$34 . 10^3$
P^{5+}	0·34	—	(2700)	(2800)	(1900)	(2800)	(2500)	(3100)	(1600)	(5300)	(500)	(830)	(960)	(870)
Ga^{3+}	0·62	2	20	15	20	20	25	20	20	15	15	6	40	40
Cr^{3+}	0·63	2	300	250	130	250	150	25	5	*	*	950	180	*
Li^{+}	0·68	1	10	10	5	20	10	10	14	10	30	20	40	50
Ni^{2+}	0·69	2	350	150	70	180	50	35	10	6	*	430	70	40
Mo^{4+}	0·70	2	*	*	*	*	*	*	*	*	*	3	*	4
Co^{2+}	0·72	5	100	45	40	60	35	35	20	25	*	85	60	10
V^{3+}	0·74	5	200	180	250	250	250	350	220	150	*	220	360	8
Zr^{4+}	0·79	10	250	200	175	250	250	275	220	300	450	220	240	1100
Mn^{2+}	0·80	—	(1100)	(1200)	(800)	(900)	(900)	(800)	(850)	(600)	(80)	(1550)	(774)	(465)
Sc^{3+}	0·81	10	*	*	*	*	*	*	*	*	*	10	*	*
Y^{3+}	0·92	15	15	15	20	20	20	20	20	30	30	25	50	200
Sr^{2+}	1·12	5	1500	1500	1500	1100	1500	1500	450	525	250	300	950	450
La^{3+}	1·14	20	*	*	*	*	*	*	*	*	75	*	*	75
Ba^{2+}	1·34	5	275	325	285	450	325	450	400	450	250	650	2600	1200
Rb^{+}	1·47	5	30	70	30	70	45	45	100	70	275	3	18	100
Cs^{+}	1·67	10	*	*	*	*	*	*	*	*	?10	—	—	—
	Fe		63	66	75	69	75	78	82	85	97	48	61	75
	Mg		37	34	25	31	25	22	18	15	3	52	39	25
	Fe		50	51	54	52	53	58	57	60	41			
	Mg		30	26	18	24	18	17	13	11	1			
	Alk.		20	23	28	24	29	25	30	29	58			
	Position		−3·2	− 2·2	1·7	1·9	− 1·3	−1·4	0·0	− 1·2	− 10·9			

Table 8 (*contd.*)

Element	B1	B2	B3	B4	B7	B9	H1	H8	H4	I	II	III
Ga × 1000/Al	0·3	0·2	0·2	0·2	0·3	0·3	0·2	0·2	0·2	0·1	0·5	0·5
Ni × 1000/Mg	6·0	3·0	2·4	4·0	1·8	1·1	0·5	0·3	—	4·8	1·6	2·4
Li × 1000/Mg	0·2	0·2	0·2	0·4	0·4	0·3	0·6	0·5	12·5	0·2	0·9	2·9
Fe^{2+}/Mg	1·2	1·5	2·3	1·6	2·3	2·5	3·5	4·1	19·2	0·8	1·3	1·8
Ni × 1000/Fe^{2+}	4·9	2·0	1·0	2·4	0·8	0·5	0·1	0·1	—	6·1	1·3	1·3
Co × 1000/Fe^{2+}	1·4	0·6	0·6	0·8	0·5	0·5	0·3	0·3	—	1·2	1·1	0·3
Fe^{3+}/Fe^{2+}	0·4	0·3	0·3	0·3	0·3	0·4	0·3	0·4	0·5	0·2	0·2	0·7
Cr × 1000/Fe^{3+}	10·3	12·0	7·0	11·4	7·5	0·9	0·2	—	—	73	16	—
V × 1000/Fe^{3+}	7·0	9·0	13·2	11·4	12·5	12·5	9·2	5·0	—	17	33	0·4
Y × 1000/Ca	0·3	0·3	0·2	0·3	0·3	0·3	0·3	0·5	1·2	0·6	1·0	14·3
Sr × 100/Ca	2·5	2·5	2·0	1·8	2·0	2·1	0·6	0·9	1·0	0·7	2·0	3·2
Sr × 100/Ca + K	2·0	2·0	1·7	1·5	1·7	1·7	0·5	0·6	0·3	0·6	1·6	0·9
Ba × 100/K	1·8	1·9	1·9	2·8	2·0	2·8	1·8	2·0	0·5	11·2	24	3·5
Rb × 100/K	0·2	0·4	0·2	0·4	0·3	0·3	0·4	0·3	0·5	0·1	0·2	0·3

Sn(10) and Pb(10) below the limits of sensitivity (in brackets) for the Black Jack teschenites.

B1–H8: Teschenites, Black Jack sill (see Table 1).

B4: Vein of microcrystalline mesostasis (composition of analcite–syenite) from teschenite H4, approx. 500 ft above lower contact, Black Jack sill.

(For specific locations of B1–H4, see WILKINSON, 1958, Fig. 2).

I–III: are from the Braefoot Outer Sill, Fife. (HIGAZY, 1952, Table 1).

I: Picroteschenite, Braefoot Bay.

II: Medium-grained teschenite, quarry near summit of Braefoot promontory.

III: Microsyenite, 330 yd north of Braefoot Pier, Dalgety Bay.

similar Fe–Mg enrichment trend. In contrast with this trend, the rocks of the Circular Head laccolith (Edwards, 1941) and the Braefoot Outer Sill (Campbell *et al.* 1933), although both olivine-bearing, fall on an almost linear Fe–Mg–alk. curve, trending towards the alk. corner.

(2) From plots of the Caledonian plutonic rocks, Nockolds (Nockolds and Mitchell, 1948) has pointed out that curves of continuous variation may be used to represent the liquid line of descent of a parental magma. Rocks whose composition is thought to have been modified by the accumulation of olivine, pyroxene

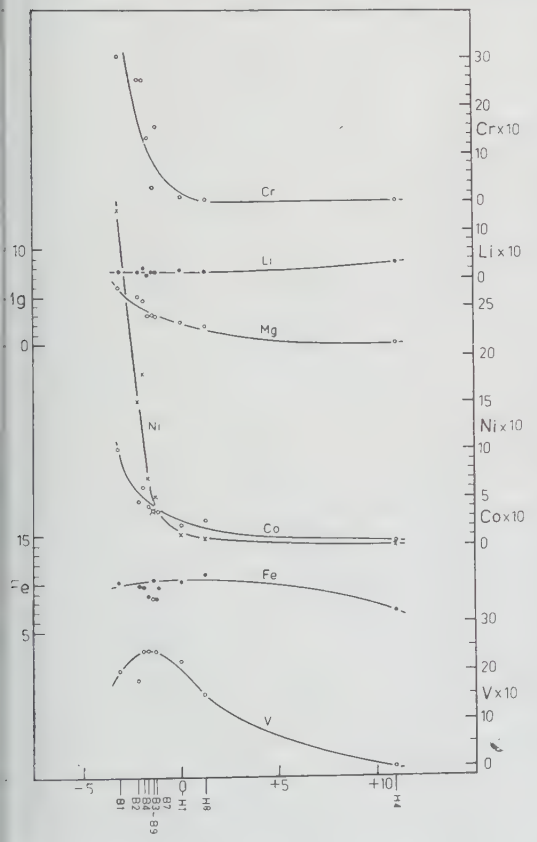

Fig. 2(a). Variation in V, Fe, Ni, Co, Mg, Li and Cr in the Black Jack teschenites.

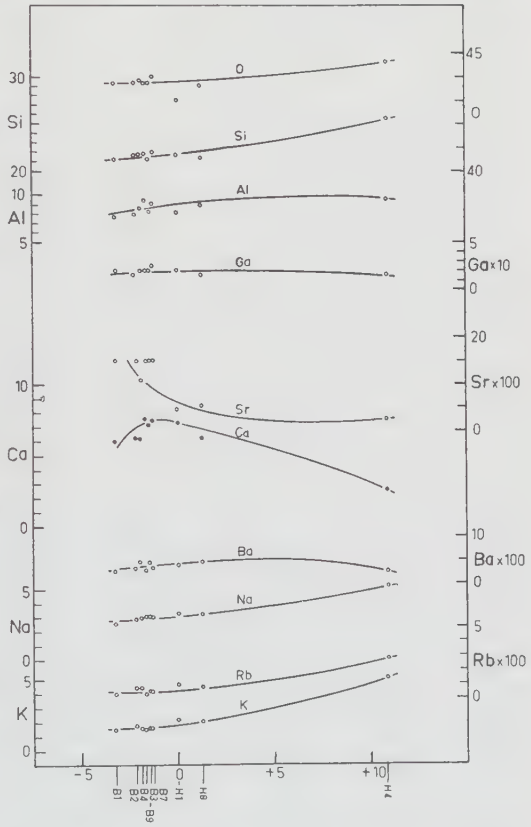

Fig. 2(b). Variation in K, Bb, Na, Ba, Ca, Sr, Ga, Al, Si and O in the Black Jack teschenites.

or feldspar generally show a scatter in relation to the liquid line of descent. The modal compositions of certain of the analysed teschenites (Table 1) would suggest that teschenites B1 (accumulation of olivine), B3 and B7 (accumulation of feldspar) and B9 (accumulation of clinopyroxene) may be regarded in such a light. However, when compared with the modes of teschenites representative of the intrusion as a whole (Wilkinson, 1958, Table 2) the above rocks are not significantly atypical. In the following discussion, a point of uncertainty is the minor element composition of the mesostasis in teschenites from successive levels in the sill.

Gallium and aluminium. With progressive differentiation, aluminium tends to increase slightly. The two points lying off the supposed line of liquid descent are teschenites B3 and B7, enriched in plagioclase. Up to heights of from 350 to 400 ft above the lower contacts, plagioclase tends to increase as olivine decreases. Gallium, if anything, shows a slight decrease. On a basis of their higher content of modal plagioclase, teschenites B3 and B7 would be expected to show enrichment in Ga, if all the gallium is considered as being camouflaged by Al. Only B7 is in accordance with this. The amount of modal titanomagnetite, a mineral in which gallium is an important trace element, significantly controls the Ga rock content; consequently B3, although enriched in plagioclase, reveals no enrichment in Ga, owing to a lower titanomagnetite content. Sandell (1949) has discussed the possibility of the effect of Ga replacing Fe^{3+} in igneous rock series.

In the teschenite rock series, the Ga/Al ratio tends to remain constant in the vicinity of 0·2, a value comparable with that found in many of the alkali series investigated by Nockolds and Allen, e.g. the Scottish Tertiary and Hawaiian series. Aluminium shows a slight decrease in the Braefoot Outer Sill, while Ga increases slightly in the early rocks and then remains steady.

Iron and magnesium. While Mg decreases regularly as the function $(\frac{1}{3}Si + K) - (Ca + Mg)$ increases, a trend controlled dominantly by a decrease in precipitated olivine together with its more fayalitic nature, the variation of Fe is not so regular. Fe tends to increase slightly with differentiation, finally decreasing perceptibly in the alkaline mesostasis. The decreased values of Fe in B3 and B7 are antipathetic with the values for Al.

Chromium. It decreases from 300 p.p.m. in teschenite B1 to less than 2 p.p.m. in teschenite H8. The change is rather slow for the teschenites from the lower 400 ft of the sill, after which the decrease is more rapid. Chromium is camouflaged principally by Fe^{3+} in titanomagnetite and clinopyroxene. In any particular teschenite the amount of Cr is more related to its previous withdrawal from the magma rather than variation in the amount of titanomagnetite and clinopyroxene separating at any time. The most abrupt change reflecting the magmatic availability of Cr occurs in teschenite B9 (500 ft above the lower contacts), which despite its enrichment in pyroxene, contains only 25 p.p.m. Cr. The Cr contents of the titanomagnetite and clinopyroxene from B9 are less than one-twelfth the Cr contents of these minerals in teschenite B7, 420 ft above the lower contacts, and representing a slightly earlier differentiation product. Teschenite B1, an early product enriched in olivine but not titanomagnetite or clinopyroxene, has a Cr content not markedly abnormal from the liquid line of descent.

In passing along the differentiation series, *vanadium* behaves in a manner similar to that in many of the alkali series investigated by Nockolds and Allen, e.g. the Scottish Tertiary, Hawaiian and Polynesian series. That is, vanadium increases to a pronounced maximum towards the middle of the basic end of the series, and then declines progressively to values below the limits of sensitivity. Such a variation in the teschenites is a reflection on the amount of vanadium in the titanomagnetites (and to a lesser extent, the clinopyroxenes) rather than the amounts of these minerals precipitating at any stage. At this stage, the titanomagnetites have a higher content of Fe^{3+}, resulting in an increase in their Fe_3O_4

content at the expense of Fe^{3+}—poor Fe_2TiO_4 in the titanomagnetite solid solutions. This change possibly facilitated entry of additional V which may have undergone slight preliminary concentration in the magma. In the later stages of evolution, the decreasing amounts of V in the magma are well illustrated by the amounts of this element in the clinopyroxenes. It may be noted that the high V content of teschenite B9 is in harmony with its higher percentage of modal clinopyroxene.

Lithium. Admitted principally by Mg in clinopyroxene, and to a lesser extent in olivine, lithium increases with differentiation, reaching a maximum in the residual alkaline mesostasis from teschenite H4 (cf. Wickman, 1943, p. 380; Goldschmidt, 1954, pp. 130–131).

Nickel and cobalt. They both decrease as the function $(\frac{1}{3}Si + K) - (Ca + Mg)$ increases. The rapid decrease in nickel stems mainly from an ever-decreasing amount of modal olivine, and reflects the ease of entry of Ni into that mineral. Cobalt decreases at a more even rate. The earliest teschenites have Ni > Co but this is soon reversed and Ni < Co. This relationship is emphasized by Nockolds and Allen for the Scottish Tertiary, Hawaiian and Polynesian series. Lundegårdh (1949) ascertained that, according to the Goldschmidt rules, the first differentiates developed by fractional crystallization of basic magmas should have the following distribution order, Cr > Ni > Co, whereas the latest differentiates should have Co > Ni > Cr. Except for B1, these relationships broadly hold for the teschenites. Considering the ratios Ni/Mg, Ni/Fe and Co/Fe, there is a fairly regular decrease from B2 to H4, i.e. along the line of liquid descent. Teschenite B1 exhibits much higher values for these ratios in relation to the general trend, and also tends to fall off the smooth curves on triangular variation diagrams. In the absence of any chilled contacts, B2 is assumed from geochemical data to have a composition approaching that of the parental magma (Wilkinson, 1958, Table 8).

Zirconium. As in the Braefoot rocks, zirconium reveals an increase in the later differentiates. It is concentrated principally in the clinopyroxene, so that the higher values for Zr in teschenite H8 reflect the concentrations of Zr in the mesostasis present in the rock (Table 8). The alkaline mesostasis from teschenite H4 reveals the maximum in Zr enrichment. The concentration of Zr "in 'residual' magmas in rock series considered to be developed by fractional crystallization" has been emphasized by Goldschmidt (1954, p. 424).

Yttrium and lanthanum. Yttrium increases with progressive differentiation until in the latest rocks it is present in amounts twice those at the beginning of crystallization. As Ca decreases, the ratio Y/Ca increases as does this value in the Scottish Tertiary, Hawaiian and Polynesian alkali series. On the other hand, lanthanum is below the limit of sensitivity (20 p.p.m.), but suddenly appears in the mesostasis H4 (75 p.p.m.). Yttrium is thus enriched in the basic rocks with respect to lanthanum, since its ionic radius favours substitution for Ca (the clinopyroxenes consistently carry 35–40 p.p.m. Y).

Calcium and strontium. Ca tends to increase at first and then decreases markedly as differentiation proceeds. Sr, however, tends to remain steady at 1500 p.p.m. in the lower 400 ft of the sill, after which it shows a marked decrease. The higher plagioclase content of B3 and B7 is not reflected in their Sr contents.

The Black Jack magma appears to have been comparatively rich in Sr, having higher values for this element than the Braefoot teschenites (Table 8). Strontium does decrease progressively in the Easter Island basalt–alkali rhyolite series but in the majority of the series investigated by Nockolds and Allen, Sr increases to a maximum and then decreases.

Barium. If anything, Ba increases to a feeble maximum and decreases slightly. The trend for Ba, at least as far as teschenite H8, is consistent with an increasing amount of alkali feldspar and analcite, the Ba content of the latter mineral increasing in the same direction.

Potassium and rubidium. The curves for these two elements are almost parallel, although in the later stages, K appears to be increasing at the greater rate. The presence of Rb in the early potash-bearing analcites possibly resulted in a slight relative impoverishment of this element in the residual liquids in the lower rocks.

The trace elements of the Black Jack teschenites reveal the same general trends as the Braefoot teschenites, although more effective removal of Cr, V, Ni and Co has occurred in the alkaline mesostasis H4 than in the Braefoot microsyenite. In the case of the residual mesostasis H4, the disappearance of Cr, V, Ni and Co recalls their absence in the Polynesia phonolites and the Scottish Tertiary trachytes. Trace element trends similar to those in the Black Jack rocks occur also in the Saltcoats biotite–teschenite and its potash-lugarite differentiate (Patterson, 1945); Ba and Sr undergo marked increases in the latter rock. Although not on the same spectacular scale, the Black Jack trends are comparable with those in the layered tholeiitic Skaergaard series.

Discussion of Results of the Mineral Analyses and the Nature of the Differentiation Process

Although the mineral series in the teschenites differ in certain aspects from the mineral series in the tholeiitic Skaergaard intrusion, a comparison of the minor elements in minerals common to both intrusions reveals a general similarity. As a consequence of milder differentiation, the minor element variations in the teschenite mineral series are not as pronounced as in the Skaergaard minerals.

The principal replacements between the various trace elements and particular major elements may be summarized as follows:

Ga for Al in plagioclase, clinopyroxene, analcite and presumably anorthoclase, and for Fe^{3+} in titanomagnetite;

Cr for Fe^{3+} in clinopyroxene and titanomagnetite;

Li for Mg in olivine and pyroxene;

Ni and Co for Fe^{2+} (and Mg to a lesser extent) in olivine, clinopyroxene and titanomagnetite;

V for Fe^{3+} in clinopyroxene and titanomagnetite and to a much less extent for Fe^{3+} in plagioclase;

Zr for Fe^{3+} in clinopyroxene;

Sc for Fe^{2+} in clinopyroxene;

Y for Ca in apatite and pyroxene, La for Ca in apatite;

Sr for Ca in plagioclase and apatite, limited replacement for Ca in clinopyroxene;

Ba for Ca in plagioclase, limited replacement for Ca in apatite, Ba for K in anorthoclase and analcite;

Rb for K in anorthoclase and analcite;

Wager and Mitchell (1951) have stressed the fact that relative changes in amount of various trace elements in a series of minerals from crystallizing basic magma result both from the interplay of crystal chemical factors and the sequence and amount of the various mineral-phases precipitated. The Goldschmidt rules predict the *presence* of minor elements, and in many cases may also give indications of differentiation trends. Ringwood's recent modifications of these rules in certain instances results in a more precise correlation between observed and anticipated trends.

It is interesting to note the similarity in the trace element distribution and trends in the various mineral series precipitated by differentiating intrusive alkali olivine-basalt and tholeiitic magmas, both fundamental parental basic magma types.

Gallium. Despite its oft-emphasized affinities for Al, gallium is present in greatest amounts in the titanomagnetites (70–80 p.p.m.), camouflaged by Fe^{3+}. Hence in the case of the teschenites, titanomagnetite may contribute as much Ga to the gallium content of the rock as the aluminous silicates; antipathetic variation in modal plagioclase and titanomagnetite may result in a relatively constant amount of Ga in the rock series.

Vanadium. In significant amounts, V is present in titanomagnetite and clinopyroxene; in both minerals, V does not reveal spectacular trends but tends to increase in the intermediate differentiation products, finally decreasing to values comparable with, or slightly less than values at the beginning of differentiation. In both cases, the V/Fe^{3+} ratio trends accord with the relative distributions proposed by Ringwood on a basis of their respective electronegativities. The V contents of the titanomagnetite and clinopyroxene bear no proportional relationship to their Fe^{3+} contents, despite variations in the order of crystallization. In general vanadium enters clinopyroxene with the greater ease.

Chromium. Camouflaged by Fe^{3+} in clinopyroxene and titanomagnetite, Cr reveals strong variation with differentiation, particularly in the upper 100 ft of the sill. Again, the preferential concentration of Cr ($r = 0{\cdot}63$) with respect to Fe^{3+} ($r = 0{\cdot}64$) is better interpreted in terms of the smaller electronegativity of Cr, rather than entirely on the basis of its slightly smaller radius. The order of crystallization of clinopyroxene and titanomagnetite is apparently important in determining the amounts of Cr present in each mineral.

Nickel and cobalt. These are important trace elements in olivine, titanomagnetite and clinopyroxene, in that order of importance. With the exception of Ni in the analysed olivines, both Ni and Co reveal a progressive decrease with differentiation, the variation of Ni being the more extreme. Recently investigated melting relationships in the Ni_2SiO_4–Mg_2SiO_4 solid solution series (Ringwood, 1956) suggest that in magmatic melts, Ni is camouflaged principally by Fe^{2+} in olivines. Nickel is removed most effectively from the magma by the precipitation of olivine. Only in H8, the most advanced teschenite differentiation product, does the Ni content of the clinopyroxene exceed that of the coexisting titanomagnetite. At

this stage the Ni content of the magma had fallen to low values and the relationships result from the earlier-precipitated clinopyroxene competing more favourably for the remaining Ni. Under magmatic conditions of absolute enrichment in Fe^{2+}, the Mg/Fe^{2+} replacement in clinopyroxenes is well known. Despite the comparatively limited degree of iron enrichment shown by the Black Jack pyroxenes, the ever-present tendency for Fe^{2+} to replace Mg with falling temperature probably resulted in comparative greater ease of entry of Ni into the pyroxene structure, as indicated by a comparison of corresponding Ni/Fe^{2+} ratios for clinopyroxene and titanomagnetite. From teschenite B2 onward, the crystallization of clinopyroxene before titanomagnetite facilitated the entry of Ni into the former mineral. In all the ferriferous mineral series, the trend of the Co/Fe^{2+} ratios is consistent with camouflage of Co by Fe^{2+}, based on a consideration of their respective radii.

Scandium. It is confined to the clinopyroxenes where it reveals enrichment relative to Fe^{2+}, in accordance with its higher charge and lower electronegativity.

Zirconium. Appreciable concentration of Zr is undergone in the clinopyroxenes, and Zr appears also in the analcites in which the Zr contents decrease with differentiation.

Yttrium and lanthanum. Y is concentrated in the apatites where it is ten times more abundant than in the clinopyroxenes (30–40 p.p.m.). La also undergoes concentration in the apatites.

Strontium and barium. As emphasized by Wager and Mitchell (1951) Sr and Ba are two elements which vary considerably in minerals possessing a common major cation and separating simultaneously. The differences are too considerable to be explained simply by order of crystallization. Thus in the Black Jack rocks the plagioclase commonly contains 3000 p.p.m. Sr while the associated clinopyroxene (15·9 per cent Ca) contains 125–175 p.p.m. Sr. The plagioclase has up to 550 p.p.m. Ba whilst in the clinopyroxene this element is present just above the limit of sensitivity. Wickman (1943) has correlated the varying ease of entry in terms of shrinkage (pyroxene) or expansion (plagioclase) of the structure in the transition of calcium from 8- to 6- co-ordination, limiting the entry of ions appreciably larger than Ca. In teschenites B9 and H8, the plagioclase contains from ten to twenty times more Ba than the associated apatite. The greatest concentrations of Ba occur in the alkali feldspar.

Rubidium. The only minerals competing for Rb were anorthoclase and analcite, where the Rb is camouflaged by K. Contrary to expectations, the more differentiated analcites do not reveal enrichment in Rb relative to K.

On the basis of the teschenite modal differentiation trends, the spatial distribution of the principal mineral series in the sill and compositional trends in the rock and mineral series, it has been concluded that *fractional crystallization* was the differentiation mechanism whereby the progressive variations were brought about, and that the residual alkaline mesostasis (= analcite syenite in composition) is a residual liquid (Wilkinson, 1958). Trace element distributions and trends in the rock and mineral series lend strong support to these conclusions. In addition to their relationships to crystal structure, in many cases the trends of certain minor elements (e.g. Co–Fe^{2+} relationships in titanomagnetite) can be correlated with the amounts of the major host elements, whose own concentrations are a

function of the temperature of crystallization. In the rocks now exposed, the order of consolidation of the sill was from the base upwards. Whilst the Goldschmidt rules may tend to oversimplify minor element trends and distributions in crystallizing magma, they can nevertheless be applied in several instances. A strong advocate of fractional crystallization as a principal factor in rock diversity, Goldschmidt (1937, p. 661) illustrated his rules by reference to trends in the Fo–Fa and Ab–An series, two continuous reaction series of prime importance during evolution of the various teschenitic fractions. The trends of the minor elements in the rock and mineral series are comparable to those discussed by Osborn (1950) in the fractionation of basic magma.

The progressive magmatic impoverishment in those elements possessing high ease of entry in higher temperature mineral phases (e.g. Ni in the olivines; Cr in clinopyroxene and titanomagnetite; Sr in plagioclase) has already been discussed. In minerals precipitated by later magmatic fractions, the concentrations of such elements fall to very low values, and ultimately the removal of these elements is complete in the residual liquid, namely the microcrystalline mesostasis. Similarly, low concentrations of an element due to difficulty of entry in early fractionated minerals result in no marked trend of the element in that particular mineral series, the element being stored up to undergo moderate enrichment in the residual liquid, e.g. Li. Certain elements reveal enrichment in this liquid owing to insignificant mineral competition during the evolution of the sill, as a result of limited precipitation of minerals possessing the optimum structural site, e.g. Rb in anorthoclase.

At certain stages during the crystallization of the intrusion, varying modal compositions in the teschenites illustrate the response to varying fractionation conditions, particularly as they affected the order of crystallization. In the case of the titanomagnetites, there is an initial decrease in the amounts of this mineral precipitated, followed by an increasing amount, the opaque mineral then being of late crystallization and showing an increase in the Fe^{3+}/Fe^{2+} ratio. In certain teschenites from the upper levels of the sill, small amounts of olivine are of late crystallization and show comparatively greater enrichment in Fa than if they were early in the crystallization sequence. Certain trace elements, e.g. Cr and V in titanomagnetite, partly respond in their behaviour to these minor fractionation variations.

Reasons have been advanced indicating that it is not necessary to invoke differential movement and accumulation of crystals (particularly olivine) under the influence of gravity in order to explain modal variations within the teschenites (Wilkinson, 1958). Most of the minor element trends in the teschenites are fairly regular along a line of supposed liquid descent, and except for certain features of B1 (e.g. Ni), there is little evidence based on minor element considerations to indicate that markedly abnormal accumulative facies are present. The utilization of trace element data along these lines should proceed with care, particularly in the absence of information indicating the modal composition of the rocks and the amounts of trace elements entering particular minerals. The relatively constant amounts of Ga in the teschenite rock series has already been discussed in terms a antipathetic variation of plagioclase and titanomagnetite.

However, as pointed out by Wager and Mitchell, the amounts of trace elements in minerals undoubtedly will provide valuable clues in petrogenetic studies. For example Drever's (1957) suggestion that the Eilean Mhuire basic rocks represent the downfaulted top of the Garbh Eilean crinanite–picrite association is substantiated by the low Cr, V, Ni and Sc contents of the Eilean Mhuire clinopyroxene where these elements are present in amounts comparable with clinopyroxene H8 from the top of the Black Jack sill.

Trace Elements in the Feeder Dykes

The feeder dykes to the sill unfortunately have been considerably altered to "white trap" (Wilkinson, 1958, pp. 25–27), only teschenite J5 being sufficiently fresh to repay chemical analysis (Fig. 1). Trace element data on the freshest dyke material is presented in Table 9. The original trace-element contents of the dykes have undoubtedly been modified by the late-stage carbonated solutions responsible for their alteration.

However certain features are worthy of comment. Relict microstructures in J13 suggest earlier idiomorphic olivines, whilst in J5 and J6 there is no evidence to indicate that olivine was ever present. In J5 and J6, Cr, V, Ni, Co and Zr are present in amounts comparable with the concentrations in those teschenites from the upper more differentiated levels of the intrusion (Table 8). Sr has decreased

Table 9. Major and trace elements of teschenite dykes

Major elements		Trace elements					
Element	Specimen J5	Element	r	s	J5	J6	J13
Si^{4+}	$203 \cdot 10^3$	P^{5+}	0·34	—	(2300)	—	—
Al^{3+}	$82 \cdot 10^3$	Ga^{3+}	0·62	2	15	12	10
Fe^{3+}	$14 \cdot 10^3$	Cr^{3+}	0·63	2	80	40	200
Mg^{2+}	$25 \cdot 10^3$	Li^{+}	0·68	1	15	10	90
Ti^{4+}	$12 \cdot 10^3$	Ni^{2+}	0·69	2	85	50	125
Fe^{2+}	$65 \cdot 10^3$	Mo^{4+}	0·70	2	5	*	*
Na^{+}	$27 \cdot 10^3$	Co^{2+}	0·72	5	30	25	30
Ca^{2+}	$51 \cdot 10^3$	V^{3+}	0·74	5	100	80	140
K^{+}	$22 \cdot 10^3$	Zr^{4+}	0·79	10	325	225	100
		Mn^{2+}	0·80	—	(700)	—	—
Fe^{3+}/Fe^{2+}	0·2	Sc^{3+}	0·81	10	*	*	20
Fe^{2+}/Mg	2·6	Y^{3+}	0·92	15	15	15	15
		Sr^{2+}	1·12	5	500	1000	300
		Ba^{2+}	1·34	5	700	625	300
		Rb^{+}	1·47	5	250	400	130
		Cs^{+}	1·67	10	10	10	*

For specimen locations, see Wilkinson (1958, Fig. 2).

appreciably, whilst the values for Ba and Rb (the latter in harmony with the increased K content of J5) are higher than any recorded in teschenites from the main sill. On the other hand, Cr, V, Ni and Co in J13 are present in amounts

similar to those in the lower teschenites e.g. teschenite B2. The relatively high Li content of J13 reflects the activity of the late-stage solutions. The high Rb content is also to be referred partly to such an origin.

Microscopic and major and trace element data on the feeder dykes, compared with the differentiation history of the sill, strongly suggest their emplacement at various stages, probably as a result of preliminary differentiation at a more deep-seated source.

Acknowledgements—The writer expresses his indebtedness to Dr. S. R. Nockolds and Mr. R. S. Allen for their determination of the trace elements and to Dr. S. R. Nockolds for helpful discussions. Financial aid under a Royal Dutch-Shell Post-graduate Scholarship is also acknowledged.

References

Ahrens L. H. (1952) The use of ionization potentials—I. Ionic radii of the elements. *Geochim. et Cosmochim. Acta* **2,** 155–169.

Campbell R., Day T. C. and Stenhouse A. G. (1933) The Braefoot Outer Sill, Fife—I. The Braefoot Promontory. *Trans. Geol. Soc. Edinb.* **12,** 342–375.

Cornwall H. R. and Rose, H. J., Jr. (1957) Minor elements in Keeweenawan lavas, Michigan. *Geochim. et Cosmochim. Acta* **12,** 209–224.

Degenhardt H. (1957) Untersuchungen zur geochemischen Verteilung des Zirkoniums in der Lithosphere. *Geochim. et Cosmochim. Acta* **11,** 279–309.

De Vore G. W. (1955a) The role of adsorption in the fractionation and distribution of elements. *J. Geol.* **63,** 159–190.

De Vore G. W. (1955b) Crystal growth and the distribution of elements. *J. Geol.* **63,** 471–494.

Drever H. I. (1957) A note on the occurrence of rhythmic layering in the Eilean Mhuire sill, Shiant Isles. *Geol. Mag.* **94,** 277–280.

Edwards A. B. (1941) The crinanite laccolith of Circular Head, Tasmania. *Proc. Roy. Soc. Vict.* **53,** 403–415.

Eskola P. (1922) The silicates of strontium and barium. *Amer. J. Sci.* **204,** 331–375.

Goldschmidt V. M. (1937) The principles of distribution of chemical elements in minerals and rocks. *J. Chem. Soc.* **1,** 655–673.

Goldschmidt V. M. (1954) *Geochemistry* p. 730. Clarendon Press, Oxford.

Hess H. H. (1949) Chemical composition and optical properties of common clinopyroxenes –I. *Amer. Min.* **34,** 621–666.

Higazy R. I. (1952) The distribution and significance of the trace elements in the Braefoot Outer Sill, Fife. *Trans. Geol. Soc. Edinb.* **15,** 150–186.

Howie R. A. (1955) The geochemistry of the charnockite series of Madras, India. *Trans. Roy. Soc. Edinb.* **62,** 725–768.

Kuroda P. K. and Sandell E. B. (1954) Geochemistry of molybdenum. *Geochim. et Cosmochim. Acta* **6,** 35–63.

Landergren S. (1948) On the geochemistry of Swedish iron ores and associated rocks. *Sverig. Geol. Unders. Afh.* **42,** 8–182.

Lundegårdh P. H. (1946) The geochemistry of magmatic iron ore. *Nature, Lond.* **157,** 625.

Lundegårdh P. H. (1949) Aspects to the geochemistry of chromium, cobalt, nickel and zinc. *Sverig. Geol. Unders. Afh.* **43,** 3–56.

Nockolds S. R. and Mitchell R. L. (1948) The geochemistry of some Caledonian plutonic rocks: A study in the relationship between the major and trace elements in igneous rocks and their minerals. *Trans. Roy. Soc. Edinb.* **61,** 533–575.

Nockolds S. R. and Allen R. (1953) The geochemistry of some igneous rock series—I. *Geochim. et Cosmochim. Acta* **4,** 105–142.

Nockolds S. R. and Allen R. (1954) The geochemistry of some igneous rock series—II. *Geochim. et Cosmochim. Acta* **5,** 245–285.

Osborn F. F. (1950) Segregation of elements during the crystallization of magma. *J. Amer. Ceram. Soc.* **33,** 219–224.

Patterson E. M. (1945) The distribution of trace elements in a Scottish Permo-Carboniferous teschenite and its lugaritic differentiate. *Geol. Mag.* **82,** 230–234.

Ringwood A. E. (1955a) The principles governing trace element distribution during magmatic crystallization.—I: The influence of electronegativity. *Geochim. et Cosmochim. Acta* **7,** 189–202.

Ringwood A. E. (1955b) The principles governing trace element distribution during magmatic crystallization —II: The role of complex formation. *Geochim. et Cosmochim. Acta* **7,** 242–254.

Ringwood A. E. (1956) Melting relationships of Ni-Mg olivines and some geochemical implications. *Geochim. et Cosmochim. Acta* **10,** 297–303.

Sahama K. and Rankama Th. G. (1950) *Geochemistry* p. 912. University of Chicago Press.

Sandell E. B. (1949) The gallium content of igneous rocks. *Amer. J. Sci.* **247,** 40–48.

Sandell E. B. and Goldich S. S. (1943) The rarer metallic elements of some American igneous rocks. *J. Geol.* **51,** 99–115, 167–189.

Shaw D. M. (1953) The camouflage principle and trace element distribution in magmatic minerals. *J. Geol.* **62,** 142–151.

Storm T. W. and Holland H. D. (1957) The distribution of nickel in the Lambertville diabase. *Geochim. et Cosmochim. Acta* **11,** 335–347.

Tilley C. E. (1950) Some aspects of magmatic evolution. *Quart. J. Geol. Soc.* **106,** 37–61.

Turekian L. K. and Kulp J. L. (1956) The geochemistry of strontium. *Geochim. et Cosmochim. Acta* **10,** 245–296.

Vincent E. A. and Phillips R. (1954) Iron–titanium oxide minerals in layered gabbros of the Skaergaard intrusion, East Greenland. *Geochim. et Cosmochim. Acta* **6,** 1–26.

Wager L. R. and Mitchell R. L. (1951) The distribution of trace elements during strong fractionation of basic magma—a further study of the Skaergaard intrusion, East Greenland. *Geochim. et Cosmochim. Acta* **1,** 129–209.

Washington H. S. and Merwin H. E. (1927) The acmitic pyroxenes. *Amer. Min.* **12,** 233–252.

Wilkinson J. F. G. (1957) Titanomagnetites from a differentiated teschenite sill. *Min. Mag.* **31,** 443–454.

Wilkinson J. F. G. (1958) The petrology of a differentiated teschenite sill near Gunnedah, New South Wales. *Amer. J. Sci.* **256,** 1–39.

Geochimica et Cosmochimica Acta, 1959, Vol. 16, pp. 151 to 180. Pergamon Press Ltd. Printed in Northern Ireland

The abundances of gallium and germanium in terrestrial materials

J. D. Burton, F. Culkin and J. P. Riley
Department of Oceanography, University of Liverpool,
Liverpool 3

(*Received* 13 *November* 1958)

Abstract—A sensitive spectrophotometric method using phenylfluorone has been applied to the determination of germanium in over 200 minerals, rocks and sediments and in sea water. The crustal abundance of germanium is about 1·7 p.p.m., which is the mean germanium content of both granitic and basic igneous rocks. The average amounts of germanium in metamorphic rocks, shales and red clays lie close to this value. The germanium content of pelagic sediments is contained entirely in their clay fraction. Of the minerals examined, sulphates, carbonates and evaporite minerals contained only very low concentrations of the element. Most oxides and silicates have germanium contents close to the mean crustal abundance. The average concentration of germanium in magmatic sulphides is less than 1 p.p.m. Sea water has been found to contain 0·06 ± 0·01 μg Ge/kg (0·82 ± 0·13 μg-atom/ton).

Gallium has been determined in sea water and in over 280 minerals, rocks and sediments using a sensitive and specific spectrophotometric method. The average crustal abundance of the element is 16·9 p.p.m. The gallium content of over 80 per cent of the thirty-three granitic rocks examined lay between 14 and 24 p.p.m. (average 18·1 p.p.m.). The average Ga : Al ratio for such rocks is $2{\cdot}35 \times 10^{-4}$. The mean gallium concentration found for twenty siliceous sediments is 9·9 p.p.m.; in general, residual sandstones and other sedimentary rocks rich in silica are poor in gallium. Hydrolysate sediments such as clays and mudstones are similar to granitic rocks in gallium content. Only traces of gallium are found in carbonate rocks (mean 0·06 p.p.m.). Pelagic clays from the Pacific, Atlantic and Indian Oceans contained an average of 22·4 p.p.m. of the element and had a Ga : Al ratio of $2{\cdot}40 \times 10^{-4}$. Most of the gallium present in the other pelagic sediments is contained in their clay fraction. The element is enriched relative to aluminium in manganese nodules (mean Ga : Al = $9{\cdot}7 \times 10^{-4}$).

The only oxide minerals examined which contain noteworthy amounts of gallium are corundum, bauxite and magnetite. With the exception of blende formed at low temperature all the sulphides investigated contained less than 3 p.p.m. of the element. Carbonate, sulphate, fluoride and evaporite minerals generally had not more than 0·15 p.p.m. Gallium is concentrated in felspars of pegmatite origin and in the late crystallizates, such as micas. Sea water contains 0·030 ± 0·007 μg of gallium/kg (0·44 ± 0·10 μg-atom/ton) and has a Ga : Al ratio of about $3{\cdot}0 \times 10^{-3}$.

Introduction

Germanium

In a critical survey of the distribution and abundances of a number of the rarer elements Fleischer (1955) has drawn attention to the dearth of information on the abundance of germanium in silicate rocks. Noddack and Noddack (1931), on the basis of unpublished spectrographic analyses of 1600 rocks and minerals, estimated an abundance of 1 p.p.m. of the element in the lithosphere; only fifteen of their published analyses include germanium (Noddack and Noddack 1931). Goldschmidt's (1937) estimate was based on the spectrographic analyses of twelve igneous and thirteen sedimentary rocks, some of which were composite samples. He found an average content of 4 p.p.m. in igneous rocks, 7 p.p.m. in sedimentary rocks, and much higher amounts in the ashes of certain coals.

Between 1937 and 1955 only ten determinations of germanium in igneous rocks (range 0·8–3·0 p.p.m. Ge) and a few determinations of the element in sedimentary rocks, other than coals, were published. On the basis of these data Fleischer considered that the estimates of Goldschmidt and the Noddacks were of the right order of magnitude but that the latter was nearer the truth.

Germanium is not detectable by normal spectrographic methods at concentrations below about 10 p.p.m. although it is detectable at much lower levels if a double arc technique is used. The determination of trace amounts of germanium has been much simplified by the development of specific chemical methods based on phenylfluorone.

Using these methods Onishi (1956) has analysed a number of rocks, mainly from Japan, and has found that the common igneous rocks are similar in germanium content, as shown by the averages: granitic rocks 1·3 p.p.m., intermediate rocks 1·5 p.p.m. basalts and diabases 1·3 p.p.m., gabbros 1·2 p.p.m., and ultramafic rocks 1·0 p.p.m. It is unlikely that the variations between the averages for the various classes are significant since the samples themselves may range from 0·8–1·8 p.p.m. Sedimentary rocks are rather poorly represented in Onishi's paper, and figures are only given for greywackes, sandstones, shale and red clay, though he concluded that sedimentary rocks are richer in germanium than igneous rocks.

Recently Wardani (1957) has carried out chemical determinations of germanium in common igneous rocks and their minerals, and in sedimentary rocks, mainly from the United States. His results are similar to those of Onishi, but tend to be somewhat lower. He postulates that the average abundance of germanium in the earth's crust is 1·0 p.p.m., compared with the figure of $1{\cdot}5 \pm 0{\cdot}5$ p.p.m. found by Onishi (1956). The data of both of these workers indicate that if there is any preferential enrichment of germanium relative to silicon in the rock-forming silicates, it is in the least-linked silicate structures, in agreement with the findings of Harris (1954).

Since germanium dioxide is more soluble in water than silica, germanium should be preferentially leached from rocks during weathering and should therefore occur in sea water. Both Buljan (1949) and Ishibashi and Shigematsu (1951) have predicted the abundance of a number of elements which have not previously been detected in sea water. Buljan's prediction is based on the hypothesis that the geochemical abundance of elements belonging to single groups of the periodic system is a function of their atomic number. This rule, which appears to hold more closely for sea water than for the lithosphere, yields a figure of 73 μg/l. for the concentration of germanium in sea water, a value which does not reflect the anomalously low terrestrial abundance of the element and is obviously too high.

Ishibashi and Shigematsu (1951) have found that if the logarithm of the ratio of the concentration of a given element in the earth's crust to its concentration in sea water is plotted against its ionic potential, the points for most elements lie on a smooth curve. They have used this curve to predict the concentrations of certain elements not yet found in sea water, and have arrived at a figure of 0·2 μg/l. for the germanium content of sea water.

Noddack and Noddack (1940) found germanium in a number of widely differing marine organisms in amounts ranging from 0·07–2·2 p.p.m. They were unable to detect it in sea water and considered that its concentration must be less than 0·1 μg/l. Bardet *et al.* (1938) carried out co-precipitation experiments using various precipitants in 60 l. samples of sea water, and although they were able to detect germanium spectrographically in some of the precipitates, they did not publish any quantitative data. Wardani (1957) referring to, as yet, unpublished work reports that the germanium content of sea water is 0·05 μg/l., which is in excellent agreement with the preliminary figure of $0{\cdot}06 \pm 0{\cdot}01$ μg/l. found by ourselves (Burton *et al.*, 1958) for sea water.

Gallium

Gallium is present in traces in most silicate rocks and minerals, but no minerals are known in which it is a principal component. In its geochemistry it is closely related to aluminium, which precedes it in Group III of the periodic table of the elements. Both elements are strongly lithophile and gallium tends to be camouflaged in aluminium minerals because of the similarity of its ionic radius and ionization potential to those of aluminium (Ga^{3+}, $r = 0{\cdot}62$ Å, $I = 30{\cdot}7V$; Al^{3+}, $r = 0{\cdot}51$ Å, $I = 28{\cdot}4V$) (Ahrens, 1952). On the other hand, since it is a transition element, it possesses siderophile and chalcophile tendencies absent from aluminium, and concentrates in the metallic phase of meteorites and in certain sulphide minerals.

On the basis of ionic radii, substitution of Ga^{3+} for Fe^{3+} ($r = 0{\cdot}64$ Å) would also be expected. High concentrations of gallium are in fact found in magnetites, but in general in silicates it is more coherent with aluminium than iron.

For many years after its discovery in blende by de Boisbaudron (1875) it was thought that gallium was an extremely rare element. The estimate of its abundance ($0{\cdot}1$–$1{\cdot}0 \times 10^{-4}$ p.p.m.) by Clarke and Washington (1926) was based entirely on its occurrence in blende, no determinations in silicates being included. Pioneer work by Hartley and Ramage (1896) showed that it was a ubiquitous constituent of silicate rocks, but it was left to Goldschmidt and Peters (1931) to provide the first quantitative picture of its distribution in rocks and minerals. Fleischer (1955) has summarized the literature on the abundance of gallium in the earth's crust and considers that the true value is slightly greater than the 15 p.p.m. found by Goldschmidt (1937, 1954).

In a recent paper Shaw (1957) has compiled all the more reliable data on the distribution of gallium and of the related elements, indium and thallium, and has critically reviewed their geochemistry. He has pointed out that most of the published analyses of silicate rocks and minerals have been carried out spectrographically and are only semiquantitative; owing to the difficulty of preparing satisfactory standards they have a precision of at best ±10–15 per cent. In a collaborative study described by Fairbairn *et al.* (1951), two standard rocks, a diabase W-1 and a granite G-1, were analysed spectrographically by five experienced spectroscopists. Their results for gallium ranged from 11–20 p.p.m. (mean 14·5 p.p.m.) for W-1 and 15–20 p.p.m. (mean 17·5 p.p.m.) for G-1. Values of 19 and $21{\cdot}5 \pm 0{\cdot}4$ and 22 and $21{\cdot}3 \pm 0{\cdot}3$ respectively were found spectrophotometrically by Onishi (personal communication) and by the present authors (Culkin and Riley, 1958a) which show that the averages of the spectrographic results tend to be low. With the spectrographic methods normally used for the analysis of silicates, the least amount of gallium which can be detected is 2 p.p.m. (Ahrens, 1954a). This is considerably greater than the amount found in many non-silicate rocks and minerals, and our knowledge of the gallium contents of these materials is therefore very scanty.

Almost the only published chemical determinations of gallium in silicate rocks are those of Sandell (1949) who determined it fluorimetrically as the oxinate after chemical separation. He analysed fourteen composite samples prepared from over 110 rocks and thirteen individual rocks, and his work in general confirmed

the findings of earlier workers. Sandell gave 15 p.p.m. gallium as the average for igneous rocks, a figure in excellent agreement with that found by Goldschmidt (1937) spectrographically.

Analytical Methods

Determination of germanium—general procedure

This paper describes investigations into the occurrence of germanium and gallium in a range of igneous, sedimentary and metamorphic rocks mainly of European origin, and in a variety of both silicate and non-silicate minerals. Particular attention has been paid to sedimentary rocks and recent pelagic sediments for which published data are very sparse. The analyses were carried out using solvent extraction procedures to concentrate the germanium and gallium, which were then determined using specific and sensitive spectrophotometric methods.

A modification of the method of Schneider and Sandell (1954) was used for the determination of germanium in silicate rocks and minerals. In their procedure, silicates are decomposed with a mixture of hydrofluoric, nitric and sulphuric acids. After removal of the volatile acids by heating, the residue is taken up in 9 N hydrochloric acid and germanium extracted with carbon tetrachloride. Germanium is back-extracted from the organic phase with water and determined photometrically with phenylfluorone. The following modifications of this procedure were introduced:

(1) Sample weights of 1–2 g were used to increase the sensitivity and precision.

(2) Three extractions with carbon tetrachloride were carried out since only about 85–90 per cent of the germanium is extracted in a single extraction; recoveries of germanium by Schneider and Sandell's method tend therefore to be about 10–15 per cent low and rather erratic.

(3) The photometric determination of germanium with phenylfluorone was performed in the presence of ethylenediaminetetra-acetic acid to suppress interference by other elements which may be extracted by carbon tetrachloride.

(4) The hydrochloric acid solution of the sample after extraction with carbon tetrachloride was retained and used for the determination of gallium, as described below.

The methods used for the dissolution of non-silicate rocks and minerals were varied according to their composition. Thus, samples of carbonates (about 10 g) were dissolved in dilute hydrochloric acid, and sulphide and oxide minerals were opened up by fusion with sodium peroxide and sodium hydroxide respectively. In each case the extraction and determination of germanium was carried out as described above.

Table 1. Recovery of germanium from rock samples

Sample	No.	Germanium added (μg)	Germanium recovered (μg)	Mean recovery
Schist	238 B.L.	0	1·2 1·4	—
		5	6·2 6·5	101
		10	11·1 11·1 11·2 11·2	99
Hornblendite	1971	0	1·0 1·2	—
		10	11·1 11·1	100
Carbonate mud	963	0	0·4 0·4	—
		5	5·2 5·3	97

In order to test the accuracy of the analytical methods used, samples of a schist (no. 238 B.L.), a hornblendite (no. 1971) and a calcareous marine mud (no. 963) were examined alone, and also with added quantities of germanium. The results, which are shown in Table 1, indicate that satisfactory recoveries of the element were obtained. Similar recoveries were obtained with oxide, sulphide and sulphate samples.

As a further test of the accuracy of the analytical method replicate analyses were made of the

standard Granite G-1 and Diabase W-1. These samples were used by Fairbairn *et al.* (1951) in a co-operative study of the precision and accuracy of chemical and spectrochemical analyses of silicate rocks. Our germanium analyses showed the presence of 1·4, 1·3, 1·3, 1·4 and 1·4 p.p.m. in G-1 and 2·0, 2·0, 2·1, 2·1 and 2·2 p.p.m. in W-1, (coefficient of variation in each case 4·0 per cent). Onishi (1956) found 0·9 and 1·6 p.p.m. respectively in these samples. The rather higher germanium contents found by our procedure is probably attributable to the use of a triple extraction for the concentration of the germanium, instead of the single extraction employed by Onishi.

Determination of germanium in sea water

Germanium was separated from sea water by a double co-precipitation with ferric hydroxide. Filtered samples of sea water (5 l.) were treated with a solution of 0·25 g of ferric alum in 10 ml of water. The precipitate was allowed to settle for 3 days, after which a second precipitation was carried out with the same weight of ferric alum. The combined precipitates were removed by centrifugation, and dissolved in hydrochloric acid. Germanium was extracted with carbon tetrachloride and determined photometrically as described above for silicates. Using this method recoveries of added germanium from sea water averaged 97 per cent. The standard deviation of the method was $\pm 0{\cdot}008$ μg/l.

Determination of gallium—general procedure

The method used for rocks and minerals was that described by Culkin and Riley (1958a). After dissolution of the sample and extraction of germanium with carbon tetrachloride, as described above, sufficient titanous chloride was added to the residual hydrochloric acid solution to reduce all the ferric iron to the ferrous state. Water was added to reduce the acid concentration to 6·5 N, and gallium was extracted with di-*iso*propyl ether. After evaporation of the solvent, the residue was dissolved in 6·5 N hydrochloric acid containing 1 per cent of titanous chloride, and gallium was determined spectrophotometrically with rhodamine *B*. Experiments in which known amounts of gallium were present showed that no gallium was extracted by carbon tetrachloride during the extraction of germanium. The accuracy of the method (coefficient of variation) is better than ± 2 per cent at about 20 p.p.m. of gallium (Culkin and Riley, 1958a). Larger samples were taken for analysis of rocks and minerals in which the gallium concentration was known to be less than 1 p.p.m.; at this level the standard deviation was $\pm 0{\cdot}02$ p.p.m.

The use of different reagents for the decomposition of the various classes of minerals was investigated. Samples of these minerals alone, and after the addition of known amounts of gallium, were dissolved and analysed. The results (Table 2) show that gallium recoveries were satisfactory and that in no case was the element lost by volatilization.

Determination of gallium in sea water

Gallium was separated from sea water by a double co-precipitation with ferric hydroxide, as described for germanium (see above). The combined precipitates were dissolved in hydrochloric acid and the gallium was extracted and determined with Rhodamine B. Using this method 93 $\pm$ 5 per cent of gallium added to sea water was recovered; the standard deviation of the method is $\pm 0{\cdot}006$ μg/l.

The Germanium Results

Germanium in non-silicate minerals

Germanium has been determined in graphite and sulphur (purity greater than 85 per cent), Table 8; oxide minerals, Table 9; sulphide minerals, Table 10; carbonate minerals, Table 11; sulphate minerals, Table 12; fluoride minerals, Table 13; evaporite minerals, Table 14; and miscellaneous non-silicate minerals, Table 15.

From the results for oxide minerals (Table 9) it appears that molecular structure is not the primary factor in determining their germanium content. There is no evidence of its association with aluminium or with titanium in anatase, rutile or

Table 2. Recovery of gallium from minerals

Sample*	Method of dissolution	Ga added (μg)	Ga found (μg)	Ga recovery (%)
2117 granite	1	0	10·5	
		5	15·5	100
		10	20·4	99
13191 magnetite	2	0	20·0	
		5	24·8	96
		5	25·0	100
9601 sulphide	3	0	3·1	
		5	8·15	101
11695 carbonate	4	0	0·1	
		5	5·1	100
11404 sulphate	5	0	0·2	
		5	5·2	100
		10	10·1	99
2796 graphite	6	0	6·7	
		5	11·8	102

(1) HF/H_2SO_4 treatment: silicates.
(2) Fusion with $KHSO_4$: oxides.
(3) $HCl/HNO_3/Br_2$: sulphides.
(4) Conc. HCl: carbonates, MnO_2.
(5) Fusion with Na_2CO_3: sulphates.
(6) Fusion with Na_2O_2: graphite.
* Details of these samples are shown in the relevant tables (pp. 168, 169, 170, 173).

ilmenite. The magnetite samples examined did not contain more germanium than did ilmenite, although it might be expected that substitution could take place more readily for tetrahedrally co-ordinated ferric ions in the antispinel structure of magnetite than for the octahedrally co-ordinated ferrous ions of ilmenite (Harris, 1954). The governing factors, which outweigh considerations of mineral structures, appear to be temperature of formation and the extent to which germanium preferentially enters any competing silicate structures.

Germanium is frequently concentrated in minerals formed at low temperatures in the last stages of magmatic differentiation. Thus, the two haematite samples from a low-temperature region (Cumberland) contained 43 and 83 p.p.m. of the element. On the other hand, magnetite, ilmenite and chromite, which are formed in the early and middle stages of magmatic differentiation, have low germanium contents. The low content found in chromite (1·4 p.p.m.) confirms other observations (Goldschmidt and Peters, 1933) that the high concentration of germanium found in this mineral by I. and W. Noddack (1931) was exceptional.

Similar principles affect the occurrence of germanium in sulphide minerals; Brewer *et al.* (1955) have discussed the effect of temperature of formation on the entry of germanium into blendes. Their conclusions are supported by the high value of 116 p.p.m. found in the low temperature blende from Derbyshire.

Ahrens (1953) has postulated that in sulphide minerals formed under conditions of low redox potential germanium occurs in the divalent state. This would explain the high concentrations of this element in certain zinc blendes, since the ionic radii of Ge^{2+} (0·74 Å) and Zn^{2+} (0·72 Å) (Ahrens, 1952) are almost identical and easy replacement should occur. On the other hand, as Brewer *et al.* (1955) have

pointed out, it is not necessary for the Ge to be in the divalent state for it to be included in blende in place of Zn, since its excess of valency electrons may enter the conduction band of the crystal or cause positive holes to be formed.

Goldschmidt and Peters (1933) have recorded a specimen of stannite from Cornwall containing 70 p.p.m. of germanium; this is unusually high for a mineral from a high-temperature region, and a specimen examined in the present work contained only 6·1 p.p.m. This is considerably richer than a specimen of chalcopyrite from the same area (0·5 p.p.m.), and may indicate that germanium concentrates in stannite in preference to other sulphides of tetragonal configuration. This substitution may perhaps occur with either Fe^{2+} or Cu^{2+} whose ionic radii (0·74 Å and 0·72 Å respectively) are similar to that of Ge^{2+} (0·74 Å).

The structure of molybdenite seems to preclude the entry of germanium, regardless of the temperature of formation; thus, there was no significant difference between the samples from Cumberland (low-temperature deposit) and New South Wales (high temperature deposit). It seems possible that germanium may be associated with antimony even in high-temperature regions.

Goldschmidt's value of about 4 p.p.m. for the average germanium content of magmatic sulphides appears to be too high, although it is quoted as a maximum value. The most usual concentration in these minerals is less than 1 p.p.m.

Germanium has not previously been detected in the commonest carbonate minerals. Its low concentration in these minerals is no doubt due to the inability of germanium to enter the coplanar carbonate grouping. The average value found for carbonate rocks is only about 0·2 p.p.m. (Table 11). Strontianite has a mean germanium content (0·5 p.p.m.), considerably higher than calcite (0·06 p.p.m.), but this trend is not maintained in the one sample of witherite examined. While replacement cannot be ruled out, it is probable that the relatively high content of germanium found in calamine was due to contamination with a small amount of blende (1·2 per cent as ZnS). It is interesting to note that Strickland (1955) found 3 p.p.m. of germanium in calamine.

The sulphates and fluorides studied contain very low concentrations of germanium. The salts obtained by evaporation of sea water would contain only about 0·002 p.p.m. of germanium (assuming 0·06 μg Ge/l.). It is evident, therefore, that some of the germanium found in the evaporite minerals must have arisen from other sources. The evaporite minerals all contained less than 0·3 per cent of water-insoluble material and less than 0·1 per cent of Fe_2O_3 (except borax which contained 0·3 per cent Fe_2O_3). Since most of the water insoluble matter was also insoluble in acid it is unlikely that it was the source of the germanium found in these minerals. The comparatively high concentration of germanium in the borax sample is noteworthy.

Germanium in silica and silicate minerals

Germanium has been determined in silica (Table 16), felspars and felspathoids (Table 17), micas (Table 18), amphiboles and pyroxenes (Table 19), and miscellaneous silicate minerals (Table 20).

One of the most prominent features of the geochemistry of germanium is that not only is it able to enter the lattices of sulphide minerals, but owing to the

similarity of its ionic radius and ionization potential (Ge^{4+} 0·53 Å, 45·7 *V*) to those of silicon (Si^{4+} 0·42 Å, 45·1 *V*), (Ahrens, 1952, 1953) it can, to a limited extent, replace silicon in silicate lattices. Its enrichment in certain silicate minerals is therefore to be expected, and it has in fact already been found in considerable amounts in topaz and zinnwaldite.

Although Goldschmidt and Peters (1933) detected up to 7 p.p.m. of germanium in quartz of various origins, the element was not found by Wardani (1957) in the quartz samples which he examined, and Harris (1954) found that quartz and felspars were both poor in the element. The germanium content of the quartz analysed in this work varied from 0·08 p.p.m. (quartzite, Table 27) to 3·5 p.p.m.

The majority of the felspars examined had germanium contents lying close to the average for igneous rocks (1·8 p.p.m.). Two, however, namely microcline (amazonite) and albite, which were from pegmatites, were much richer in germanium. The germanium contents of the common felspathoids examined were less than half those of the felspars: they are related to the higher silica contents of the latter and illustrate the correlation between silicon and germanium (Harris, 1954). The occurrence of relatively high concentrations of germanium in amazonite and the rare caesium mineral pollucite is probably explicable by the fact that, like many other trace elements, it does not fit readily into the common lattice positions and is therefore concentrated in pegmatites (Ahrens, 1945).

The average concentration of germanium found in the micas examined is slightly higher than the average found for igneous rocks. This difference is probably not significant on account of the small number of samples examined. Goldschmidt and Peters (1933) found about 70 p.p.m. of the element in lepidolite, whereas the sample of this mineral analysed in the present work only contained 3·3 p.p.m.

The data for the pyroxenes and amphiboles (Table 19) are in agreement with Wickman's (1943) hypothesis that germanium is enriched in the least linked silicate minerals, their average germanium content being over 50 per cent greater than the average for felspars.

Among the miscellaneous silicate minerals germanium is only appreciably concentrated in yttrotitanite and topaz. The high germanium content of the latter was noted by Goldschmidt and Peters (1933) and by Oftedal (1940).

Germanium in igneous rocks

Thirty-three granitic rocks (Table 21) were examined and their mean germanium content, 1·7 p.p.m., is identical with that of the ten basic igneous rocks examined (Table 22). This value and the "normal" frequency distribution of the results is very similar to those found by Onishi for Japanese and some American rocks, and by Wardani for American rocks (cf. Table 3).

These results confirm the findings of both Onishi and Wardani that there is no significant difference between the germanium contents of acidic and basic igneous rocks. In general our results are rather higher and show a larger spread; this may be caused by the fact that the samples were taken from a wider area.

The lavas examined (Table 23) fall into two groups with regard to their germanium content. The samples from Hawaii have a mean germanium concentration of 3·3 p.p.m. as compared with 2·1 p.p.m. for the remainder.

Table 3. Germanium content of igneous rocks (p.p.m.)

Rock type	Onishi			Wardani			This work		
	Range	Mean	No. of samples	Range	Mean	No. of samples	Range	Mean	No. of samples
Granitic igneous	0·7–1·8	1·3	43	0·9–1·5	1·1	15	0·5–3·2	1·7	33
Basic igneous	1·0–1·7	1·3	15	1·2–1·4	1·3	6	0·7–3·1	1·7	10
Gabbros	0·8–1·8	1·2	20	0·8–1·5	1·1	4			

Germanium in sediments

The germanium contents of the sedimentary rocks examined (Table 25) may be divided into two main categories, the carbonate sediments and the siliceous sediments. The germanium concentrations of the carbonate rocks average 0·09 p.p.m. and are very similar to the calcite samples shown in Table 11. It is interesting to compare the figures for limestones with the germanium contents of modern mollusc shells (Table 4), which in each case are slightly richer in the element.

Table 4. Germanium in mollusc shells

Organism	Ge (p.p.m.)
Pecten maximus	0·15
Mytilus edulis	0·14
Chlamys opercularis	0·19
Nucella lapillus	0·28
Calliostoma zizyphinum	0·23
Littorina littoralis	0·41
Littorina littorea	0·35

The average figure (2·2 p.p.m.) found for four shales from the British Isles is lower than that found by Goldschmidt and Peters (1933) for European shales (3·5 p.p.m.). Onishi (1956) found averages of 1·6 and 1.7 p.p.m. respectively in Japanese shales, and Wardani (1957) determined an average of 1·2 p.p.m. in six North American shales. All these figures are consistent and very much less than the 7 p.p.m. recorded by Preuss (1940) for thirty-six German shales and, although higher germanium concentrations have been reported in shales from coal measures (Breger and Schopf, 1955), it seems likely that the results of Preuss are subject to a systematic error.

Germanium in metamorphic rocks

Metasediments (Table 27) have a mean value of 1·7 p.p.m. of germanium, which is very similar to the average for sedimentary rocks and the crust. The

rather high mean value of 2·7 p.p.m. for the germanium content of metamorphosed igneous rocks (Table 26) is caused by the high germanium contents of samples nos. 2255 and 1550.

Germanium in recent marine sediments

Germanium has been determined in a variety of recent marine sediments from the principal oceans, and it shows a range of 0·0–2·8 p.p.m. (Table 28).

The red clay samples analysed contained 2·1–2·7 p.p.m. of germanium (mean 2·4 p.p.m.), which agrees satisfactorily with the average of 2·0 p.p.m. for twenty-seven pelagic clays from the Pacific Ocean published by Wardani (1957) in a preliminary report. Onishi (1956), on the other hand, found only 1·6 p.p.m. of the element in two composite samples of red clay from the same ocean. The analysis of a 5 m core of undisturbed clay from the North Atlantic showed that there was no significant vertical variation in the germanium content of the sediment column during its period of deposition. The red clays are slightly richer in germanium than the average igneous rocks (1·7 p.p.m.), from which they are probably indirectly formed by weathering. Much germanium finds its way into the ocean and thence into sediments in the form of clay minerals, which, as they are derived from micas and other sheet minerals, will be rich in germanium. Germanium is also certainly transported in solution together with dissolved silica. Some differentiation of dissolved silicon and germanium takes place biologically since germanium, unlike silicon, is not utilized by diatoms (Riley, unpublished work). This probably results in a relative enrichment of the oceans in germanium with respect to silicon (see below). Much of the silicon removed in this way is later deposited, together with varying amounts of suspended clay, as diatomaceous ooze or as gelatinous silica. The germanium concentration in the oceans is presumably kept static by some adsorption or ion exchange mechanism with the marine clays or suspended iron hydroxide.

The germanium contents of the calcareous oozes and muds are generally in inverse proportion to their total calcium + magnesium contents. This is to be expected in view of the inability of the element to substitute for carbon in the carbonate grouping (p. 155). In these samples the germanium is wholly resident in their clay fractions. The latter are found by calculation to contain an average of 2·1 p.p.m., a figure in close agreement with that found for red clays, to which they are chemically and mineralogically akin.

Similar reasoning may be applied to the siliceous oozes which are composed of the remains of siliceous organisms together with varying amounts of clay similar in composition to red clay. The clay contents of such oozes may be calculated roughly from their silica contents, and it again appears that if we assume germanium to be absent from the siliceous organisms (*vide supra*), then the germanium content of the clay fraction is in general about 2·0 p.p.m.

Full chemical and mineralogical details of most of the oozes and clay samples shown in Table 28 are to be published in a paper in course of preparation.

The germanium content of the acid soluble fraction of manganese nodules probably represents germanium which has been removed from sea-water by the scavenging action of the oxides and hydroxides of iron and manganese as described by Goldberg (1954).

In order to investigate the scavenging action of various precipitates for germanium, samples of filtered sea water (5 l.), enriched with 10 μg of germanium, were treated with a solution of the salt of the element concerned. The hydroxide which formed by the action of the natural alkalinity of the sea water was allowed to precipitate and after 4 days was analysed for germanium. Blank tests were also run on unenriched sea water. The precipitate of manganese dioxide was produced by treating the sea water with 10 ml of 0·1 N potassium permanganate and 10 ml of ethyl alcohol. These tests (Table 5) showed that ferric hydroxide and manganese

Table 5. Co-precipitation of germanium (10 μg) from sea water (5 l.)

Precipitate	Form in which element was added	Wt. of element (mg)	Ge co-precipitated (%)
$Fe(OH)_3$	$FeNH_4(SO_4)_2 \cdot 12H_2O$	30	95
$Al(OH)_3$	$NH_4Al(SO_4)_2 \cdot 12H_2O$	12	24
$Cr(OH)_3$	$Cr(NO_3)_3 \cdot 9H_2O$	25	5
$MnO_2 \cdot xH_2O$	$KMnO_4$	11	69

dioxide were both effective scavengers of germanium from sea water. Further tests were also made attempting to co-precipitate germanium from acidified sea water as sulphide, with the sulphides of tin, lead, copper and bismuth; in each case less than 10 per cent of the germanium in the water was co-precipitated.

Germanium in sea water

Germanium has been determined in ten samples of sea water from the English Channel, Irish Sea and North Atlantic. The results, (Table 29), show that within the limits of experimental error, there is no variation in germanium content with either depth or position. The average germanium content (0·06 $\pm$ 0·01 μg/kg or 0·82 $\pm$ 0·13 μg-atom/ton) is in good agreement with the value found by Wardani (0·05 μg/kg)(cf. Onishi, 1956) and of the same order as the concentration (0·2 μg/l.) predicted by Ishibashi and Shigematsu (1951).

Germanium is present in sea water in much more constant amounts than silicon, which varies from 10 to 2500μg/kg. This constancy is probably due to the fact that unlike silicon it is not utilized by plankton or sponges in the formation of their shells and hard parts. Germanium is much enriched in sea water relative to silicon. If a value of 100 μg/l. is assumed for the average silicon content of sea water, then the Si : Ge ratio in sea water is 1700 : 1 as compared with a ratio of 170,000 : 1 in the lithosphere.

The germanium content of sea water may be maintained at this low level either by mechanisms of adsorption as discussed above (p. 158) or by ion exchange with clays as suggested by Goldschmidt (1954).

The Gallium Results

Gallium in non-silicate minerals

The gallium contents of sulphur, graphite and some oxide, sulphide, sulphate, carbonate, fluoride, evaporite and miscellaneous minerals are shown in Tables 8–15.

The comparatively high gallium contents (average 7·1 p.p.m.) of the four graphite samples of various geographical origins are probably indicative of their organic origin. Goldschmidt (1937) considers that a biological enrichment process is responsible for the high concentrations of gallium, germanium and certain other rare elements in the ashes of some coals. It is probable, since graphite is the final product of the process by which coal is formed from organic matter, that any gallium present in coal undergoing graphitization would remain in the graphite formed.

The ability of gallium ($r = 0{\cdot}62$ Å) to replace aluminium ($r = 0{\cdot}51$ Å) is most clearly seen in the oxide minerals (Table 9). High concentrations of the element occur not only in bauxite but also in corundum, in which it has not previously been detected (Pearson, 1955). The amounts found in bauxite are comparable with those determined by Majumdar and Sarkar (1947) and Gordon and Murata (1952).

Minerals, such as magnetite and franklinite, which are products of the early and middle stages of magmatic differentiation, were also found to contain high concentrations (20–90 p.p.m.) of gallium which must replace Fe^{3-} ($r = 0{\cdot}64$ Å). On the other hand it is only present in small amounts in haematite, goethite and limonite which are formed by hydrothermal or sedimentation processes. Quite a high concentration of gallium was found in chromite; the association of gallium with chromium is perhaps to be expected because of the similarity of their ionic radii (Cr^{3+}, $r = 0{\cdot}63$ Å).

The occurrence of gallium in sulphide minerals is almost entirely restricted to blende and germanite and it is clear that its chalcophile behaviour is most strongly affected by its similarity to zinc. Morris and Brewer (1954) have summarized the literature on the occurrence of gallium in blendes and have concluded that, like germanium, it is concentrated most strongly in the low temperature varieties. This is a possible explanation of the difference between the two samples examined, the sample from Derbyshire (111 p.p.m.) being from a low-temperature region and that from Jugoslavia (2·2 p.p.m.) from a high-temperature region. Morris and Brewer (1954) consider that gallium is present in blende as a solid solution of the sulphide of either Ga^{2+} or Ga^{3+}. Gallium is not concentrated in the sulphides of arsenic, antimony, tin, iron, molybdenum or lead.

The only carbonate minerals containing significant amounts of gallium were siderite (average 0·6 p.p.m.) and calamine (1·3 p.p.m.); the presence of gallium in the latter is explicable by contamination with 1·2 per cent of blende. The remaining carbonates averaged about 0·1 p.p.m. which is about the same as that found by Culkin and Riley (1958b) for gallium in mollusc shells. The reluctance of gallium to enter carbonate minerals is probably due to the fact that it does not form a carbonate but instead either goes into solution as the gallate ion or precipitates as its hydroxide.

The very small concentrations of gallium found in most of the sulphate, fluoride and evaporite minerals examined (Tables 12, 13 and 14) are in fair agreement with what would be found on evaporation of sea water containing 0·03 μg Ga/l. Although cryolite is rich in aluminium, Goldschmidt and Peters (1933) were unable to detect gallium spectrographically in a specimen from

Greenland; our work has confirmed their observations that only small concentrations of gallium are present. Goldschmidt and Peters concluded that during the formation of cryolite the large Ga^{3+} ion was rejected in favour of the aluminium ion and was instead incorporated in the accompanying sphalerite. Wickman (1943) has advanced a thermodynamical explanation for the relative enrichment of aluminium in cryolite.

Gallium in silicate minerals

The gallium contents of the silicate minerals examined are shown in Tables 16–20. In general, as would be expected, the concentration of gallium in quartz samples is very low. In the felspars (Table 17) there is considerable variation in gallium content. Two samples of amazonite have an average concentration of 58 p.p.m. and albite from Virginia contains 46 p.p.m., whereas another albite from Italy has only 4·7 p.p.m. In general, as found by Bell (1955), felspars of pegmatite origin are much richer in gallium than other felspars, a similar phenomenon to that observed with germanium (p. 156). The gallium content of the non-pegmatite felspars is fairly constant with an average of 15·1 p.p.m.

The felspathoids (mean 14·7 p.p.m.) are similar in their gallium content to the felspars. The figures for nepheline and sodalite are much lower than those found by Goldschmidt and Peters (1933) (74 and 44–74 respectively). Those for leucite and pollucite are slightly higher than those values recorded by Goldschmidt and Peters (1933) and Ahrens (1947) (7, 5–10 p.p.m. respectively). Ahrens has commented on the low gallium content of pollucite compared with other pegmatite minerals; he has attributed this to the lack of a site in its lattice capable of holding medium-sized ions in sixfold co-ordination.

The tendency for gallium to concentrate in the late crystallizates is well illustrated by the micas, which have the highest gallium contents found in this work. As Goldschmidt and Peters (1933), Borovik and Sosedko (1937) and Nockolds and Mitchell (1948) have demonstrated, muscovite and phlogopite have a greater affinity for gallium than has biotite.

The hornblendes (Table 19) examined were quite uniform in their gallium contents (mean 13·4 p.p.m.) but the non-aluminous amphiboles, asbestos and actinolite were much poorer. The low gallium contents of the pyroxenes found by earlier workers (Shaw, 1957, Table 8) were confirmed.

Gallium in igneous rocks

The gallium contents of the various classes of igneous rocks examined are shown in Tables 21–23. The gallium concentrations of thirty-three granitic rocks lie in the range 9·1–43·1 p.p.m. of which 60 per cent of the samples contain between 15–22 p.p.m. and over 80 per cent between 14 and 24 p.p.m. The average value for these granitic rocks (18·1 p.p.m.) is in excellent agreement with the average of 18·8 p.p.m. calculated by Fleischer (1955) from the analyses of 209 rocks containing more than 65 per cent SiO_2. Ahrens (1954b) found an average of 17 p.p.m. in Canadian granites; the same figure was found by Sandell (1949) for the average gallium content of seven composite granite samples using a fluorimetric method. If Daly's (1933) figure of 7·7 per cent is assumed for the abundance of

aluminium in granitic rocks, a gallium content of 18·1 p.p.m. corresponds to a Ga : Al ratio of $2{\cdot}35 \times 10^{-4}$.

Some of the very high gallium contents reported for granites by certain workers seem to be due to systematic errors. Sahama (1954) found 74 p.p.m. in a composite of fifty-four samples of Rapakivi granite and Rankama (1946) found the same amount in twelve other granites from Finland. We have found 16·9 p.p.m. in a sample of Rapakivi granite and an average of 21·1 p.p.m. (range 10·5–43·1) in five other Finnish granites; similar concentrations have been recorded by Webber (1952).

The spread of gallium concentrations found in the migmatite rocks and in the lavas and tuffs closely resembles that of the granitic rocks, and the average values for all types are identical.

The average gallium content found for ten basic rocks (11·5 p.p.m.) is in excellent agreement with the value found fluorimetrically by Sandell for a composite sample of twenty-four basic rocks. This agreement cannot be considered very significant in view of the small number of samples examined and of the higher concentrations recorded by other workers for this class of rocks (cf. Shaw 1957, Table 4).

Gallium in sedimentary rocks

The average gallium content of the twenty siliceous sediments examined is 9·9 p.p.m. (Table 25), which is only about half that of igneous rocks. The exact value of the mean is probably not significant since some of the samples examined were quite poor in aluminium. In general, residual sandstones and other rocks rich in silica are poor in gallium because of their low aluminium content; on the other hand, the hydrolysate sediments, such as clays and mudstones, have gallium contents similar to those of granitic rocks.

The carbonate sediments are quite uniform in gallium content (average 0·06 p.p.m.), and this figure confirms the non-association of the element with carbonate minerals discussed on p. 160. The concentration of gallium found in drewite and in most of the modern mollusc shells examined by the authors (Culkin and Riley, 1958b) lay close to the average for chalks and limestones.

Gallium in metamorphic rocks

The gallium contents of metamorphosed igneous rocks and metasediments are shown in Tables 26 and 27. The average for metamorphosed igneous rocks (11·6 p.p.m.) is distinctly lower than that for granitic rocks, but owing to the small number of samples examined no definite conclusion can be drawn. Among the metasediments those containing much silica and little alumina are poor in gallium. The average Ga : Al ratio ($2{\cdot}0 \times 10^{-4}$) of those samples (all from Eire) for which aluminium contents are available is similar to that of igneous rocks.

Gallium in recent marine sediments

Very little work has been done on the gallium contents of pelagic sediments since the pioneer investigations of Goldschmidt and Peters (1933), who found

concentrations of gallium in red clays, calcareous and siliceous oozes of 4–22, 4 and 4–7 p.p.m. respectively. Recently Goldberg and Arrhenius (1958) have published semiquantitative spectrographic analyses of twenty-six pelagic sediments from the Eastern Pacific Ocean. Six samples of dark brown clay contained 19–22 p.p.m. of gallium (average 21 p.p.m.) and one sample of globigerina ooze contained 13 p.p.m. (34 p.p.m. in the residue after removal of carbonate with acid). Gallium was not detected in two foraminiferal oozes.

The gallium contents of the pelagic sediments examined in this work are shown in Table 28. The pelagic clay samples contain a fairly uniform concentration of gallium (20–28 p.p.m.). Their mean (22·4 p.p.m.) for the six stations investigated is in excellent agreement with that found by Goldberg and Arrhenius. The average Ga : Al ratio of these clays ($2{\cdot}40 \times 10^{-4}$) is very close to that of granitic rocks ($2{\cdot}35 \times 10^{-4}$); this suggests that little differentiation of the two elements has occurred during the weathering and degradation of terrestrial rocks and the deposition of their decomposition products as clays on the ocean floor. It should be noted, however, that gallium is enriched in the pelagic clays compared with granitic rocks, on account of the higher aluminium content of the clays. Investigation of an undisturbed red clay from the Atlantic Ocean has shown no significant variation of either aluminium or gallium concentration with depth down the core.

As in the case of germanium the gallium contents of the siliceous and globigerina oozes are inversely related to their silica and carbonate contents; when allowance is made for these, the gallium contents of their clay fractions are found to be similar to those of the pelagic clays.

The manganese nodules examined contained 15·7–21·5 p.p.m. of gallium in their acid-soluble fractions. Their Ga : Al ratios (average $9{\cdot}7 \times 10^{-4}$) although variable, are all considerably greater than the average for pelagic sediments; this ratio probably reflects the fact that most of the aluminium and gallium which the nodules contain is directly scavenged from sea water, in which the Ga : Al ratio is about 3×10^{-3} (*vide infra*). The active agent in this scavenging process is probably highly adsorptive colloidal ferric hydroxide, which loses its charge and accretes with manganese oxides or hydroxides to form the nodules (Goldberg, 1954).

Details of the chemical and mineralogical compositions of most of the samples shown in Table 28 are to be published in a paper being prepared.

The adsorptive properties of colloidal oxides and hydroxides were investigated. Samples (5 l.) of filtered sea water enriched, with 1 μg of gallium, were treated with salts of aluminium, chromium, iron and manganese (equivalent to 25 mg of the metal) as described on p. 159. The percentages of gallium co-precipitated from the sea water by a single precipitation were as follows: Al, 58; Cr, 65; Fe, 75; Mn, 27.

Gallium in sea-water

The occurrence of gallium in sea-water has received little attention owing to the lack of sufficiently sensitive analytical methods. Del Campo and Rodeja (1914) and Bardet *et al.* (1938) detected the element in sea-water spectrographically. Noddack and Noddack (1940) found 0·5 μg of gallium/l. in the water of Gullmars Fjord, Göteborg, Sweden; this analysis can scarcely be considered to be representative of ocean water, since the sample was taken from a land-locked fjord.

Ishibashi and Shigematsu (1951) have predicted the abundance of gallium in sea-water to be 0·001 μg/l.

Gallium has been determined in eleven samples of sea-water (mainly surface samples). Before analysis the samples were passed through a filter having an average pore size of 1·5 μ. The results (Table 29) show that the average gallium content of sea-water is $0{\cdot}031 \pm 0{\cdot}007$ μg/kg ($0{\cdot}44 \pm 0{\cdot}09$ μg-atom/ton) and that there is no significant variation with depth or position. This value. although very much less than that found by the Noddacks, is much more in line with the relative abundance of the element in the lithosphere.

Gallium is enriched in sea-water relative to aluminium. If an average aluminium concentration of 10 μg/l. is assumed for sea-water (Simons *et al.*, 1953, Greenhalgh and Riley, unpublished work), then the Ga : Al ratio for sea-water is 3×10^{-3} compared with the average of about $2{\cdot}2 \times 10^{-4}$ for the lithosphere. This enrichment of sea-water in gallium relative to aluminium has been predicted by Goldschmidt (1954).

The fate of gallium in weathering processes

In order to investigate the behaviour of gallium in weathering of a granite to a laterite, samples taken at 30 cm vertical intervals in a laterite deposit were analysed for gallium, aluminium and iron. The deposit itself is situated 35 miles

Table 6. The occurrence of gallium, aluminium and iron in a laterite

Sample no.	Depth (cm)	Ga (μg/g)	Al^{3+} (%)	$\frac{Ga^{3+}}{Al^{3+}} \times 10^4$	Fe^{3+} (%)	Fe^{2+} (%)	$\frac{Ga^{3+}}{Fe^{3+}} \times 10^4$
1	Top of section	27·2	8·44	3·22	3·19	0·16	8·5
2	30	27·0	8·41	3·21	3·13	0·11	8·6
3	60	26·0	8·29	3·14	2·95	0·27	8·8
4	90	27·1	8·45	3·21	3·12	0·22	8·7
5	120	25·9	8·37	3·09	3·23	0·11	8·0
6	150	25·2	8·39	3·06	3·22	0·11	7·8
7	180	25·7	8·33	3·09	3·17	0·17	8·1
8	210	26·1	8·08	3·23	3·17	0·15	8·2
9	240	24·1	7·99	3·01	3·17	0·17	7·6
10	270	21·7	7·41	2·93	2·63	0·17	8·3
11	300	21·6	7·30	2·96	2·13	0·12	10·1
12	Granite	$21{\cdot}9 \pm 0{\cdot}15$	6·59	$3{\cdot}32 \pm 0{\cdot}02$	1·00	0·94	21·9

S.E. of Kaduna, Northern Nigeria, and is approximately 3·3 m thick. It had been formed by alteration of a coarse foliated biotite granite (CL 12), which had the approximate composition: Biotite 10 per cent; magnetite 5 per cent; quartz 15 per cent; potassium felspar (orthoclase or microcline) 70 per cent. The results (Table 6) show that the laterite column and the original granite had average Ga : Al ratios of $3{\cdot}11 \pm 0{\cdot}11$ and $3{\cdot}32 \pm 0{\cdot}02$ respectively, hence there is possibly a slight enrichment of aluminium relative to gallium in the former as predicted by

Goldschmidt (1954). On the other hand, the lack of coherence between gallium and ferric iron during weathering is very pronounced.

Conclusions

The occurrence of germanium in minerals in appreciable amounts is confined to the oxide, sulphide and silicate minerals, and only very small amounts occur in carbonates, sulphates and evaporite minerals. In general the amounts of the element found in minerals and rocks are only about one third of those found by Goldschmidt.

The average amount of the element found in acidic igneous rocks (1·7 p.p.m.) and basic igneous rocks (1·7 p.p.m.) are identical and agree quite well with the amounts found by Onishi (1956) (1·3 p.p.m. and 1·3 p.p.m., respectively). The average germanium content of igneous rocks is about 1·7 p.p.m. and this figure probably approximates to the average abundance of the element in the earth's crust. The distribution of germanium in igneous rocks and minerals does not seem to directly follow that of any of their major constituents. There is some evidence that the element substitutes for silicon most readily and most frequently in the least cross-linked silicate minerals, as suggested by Wickman (1943) and Harris (1954).

The germanium content of the siliceous sedimentary rocks (average 1·5 p.p.m.) examined shows a much larger scatter than the igneous rocks, but there are insufficient results to draw any definite conclusions. In the recent marine sediments, however, the germanium is entirely confined to their clay fraction, which contains about 2·2 p.p.m. The calcareous and siliceous remains of marine plants and animals which usually constitute the remainder of the oozes and clays are devoid of germanium.

Crustal abundance of gallium

The most reliable estimates of the crustal abundance of gallium are shown in Table 7; they have generally been calculated on the assumption that the abundance

Table 7. Crustal abundance of gallium

Reference	Abundance (p.p.m.)
Goldschmidt and Peters (1933)	15
Sandell (1949)	15
Bell (1955)	15
Fleischer (1955)	15
Shaw (1957)	19
This paper	17

is the concentration of gallium in the average igneous rock. The figure of 17 p.p.m. found in this work is the weighted mean of the average gallium contents shown in Tables 21–24.

Fleischer (1955) considered that the figure of 15 p.p.m. which he obtained after

a thorough survey of the literature was close to the true value but was probably slightly low. Shaw (1957) has reassessed Fleischer's data on the grounds that the majority of igneous rocks are in the basic or intermediate-silicic ranges. He considers that the crustal abundance of the element is best represented by the average of these two classes.

Many of the data from which the estimates in Table 7 were compiled are only semiquantitative and in view of this, the agreement between them is surprisingly good.

Acknowledgements—The authors wish to thank the Trustees of the British Museum for the gift of a number of recent marine sediments and manganese nodules, Dr. D. Ericson of the Lamont Geological Observatory for the red clay core, Dr. G. Arrhenius of the Scripps Institution of Oceanography for other pelagic sediments, and Mr. R. N. Cope for the collection of the laterite samples. They would also like to thank Dr. B. Leake for his helpful suggestions and criticism, and Mr. F. A. J. Armstrong for providing many of the sea-water samples. One of us (J. D. B.) was in receipt of a training grant from the Development Commission of the Ministry of Agriculture and Fisheries during part of the work.

References

Ahrens L. H. (1945) Quantitative spectrochemical examination of minor constituents in Pollucite. *Amer. Min.* **30,** 616–622.

Ahrens L. H. (1947) Analyses of minor constituents of Pollucite. *Amer. Min.* **32,** 44–51.

Ahrens L. H. (1952) The use of ionization potentials. Part I. Ionic radii of the elements. *Geochim. et Cosmochim. Acta* **2,** 155–169.

Ahrens L. H. (1953) The use of ionization potentials. Part II. Anion affinity and geochemistry. *Geochim. et Cosmochim. Acta* **3,** 8.

Ahrens L. H. (1954a) *Quantitative Spectrochemical Analysis of Silicates.* Pergamon Press, London.

Ahrens L. H. (1954b) The lognormal distribution of the elements. *Geochim. et Cosmochim. Acta* **5,** 49–73, 121–131.

Bardet J., Tchakirian A. and Lagrange R. (1938) Recherche spectrographique des éléments existant a l'état de traces. *C. R. Acad. Sci., Paris* **206,** 450.

Bell C. K. (1955) Some aspects of the geochemistry of gallium. *Bull. Geol. Soc. Amer.* **6,** 1529–1530.

Boisbaudron L. de (1875) Caractères chimiques et spectroscopiques d'un nouveau métal, le Gallium découvert dans une blende de la mine de Pierrefitte, vallée d'Argeles. (Pyrénées). *C. R. Acad. Sci., Paris* **81,** 493.

Borovik S. A. and Sosedko A. F. (1939) Ga in mineral samples collected by the expedition of the Lomonosof Institute of the Academy of Sciences of the U.R.S.S. *Dokl. Akad. Nauk SSSR* **14,** 31–34.

Breger I. A. and Schopf J. M. (1955) Germanium and uranium in coalfield wood from upper Devonian black shale. *Geochim. et Cosmochim. Acta* **7,** 287.

Brewer F. M., Cox J. D. and Morris D. F. C. (1955) The occurrence of germanium in blende. *Geochim. et Cosmochim. Acta* **8,** 131–5.

Buljan M. (1949) The occurrence of elements in sea-water and in the earth's crust in relation to the periodic system of elements. *Acta Adriat.* **4,** (6), 36.

Burton J. D., Culkin F. and Riley J. P. (1958) Germanium and Gallium in sea-water. *Nature, Lond.* **181,** 179–180.

Campo A. del and Rodeja V. G. (1914) Espectrografia Oceanografica. *An. Soc. Esp. Fis. Quim.* **12,** 78.

Clarke F. W. and Washington H. S. (1924) The data of geochemistry. *U.S. Geol. Surv. Prof. Pap.* 127, p. 21.

Culkin F. and Riley J. P. (1958a) The spectrophotometric determination of gallium in rocks and minerals. *Analyst* **83,** 208–212.

Culkin F. and Riley J. P. (1958b) The occurrence of gallium in marine organisms. *J. Mar. Biol. Ass. U.K.* **37,** 607–615.

Daly R. A. (1933) *Igneous Rocks and the Depths of the Earth.* McGraw-Hill, New York.

Fairbairn H. W., Schlecht W. G., Stevens R. E., Dennen W. H., Ahrens L. H. and Chayes F. (1951) A Co-operative Investigation of Precision and Accuracy in Chemical, Specsrochemical and Modal Analysis of Silicate Rocks. *Bull. U.S. Geol. Surv.* No. 980.

Fleischer M. (1955) Estimates of the abundances of some chemical elements and their reliability. *Spec. Pap. Geol. Soc. Amer.* No. 62, 145–154.

Goldberg E. D. (1954) Marine geochemistry. I. Chemical scavengers of the sea. *J. Geol.* **62,** 249–265.

Goldberg E. D. and Arrhenius G. O. S. (1958) Chemistry of Pacific pelagic sediments. *Geochim. et Cosmochim. Acta* **13,** 153–212.

Goldschmidt V. M. (1937) The principles of distribution of chemical elements in minerals and rocks. *J. Chem. Soc.* 655.

Goldschmidt V. M. (1954) *Geochemistry.* Oxford University Press.

Goldschmidt V. M. and Peters C. (1931) Zur Geochemie des Ga. *Nachr. Ges. Wiss. Göttingen, Math. Phys. Kl.* I, 165–183.

Goldschmidt V. M. and Peters C. (1933) Zur Geochemie des Germaniums. *Nachr. Ges. Wiss. Göttingen, Math. Phys. Kl.* III, **31,** 141–166.

Gordon M. and Murata K. J. (1952) Minor elements in Arkansas bauxite. *Econ. Geol.* **47,** 169.

Harris P. G. (1954) Distribution of germanium among co-existing phases of partly glassy rocks. *Geochim. et Cosmochim. Acta* **5,** 185.

Hartley W. N. and Ramage H. (1896) On the occurrence of gallium in the clay-ironstone of the Cleveland District of Yorkshire: Determination of gallium in blast-furnace iron from Middlesbrough. *Proc. Roy. Soc.* **60,** 393.

Ishibashi M. and Shigematsu T. (1951) Chemical studies of the Ocean. XL: On the regularities of the amounts of elements. *Bull. Inst. Chem. Res. Kyoto* **27,** 42.

Majumdar A. and Sarkar P. B. (1947) Ga content in Indian bauxites. *Sci. & Cult.* **13,** 75.

Morris D. F. C. and Brewer F. M. (1954) The occurrence of Ga in blende. *Geochim. et Cosmochim. Acta* **5,** 134–141.

Noddack I. and Noddack W. (1931) Die geochemie des Rheniums. *Z. phys. Chem.* A **154,** 214–225.

Noddack I. and Noddack W. (1940) Die Haüfigkeiten der Schwermetalle in Meerestieren. *Ark. Zool.* **32,** 1.

Nockolds S. R. and Mitchell, R. L. (1948) The geochemistry of some Caledonian plutonic rocks. *Trans. Roy. Soc. Edinb.* **61,** 533–575.

Oftedal I. (1940) Untersuchungen über die Nebenbestandteile von Erzmineralen norwegischer zinkblende führender Vorkommen. *Skr. Norske VidnskAkad. Mat. Nat. Kl.* No. 8.

Onishi H. (1956) Notes on the geochemistry of germanium. *Bull. Chem. Soc. Japan* **29,** 686–694.

Onishi H. and Sandell E. B. (1955) Photometric determination of gallium with Rhodamine B. *Analyt. Chim. Acta* **13,** 159.

Preuss E. (1940) Beitrage zur spektralanalytischen Methodik II. Bestimmung von Zn, Cd, Hg, In, Tl, Ge, Sn, Pb, Sb und Bi durch fraktionierte Destillation. *Z. angew. Miner.* **3,** 8–20.

Rankama K. (1946) On the geochemical differentiation in the earth's crust. *Bull. Comm. Géol. Finl.* No. 137.

Sahama T. G. (1945) On the chemistry of the east Fenno-scandian rapakivi granites. *C. R. Soc. Géol. Finl. No.* 18, 15–64.

Sandell E. B. (1949) The Ga content of igneous rocks. *Amer. J. Sci.* **247,** 40–48.

Schneider W. A. and Sandell E. B. (1954) Photometric determination of traces of germanium after carbon tetrachloride extraction. *Mikrochim. Acta* 263.

Shaw D. M. (1957) *Physics and Chemistry of the Earth* Vol. II, pp. 164–211. Pergamon Press, London.

Simons L. H., Monaghan P. H. and Taggert M. S. (1953) Aluminium and iron in Atlantic and Gulf of Mexico waters. *Analyt. Chem.* **25,** 989–990.

Strickland E. H. (1955) Rapid determination of microgram quantities of germanium. *Analyst* **80,** 548.

Wardani S. A. (1957) On the geochemistry of germanium. *Geochim. et Cosmochim. Acta* **13,** 5–19.

Webber G. R. (1952) Spectrochemical analysis of the White Mountain magma series and some Finnish granites. M.Sc. Thesis, McMaster University (unpublished).

Wickman F. E. (1943) Some aspects of the geochemistry of igneous rocks and of differentiation by crystallization. *Geol. Fören. Stockh. Förh.* **65,** 371.

Table 8. Gallium and germanium in sulphur and graphite

Cat. no.	Mineral	Locality	Ge (p.p.m.)	Ga (p.p.m.)
T.S.T.2796	Graphite	Borrowdale, Cumberland	2·6	6·7
	Graphite	Cumberland	1·0	9·6
	Graphite	Greenland	1·3	5·6
	Graphite	Ceylon	0·3	6·4
14874	Sulphur	La Familia Mine, Almeria, Spain	0·3	0·3

Table 9. Gallium and germanium in oxide minerals

Cat. no.	Mineral	Formula	Locality	Ge (p.p.m.)	Ga (p.p.m.)
Simple oxide minerals					
	Anatase	TiO_2	La Grave, French Alps	1·1	0·8
14735	Cassiterite	SnO_2	St. Austell, Cornwall	2·1	6·2
	Corundum	Al_2O_3	Franklin, N. Carolina	0·8	99·7
12756	Haematite	Fe_2O_3	Paracuti, Brazil	2·6	1·2
12672	Haematite	Fe_2O_3	Unknown	1·3	1·2
12716	Haematite	Fe_2O_3	Cumberland	83	2·1
12733	Haematite	Fe_2O_3	Cumberland	43	1·6
13396	Pyrolusite	MnO_2	Aberdeenshire	3·8	2·9
13271	Pyrolusite	MnO_2	Jamda, India	1·2	2·7
12514	Rutile	TiO_2	Unknown	0·7	1·9
Hydrated oxides					
10368	Bauxite	$Al_2O_3 \cdot 2H_2O$	Katni, Cen. Prov. India	0·8	104
12881	Bauxite	$Al_2O_3 \cdot 2H_2O$	Pereille, France	2·1	83·9
12927	Goethite	$Fe_2O_3 \cdot H_2O$	Unknown	0·3	1·3
8528	Limonite	$Fe_2O_3 \cdot nH_2O$	Quarff, Shetland	<0·02	0·5
12637	Limonite	$Fe_2O_3 \cdot nH_2O$	Fyfield, Northants.	1·0	6·0
Multiple oxides					
13141	Chromite	$FeCr_2O_4$	Borchills, Baltimore	1·4	17·9
	Franklinite	$ZnFe_2O_4$	Franklin, New Jersey	1·4	14·4
8052	Ilmenite	$FeTiO_3$	Connecticut	0·8	8·7
	Ilmenite (ex Iron sand)	$FeTiO_3$	W. coast, S. America	2·7	1·4
13191	Magnetite	Fe_3O_4	Iser, Bohemia	1·2	20·0
12737	Magnetite	Fe_3O_4	Pretoria, S. Africa	3·1	88·6
13420	Magnetite	Fe_3O_4	Taberg, Switzerland	1·2	51·2
12750	Magnetic iron sand	Fe_3O_4	Seacombe, Cheshire	0·6	28·5

Table 10. Gallium and germanium in sulphide minerals

Cat. no.	Mineral	Formula	Locality	Ge (p.p.m.)	Ga (p.p.m.)
15042	Arsenopyrite	$FeAsS$	Cornwall	1·6	0·37
1672	Blende	ZnS	Trepea, Jugoslavia	0·7	2·2
16304	Blende	ZnS	Derbyshire	116	111
9527	Bornite	Cu_5FeS_4	Australia	0·05	2·88
12563	Chalcopyrite	$CuFeS_2$	Devon	0·5	0·22
15259	Cinnabar	HgS	Almaden, Spain	1·9	0·40
10072	Galena	PbS	Cumberland	0·6	0·08
T.S.T.2090	Galena	PbS	Granada, Spain	1·2	0·12
15909	Jamesonite	$Pb_4FeSb_6S_{14}$	Cornwall	3·4	0·02
12518	Marcasite	FeS_2	Folkestone	0·8	0·81
13146	Molybdenite	MoS_2	Tarnworth, N.S.W.	1·4	0·38
14539	Molybdenite	MoS_2	Aldfield, Pontiac Co., Quebec	1·6	0·28
G.H.M.237	Molybdenite	MoS_2	Carrick Fell, Cumberland	1·1	2·1
15040	Orpiment	As_2S_3	Idjowa, Hungary	1·1	0·85
15888	Pyrite	FeS_2	Drunwhindle	0·7	0·08
12599	Pyrite	FeS_2	Unknown	0·4	0·67
12602	Pyrite	FeS_2	Unknown	0·6	0·71
9601	Pyrrhotite	$Fe_{1-x}S$	Roughtingill, Cumberland	0·5	3·1
15020	Realgar	AsS	Hungary	0·5	2·0
11716	Stannite	Cu_2FeSnS_4	Cornwall	6·1	2·9
15068	Stibnite	Sb_2S_3	Ichinokawa, Japan	10·0	0·54

Table 11. Gallium and germanium in carbonate minerals

Cat. no.	Mineral	Formula	Locality	Ge (p.p.m.)	Ga (p.p.m.)
	Aragonite*	$CaCO_3$	Andros Islands, Bahamas	0·04	0·06
	Calamine	$ZnCO_3$	Laurium, Greece	1·40	1·3
T.S.T.634	Calcite	$CaCO_3$	Bex, Switzerland	0·07	0·3
4450	Calcite†	$CaCO_3$	Unknown	0·08	0·13
15537	Calcite‡	$CaCO_3$	Unknown	0·06	0·10
B.L.762	Calcite§	$CaCO_3$	Cashel, Co. Galway	0·05	0·5
4993	Cerrusite	$PbCO_3$	Mold, N. Wales	0·26	0·04
11342	Dolomite	$CaCO_3MgCO_3$	Newton Stewart, Galloway	0·17	0·07
11349	Magnesite	$MgCO_3$	Greek Archipelago	0·22	0·07
11351	Magnesite	$MgCO_3$	Frankenstein, Silesia	0·02	0·05
15192	Rhodochrosite	$MnCO_3$	Unknown	0·02	0·09
12498	Siderite	$FeCO_3$	Clay Pit, Rainford, Lancs.	0·12	0·8
12631	Siderite	$FeCO_3$	Bathgate, Linlithgow	0·45	0·4
11487	Strontianite	$SrCO_3$	Weardale, Yorks.	0·58	0·02
11698	Strontianite	$SrCO_3$	Strontian, Argyll	0·48	0·08
11567	Strontianite	$SrCO_3$	Strontian, Argyll	0·44	0.09
11695	Witherite	$BaCO_3$	Anglezark, Lancs.	0·18	0·1

* Drewite. † Mudstone, Carboniferous. ‡ Oolitic limestone, carboniferous. § Metamorphosed limestone.

Table. 12. Gallium and germanium in sulphate minerals

Cat no.	Mineral	Formula	Locality	Ge (p.p.m.)	Ga (p.p.m.)
12377	Anhydrite	$CaSO_4$	Sweden	0·23	0·05
11502	Barytes	$BaSO_4$	Glen Sannox, Arran	0·56	0·49
11440	Barytes	$BaSO_4$	Dufton	1·05	0·04
11423	Barytes	$BaSO_4$	Seater, Pomona, Orkney	0·29	0·2
11438	Barytes	$BaSO_4$	Fuller's earth pit, Nutfield	1·47	0·2
11404	Barytes	$BaSO_4$	Stromness, Orkney	0·28	0·2
11584	Celestite	$SrSO_4$	Banks of Nidd, Knaresborough	0·38	0·02
11580	Celestite	$SrSO_4$	Kingston, Ontario, Canada	1·08	0·03
11594	Celestite	$SrSO_4$	Yate, Nr. Bristol	0·10	0·02
11680	Celestite	$SrSO_4$	Bristol	0·31	0·03
12300	Gypsum	$CaSO_4 2H_2O$	British Columbia	0·22	0·09
12385	Gypsum	$CaSO_4 2H_2O$	Niagara	0·41	0·06
12381	Gypsum	$CaSO_4 2H_2O$	Montmartre, Paris	0·33	0·08
12389	Gypsum	$CaSO_4 2H_2O$	Belfast	0·60	0·00
12380	Gypsum	$CaSO_4 2H_2O$	Bunny, Notts.	0·13	0·07
	Kieserite	$MgSO_4 H_2O$	Stassfurt	0·02	0·09

Table 13. Gallium and germanium in fluoride minerals

Cat. no.	Mineral	Formula	Locality	Ge (p.p.m.)	Ga (p.p.m.)
12154	Fluorite	CaF_2	Castleton, Derbyshire	0·94	0·02
12184	Fluorite	CaF_2	Beeralston, Devon	0·67	0·01
150	Fluorite	CaF_2	Weardale, Yorks	0·43	0·02
15193	Cryolite	Na_3AlF_6	Arkisutfjord, Greenland	0·16	3·0

Table 14. Gallium and germanium in evaporite minerals

Cat. no.	Mineral	Formula	Locality	Ge (p.p.m.)	Ga (p.p.m.)
T.S.T.10	Halite	NaCl	Cheshire	0·04	<0·02
	Halite	NaCl	Stassfurt	0·00	<0·02
	Bay Salt	NaCl	Brinepans, Northwich, Cheshire	0·09	<0·02
T.S.T.31	Carnallite	$KClMgCl_2 \cdot 6H_2O$	Stassfurt	0·05	0·03
	Kainite	$MgSO_4KCl \cdot 3H_2O$	Stassfurt	0·07	0·07
	Kieserite	$MgSO_4 \cdot H_2O$	Stassfurt	0·02	0·09
	Borax	$Na_2B_4O_7 \cdot 10H_2O$	Tibet	1·35	1·8
	Borocalcite	$Ca_4B_{10}O_{19} \cdot 9H_2O$	Unknown	0·11	<0·002

Table 15. Gallium and germanium in miscellaneous non-silicate minerals

Cat. no.	Mineral	Locality	Ge (p.p.m.)	Ga (p.p.m.)
F.W.11,162	Jet	Whitby, Yorks.	2·0	1·1
	Monazite	Travancore, India	0·44	1·3
13178	Scheelite	Cumberland	1·20	0·0
	Wolframite	Spain	0·59	0·3

Table 16. Gallium and germanium in silica

Cat no.	Mineral	Locality	Ge (p.p.m.)	Ga (p.p.m.)
1293	Quartz	Naragata Deleme Mine, Nigeria	1·5	0·02
	Quartz	Cumberland	0·4	0·008
4840	Quartz	Anglesey	0·08	1·6
11330	Quartz	Unknown	3·5	2·0
4836	Jasper	Mona Complex, Newborough Downs, Anglesey	2·3	1·2

Table 17. Gallium and germanium in felspars and felspathoids

Cat. no.	Mineral	Locality	Ge (p.p.m.)	Ga (p.p.m.)
7649	Orthoclase	Baveno, Italy	1·9	13·5
183 BL	Orthoclase	Inishdugga Granite, Co. Galway	2·0	8·8
	Moonstone	Ceylon	2·2	24·7
13	Microcline	Derryrona, Co. Donegal	5·0	20·1
	Amazonite	York River, Banneroff, Canada	7·8	66·6
7625	Amazonite	Colorado	10·7	50·7
7655	Albite	Amelia Co., Virginia	9·5	46·1
7244	Albite	Dorio, Italy	4·4	4·7
	Oligoclase	Twedestrand, Norway	2·0	12·9
7657	Labradorite	Labrador	1·1	10·0
	Sanidine	Dracherfels	2·3	14·7
7647	Anorthoclase	Kilimanjaro	1·2	16·0
7611	Leucite	Vesuvius	0·91	11·1
7620	Nepheline	Arkansas	0·65	20·2
8774	Sodalite	Princess Quarry, Bancroft	0·32	15·1
	Pollucite	Elba	12·5	12·5

Table 18. Gallium and germanium in micas

Cat. no.	Mineral	Locality	Ge (p.p.m.)	Ga (p.p.m.)
16532	Lepidomelane*	Unknown	2·1	6·7
510	Lepidolite	St. Dennis, Cornwall	3·3	109·3
	Biotite	Sebastopol, Renfrew Co., Ontario	1·3	33·0
	Muscovite	Pied des Monts., Quebec	3·2	174·1
	Phlogopite	Portland, Labelle Co., Quebec	2·2	101·1

* SiO_2 = 35·5; Al_2O_3 = 17·6 per cent.

Table 19. Gallium and germanium in amphiboles and pyroxenes

Cat. no.	Mineral	Locality	Ge (p.p.m.)	Ga (p.p.m.)
	Asbestos	Shabani Mine, Rhodesia	2·2	1·4
1363	Actinolite*	Cashel, Co. Galway	1·5	3·6
2108 B.L.	Brown Hornblende	Garroman, Co. Galway	1·6	11·7
1187 B.L.	Hornblende (ex metamorphosed gabbro)	Lettershinna, Co. Galway	2·0	14·9
1443 B.L.	Hornblende (ex metamorphosed gabbro)	Lough Wheelaun Intrusion, Co. Galway	3·4	20·4
1798 B.L.	Hornblende† (ex metamorphosed gabbro)	Cashel, Co. Galway	3·0	11·3
1396 B.L.	Hornblende‡ (ex metamorphosed pyroxenite)	S of Cashel, Co. Galway	2·8	9·0
2127 B.L.	Hornblende (ex metamorphosed ultrabasic rock)	Invermore, Co. Galway	2·0	10·4
2109 B.L.	Hornblende (ex metamorphosed ultra basic rock)	Garroman, Co. Galway	2·4	16·1
T.S.T.984	Granular Augite	Arendal	2·4	4·7
T.S.T.2890	Hypersthene	L. Scavay, Skye	2·9	6·8
	Monoclinic pyroxene	Dillage, Labrador	1·3	5·7

* From actinolite–tremolite nodule. † 48·80% SiO_2; 7·30% Al_2O_3. ‡ 50·31% SiO_2; 5·89% Al_2O_3.

Table 20. Gallium and germanium in miscellaneous silicate minerals

Cat. no.	Mineral	Locality	Ge (p.p.m.)	Ga (p.p.m.)
15485	Beryl	West Chester, Penn.	2·2	8·2
8772	Orthite	Cardiff, Ontario	3·1	33·5
	Scapolite	Unknown	2·1	0·0
	Talc	Unknown	2·0	11·6
G.H.M. 72	Topaz	Brazil	11·1	3·5
7196	Topaz	Trumbull, U.S.A.	91·5	0·8
	Tourmaline	Valleneuve, Quebec	1·7	14·0
	Yttrotitanite	Unknown	8·7	10·5
	Zircon	Unknown	1·5	0·8

Table 21. Gallium and germanium in granitic rocks

Cat. no.	Rock	Locality	Ge (p.p.m.)	Ga (p.p.m.)
1362	Granite	Hereford Beacon, Worcs.	2·1	11·5
1386	Granite	Foxdale, Isle of Man	0·8	31·0
1416	Granite	Dhoon, Isle of Man	2·7	13·6
1533	Biotite–hornblende granite	Madras, India	1·5	19·5
2118	Granite	Vakkara, West Finland	1·5	43·1
2157	Biotite granite	Suodieniemi, Finland	1·3	20·7
4630	Gweebarra granite	Lough Nambraddan, Co. Donegal	0·5	15·8
5192	Granite	Land's End, Cornwall	1·3	21·4
2140 B.L.	Granite	Errisberg Townland, Galway, Eire	1·4	15·1
189 B.L.	Granite	Inishdugga, Galway, Eire	0·8	12·9
10546	Etive granite	Laggan Dam, Scotland	0·8	17·0
	Murvey alkali granite	Molybdenite Prospect, Murvey, Eire.	1·9	21·3
	Shap granite	Shap, England	3·2	24·4
5022	Granite	Mallopo Hills, Bulawayo	1·9	22·2
4956	Post bothnian granite	Siuro, Finland	2·2	19·9
2117	Granite	Eurajoki, Finland	0·5	10·5
5081	Granite gneiss	Inchbae, Scotland	1·0	18·7
1950	Granite	Castle an Dinas, Cornwall	2·7	18·0
1544	Hornblende–biotite granite	Newry, Co. Down	2·4	17·5
1639	Biotite–hornblende granite	Ronez Quay, Guernsey	2·2	19·0
2122	Tourmaline granite	Lillaijen, W. Finland	2·5	14·0
2112	Granite	Sappi Islands, Finland	2·1	17·3
2120	Rapakivi granite	Heinjoki, Finland	2·3	16·9
2033 B.L.	Roundstone granite	Cashel, Co. Galway, Eire	1·9	13·5
2085 B.L.	Galway granite	Invermore, Co. Galway, Eire	2·3	16·5
1634	Tonalite	L'Ancresse, Guernsey	2·3	9·1
8769	Syenite	Deer Lake, Cardiff Township, Canada	0·6	16·1
11·7	Syeno–dolerite	Graven, Shetland	1·5	20·7
4219	Muscovite–pegmatite	(pneumolytic zone) Malvern	2·1	14·2
10655	Biotite–epidote granite	Spiggie, Shetland	3·1	17·1
925	Granite	Omey Island, Connemara, Eire	1·6	11·5
P-6	Granite	Intrusion within Omey Island granite, Eire	2·5	16·2
G-1	Granite	Westerly, Rhode Island	1·4	21·3
	33 samples	mean	1·7	18·1

Table 22. Gallium and germanium in basic igneous rocks

Cat. no.	Rock	Locality	Ge (p.p.m.)	Ga (p.p.m.)
13639	Lamprophyre	E. Quarff, Shetland	1·6	18·8
8535	Lamprophyre*	E. Quarff, Shetland	3·1	6·2
239 B.L.	Lamprophyre	Ballyconneely, Co. Galway	0·7	15·3
2113	Dolerite	Sappi Island, W. Finland	1·8	11·5
2798	Metadolerite	Dhambad, India	1·9	14·0
2817	Peridotite†	Loch Inver, Scotland	1·5	10·5‡
2275	Olivine–norite	Insch, Aberdeen	2·2	14·4
1599	Norite–hartzbergite	Dorset, Southern Rhodesia	0·8	1·3
1596	Lherzolite	Western Pipe, Kimberley	1·4	1·0
W-1	Diabase	Centerville, Virginia	2·1	21·5
	10 samples	mean	1·7	11·5

* In old Red Sandstone breccia.
† Precaledonian dyke in Lewisian granite; examination of a thin section showed some alteration to tremolite and chlorite.
‡ Average of two determinations (10·5 and 10·5 p.p.m.) Al_2O_3, 5·2%.

Table 23. Gallium and germanium in lavas and tuffs

Cat. no.	Rock*	Locality	Ge (p.p.m.)	Ga (p.p.m.)	Al_2O_3 (%)	Ga/Al $\times 10^4$
745	Andesite	Wolf's Castle	2·3	11·5	—	—
4385	Andesite	Mauna Kea, Hawaii*	3·7	22·0	19·5	2·1
4380	Hypersthene basalt	Mauna Loa, Hawaii, 1887*	3·2	16·1	11·7	2·6
4381	Picritic basalt	Mauna Loa, Hawaii, 1868*	2·8	12·4	9·4	2·5
4378	Olivine basalt	Haulalai, Hawaii, 1801	2·8	18·1	10·9	3·1
4382	Olivine basalt	Mauna Loa, Hawaii, 1919*	3·4	19·3	11·8	3·1
3023	Olivine basalt	Nairobi, Kenya	1·8	19·4	12·2	3·0
3025	Phonolite	Nairobi, Kenya	2·1	18·9	19·8	1·8
3029	Nephelinite	Nairobi, Kenya	2·2	23·1	20·0	2·2
		9 samples mean	2·7	17·9	—	—

* Analyses of 4378–4385 in *Hawaii Division of Hydrography Bull.* **9**, 202–6.

Table 24. Gallium and germanium in migmatite rocks

Cat. no.	Rock	Locality	Ge (p.p.m.)	Ga (p.p.m.)
1731 B.L.	Biotite–hornblende-labradorite-quartz gneiss	Kanes Lough, Co. Galway	3·3	20·8
1318 B.L.	Quartz-andesine-labradorite–hornblende–chlorite gneiss*	Glenturkan Lough, Cashel, Co. Galway	2·0	19·7
504 B.L.	Quartz–microcline–oligoclase gneiss†	Cashel, Co. Galway	2·0	10·9
4232	Ultra basic greenstone	Calwell Park Quarry, Malvern, Worcs.	1·0	20·0
3507	Hornblende gneiss	Laxford, Scotland	2·8	14·2
2145 A.B.	Migmatite	Blaberslandet Is., Finland	2·1	22·4
	6 samples	mean	2·2	18·0

* 60·5% SiO_2; 13·4% Al_2O_3. † 73·2% SiO_2; 11·4% Al_2O_3.

Table 25. Gallium and germanium in sedimentary rocks

Rock	Locality	Ge (p.p.m)	Ga (p.p.m)
Mudstone interbedded with graptolitic siltstone	Wenlock, W of Llanfyllin	2·2	16·2
Mudstone interbedded with greywacke	Wenlock, W of Llanfyllin	1·3	21·2
Sandy, sideritic mudstone, Main oolite ironstone	Northamptonshire	0·8	10·2
Siltstone, wenlock, Silurian	Ludlow, Salop	0·8	4·1
Micaceous siltstone, Ordovician	Minsterley, Salop	2·5	20·1
Greywacke, Cambrian	Harlech Dome, Merionethshire	1·4	15·0
Shale (graptolitic)	Hartfell, S. Uplands, Scotland	1·4	8·6
Black shale, Cambrian	Tremadoc, Merionethshire	3·2	21·3
Black shale, Carboniferous	Rhydymwyn, Flintshire	0·9	2·8
Black shale, rhaetic Jurassic	Westbury-on-Severn, Glos.	1·5	4·3
Shale, headon beds, Oligocene	Yarmouth, I. of Wight.	3·2	9·8
Sandstone. Upper mottled bunter	Runcorn	2·1	3·9
Coarse sandstone, caradoc, Ordovician	Church Stretton, Salop.	0·2	0·83
Eday sandstone, Devonian	Hoy, Orkney	1·2	5·3
Sandstone, caradoc, Ordovician	Nr. Church Stretton, Salop	1·9	11·8
Grit, upper llandovery (or older); Silurian	Connemara, Eire	1·2	7·3
Chert "Millstone grit" facies, Carboniferous	Holywell, Flintshire	0·4	2·4
Breccia, brockram, Permian	Nr. Appleby, Westmorland	0·8	0·8
Clay, wealden, Cretaceous	Nr. Corfe Castle, Dorset	1·5	14·5
Fireclay, senonian, Upper Cretaceous	N of Aswan, Egypt	1·2	15·9
Limestone (oolitic), Jurassic	Leckhampton Hill, Cheltenham	0·1	0·02
Limestone (oolitic), Carboniferous	Loc. unknown	0·07	0·10
Limestone, Carboniferous	Corwen, Merionethshire	0·09	0·06
Chalk, coranguinum zone, Cretaceous	Nr. Clandon, Surrey	0·05	0·03
Chalk, subglobosus zone, Cretaceous	Culver Cliff, I. of Wight	0·03	0·08
Dolomite	Newton Stewart, Galloway	0·17	0·07

Table 26. Gallium and germanium in metamorphosed-igneous rocks

Cat. no.	Rock	Locality	Ge (p.p.m.)	Ga (p.p.m.)
2255	Hypersthene–augite garnet felspar rock	Scourie, Scotland	3·9	9·0
1550	Cromaltite (melanite pyroxenite)	Ledmore, Assynt. Scotland	3·7	13·9
1576	Eclogite	Victor Roberts Pipe, Kimberley	2·2	8·8
1597 B.L.	Olivine–bronzite–clinopyroxene bytownite*	Lough Wheelaun intrusion, Connemara, Eire	2·3	8·4
931	Hornblende–labradorite rock†	Cashel, Co. Galway, Eire	1·3	18·0
	5 samples	mean	2·7	11·6

* 46·0%, SiO_2; 6·1%, Al_2O_3. † 52·6%, SiO_2; 6·1%, Al_2O_3.

Table 27. Gallium and germanium in metasediments

Cat. no.	Rock	Locality	Ge (p.p.m.)	Ga (p.p.m.)
4840	Gwna quartzite	Llangefni, Anglesey	0·08	1·6
11901	Graphitic quartzite	Shetland Isles	2·2	3·8
250 B.L.	Siliceous granulite	Ballyconneely, Co. Galway	1·2	7·7
2140	Siliceous granulite	Ballinaboy, Co. Galway	2·0	3·9
1360	Mica schist	Holland Arms, Anglesey	1·4	12·3
250	Graphitic schist	Nr. Newcastle, New Brunswick	2·3	32·9
1714 B.L.	Biotite–sericite–quartz–sillimanite schist*	Cashel, Co. Galway	2·9	37·4
2096 B.L.	Biotite–sericite–quartz–garnet schist†	Derryadd, West Cashel	0·9	31·8
734 B.L.	Sericite-chlorite–garnet schist‡	Cashel, Co. Galway	1·5	33·4
672 B.L.	Biotite–andesine–sillimanite schist§	Cashel, Co. Galway	1·6	27·8
304 B.L.	Staurolite–biotite–quartz–garnet schist**	Rinvyle, Co. Galway	2·1	11·9
238 B.L.	Garnet–staurolite–muscovite–biotite–quartz schist††	Rinvyle, Co. Galway	1·3	21·1
1431 B.L.	Garnet–cordierite–biotite hornfels‡‡	Lough Wheelaun, Co. Galway	1·2	23·3
1338 B.L.	Striped amphibolite	Athry, Co. Galway	2·7	13·8
763 A	Striped amphibolite	Cashel, Co. Galway	1·5	16·8
	15 samples	mean	1·7	18·6

* 46·1%, SiO_2; 23·6%, Al_2O_3. § 42·6%, SiO_2; 27·4%, Al_2O_3. †† 48·0%, SiO_2; 27·8%, Al_2O_3.
† 48·2%, SiO_2; 23·4%, Al_2O_3. ** 46·4%, SiO_2; 30·4%, Al_2O_3. ‡‡ 38·9%, SiO_2; 23·2%, Al_2O_3.
‡ 44·1%, SiO_2; 26·8%, Al_2O_3.

Table 28. Gallium and germanium in recent marine sediments

Sample	Sea or ocean	Lat.	Long.	Depth (m)	Ge (p.p.m.)	Ga (p.p.m.)
Diatomaceous ooze[1]	S. Atlantic	46°35′S	24°15·5′W	4402	1·8	15·6
Diatomaceous ooze[2]	S. Atlantic	62°56′S	59°50′W	949	1·6	13·7
Diatomaceous ooze[3]	S. Atlantic	55°52′S	56°53′W	4344	1·4	—
Diatomaceous ooze[4]	S. Atlantic	66°40·5′S	71°01′W	531	2·2	16·2
Diatomaceous ooze[5]	S. Atlantic	62°57′S	60°21·5′W	967	1·1	13·4
Globigerina ooze[6]	S. Atlantic	48°35′S	53°34′W	4136	1·4	17·7
Globigerina ooze[7]	S. Atlantic	26°07′S	14°36′W	3195	0·0	3·7
Pteropod ooze[8]	N. Atlantic	38°30′N	31°14′W	1828	0·6	—
Radiolarian ooze[9]	S. Atlantic	50°26′S	30°27′W	5000	2·0	10·9
Red clay[10]	N. Pacific	30°22′N	154°56′W	5400	2·7	28·0
Red clay[11]	N. Pacific	43°49′N	143°07′W	4270	—	21·3
Red clay[12]	N. Pacific	29°24′N	153°06′W	3460	—	21·6
Red clay[13]	N. Pacific	31°05′N	135°24′W	4940	—	19·5
Red clay[14]	Indian	6°52′N	67°12′E	4793	2·8	21·0
Red clay core[15] top ± 2 cm	N. Atlantic	24°35′N	64°02′W	5395	2·3	22·0
Red clay core 50 cm	N. Atlantic	24°35′N	64°02′W	5395	2·1	22·8
Red clay core 100 cm	N. Atlantic	24°35′N	64·02′W	5395	2·4	25·5
Red clay core 150 cm	N. Atlantic	24°35′N	64°02′W	5395	2·6	23·2
Red clay core 200 cm	N. Atlantic	24°35′N	64°02′W	5395	2·3	23·5
Red clay core 250 cm	N. Atlantic	24°35′N	64°02′W	5395	2·3	26·1
Red clay core 300 cm	N. Atlantic	24°35′N	64°02′W	5395	2·3	21·2
Red clay core 350 cm	N. Atlantic	24°35′N	64°02′W	5395	2·3	22·4
Red clay core 400 cm	N. Atlantic	24°35′N	64°02′W	5395	2·1	20·4
Red clay core 450 cm	N. Atlantic	24°35′N	64°02′W	5395	2·1	24·4
Red clay core 500 cm	N. Atlantic	24°35′N	64°02′W	5395	2·6	21·8
Deep sea calcareous clay[16]	Mediterranean	35°55′N	17°29′E	3956	1·0	6·5
Deep sea calcareous clay[17]	Mediterranean	35°55′N	17°29′E	3956	1·0	8·5
Deep sea calcareous clay[18]	Indian	01°06·5′N	85°36′E	4464	0·9	5·7
Green mud	N. Atlantic	44°38′N	55°47′W	1049	1·4	8·8
Manganese nodule[19]	N. Pacific	37°41′N	177°04′W	5303	1·8[22]	21·5[22]
Manganese nodule[20]	S. Pacific	13°28′S	149°30′W	4300	3·2[22]	18·3[22]
Manganese nodule[21]	N. Pacific	37°52′N	160°17′W	5011	—	15·7[22]

[1] Discovery St. No. 10, 13/2/26. Total $CaCO_3 + MgCO_3 = 2{\cdot}7\%$, $SiO_2 = 67{\cdot}4\%$, $Al_2O_3 = 11{\cdot}3\%$, Ga : Al = $2{\cdot}6 \times 10^{-4}$.

[2] Discovery St. No. 203, 5/4/27, Bransfield Strait, S. Shetlands.

[3] Discovery St. W.S. 468, 9/11/29, $SiO_2 = 61{\cdot}4\%$.

[4] Discovery St. W.S. 514, 11/2/30.

[5] Discovery St. N. 26/2/27.

[6] Discovery St. No. 64.

[7] Discovery St. D. Total $CaCO_3 + MgCO_3 = 92{\cdot}6\%$, $SiO_2 = 2{\cdot}2\%$.

[8] Challenger St. No. 73, $CaCO_3 = 73{\cdot}5\%$.

[9] Discovery St. No. 11, 16/2/26. $SiO_2 = 66{\cdot}9\%$.

[10] Challenger St. No. 256, British Museum No. M 320; Total $CaCO_3 + MgCO_3 = 1{\cdot}78\%$, $SiO_2 = 55{\cdot}4\%$, $Al_2O_3 = 19{\cdot}1\%$, Ga : Al = $2{\cdot}8 \times 10^{-4}$.

[11] Scripps Institute of Oceanography, "Cusp" Expedition, Station 14 G. Total $CaCO_3 + MgCO_3 = 1{\cdot}06\%$, $SiO_2 = 55{\cdot}2\%$, $Al_2O_3 = 17{\cdot}4\%$, Ga : Al = $2{\cdot}3 \times 10^{-4}$.

[12] Scripps Institute of Oceanography "Chinook" Expedition, Station 1a-c. Total $CaCO_3 + MgCO_3 = 0{\cdot}95\%$, $SiO_2 = 55{\cdot}5\%$, $Al_2O_3 = 17{\cdot}5\%$, Ga : Al = $2{\cdot}3 \times 10^{-4}$.

[13] Scripps Institute of Oceanography "Cusp" Expedition, Station 1G. Total $CaCO_3 + MgCO_3 = 0{\cdot}83\%$, $SiO_2 = 53{\cdot}9\%$, $Al_2O_3 = 17{\cdot}5\%$, Ga : Al = $2{\cdot}1 \times 10^{-4}$.

[14] John Murray Expedition St. No. 166, British Museum No. 96626 (A 51) 28·7 cm from top of core: Total $CaCO_3 + MgCO_3 = 3{\cdot}82\%$, $SiO_2 = 54{\cdot}7\%$, $Al_2O_3 = 16{\cdot}3\%$, Ga : Al = $2{\cdot}4 \times 10^{-4}$.

[15] Columbia University, Lamont, Geological Observatory. Core A_{172-19} Station was on a small hill at the southern boundary of Bermuda Rise. The core showed no traces of material deposited by turbidity currents. Average composition: Total $CaCO_3 + MgCO_3 = 2{\cdot}7\%$, $SiO_2 = 53{\cdot}2\%$, $Al_2O_3 = 19{\cdot}1\%$, Ga = 23·0 p.p.m. Ga : Al = $2{\cdot}3 \times 10^{-4}$.

[16] Discovery St. No. 2911 S.T.P.(A) 21/11/51, pilot core. Sample consisted of clay admixed with 54·5% $CaCO_3 + MgCO_3$ (mainly globigerina and pteropods). $SiO_2 = 22{\cdot}1\%$, $Al_2O_3 = 7{\cdot}6\%$, Ga : Al = $1{\cdot}6 \times 10^{-4}$.

[17] Discovery St. No. 2911 S.T.P. (B). Sample consisted of clay admixed with 60·2% $CaCO_3 + MgCO_3$ (mainly globigerina and pteropods). $SiO_2 = 25{\cdot}1\%$, $Al_2O_3 = 8{\cdot}7\%$, Ga : Al = $1{\cdot}8 \times 10^{-4}$.

[18] Discovery St. No. 2896 S.T.P. Sample consisted of clay admixed with 58·5% $CaCO_3 + MgCO_3$ (mainly globigerina). $SiO_2 = 24{\cdot}2\%$, $Al_2O_3 = 6{\cdot}6\%$, Ga : Al = $1{\cdot}8 \times 10^{-4}$.

[19] Challenger St. No. 248. British Museum No. M313. 2·5% Al in acid soluble part, Ga : Al = $8{\cdot}6 \times 10^{-4}$.

[20] Challenger St. No. 276. 3·2% Al in acid soluble part. Ga : Al = $5{\cdot}8 \times 10^{-4}$.

[21] Challenger St. No. 252. British Museum No. M316. 1·06% Al in acid soluble part. Ga : Al = $14{\cdot}8 \times 10^{-4}$.

[22] In acid-soluble part.

Table 29. Germanium and gallium contents of sea waters

Date	Station	Lat.	Long.	Sounding (m)	Depth (m)	Cl (‰)	Ge (μg/l.)	Ga (μg/l.)
5/57 (Composite)	Irish Sea	—	—	—	Surface	19·10	—	0·030 0·026 0·026
2/57 (Composite)	Kish	53°20′N	5°17′W	140	Surface	18·91	0·06	0·03
2/57 (Composite)	Bardsey	52°45′N	4°47′W	—	Surface	18·93	0·05	0·02
5/5/57	E-1	50°50′N	4°22′W	70	Surface	19·52	0·05	—
5/5/57	L-5	50°18′N	4°11′W	40	Surface	18·45	0·06	—
5/5/57	—	48°25′N	9°53′W	790	Surface	19·71	0·06	0·04
5/5/57	—	48°25′N	9°53′W	790	260–300*	19·69	0·06	0·05
6/5/57	—	47°47′N	9°18′W	3900	Surface	19·49	0·06	0·02
6/5/57	—	47°47′N	9°18′W	3900	240–270*	19·71	0·06	0·02
6/5/57	—	47°47′N	9°18′W	3900	3660–3690*	19·34	0·07	0·04
9/5/57	E-2	49°27′N	4°42′W	95	Surface	19·72	0·06	0·03

* Collected using several water bottles at 10 m intervals.

Geochimica et Cosmochimica Acta, 1959, Vol. 16, pp. 181 to 191. Pergamon Press Ltd. Printed in Northern Ireland

Radon in the New Zealand geothermal regions*

R. E. Belin
Snowy Mountains Hydro-electric Authority, Cooma, N.S.W., Australia

(*Received* 21 *April* 1958; *in revised form* 16 *January* 1959)

Abstract—Measurements have been made on radon and thoron associated with gas and condensate samples from fumaroles and pools, situated along the Rotorua–Taupo graben. Methods of collection and measurement are briefly described.

The values of radon to gas (R_g) range from $0{\cdot}8 \times 10^{-9}$ to 320×10^{-9} curies/litre (c/l.) for pools and $0{\cdot}32 \times 10^{-9}$ to 340×10^{-9} c/l. for fumaroles. Radon to condensate values (R_c) for fumaroles fall in the range of 7×10^{-9} to 340×10^{-9} c/l. of condensate.

Variations in discharges of radon and thoron have been related to geology, i.e. there is a greater radioactive discharge from acid igneous regions than from intermediate igneous regions. The ratio of the average of the R_c-values for fumaroles in the acid igneous region to the average of the R_c-values for fumaroles in the intermediate igneous regions is equal, within experimental error, to the ratio of the γ-counting rates of the surface rocks of the two regions. It is therefore suggested that it is steam or water which is responsible for bringing the radioactive gases to the earth's surface.

Introduction

In New Zealand, measurements of radon accompanying fumarole gases have been confined in the past to Karapiti (712)† (Rogers, 1926; Grigg and Rogers, 1929). A few determinations of radon dissolved in thermal waters have also been made (Maclaurin and Wright, 1911; Grigg and Rogers, 1929); but none on the radon accompanying gases emerging from hot pools or springs. Kuroda (1944) and Kuroda and Yokoyama (1948, 1949), in Japan, made many observations on radon and thoron as well as other radioactive elements emerging from hot pools while Iwasaki *et al.* (1951) reported on the radioactive constituents of fumarolic discharges. In Italy Straniero (1951) claimed that the radioactivity accompanying the steam was direct evidence of deep origin.

Radon in geothermal pools ranges over quite wide limits (Maclaurin and Wright, 1911; Grigg and Rogers, 1929; Schlundt, 1935; Kuroda, 1944; Kuroda and Yokoyama, 1948, 1949), and is seldom in equilibrium with either its parents or its daughters. This is to be expected as the radon concentration in geothermal pools, if it is released from the near surface rocks and brought to the surface by the water, is affected by such variable factors as:

(1) The solubility of radon in waters varying in pH and temperature.
(2) The emanating power of the rock containing the parent radioactive material.
(3) The differential leaching of subterranean rocks by hot, often acid, waters (this will bring up varying amounts of the radioactive elements, e.g. the radium observed in Japanese mineral springs (Kuroda, 1944) is far in excess of the amount which would be in equilibrium with the uranium present).

---

* The work herein described was carried out while the author was attached to the Dominion Physical Laboratory, D.S.I.R., Lower Hutt, New Zealand.

† *Note:* The pool and fumarole numbering is that adopted by the New Zealand Geological Survey. The exact locations, defined by the numbers, are given in their detailed maps of the areas.

(4) The differential precipitation of a radioactive element (this could create subterranean deposits which, with a subsequent geological change, could be brought slowly to the surface or could explain the high radon contents of some pools or fumaroles).
(5) The time of travel of the flushing fluid through the radon producing areas.
(6) The surface area exposed to the flushing fluid.
(7) The rate of separation of other gases, flushing radon from the water.

It may be possible to simplify this complicated picture by examining the radioactivity of fumaroles. The object of this investigation therefore was to measure and compare radioactive emanations, accompanying discharges of fumaroles, of the andesite regions (Tongariro, Ngauruhoe and White Island) with those of the acid igneous region (between Tokaanu and White Island) (New Zealand Geological Survey, 1948), see Fig. 1. The experiment was extended to a comparison of radon accompanying the gases rising from pools in the two regions.

Methods of Sampling and Measurement

Pools. Generally only pools with a steady gas outflow were sampled, unless their selection was determined by criteria such as abnormal radioactivity of sinter deposits as at pool 419 Waiora (Belin, 1957). Sampling proceeded by displacing hot pool water, from a glass flask, by gas from the pool.

For comparison, samples were collected from a few boiling pools by covering the most active spot by a large, heavy, submerged funnel. This created a jet of steam from the stem, and collection proceeded as for fumaroles.

Fumaroles. In general, a hole was drilled several feet from the vent in such a place as to strike the main steam flow. A sampling pipe sealed into the hole ensured a steady flow of steam and gas. With fumaroles discharging from amongst rocks a sampling pipe was inserted into the most vigorous part. By restricting the opening of small vents, a steady flow was assured.

Collection proceeded by connecting the sampling pipe to a 880 ml vacuum-tight condenser which had previously been filled with gas-free hot water. This was driven out by the gas–steam mixture and a sample of gas and water was then collected by condensation. Considerable care was always taken to avoid air contamination.

Radon estimation. A measurable amount of the collected gas assumed to be all CO_2 (CO_2 normally comprises 85 per cent or more of the gas (Wilson, personal communication; Wilson, 1949)) was transferred to a 1·67 l. copper ionization chamber. Three hours after the transfer, when Rn and its daughters had reached equilibrium, the ionization current was measured using either a d.c. feedback amplifier range from 10^{-10} to 10^{-13} A, or a pulse amplifier recorder for currents less than 10^{-13} A. By calibration, the radon in the chamber and hence the total amount of radon in the sample was estimated. In so doing the Rn distribution coefficient, given by Hevesy and Paneth (1938), between air and water was assumed for the Rn distribution between gas and condensate. The Rn thus found was corrected for decay since collection.

Thoron estimation. Since thoron has only a 54 sec half-life, after a short space of time, only ThB will be present in a sample. Slowly its daughters will build up

and by the time the flask is opened, usually about 3 hr after collection, equilibrium conditions will have been established. In addition, radon and its daughters RaA, RaB and RaC, will also be near equilibrium. ThB, RaB, are isotopes of lead and their extraction followed the procedure used for minute traces of this element. The precipitate containing RaB, RaC, ThB and ThC was assayed by an end-window geiger counter. The ThB contribution to the count rate and thence the absolute disintegration rate of thoron at the time of collection was deduced.

Results

Pools. Only radon estimations were made on the gases emerging from pools and these are given in Table 1 as a value of R_g i.e. Rn to gas, assumed to be CO_2 at s.t.p. Fig. 1 gives the geographical positions of the various areas mentioned

Table 1. Radon content of gases rising from geothermal pools

Area	Pool no. and/or name	Temp.* (°C)	pH*	R_g radon/gas (c/l. $\times 10^9$)
Wairakei	29	89	7·8	95
	Opal Pool (113)	87	6·0	320
	117	68	2·6	70
Waiora	427	49	2·4	50
	443	82	2·5	8
	Twin Opal (419)	82	2·3	22
Spa	33	83	3·0	60
	78	63	5·7	113
Rotokaua	2	98	1·95	6
	7	57	2·5	14
	37	89	3·6	12
Orakei Korako	Pysche's Bath			19
	Foot Bath	98		56
	Hochstetter	100		21
	Kehurangi	98		29
Ketetahi	Nearest Ahi†	60		0·8
White Island	Pool on SE side	98		7

* Temperatures and pH were supplied by the Geological Survey.

† Ahi is the largest fumarole in the Ketetahi thermal area on the slopes of the dormant volcano Tongariro.

in Tables 1, 2, 3 and 4. In each pool a minimum of two determinations were made. The results are expressed in curies/litre (c/l.) of gas. The errors in R_g are of the same order as that explained below for fumaroles.

Table 2 includes the values of R_g in curies of radon/litre (c/l.) of gas at s.t.p. and the values of R_c in curies of radon/litre (c/l.) of water from condensed steam

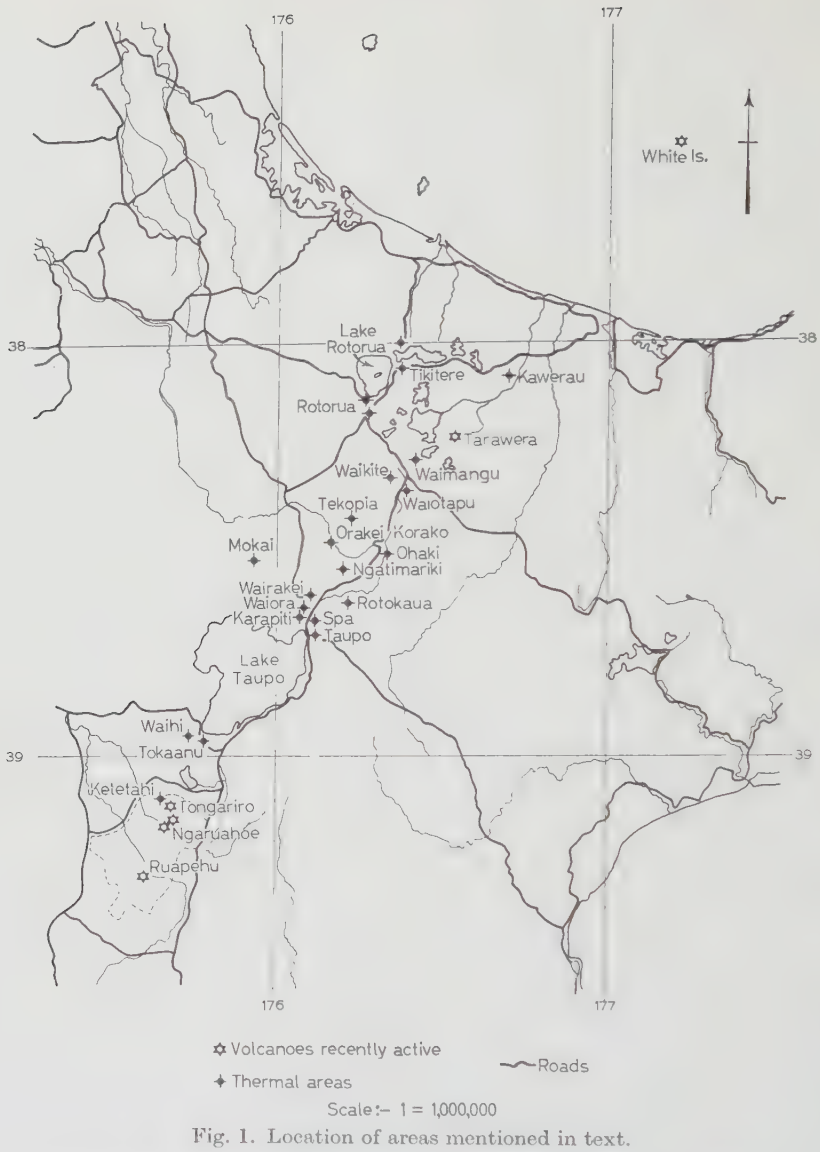

Fig. 1. Location of areas mentioned in text.

for four pools – two at Wairakei and two near Karapiti. These samples were collected by the alternative fumarole method described for boiling pools.

Fumaroles. In Table 3, the radon content of all the fumaroles examined is expressed in curies/litre (c/l.) of gas at s.t.p. – the R_v value – and curies/litre (c/l.) of condensate – the R_c value. (There are not many other fumaroles in the acid igneous region than those given in Table 3.)

Typical examples of variation in R_v can be gauged by comparing individual measurements of Big Donald and of Schubert's Fairy. At both fumaroles three determinations were made, spread over a period of several days. For Big Donald

Table 2. Radon associated with some boiling pools (gases collected by the fumarole method)

Area	Pool no.	Temp. (°C)	R_g radon/gas (c/l. × 10^9)	R_c radon/condensate (c/l. × 10^9)	No. of samples
Near	681	100	180	330	3
Karapiti	682	100	160	340	2
Wairakei	60	100	115	770	2
	222	100	58	170	2

Table 3. Radon associated with fumarole discharges*

Area	Type of surface material	Fumarole no. and/or name	Temp. (°C)	R_g radon/gas (c/l. × 10^9)	R_c radon/condensate (c/l. × 10^9)	No. of samples
White Island	Intermediate igneous (andesite)	Big Donald	580	3·4	94	3
		Schubert's Fairy	180	8·4	50	3
		D.P. Fumarole	108	2·8	65	2
Waiotapu	Acid igneous (pumice of rhyolitic comp.)			25	120	1
Wairakei	Acid igneous (pumice of rhyolitic comp.)	612		18	40	2
		604		19	200	2
Waiora	Acid igneous (pumice of rhyolitic comp.)	557		20	340	1
		small one near 557		15	170	1
Karapiti	Acid igneous (pumice of rhyolitic comp.)	712	114	340	250	7
		712A		330	110	5
Spa	Acid igneous (pumice of rhyolitic comp.)	Bore 1		20	64	2
Tokaanu	Intermediate/ igneous (andesite)	Near Thermal Baths		1·5	87	1
Ketetahi	Intermediate/ igneous (andesite)	Ahi†	105	1·2	74	2
Ngauruhoe	Intermediate/ igneous (andesite)	‡		0·32	7	2

* All fumarole temperatures except those marked are near or equal to 100°C. Ngauruhoe gas temperatures were not measured but the main vents here are probably hotter than Big Donald on White Island.

† Corrected to 760 mm of Hg.

‡ Only fumaroles around the rim of the crater could be approached.

Table 4. Thoron associated with the discharges from three fumaroles

Area	Fumarole no. and/or name	Temp. (°C)	T_g thoron/gas (c/l. $\times 10^9$)	T_c thoron/ condensate (c/l. $\times 10^9$)	No. of determinations
Karapiti	712	114	740	5700	3
Waiotapu			220	1200	1
White Island	Big Donald	580	60	2200	2

and Schubert's Fairy the results were, respectively, 2·52, 4·31, 3·29 c/l. and 8·83, 8·44, 8·18 c/l. Variations as large as those for Big Donald are not fully understood and may result from actual variations in radon content of the fumarole or possibly the change in position of the sampling pipe, hence changing collecting conditions. Under such circumstances it is not possible to estimate reliable errors, however, if the fumarole discharge were assumed constant then the standard deviation in all cases is $\leqslant \pm 10$ per cent. Errors in counting are insignificant compared to this.

From measurements made on Karapiti (712) in 1953 by the writer and F. B. Knox it appears there has been a slight drop in radon concentration since then. Unfortunately in these early measurements an unknown quantity of air entered the collection flask, thus accurate comparison with the more recent results is not possible. Grigg and Rogers (1929) found $0{\cdot}36 \times 10^{-8}$ curies of radon per litre of condensate. This is a factor of 70 lower than the present determination. Should the earlier figures be reliable then it appears that the radon content of Karapiti (712) fluctuates widely.

Samples collected from Ngauruhoe on an earlier occasion were discarded as it was then thought that air had so seriously contaminated the sample as to make it worthless. However, more careful sampling later established that approximately 85 per cent of the emerging gas was actually air (Wilson, personal communication), It is quite conceivable that on a new crater where consolidation of rocks is not complete air could be sucked in by venturi action. The figure given in Table 3 has been corrected for the air present.

The values of T_g in curies of thoron per litre (c/l.) of gas at s.t.p. and T_c in curies of thoron per litre of condensate (c/l.) for three fumaroles, Karapiti, Waiotapu and Big Donald, are given in Table 4. Errors are of the order of ± 20 per cent. The T_g values for Ngauruhoe, Ketetahi, Tokaanu and the fumaroles on White Island, except Big Donald, were less than 15×10^{-9} c/l., the lower limit of the method. Fumaroles 604 and 557 at Waiora were not sampled for thoron.

Table 5 gives the average values, $\bar{R}_g$ of R_g and $\bar{R}_c$ of R_c, for the acid igneous region, the intermediate igneous regions and for Karapiti (712 and 712A). The value of $\bar{R}_g$ for the acid igneous region excludes Karapiti.

Factors Influencing Radon Discharge

If all the radon were to originate in a magma which is common to all the thermal areas, then the discharges from those areas of highest temperature, where the magma is presumably closest to the earth's surface, should have the highest

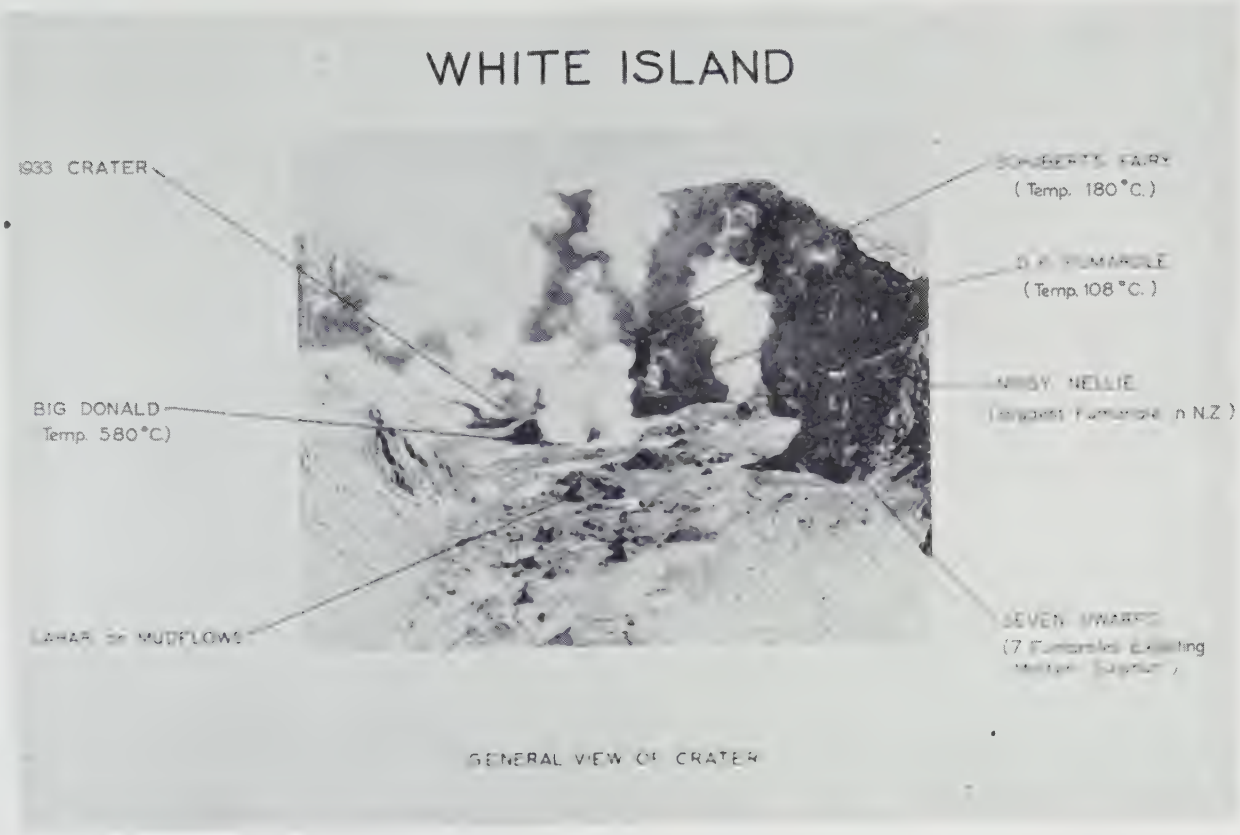

Fig. 2. General view of White Island crater

radon content. This is not substantiated by examination of Table 3. It is therefore more probable that radon at the surface is released largely from the last of the rocks through which the flushing fluid (either gas or water or both) passes.

Table 5.

Region	Average of R_g $\bar{R}_g$	Average of R_c $\bar{R}_c$
Acid	*19 ± 1	17·7 ± 4·4
Intermediate	4·2 ± 0·8	7·7 ± 0·8
Karapiti (712 and 712A)	350 ± 35	20 ± 3

* Excludes Karapiti (712 and 712A).

Much of the surface material in the acid igneous region is rhyolitic tuff which presents zones of high porosity and surface area/unit volume. This material in the Taupo area extends to a depth of 2000–3000 ft and rests on an extensive sheet of ignimbrite 4000–5000 ft thick (Healy, personal communication). Near the surface it is probable that water migrates through these porous zones and because of the high surface area exposed to the flushing fluid may account in part for the high radon content of the gases in these areas. The surface intermediate igneous material of White Island and Tongariro consists largely of breccias, tuffs, lava flows and possibly congealed lava at shallow depth. The mechanics of fluid flow in these areas near the surface may therefore be similar to that postulated for the acid areas. Other factors influencing the radon content of the geothermal discharges if water is the flushing fluid were enumerated in the introduction and will not be discussed further. In the absence of a sounder knowledge of the mechanisms involved, similarity between rhyolite and andesite regions, excluding Tokaanu and Ngauruhoe, will be assumed, and the dependence of radon content in terms of R_g and R_c on the radioactivity contained in the near surface rocks will be investigated.

In this comparison Ngauruhoe and Tokaanu have been excluded for the following reasons:

(1) At Ngauruhoe, the only active lava volcano of the group, congealed lava near the surface would present a much lower surface area to the flushing fluid and may account for the much lower radon content of the discharge here compared with other andesite areas. Also here the short distance of travel of the meteoric water to and from the magma may also in part be the cause for this low value (see Table 3). Further Ngauruhoe's lava has recently been classified as more basic than andesite (Steiner, personal communication) thus other factors being equal the radon content of its discharge may be expected to be less than that from andesite areas (see below).

(2) At Tokaanu the geology is a little uncertain. The surface material is composed largely of andesite lava flows and tuffs, and may extend to a depth of a few hundred feet and probably rests on acid igneous rock of unknown thickness (Healy, personal communication).

Radon in Fumaroles

Statistical treatment

The results, except for those of Ngauruhoe and Tokaanu, given in Table 3 have been examined by the application of the small or exact sampling theory (Kenney, 1943). This places the values of R_g into three distinct universes—R_g values for (a) the intermediate igneous regions; (b) the acid igneous region; (c) Karapiti (712 and 712A).

The values of R_c examined in the same light were found to belong to two distinct universes, R_c values of: (a) the intermediate igneous regions; (b) the acid igneous region. These observations indicate that both the R_g and R_c values are related to the surface rock material. The R_g value for Karapiti is the one exception and is therefore probably a special case.

In the case of Tokaanu the exact sampling theory suggests grouping the R_g and R_c values from there with those of the andesite regions. This, together with Healy's observation (above), further supports the theory that radon is released from the last of the rocks through which the water and gas pass.

The relation between radon and the near surface rock

The radium content of igneous rocks increases with increasing silica content (Evans and Goodman, 1941). This implies that, if the Rn is picked up by fluids, and if other factors are similar, the radon content of the fumaroles discharging from acid igneous rocks, mainly of rhyloitic composition, will be greater than that from intermediate igneous rocks (andesite). The figures in Table 3 support this view, i.e. the fumaroles in the rhyolitic region, particularly around Taupo are higher in Rn content than fumaroles emerging from the pure andesite cones of White Island, Tongariro and Ngauruhoe, where it is considered that acid igneous rock is completely absent even at depth (Fleming and Steiner, 1951).

The radium content of many igneous rocks has been measured by Evans and Goodman (1941). From a summary of radioactivities they give:

$$\frac{\text{Radium content of acid igneous rocks}}{\text{radium content of intermediate igneous rocks}} \doteqdot 3$$

From the figures of Gibbs and McCallum (1955) the ratio of the γ-counting rates of Taupo ash to Tongariro ash (not of recent origin) was deduced as $2{\cdot}1 \pm 0{\cdot}1$ but they do not specify the radioactive constituents.

From Table 5

$$\frac{\bar{R}_g - \text{acid}}{\bar{R}_g - \text{intermediate}} = 4{\cdot}5 \pm 0{\cdot}9 \qquad (1)$$

and

$$\frac{\bar{R}_c - \text{acid}}{\bar{R}_c - \text{intermediate}} = 2{\cdot}3 \pm 0{\cdot}5 \qquad (2)$$

The closeness of this last ratio to that deduced from the results of Gibbs and McCallum (1955), and to that given by Evans and Goodman (1941), suggests that radon is associated with steam (or water).

The flushing fluid

From Table 3

$$\frac{R_c/R_g \text{ (acid)}}{R_c/R_g \text{ (Karapiti)}} = \frac{\text{gas/condensate (acid)}}{\text{gas/condensate (Karapiti)}} = 18{\cdot}3 \pm 3{\cdot}8 \qquad (3)$$

$$\frac{R_c/R_g \text{ (intermediate)}}{R_c/R_g \text{ (acid)}} = \frac{\text{gas/condensate (intermediate)}}{\text{gas/condensate (acid)}} = 2{\cdot}0 \pm 0{\cdot}2 \qquad (4)$$

R_c/R_g (acid) excludes Karapiti (712 and 712A).

Ratio (3) resolves the Karapiti R_g anomaly (i.e. there the high value of R_g with respect to other R_g values in the acid igneous region is explained completely by the much lower gas content). Since the high R_g value here is explained and the R_c value fits in with the rest of the acid igneous region it is reasonable to believe that it is the water which collects the radon and brings it to the surface.

Ratio (4), $2{\cdot}0 \pm 0{\cdot}2$, suggests that ratio (1), $4{\cdot}5 \pm 0{\cdot}9$, could be modified to allow for the much greater proportion of gas emerging from the intermediate igneous regions. Two volumes of gas rising from these regions can be compared with one volume of gas rising from the acid igneous region by dividing ratio (1) by ratio (4), with the result $2{\cdot}3 \pm 0{\cdot}2$. This is the same as the R_c ratio (ratio (2)) of the two regions. This could be expected purely from the Rn equipartition laws between gas and water, since the volume of condensate is small compared to that of the gas and the solubility of Rn in water is small. This poses the question as to whether Rn is collected by gas or by water—the latter is preferred after evaluating the apparent Karapiti anomally and from purely physical considerations. Faul *et al.* (1951) found maximum Rn concentrations of $0{\cdot}5 \times 10^{-9}$ c/l. (s.t.p.) in natural gas wells and suggested the radon origin to be in the immediate vicinity of the bore. If radon were collected by the gas then a higher radon content may be expected as the gas probably sweeps out a greater volume than that in the immediate vicinity of the bore. This together with the above observations focuses attention on Rn being collected by the water.

The scatter of R_c in the acid igneous region suggests that if radon is associated with steam then the volumes flushed by the steam emerging from fumaroles differ and are not necessarily related to steam output. Compare, for example 712 and 712A, where the former has a steam discharge several times that of the latter. Other factors affecting this scatter of R_c have been given in the introduction. R_g or R_c appear to bear no relation to other fumarolic activity, e.g. on White Island there is little difference between the hottest, most vigorous fumarole and the relatively cold small D.P. fumarole nearby. In the acid igneous region Karapiti (712) is by far the most vigorous (measured output 16,000 kg/hr of steam (Ledger, personal communication)) and it has the highest R_g value (already resolved) and a high R_c value. These observations appear to be contradictory to those of Iwasaki *et al.* (1951), who found that fumaroles of small discharge capacity showed higher radioactivity than those of large discharge capacity. This observation is supported by comparison of Karapiti (712) and Big Donald, but in this one case only in the present investigation, and disregards other physical differences.

Radon in Pools

The R_g values of the pools present a similar picture, in that they are higher in the acid igneous areas than in the intermediate igneous areas. The highest value is as high as the highest measured in Japan (Kuroda, 1944) and U.S.A. (Schlundt, 1935).

The pools sampled by the fumarole technique give figures for R_g comparable to those obtained by the simpler collecting method used in the Wairakei area.

Since the R_g values are dependent upon the gas present and hence on the ratio of gas to water they can fluctuate widely, refer to Karapiti for example. Thus R_g values for pools are not necessarily the same as for fumaroles nearby—the R_c values, if radon is associated with water, should be the same for pools and for fumaroles if the latter result from water flashing to steam below the earth's surface. Support for this is found by comparing the R_c values in Tables 2 and 3. This suggests that all fumaroles in this region are created by water flashing to steam from a pool or other reservoir below the earth's surface.

The R_g values for the fumaroles of the Waiora Valley are of the same order as that for the pools nearby. At Ketetahi the one pool measured gives approximately the same value of R_g as obtained from Ahi. No fumaroles existed in the other areas examined.

Thoron in Fumaroles

From Table 4 the ratio of the mean value of T_c for the acid igneous region, Karapiti and Waiotapu, to the value of T_c for the intermediate igneous region, White Island, is approximately 3 : 1. Evans and Goodman (1941) gave approximately 3 : 1 for the ratio of thorium in acid igneous rocks to thorium in intermediate igneous rock. The closeness of these ratios gives further evidence supporting the theory that radioactive emanations are associated with the emerging steam or water and are not related to the CO_2 content.

Further evidence of the short-lived thoron in fumarole discharges implies that this element emanates from rocks near the earth's surface.

Conclusion

Results of this investigation suggest that steam (or water) is responsible for the collection of radon and thoron from rocks near the earth's surface. This view is supported by:

(a) The radon content of the discharge from pools and fumaroles appears to be related to the radioactivity of the surface material, i.e. more radon emerges from the acid igneous region than from the intermediate igneous regions.

(b) The ratio of the average of the radon to condensate values of fumaroles in the acid igneous region to the average of the radon to condensate values of fumaroles in the intermediate igneous regions is equal, within experimental error, to the ratio of the γ-counting rates of the surface rocks of the two regions.

(c) The ratio of the same values for thoron is approximately equal to the ratio of the thorium in the surface rocks of the two regions.

(d) Radon to condensate values for pools are consistent with the evidence that fumaroles result from water flashing to steam below the earth's surface.

Acknowledgements—The writer wishes to acknowledge Messrs. F. B. Knox, A. E. Bainbridge, and K. A. Bargh for having at various times assisted and often contributed towards methods of gas collection and measurement. The ionization current meters were designed by Mr. G. J. Ferguson. Fig. 1 is a map which has been reproduced with the permission of the Director of the Geological Survey, Department of Scientific and Industrial Research, New Zealand. Finally, he wishes to thank Mr. W. H. Ward, Director, Dominion Physical Laboratory for his critical but constructive comments.

References

Belin R. E. (1957) A gamma radioactivity survey of some of the geothermal areas of the North Island of New Zealand. *N.Z. J. Geol. Geophys.* **1,** 156–165.

Evans R. and Goodman C. (1941) Radioactivity of rocks. *Bull. Geol. Soc. Amer.* **52,** 459–490.

Faul H., Gott G. B., Manger G. E., Mytton J. W. and Sakakura A. Y. (1953) Radon and helium in natural gas. *Proceedings of the Conference on Nuclear Processes in Geologic Settings* University of Chicago.

Fleming C. and Steiner A. (1951) Sediments below Ruapehu Volcano. *N.Z. J. Sci. Tech.* **32,** No. 6, 31–32.

Gibbs H. S. and McCallum G. J. (1955) Natural radioactivity of soils. *N.Z. J. Sci. Tech.* **37,** No. 3, 354–368.

Grigg F. J. T. and Rogers M. N. (1929) Radioactivity and chemical composition of some N.Z. Waters. *N.Z. J. Sci. Tech.* **11,** 216–219.

Hevesy G. and Paneth F. A. (1938) *A Manual of Radioactivity* p. 306. Oxford University Press, London.

Iwasaki I. and Isimori J. and Hataye I. (1951) Geochemical investigation of volcanoes in Japan—XXIX. Radioactive constituents of fumarolic gases. *J. Chem. Soc. Japan* **72,** 736–739.

Kenney J. F. (1943) *Mathematics of Statistics* Pt. 2. Van Nostrand, New York.

Kuroda K. (1944) Radioactive springs discovered in Masutomi. *Bull. Chem. Soc. Japan* **19,** No. 3, 33–83.

Kuroda K. and Yokoyama Y. (1948) On the equilibrium of the radioactive elements in the hydrosphere—I and II. *Bull. Chem. Soc. Japan* **21,** 52–63.

Kuroda K. and Yokoyama Y. (1949) On the equilibrium of the radioactive elements in the hydrosphere—III and IV. *Bull. Chem. Soc. Japan* **22,** 34–45.

McLaurin J. S. and Wright C. M. (1911) Radioactivity of the thermal water of Rotorua, Taupo and Te Aroha. *Dominion Laboratory Forthy-fourth Annual Report* p. 63.

New Zealand Geological Survey (1948) The outline of the geology of New Zealand. *Symposium of officers of the New Zealand Geological Survey.*

Rogers M. N. (1926) Radioactivity of the Karapiti Blowhole. *Trans. Proc. N.Z. Inst.* **57,** 892.

Schlundt H. (1935) Radioactivity of the spring waters in the hot spring area of Arkansas. *Amer. J. Sci.* **30,** 45–50.

Straniero D. (1951 and 1952) Italy's geothermal steam—I and II. *N.Z. Elect. J.* 1016–1019; 115–119.

Wilson S. H. (1949) The chemical investigation of the hot springs of the New Zealand thermal region. *Seventh Pacific Science Congress of the Pacific Science Association* p. 449–469.

Geochimica et Cosmochimica Acta, 1959, Vol. 16, pp. 192 to 193. Pergamon Press Ltd. Printed in Northern Ireland

GEOCHEMICAL NOTE

Constitution of the mantle—a revision*

(*Received* 20 *October* 1958)

In some papers recently published (Ringwood, 1958, Parts I, II, III) the nature of the phase transition zone in the mantle between 2–400 km and 900 km has been extensively discussed. The large width of the transition zone was attributed primarily to the presence of a high temperature gradient in this region combined with a high pressure gradient dP/dT for the transitions, and secondarily to solid solution effects among the participating phases. Subsequent data have shown that the relative importance of these factors should be reversed.

The slope dP/dT of the olivine–spinel transition in Mg_2SiO_4 was estimated very tentatively as 100 bars/degree. This implies an entropy change of 10 cals/mole per degree. Meijering and Rooymans (in press) have pointed out that the entropy change would probably be substantially less than this, which means that dP/dT would probably be proportionally smaller. Roy and Roy (1954) have determined the initial slope dP/dT for the olivine–spinel transition in Mg_2GeO_4 as 40 bars/degree, and the corresponding value for Mg_2SiO_4 may well be close to this. At higher temperatures and pressures it would probably be somewhat larger. This is supported by the later work on the transition in Mg_2SiO_4 at 600°C, which was presented as an appendix to Part II. This showed that the transition pressure was substantially higher than the calculated value at 600°C. This result was obtained too late for incorporation of its implications in the manuscript.

As a result of the smaller gradient, the width imparted to the transition region by any plausible temperature distribution is less than previously assumed.

On the other hand, an investigation by Meijering and Rooymans (in press) has shown that solid solution effects are more important than previously supposed in spreading the transition region. They made a thermodynamic study of the olivine spinel transition as a function of pressure at constant temperature, in the ternary system MgO–FeO–SiO_2 and concluded that solid solution effects could spread the transition over a range of several hundred kilometres.

A further contribution to the transition range, which has not previously been considered, is made by solid solution between diopside and enstatite which occurs at temperatures above 1200°C. A small amount of diopside (which is probably present) would extend upwards the pressure required for solid solution of $MgSiO_3$ in Mg_2SiO_4 spinel, or for decomposition of $MgSiO_3$ into Mg_2SiO_4 spinel and SiO_2 (coesite).

In view of these considerations it seems reasonable to attribute the transition range in the mantle largely to solid solution effects. This does not exclude the possibility of a high temperature gradient in this region, which may be supported by other evidence (Tozer, in manuscript). The influence of the temperature gradient in spreading the transition region would still be important, but not dominant.

* Paper No. 172 published under the auspices of the Committee of Experimental Geology and Geophysics and the Division of Geological Sciences at Harvard University.

A diagram illustrating the revised interpretation is presented (Fig. 1).

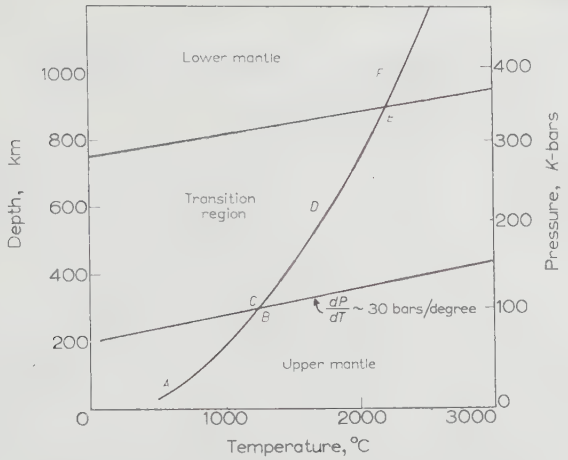

Fig. 1. Possible relationship between transition zone and temperature distribution in the mantle. Letters on temperature depth curve refer to phase assemblages which may be present (Ringwood, Part III), 1958.

A. Olivine $\left(\frac{MgO}{FeO} \sim 5\right)$, enstatite $\left(\frac{MgO}{FeO} \sim 5\right)$, small amounts of diopside-jadeite solid solution, pyrope rich garnet.

B. Olivine, enstatite-diopside-jadeite solid solution (henceforth called "pyroxene"), minor garnet.

C. Olivine, pyroxene, iron-rich spinel.

D. Spinel $\left(\frac{MgO}{FeO} \sim 5\right)$, pyroxene.

E. Disordered, non stoichiometric spinel, containing $(MgFe)SiO_3$ in solid solution, minor diopsidic pyroxene.

F. Homogeneous, highly disordered, spinel solid solution.

Notes:

(I) Disappearance of garnet between *B* and *C* is controlled by solubility of Al_2O_3 and Cr_2O_3 in spinel and pyroxene. All other components present in garnet are readily soluble in these phases. In regions where Al_2O_3 is locally concentrated, garnet may persist as a phase, to greater depths.

(II) Principal transition between *C* and *D* is the olivine–spinel inversion, which takes place over a substantial depth range due to Mg–Fe solid solution.

(III) Principal equilibria involved in spinel-pyroxene solid solution between *D* and *E* are:

$$2(MgFe)SiO_3 \rightarrow (MgFe)_2SiO_4 \text{ (spinel)} + SiO_2 \text{ (Coesite)}$$

$$(MgFe)_2SiO_4 \text{ (Spinel)} + SiO_2 \text{(coesite)} \rightarrow \text{non-stoichiometric defect spinel.}$$

Acknowledgement—The author is indebted to Drs. Meijering and Rooymans for a pre-print of their paper.

A. E. Ringwood

Department of Geophysics, Australian National University
Canberra, A. C. T., Australia

References

Meijering J. L. and Rooymans C. J. M. (1958) On the Olivine–Spinel transition in the earth's mantle. *Proc. Kon. Ned. Akad.* (in press).

Ringwood A. E. (1958) Constitution of the mantle: Parts I, II and III. *Geochim. et Cosmoschim. Acta* **13**, 303–321; **15**, 18–29 and 195–212.

Roy D. M. and Roy R. (1954) *Amer. Min.* **39**, 957.

Tozer D. In preparation.

Geochimica et Cosmochimica Acta, 1959, Vol. 16, pp. 194 to 196. Pergamon Press Ltd. Printed in Northern Ireland

LETTERS TO THE EDITORS

A typical parent meteorite body—a reply to Dr. J. F. Lovering

(*Received* 17 *December* 1958)

In a preceding issue of this journal I criticized certain arguments in a paper by Dr. J. F Lovering. In this, the criticism was directed specifically to points in Lovering's papers and these were numbered according to the organization of his paper. Now a reply appears with twelve points. Under these circumstances a discussion could become a divergent series and hence I wish to be very brief in my counter-reply. Lovering says: "In his comments Professor Urey has brought up a number of points which would appear to be mainly based on his *personal* views concerning the origin of meteorites. These will not be discussed in this plan but only certain specific matters of fact." I re-read my comments in order to understand to what opinions this statement refers. Apparently it relates to my contention that the iron meteorites were not a part of a core of the meteorite planet. But this is a conclusion based on arguments given in the last paragraph of my comment. I maintain that it is to himself that Lovering's remarks quoted above apply. In 1953, Henderson presented his evidence for the small size of the primary iron–nickel masses and this has been part of my thinking since then and has appeared in a number of my publications. It is not as extensive as we should like it to be, but there is no evidence for the contrary view that parent meteorite planets had cores. These matters are part of the "facts". Accepting them, the argument in regard to the origin of the iron meteorites follows an entirely different course from that outlined by Lovering and, in fact, much of his discussion is beside the point. Lovering has executed a magnificent ploy of "one-upmanship"*, i.e. when one does not wish to face the evidence he accuses the other person of arbitrarily following his personal views. It certainly confuses one's opponent to a point where even he must study his work to find out what it is all about!

Lovering's discussion shows how doubtful his entire argument is, and to bring this out was the sole purpose of my comment. Averaging poor data or even good data which varies widely for unknown reasons leads to doubtful results. Also, one should try to be responsible for the reliability of references and not to promulgate incorrect conclusions into the indefinite future.

In regard to his point (11), Lovering has not understood my comment. It was a brief statement covering very divergent lines of argument. However, this did not refer only to the arguments in regard to the chondritic meteorites, though it includes this particular argument. The great diversity of chemical composition and structure of the iron meteorites is partly explained as being due to the separate preparation of each of the metal masses of which they are composed. The indications that the parent metal masses were of the size of the metal meteorites is consistent with this conclusion and the evidence for the small size may be repeated again.

(a) The surface features of the iron meteorites (re-entrant holes, bridges, etc.) show in many cases that they are not fragments of a larger metal mass (Henderson).

(b) The large proportion of stony irons observed to fall indicates that the ratio of silicate-metal surface to volume of the metal was large.

(c) The absence of great distortion of the Widmannstätten figures show that the violent disruption required to break up a massive metal mass did not occur.

Harold C. Urey

University of California
La Jolla, California, U.S.A.

* For definitions, see Stephen Potter.

A typical parent meteorite body—reply to Professor Urey

At the present time there are apparently two completely different schools of thought with regard to the origin of the primary meteorites—(1) the view held by Professor Urey that they were essentially small bodies of the same order of size of the metal meteorites themselves, and (2) that they originated within one or more larger bodies, probably of lunar dimensions, with silicate mantles and metal cores. It is too early to decide finally between these hypotheses.

In my two papers I described some logical consequences of the second assumption. Professor Urey made twelve specific criticisms of matters of fact and these I have answered. His further letter adds nothing scientific to the discussion and I must object to his statement that "there is no evidence for the contrary view that parent meteorite planets had cores. These matters are part of the 'facts' ". This statement could give a completely wrong impression of the position. Obviously the whole matter needs arguing at considerable length but it would be inappropriate to do so here.

J. F. Lovering

Department of Geophysics
Australian National University
Canberra A.C.T.
Australia

Further comments on the vanadium–calcium line coincidence at 3185 Å

(*Received* 11 *February* 1959)

The following remarks are pertinent to the recent note by Shaw (1958) on a calcium coincidence with the vanadium line at 3185·4 Å.

(a) This coincidence has been recognized in this laboratory for many years, it having been referred to previously by various workers. Kvalheim (1942) states that "V 3185 coincides with the weak Ca-line 3185, but this does not disturb the analysis except when the Ca content is high and the V-line at the same time very weak". Harvey (1947) suggests that there is interference of V 3185·4 Å when calcium is a major constituent. Russell and Saunders (1925) list several Ca lines near 3185, one of them being 3185·22 Å. The Ca line in question is reported in the wavelength tables of Kayser and Konen (1932). In the calcium spectrum reproduced by Gatterer and Junkes (1947), there is a group of lines in this spectral region including one near 3185 Å.

(b) In the study by Scott (1945) of the effect of extraneous elements on spectral line intensity, two vanadium lines were used, 4379·2 Å and 3185·4 Å. Calcium compounds produced enhancement in both cases, although the effect was more marked with V 3185·4 Å. While the calcium interference at 3185 Å explains why there was a greater effect with V 3185·4 Å than with V 4379·2 Å, it does not "confirm that the so-called enhancement is spurious" as claimed by Shaw. We have not been able to obtain any evidence of a significant coincidence of a calcium line with V 4379·2 Å.

(c) With regard to the value of 240 p.p.m. for vanadium in the standard diabase W-1 (Ahrens, 1954) it should be pointed out that the result obtained in this laboratory (220 p.p.m.) is not open to the criticism put forward by Shaw, since, as stated by Mitchell (1948), V 4379·2 Å is used for the semiquantitative analysis of rocks. V 3185·4 Å is used in this laboratory only for the quantitative analysis of concentrates of soil extracts, plants, etc, from which calcium is removed during the chemical concentration prior to arcing (Mitchell, 1948).

While we agree with Shaw's conclusion that V 3185·4 Å should not be used for vanadium determinations in calcium-rich samples, we cannot agree that this coincidence has been disregarded by other workers. We consider that the enhancement of vanadium by calcium in the arc is a real effect.

R. O. Scott
D. J. Swaine

Department of Spectrochemistry
The Macaulay Institute for Soil Research
Aberdeen, Scotland

References

Ahrens L. H. (1954) *Quantitative Spectrochemical Analysis of Silicates* p. 29. Pergamon Press, London.

Gatterer A. and Junkes J. (1947) *Atlas der Restlinien. Spektren von 30 Chemischen Elementen.* Specola Vaticana.

Harvey C. E. (1947) *A Method of Semi-quantitative Spectrographic Analysis* p. 271. Applied Research Laboratories, Calfornia.

Kayser H. and Konen H. (1932) *Handbuch der Spectroscopie* Vol. VIII (i), p. 355. Hirzel, Leipzig.

Kvalheim A. (1942) On the spectrochemical determination of vanadium in iron ores and slags. *Norsk Geol. Tidsskr.* **21,** 245–267.

Mitchell R. L. (1948) The Spectrographic Analysis of Soils, Plants and Related Materials p. 84 and p. 88. *Tech. Commun. Bur. Soil Sci., Harpenden,* No. 44.

Russell H. N. and Saunders F. A. (1925) New regularities in the spectra of the alkaline earths. *Astrophys. J.* **61,** 38–69.

Scott R. O. (1945) The effect of extraneous elements on spectral line intensity in the cathode layer arc. *J. Soc. Chem. Ind., Lond.* **64,** 189–194.

Shaw D. M. (1958) A vanadium–calcium spectral line coincidence at 3185 Å and its effect on vanadium abundance data. *Geochim. et Cosmochim. Acta* **15,** 159–161.

OBITUARY

F. A. PANETH 1887–1958

Friedrich Adolph Paneth, one of the founders and original editors of this journal, died in Vienna on 17 September 1958. Born in Vienna in 1887, he received his early training at the Universities of Vienna, Munich and Glasgow, respectively under Skraup, von Baeyer and Soddy. He occupied Chairs at the Prague Institute of Technology, at the universities of Hamburg and Berlin and was Professor and Director of the Chemical Laboratories at Koenigsburg before coming to England to work at Imperial College, being appointed in 1938 Reader in Atomic Chemistry. In 1939 he became Professor of Chemistry at Durham. His earlier work included the development of the use of radioactive tracers, the discovery of the hydrides of several metals and studies of the transient free aliphatic radicals. In later life his interests turned towards geochemistry and cosmochemistry; he devised precise methods for the determination of helium and among other tasks he was entrusted with the investigation of gases collected from the upper atmosphere by rocket missiles fired in the United States. He also applied the helium method to the determination of the ages of meteorites.

His distinguished contributions to chemistry were recognized in 1947 by his election to the Royal Society, and by honours from many other learned societies. In 1949 he was President of the Joint Commission on Radioactivity of the International Council of Scientific Unions.

During World War II he spent 2 years as Head of the Chemistry division of the British-Canadian Atomic Energy Laboratory in Montreal. Upon returning to Durham, his efforts led to the foundation of the Londonderry Laboratory for Radiochemistry to which he attracted researchers from many parts of the world. He retired from the Durham Chair in 1953, and became a Director in the Max-Planck-Institüt für Chemie, Mainz.

A man of great personal charm and of formidable linguistic ability, Professor Paneth will be remembered by friends in many countries, not least by those who work in the borderland between chemistry, geology and astronomy.

K. C. Dunham

Department of Geology
University Science Laboratories
Durham

Geochimica et Cosmochimica Acta, 1959, Vol. 16, p. 197. Pergamon Press Ltd. Printed in Northern Ireland

Book review

V. I. Lebedev: **Osnovy Energeticheskogo Analiza Geokhimicheskikh Protsessov (Fundamentals of the Energetic Analysis of Geochemical Processes)**. Izdatelstvo Leningradskogo Universiteta, 1957. 342 pp. 23 roubles, 50 kopeks.

"In this book an attempt is made to introduce to geochemistry new concepts necessary for understanding natural processes developed by physics and chemistry in the last 15 or 20 years and to give solutions for the more general problems of geochemistry" (p. 2, reviewer's translation). To this end the first third of the book is devoted to an exposition of the basic principles of atomic structure and chemical bonding. Next, the generalizations are made that assemblages tend to be composed of minerals with the densest packing (somewhat modified by the exact nature of bonding) and with the maximum energy of bonding. The latter principle is most used in the subsequent argument. The approach, although not entirely unfamiliar in the West, has been most extensively developed in Russia, under the influence of Fersman. The energy values that Lebedev uses commonly are heats of formation, as calculated by Born–Haber cycles or as measured. Among the problems to which these methods are applied are the distribution of elements between sulphur and oxygen compounds, interpretation of the reaction series, and problems of the migration of elements. Lebedev states "these methods do not replace the more precise and universal thermodynamic analysis, the application of which to natural processes, unfortunately, is limited by the extraordinary complexity of natural processes . . ." (p. 156). It is to be regretted that, in actuality, Lebedev does allow his methods of energetic analysis to replace the thermodynamic methods. Although the various thermodynamic functions are introduced, there is little appreciation of the specific uses of each.

The treatment of the polymorphism of the Al_2SiO_5 minerals may be taken as an example of Lebedev's approach. The discussion is based on the heats of formation, which he usually simply calls "energy". The values of Neumann (1925) are accepted uncritically, although at present they are generally used with great caution, if at all. First, Lebedev states as a paradox the fact that kyanite is the densest phase while sillimanite has the highest energy content, which he resolves by consideration of the crystal structures (p. 151). Later, he uses such facts as the appearance of the lower density sillimanite in the deeper zones of metamorphism as examples of the dangers of reliance on Le Chatelier's Principle (p. 185). The quantitative counterpart of the Principle, the Clapeyron–Clausius equation, is entirely unmentioned. Finally, he concludes that, as sillimanite has the lowest energy level, kyanite and andalusite are metastable forms, whose appearance is controlled by kinetic factors (p. 193).

The final chapter presents, as a logical outgrowth of such analysis, the theory, which Lebedev and his co-workers have earlier published in a series of papers, that the geochemical cycle is run by solar energy, absorbed by "geochemical accumulators" in the weathering zone and released during metamorphism at depth. (A remarkably similar, but demonstrably independent, thesis was presented by V. A. Saull in this journal, 1955.) The criticism of, among others, Korzhinsky, who demonstrated that the theory can not be reconciled with the laws of thermodynamics, is acknowledged but not refuted.

Perhaps the most important development in geochemistry in the last 15 or 20 years is the realization that the old science of thermodynamics provides a rigid framework for geochemical theory, only in terms of which can the newer discoveries in chemistry and physics be properly applied. Comparison with any of several recent works in which this is accepted makes Lebedev's book appear rather deficient. Nevertheless, a geochemist, particularly one not too familiar with the recent Russian literature, could hardly fail to obtain many stimulating ideas from this book.

D. J. Milton

Department of Geology
Harvard University
Cambridge, Mass.

Geochimica et Cosmochimica Acta, 1959, Vol. 16, p. 198. Pergamon Press Ltd. Printed in Northern Ireland.

MEETING ANNOUNCEMENTS

A Symposium on Petroleum Geochemistry at Fordham University, during the 5th World Petroleum Congress

A SYMPOSIUM on petroleum geochemistry will be held at Fordham University, New York 58, N.Y., on Thursday evening, June 4, 1959. The meeting will consist of an informal, open discussion of papers submitted by researchers who are active in this and related scientific fields. The papers will be preprinted and will be distributed upon request to all who wish to attend the meeting. These are some of the contributions to the program:

Synthesis of organic compounds in the atmosphere of the primitive earth;
Reactions of biochemicals during rock formation;
Thermal alteration of chlorophyll;
Bacterial activity in recent sediments;
Petroleum genesis and accumulation mechanisms;
The sedimentary strata as a chromatographic column;
Nitrogen, noble gas and carbon isotope geochemistry;
Recent U.S. and foreign developments in geochemical exploration for oil.

Inquiries should be addressed to the members of the program committee: Professor BARTHOLOMEW NAGY, Department of Chemistry, Fordham University, Chairman; Dr. E. G. BAKER, Esso Research and Engineering Company, P.O. Box 51, Linden, New Jersey; or to Professor PAUL A. WITHERSPOON, Department of Petroleum Engineering, University of California, Berkeley 4, California. The discussion moderator will be DR G. D. HOBSON, Imperial College of Science and Technology, University of London, England.

Although the symposium is not an official part of the 5th World Petroleum Congress, Congress registrants may recieve information and preprints at the document counter in the registration area in the New York Colliseum.

Symposium on Geochemistry

A SYMPOSIUM on geochemistry organized by the Commission on Geochemistry of the International Union of Pure and Applied Chemistry will be held in Göttingen, Germany, on August 21st and 22nd, 1959, to be followed by two days' field excursions. The topics for discussion at the Symposium are:

(1) Stable nuclides in geochemistry;
(2) Long-lived radionuclides in natural systems;
(3) Geochemistry of the halogens;
(4) Geochemical aspects of life on earth.

Introductory lectures will be held as follows: for (1) by RANKAMA, for (2) HARRISON BROWN, for (3) by CORRENS and for (4) by OPARIN and UREY, who will extend invitations for further contributions.

The excursions will comprise a day's visit to the Harz and another one to the Zechstein salt deposits along the Werra.

The local chairman of the Symposium is Professor C. W. CORRENS, Sedimentpetrographisches Institüt, Göttingen, Lotzestrasse 13, Germany.

ERRATA

S. A. EL WARDANI: Marine geochemistry of germanium and the origin of Pacific pelagic clay minerals

Geochim. et Cosmochim. Acta **15**, 237–254.

THE following corrections should be made:

p. 241, line 1: delete 'aluminium'; substitute 'biogenous' for 'hydrogenous';
line 2: delete 'authigenic';
p. 244, VIII, line 7: delete 'quartz, detrital igneous minerals'.

M. HOOKER: Data of rock analyses—V.

Geochim. et Cosmochim. Acta **15**, 342–369.

THE following additions and corrections were notified too late for inclusion in the above article:

p. 359, line 18: for EDWARDS 1942b read EDWARDS 1941b;
p. 360, lines 22–23 ('Amphibolite'): add JOPLIN 1939; SIMPSON 1916;
line 34: for RICHARD read RICHARDS;
line 36: for COLDWITZ read COLDITZ;
p. 361. line 20: for EDWARDS and CRAWFORD 1950 read EDWARDS and CRAWFORD 1940;
p. 363, line 49: for ANDREWS 116 read ANDREWS 1916;
p. 365, lines 38–45 ('Meteorite'): add HODGE-SMITH and EDWARDS 1941;
line 47: for REID A. J. read REID A. M.;
p. 367, line 29: for EKWARDS read EDWARDS;
line 31: for BYRAN read BRYAN.

W. S. BROECKER and A. WALTON: The geochemistry of C^{14} in fresh-water systems (This issue, pp. 15–38.)

Notes added in press:

1. (See p. 18). It should be noted that the C^{13} analyses were made on the counting gas. Although fractionation during the preparation of this gas is probably small, caution should be exercised when comparing the δC^{31} results with those published by workers preparing samples under controlled conditions.

2. (See p. 28). DR. HARMON CRAIG has pointed out to the authors that he has unpublished evidence which strongly suggests that the dissolved bicarbonate in river water is largely derived from organic material rather than atmospheric CO_2. If this is the case the length of storage of the carbon in the organic form would influence the C^{14}/C^{12} ratio in river water. Thus a much greater time lag would exist before the appearance of significant amounts of H-bomb C^{14} in fresh-water streams. In this case the ΔC^{14} values given in column 2 (Table 6) and the exchange rates in column 5 would be most nearly correct.

INFORMATION FOR CONTRIBUTORS

I. GENERAL

1. Papers on geochemistry should be submitted to the appropriate Executive Editor (*Papers on cosmochemistry should be sent to Prof. W. A. Wahl*). Papers submitted for publication will naturally be judged from the standpoint of scientific originality and novelty. Technical details of apparatus used in scientific investigation can, however, be presented in brief notes. Critical comments or preliminary results requiring early publication should be submitted as letters to the editors. Where possible, letters should be confined to 500 words. The preparation of progress reports and review articles will be invited by the editors from time to time. The journal appears as independent and complete numbers, which are combined into volumes of about 300 pages.

2. Only papers which have not been previously published can be accepted. Authors must agree not to publish elsewhere a paper submitted to and accepted by *Geochimica et Cosmochimica Acta*.

3. Fifty reprints of each paper are provided free. Additional copies can be purchased if ordered at the time the first proofs are returned. A reprint order form will accompany first proofs.

II. SCRIPT REQUIREMENTS

1. Scripts must be written in one of the three official languages—English, French or German.

2. The script should be typed (not a carbon copy). The text must be ready for printing and should be carefully checked for errors. Authors will receive proofs for correction.

3. Illustrations should accompany the script, mounted on separate sheets. Line diagrams that require to be redrawn should include all relevant details. Half-tone illustrations should be restricted to the minimum necessary. Photographs should be enlarged sufficiently to permit their clear reproduction, and if words or numbers appear on them, two copies should be sent, one clearly printed and the other without inscription. All illustrations should be provided with descriptive legends, which should be given on a separate sheet. Any lettering on diagrams—other than Greek letters, symbols, etc.—should be stencilled and should be sufficiently large and bold to permit reproduction when the diagram has been reduced to a size suitable for inclusion in the journal.

4. References in the text should be given by quoting the author's name and year of publication, i.e. AHRENS (1952). **Full references should be listed at the end of each paper, in alphabetical order, in the following manner:**

AHRENS, L. H. (1952) The use of ionization potentials—I. Ionic radii of the elements. *Geochim. et Cosmochim. Acta* **2**, 155–169.

and should include the full title of the article, standard abbreviated title of the journal, year, volume number and inclusive page numbers. References to books should include the total number of pages.

5. The text of articles submitted should be concise and in a readily understandable style. The technical description of the methods used should only be given in detail when such methods are new. The essential contents of each paper should be briefly recapitulated in an abstract in English. Such an abstract, may, however, be submitted by the author in the language of the original typescript for translation into English by the editorial staff.

6. To conserve space, authors are requested to mark less important portions of the paper (such as description of methods, record of experimental results, etc.) for printing in smaller type.

7. Indices of refraction should be denoted by the symbols α, β, γ, ω, ε, n, and vibration directions by X, Y, Z, O and E.

Pergamon Press are also publishers of the following Journals:

JOURNAL OF NUCLEAR ENERGY (*including* THE SOVIET JOURNAL OF ATOMIC ENERGY*). PART A: REACTOR SCIENCE; PART B: REACTOR TECHNOLOGY
HEALTH PHYSICS (*The Official Journal of the Health Physics Society*)
JOURNAL OF INORGANIC AND NUCLEAR CHEMISTRY
TETRAHEDRON (*The International Journal of Organic Chemistry*)
TALANTA (*An International Journal of Analytical Chemistry*)
INTERNATIONAL JOURNAL OF APPLIED RADIATION AND ISOTOPES
BIOCHEMICAL PHARMACOLOGY
ARCHIVES OF ORAL BIOLOGY
* BIOPHYSICS
* JOURNAL OF MICROBIOLOGY, EPIDEMOLOGY AND IMMUNOBIOLOGY
* PROBLEMS OF HEMATOLOGY AND BLOOD TRANSFUSION
* PROBLEMS OF VIROLOGY
* PROBLEMS OF ONCOLOGY
* SECHENOV PHYSIOLOGICAL JOURNAL OF THE U.S.S.R.
* PAVLOV JOURNAL OF HIGHER NERVOUS ACTIVITY
* ELECTRIC TECHNOLOGY, U.S.S.R.
* RADIO ENGINEERING
* RADIO ENGINEERING AND ELECTRONICS
* TELECOMMUNICATIONS
* PHYSICS OF METALS AND METALLOGRAPHY
* THE ABSTRACTS JOURNAL OF METALLURGY
* APPLIED MATHEMATICS AND MECHANICS
CHEMICAL ENGINEERING SCIENCE
JOURNAL OF ATMOSPHERIC AND TERRESTRIAL PHYSICS
PLANETARY AND SPACE SCIENCE
BULLETIN GÉODÉSIQUE
ANNALS OF THE INTERNATIONAL GEOPHYSICAL YEAR
SPECTROCHIMICA ACTA
JOURNAL OF THE MECHANICS AND PHYSICS OF SOLIDS
ACTA METALLURGICA
(*for the Board of Governors of Acta Metallurgica*)
INTERNATIONAL JOURNAL OF THE PHYSICS AND CHEMISTRY OF SOLIDS
DEEP-SEA RESEARCH
JOURNAL OF NEUROCHEMISTRY
JOURNAL OF PSYCHOSOMATIC RESEARCH
JOURNAL OF INSECT PHYSIOLOGY
INTERNATIONAL JOURNAL OF AIR POLLUTION
INTERNATIONAL ABSTRACTS OF BIOLOGICAL SCIENCES
(*for Biological and Medical Abstracts Ltd.*)
RHEOLOGY ABSTRACTS
VACUUM
OPERATIONAL RESEARCH QUARTERLY
ANNALS OF OCCUPATIONAL HYGIENE
ELECTROCHIMICA ACTA

* *Translations of Russian journals published on behalf of the Pergamon Institute, a non-profit-making foundation*

Leaflets giving further details and subscription rates of each of these journals are available on request

FILED IN STACKS
10 Aug. 1955
19 Aug 1950
20 Apr 64
5 Jul 54
4 Sep 64

THE GEOCHEMICAL SOCIETY

OFFICERS

FARRINGTON DANIELS, President
JOHN F. SCHAIRER, Vice-President
KONRAD B. KRAUSKOPF, Secretary
GEORGE T. FAUST, Treasurer

COUNCILLORS

WILLARD F. LIBBY, 1956–1958
HATTEN S. YODER, 1956–1958
JOHN A. S. ADAMS, 1957–1959
ALFRED O. NIER, 1957–1959
E. F. OSBORN, 1958–1960
H. G. THODE, 1958–1960

REGIONAL VICE-PRESIDENTS

LOUIS H. AHRENS
RUI RIBEIRO FRANCO
ING. GEORGES ORDOÑEZ
C. W. CORRENS
WILLIAM S. FYFE
KEN SUGAWARA

COMMITTEES

Auditing Committee:
JOSEPH J. TREGONING, Chairman
WILLIAM L. HILL
C. R. NASSER

Constitution and By-Laws Committee:
MICHAEL FLEISCHER, Chairman
JULIAN R. GOLDSMITH
DENIS M. SHAW

Education Committee:
H. D. HOLLAND, Chairman
J. A. S. ADAMS
D. M. HENDERSON
KURT E. LOWE
G. D. NICHOLLS

Membership Committee:
R. M. GARRELS, Chairman
HARVEY C. DIEBL
CHESTER B. SLAWSON
JAMES E. SLOSSON

Nominating Committee:
D. E. WHITE, Chairman
GEORGE EDWARDS
A. E. ENGEL
W. D. KELLER
T. G. SAHAMA
D. M. SHAW

Programme Committee:
H. T. EVANS, Chairman
GORDON J. F. MACDONALD
H. E. LOWENSTAM

Publications Committee:
E. W. HEINRICH, Chairman
JULIAN R. GOLDSMITH
JOHN C. MAXWELL
N. W. RAKESTRAW
S. C. ROBINSON
L. R. WAGER

Research Committee:
C. G. DODD, Chairman
LOUIS H. AHRENS
W. F. BRADLEY
C. W. CORRENS
RUI RIBEIRO FRANCO
WILLIAM S. FYFE
ING. GEORGES ORDOÑEZ
R. A. ROWLAND
KEN SUGAWARA
T. G. THOMPSON
G. W. WETHERILL

Russian Translations Committee:
EARL INGERSON

Seal Committee:
ALVIN VAN VALKENBURG, JR., Chairman
MARGARET D. FOSTER
JEWELL GLASS
EDWIN ROEDDER

Standards Committee:
HARRY A. BRIGHT, Chairman
FELIX CHAYES
ALBERT E. J. ENGEL
SAMUEL S. GOLDICH
KIGUMA J. MURATA
GEORGES S. SWITZER

Tellers Committee:
CHARLES MEYER, Chairman
HENRY R. CORNWALL
COLIN O. HUTTON